Title

Glycomimetics via radical polymerization: The effect of saccharide identity, connectivity, and architecture on biological interactions

Author

Liau, Walter Tsu-i

Publication Date

2017

Peer reviewed|Thesis/dissertation

UNIVERSITY OF CALIFORNIA

Los Angeles

Glycomimetics via radical polymerization: The effect of saccharide identity, connectivity, and architecture on biological interactions

A dissertation submitted in partial satisfaction

of the requirements for the degree

Doctor of Philosophy in Bioengineering

by

Walter Tsu-i Liau

2017

ABSTRACT OF THE DISSERATION

Glycomimetics via radical polymerization: The effect of saccharide identity, connectivity, and architecture on biological interactions

by

Walter Tsu-i Liau

Doctor of Philosophy in Bioengineering

University of California, Los Angeles, 2017

Professor Andrea M. Kasko, Chair

Polysaccharides are polymeric chains comprised of saccharides connected through glycosidic bonds that have important biological functions, such as energy storage, structure, and cell signaling. Although polysaccharides are ubiquitous in nature, there are limited tools for examining their roles due to the complexity of polysaccharide synthesis. In order to synthesize well-defined polysaccharides, selective protection/deprotection techniques are employed that require tedious purification at each intermediate. In order to facilitate the creation of high molecular weight saccharide-bearing polymers, glycopolymers can be created as an alternative. Glycopolymers emulate the interactions observed in natural polysaccharides through the use of synthetic analogues.

Glycopolymers are synthetic polymers that present saccharide side groups. Although glycopolymers have been produced with control over saccharide identity and molecular weight, only limited investigations have been conducted to incorporate cationic charge or control branched architecture. Currently, cationic charge is incorporated through the copolymerization of cationic monomers with glycomonomers, but the inclusion of cationic monomers has led to

increased cytotoxicity. There have been no examples of glycopolymers utilizing the inherent charge available on amino-sugars, such as glucosamine. In addition, branched glycopolymers have previously been studied using atom-transfer radical polymerization, but the polymerization technique is incompatible with amine-containing monomers and requires removal of the copper catalyst. Reversible addition-fragmentation chain transfer (RAFT) polymerization is an alternative technique for glycopolymer synthesis, but branching has only been introduced using crosslinkers that result in gelation at high degrees of incorporation. To address these limitations, new cationic glycomonomers and RAFT branching units have been synthesized.

Using these new tools, in addition to those currently available for glycopolymer synthesis, a number of biomedical applications were investigated: bacterial attachment on glycopolymer-modified surfaces, lectin interaction with 3D constructs that present saccharides at different densities, antibacterial activity of a cationic glycopolymer, and potential usage of a cationic glycopolymer in gene transfection.

Using a set of four glycomonomers synthesized from glucose, galactose, mannose, and *N*-acetyl glucosamine, glycopolymer of various saccharide identities were polymerized via RAFT polymerization and conjugated to gold surfaces to investigate the attachment of *Shewanella oneidensis* and *Vibrio cholerae*. Polymeric mannose was seen to encourage significantly more attachment than monomeric mannose, polymeric galactose, and polymeric *N*-acetyl glucosamine.

Using a RAFT branching unit, amphiphilic glycopolymers were polymerized and self-assembled into nanoparticles with control over the surface saccharide density without affecting size and morphology. The nanoparticles with increased branching bound more lectin compared to nanoparticles without branching and glycopolymers in solution.

Using a cationic glycomonomer, a chitosan-mimic was polymerized and investigated for similarities in bioactivity. In antibacterial studies, the cationic glycopolymer closely mimicked the ability of chitosan to inhibit bacterial growth above a threshold molecular weight. Unlike chitosan, the glycopolymer was also soluble in neutral and basic buffer and maintained its ability to inhibit bacterial growth. As a transfection agent, the glycopolymer was able to induce gene expression with less cytotoxicity than poly(ethylenimine), the standard synthetic transfection agent, but with more cytotoxicity than chitosan. With optimization, the chitosan-mimic can be an efficient transfection agent with low cytotoxicity.

We have described the addition of new synthetic tools for creating cationic glycopolymers and hyperbranched glycopolymers. The applications presented demonstrate the importance of control over saccharide identity, branching, and charge in glycomimetic systems and can be applied to the design of new therapeutics and devices.

The dissertation of Walter Tsu-i Liau is approved.

Tatiana Segura

Gerard C. L. Wong

Isaac Yang

Andrea M. Kasko, Committee Chair

University of California, Los Angeles

2017

To my God and

all those whom He has place in my heart

TABLE OF CONTENTS

LIST OF FIGURES

LIST OF SCHEMES

LIST OF TABLES

ACKNOWLEDGEMENTS

Without the support of numerous individuals, the work presented in this dissertation would not have been possible. Although I could never enumerate all the kind acts of support, I'd like to recognize a few key people that have played a critical factor throughout the work presented in this dissertation.

First and foremost, I'd like to thank my research advisor, Professor Andrea M. Kasko, without whom I would not have the opportunity to conduct the body of work presented in this dissertation. Although there were many periods of frustration throughout the years, her advice and encouragement always helped me to persevere with my investigations and to mold me into a proper researcher.

To the members of the Kasko lab, thank you for the many hours of companionship in shared experiences of trials and tribulations. Without such supportive comrades, graduate school would have been unbearable. A special thanks to Professor Donald R. Griffin for his pioneering work that helped establish this lab and his generosity in making sure I looked my best at graduation. To Dr. Kenneth Lin, I owe a particular word of gratitude for his work in establishing the glycomimetics project, which I was so fortunate to continue, and his patience in training me in numerous synthetic techniques, however unconventional they may have ended up being. To Dr. Brianna Upton, thank you for the numerous pep talks during lunch, help with all things related to chemistry and the UCLA Chemistry and Biochemistry department, baked goods, making me a fun person in lab, and waiting for me to remove our final graduation chain link. Without your companionship through the roughest times, I would not have made it to the end. To Dr. Darice Wong, thank you for your sage advice throughout my PhD career and especially during our annual Georgetown Cupcakes trek. You really helped to put everything into perspective and

encouraged me to keep working at it. To Shadi Kordbacheh, thank you for your willingness to help take mass spectrometry samples and daily words of encouragement; you're the best! Last, but not least, I'd like to thank my capable undergraduate researcher David Teng, who was not only a helping hand in the beginning stages of the synthesis of the Fmoc-protected cationic glycomonomers, but also a brother-in-arms with struggles inside and outside of lab.

I would like to thank our collaborators in Paul Weiss's lab and the Gerard Wong's lab at UCLA. Thomas Young for his work in creating and characterizing the saccharide surfaces, and Calvin Lee for his work in tracking *Vibrio cholerae* presented in Chapter 5. I would like to thank our collaborators in Sébastien Lecommandoux's lab at the University of Bordeaux. Colin Bonduelle for his work training me in self-assembly techniques and his assistance with TEM imaging presented in Chapter 6. I would like to thank our collaborators in Ren Sun's lab at UCLA. Sara Shu for her help in providing pEGFP-C1, running agarose gels, and assisting in transfection experiments with HEK293 cells presented in Chapter 8. I am also indebted to the National Science Foundation and the Materials Creation Training Program for their support throughout this work. Portions of Chapter 4 and the entirety of Chapter 6 were adapted with permission from *Biomacromolecules* **16,** 284–94 (2015).

Lastly, I would like to thank my spiritual family of which my biological family is a part. Thank you Mom and Dad for your undying support throughout my entire life, in providing every opportunity for me and instilling me with all the skills and virtues I needed to succeed. Many thanks to my sisters Grace and Joyce and their remembrance of my birthday, their constant reminders to spend some time with our family, and Grace's numerous rides home and dinners late at night. To my spiritual companions Lampstand, Ben, Chris, Matt, Mark, Ruolin, Josh, David, Jason, Eric, Brian, Enoch, Ryan, Katherine, Priscilla, Prisca, Valerie, Sara, Angel, and

Julianna, thank you for all the fellowship, prayers, encouragement, hugs, meals, outings, and memories. You have made the monotonic life of a graduate student fun, exciting, and an absolute joy that I will treasure my entire life.

It has been an honor to pass through this experience at UCLA with the loving support of so many people. I am eternally grateful. Thank you.

VITA

2007	Bachelor of Science in Engineering
	Harvey Mudd College
2015	Master of Science in Bioengineering
	University of California, Los Angeles

PUBLICATIONS

Liau, W. T., Bonduelle, C., Brochet, M., Lecommandoux, S. & Kasko, A. M. Synthesis, characterization, and biological interaction of glyconanoparticles with controlled branching. Biomacromolecules 16, 284–94 (2015).

CHAPTER 1

Introduction

1.1. Polysaccharides in biomedicine

Polysaccharides, polymeric chains comprised of saccharides connected through glycosidic bonds, are ubiquitous in nature and function in a variety of ways, including energy storage, structure, and cell signaling. Their function is dictated by a number of characteristics, such as saccharide identity, connectivity, and architecture. Due to the ubiquity of polysaccharides in the body, polysaccharides have been investigated for their biomedical applications. For example, heparin has been used as an anticoagulant, and chitosan has been investigated for its antimicrobial properties.[1] While polysaccharides isolated from natural sources are promising as therapeutics, they are limited by a lack of control over architecture and molecular weight, by difficulty in purification, and by batch-to-batch variability. To overcome the limitations of natural polysaccharides, polysaccharides have been created synthetically. Their synthesis, however, is subject to tedious protection/deprotection chemistry and purification techniques for each intermediate, making high yields and high molecular weights impractical.[2–6] Glycopolymers have been used as an alternative to synthetic polysaccharides. Glycopolymers are polymers composed of a synthetic backbone with saccharide side groups and provide good synthetic control over saccharide identity and connectivity.[7,8]

1.2. Glycomonomer synthesis

Glycopolymers can be created via two methods: post-polymerization conjugation and direct polymerization. Post-polymerization conjugation attaches saccharide units to a preformed

polymer backbone. While this method allows for facile synthesis of the polymer backbone and saccharide units separately, their conjugation requires the incorporation of an additional linkage often not found in natural polysaccharides (e.g. amide bonds or triazole rings) and high conjugation efficiency is difficult to achieve. Direct polymerization requires the synthesis of glycomonomers, but ensures a saccharide at every repeat unit. Glycomonomers are synthesized from the modification of monosaccharides with polymerizable moieties. Monosaccharides, however, present numerous alcohol moieties for modification. In order to create a uniform sample of glycomonomer, selective protection/deprotection chemistry is applied. Most glycomonomers have polymerizable groups attached through a glycosidic bond at the anomeric position due to its increased reactivity or to the primary alcohol due to the selectivity of protecting groups. While multiple glycomonomers have been developed, glycomonomers have not been developed that present cationic charge. Currently, cationic charge is introduced through the copolymerization of a glycomonomer with a cationic monomer, but the usage of cationic monomers typically results in increased cytotoxicity. In order to create biocompatible cationic glycopolymers, cationic glycomonomers need to be developed that closely resemble the units found in natural polysaccharides.

1.3. Glycopolymer synthesis

Glycopolymers can be polymerized through a variety of techniques, but free-radical polymerization is particularly powerful, since it affords high flexibility in polymerization conditions, such as monomer, solvent, and temperature. Free-radical polymerization, however, can produce highly disperse polymer samples resulting from the premature termination of propagating chains. Controlled free-radical polymerization techniques, which reversibly maintain most propagating chains in a dormant state to avoid premature termination, can be used to

polymerize glycopolymers with control over molecular weight and limit dispersity.[7–14] While branching plays a key role in the physical and biological properties of polysaccharides, few examples of branched glycopolymers have been reported.[15–18] Initially, our group investigated hyperbranched glycopolymers made via atom-transfer radical polymerization (ATRP).[19] ATRP controls molecular weight by the reversible deactivation of propagating chains through use of a copper catalyst, but it also carries certain limitations, which include the inability to polymerize amine-containing monomers due to competitive complex formation with the copper catalyst and the need to remove the copper catalyst post-polymerization.[20]

As an alternative, reversible addition-fragmentation chain transfer (RAFT) polymerization is a versatile technique that is compatible with a wide variety of solvents, monomers, and initiators.[21] RAFT polymerization controls molecular weight through the use of a chain transfer agent (CTA) that reversibly holds propagating chains in a dormant state as radicals are transferred from one chain to another at a high rate.[21] At the completion of a RAFT polymerization, the CTA remains attached to the chain end and allows for reinitiation to continue chain propagation or is susceptible to facile chain end modification.[22] Branching in glycopolymers created via RAFT polymerization, however, is currently introduced using a homobifunctional crosslinker, such as ethylene glycol dimethacrylate.[23] Since the branching unit is a crosslinker, gelation has been observed when attempting high degrees of branching.[24–26] In order to facilitate the creation of highly branched glycopolymers via RAFT polymerization, polymerizable chain transfer agents need to be developed that containing a RAFT chain transfer moiety for chain propagation and a polymerizable moiety for incorporation into another polymer chain.

1.4. Dissertation focus

1.4.1. Overview

The aim of this dissertation is to create new glycomimetic tools for controlling and understanding cellular interactions with polysaccharides. Previous research in the field has developed a number of tools including glycomonomrs that contain a variety of saccharide identities, such as glucose, galactose, mannose, and *N*-acetyl glucosamine, but there has yet to be an example of a cationic glycomonomer. In addition, although branched glycopolymers have been previously studied using an ATRP initiator-monomer, the limitations of ATRP (inability to polymerize amine-containing monomers and removal of the copper catalyst) has shifted interest to using RAFT polymerization. Branched glycopolymers are created via RAFT polymerization, however, it currently utilizes a crosslinker that leads to gelation at high degrees of branching. In order to form hyperbranched glycopolymers via RAFT polymerization, an alcohol-bearing CTA is required to attach a polymerizable group. In order to address the current limitations, the main focus of this dissertation is to create new glycopolymer tools to further bridge the gap between natural polysaccharides and synthetic glycopolymers and to use these tools to investigate biological interactions.

1.4.2. Significance

In this dissertation, we utilize the newly developed tools for polymerizing cationic glycopolymers and for polymerizing branched glycopolymers to investigate four biomedical applications: bacterial attachment on glycopolymer surfaces, lectin interaction with 3D constructs that present saccharides at different densities, antibacterial activity of a cationic glycopolymer, and potential usage of a cationic glycopolymer in gene transfection.

While there have been examples of monosaccharides surfaces and some limited examples of glycopolymer surfaces, surfaces have not been created with the full spectrum of glycopolymers nor with patterned regions. The natural glycocalyx is a complex array of biomolecules. In the same way, patterned surfaces can have profound usefulness in directing the location and activity of bacteria through the presentation of different saccharide identities. Glycopolymers created via RAFT polymerization allow for facile control of saccharide identity and formation of glycopolymer surfaces on gold. Using RAFT polymerization, we created glycopolymers of different saccharide identities and modified gold surfaces to investigate the avidity of bacteria with each glycopolymer surface.

Although interactions with glycopolymers in solution and on 2D substrates have numerous biomedical applications, the natural presentation of saccharides is on the surface of 3D constructs. Previous investigations polymerized glycopolymers from a 3D protein, but the use of a protein limited the polymerization sites to the locations of initiator attachment and also complicated the characterization of the glycopolymers produced. Using RAFT polymerization, we created amphiphilic glycopolymers and formed nanoparticles through self-assembly techniques. The incorporation of a polymerizable CTA allowed for control of the saccharide density on the surface.

Finally, cationic polymers have a variety of biomedical applications, including as an antimicrobial and as a transfection agent. Much of the interest in cationic polysaccharides comes from the unique antimicrobial and biocompatible attributes of chitosan. Chitosan, as a naturally-derived polysaccharide, suffers from a lack of control over molecular weight and difficulty in purification. Furthermore, chitosan is only soluble in acidic media. In order to overcome these limitations, research has sought to create synthetic cationic glycopolymers by the copolymerize

of cationic monomers with glycomonomer or create cationic polysaccharides through the chemical modification of other neutral polysaccharides. Both approaches, however, are difficult to characterize and suffer from limited therapeutic activity. Alternatively, we designed a cationic polymer that closely resembles chitosan in structure and investigated its potential as an antimicrobial and as a transfection agent.

1.4.3. Outline of chapters

Chapter 2 gives an overview of current synthetic techniques for creating glycomic tools and their biomedical applications. Chapter 3 describes the synthesis of a library of glycopolymer tools, including new cationic glycomonomers and branching units for RAFT polymerization. Chapter 4 details the polymerization of three sets of glycopolymers: 1) glycopolymers with a variety of saccharide identities attached to the polymer backbone through a glycosidic bond, 2) linear and branched glycopolymers and linear and branched amphiphilic glycopolymers of various molecular weights with galactose attached through the primary alcohol to the polymer backbone, and 3) a cationic methyl glucosaminoside glycopolymer with various molecular weights isolated via fractional precipitation.

Chapter 5 describes the formation of surfaces using the first set of glycopolymers synthesized in Chapter 4 to investigate bacterial attachment. Chapter 6 describes the formation of nanoparticles using the amphiphilic glycopolymers in the second set of glycopolymers synthesized in Chapter 4 to investigate lectin interaction with 3D constructs that present saccharides at different densities. Chapter 7 describes the investigation of the antibacterial property of the cationic glycopolymer synthesized in Chapter 4. Chapter 8 describes the investigation of using the cationic glycopolymer synthesized in Chapter 4 as a transfection agent.

Chapter 8 gives the conclusions drawn from this dissertation along with potential directions leading from this body of work.

CHAPTER 2

Background

Polysaccharides, peptides, and nucleic acids comprise the three main classes of biopolymers found in nature. Historically, polysaccharides have been considered an energy source or for structural support, which in turn are useful to humans as food, clothing, and paper. With more recent discoveries and development of analytical techniques, the role of polysaccharides in cell signaling, pathogen recognition, and disease states have been better understood allowing the design of improved biomedical treatments.[27–29] Polysaccharides isolated for biomedical purposes were initially derived from natural sources. For example, heparin, originally isolated from dog liver[30,31] and more contemporarily from the mucosal tissue of meat animals, is one of the oldest carbohydrate drugs still in widespread clinical use as an anticoagulant.[32]

Natural polysaccharides, however, suffer from a number of short-comings, such as limited supply of source organisms, lack of control over molecular weight, and difficulty of purification, which lead to batch-to-batch variations. In 2008, Baxter Healthcare Corporation recalled nine lots of heparin linked to over 200 deaths in the United States.[33] Such instances exemplify the need for synthetic alternatives to naturally-derived polysaccharide therapeutics. Two approaches have been taken to create synthetic alternatives: synthetic polysaccharides (synthetic duplicates of their natural counterparts) and glycomimetics (synthetic polymers that present saccharide side groups endeavoring to replicate the effects of natural polysaccharides).

2.1. Synthetic polysaccharides

Synthetic polysaccharides are produced through the successive formation of glycosidic bonds between the anomeric carbon of a glycosyl donor and one of the hydroxyl groups of a glycosyl acceptor.[3] A number of challenges, however, frustrate the creation of synthetic polysaccharides. First, both the glycosyl donor and acceptor are inherently unreactive, so anomeric activation is typically necessary on the glycosyl donor (Scheme 2.1a). Additionally, the bioactivity of the polysaccharide is affected by the stereoselectivity of the glycosyl linkage (α versus β) and thus needs to be carefully controlled (Scheme 2.1b). Finally, the regioselectivity of the linkage also affects bioactivity, so extensive protection/deprotection strategies are required to ensure the appropriate glycosidic linkages are formed. Two strategies for polysaccharides synthesis are typically employed: enzymatic or chemical.

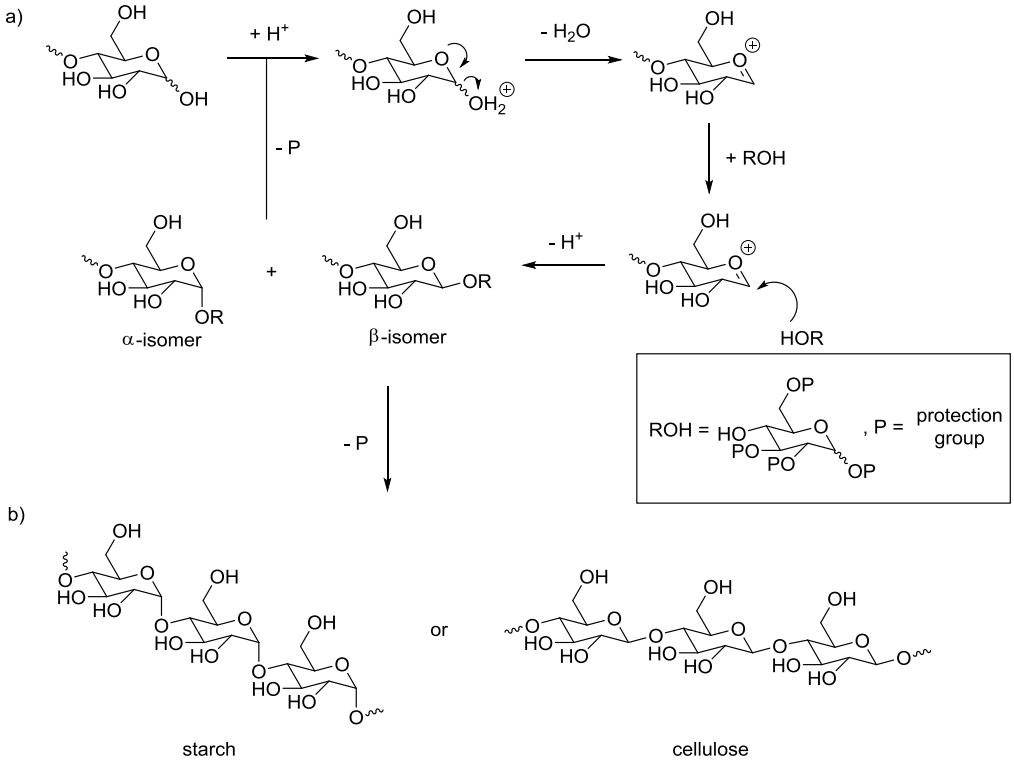

Scheme 2.1. Synthesis of synthetic polysaccharide with a) glycosyl donor activation and b) resultant polysaccharide with different bioactivity based on stereoselectivity of the glycosidic linkage.

2.1.1. Enzymatic synthesis

In order to mimic how polysaccharides are naturally constructed, enzymes can be isolated or engineered to form specific glycosidic linkages. In general, these enzymes fall into two categories: glycosyltransferases and glycosidases.[34] Glycosyltransferases utilize nucleotide sugars and glycosyl phosphates as glycosyl donors, the sugar that provides the anomeric alcohol in the glycosidic bond, to add saccharides to a growing saccharide chain.[35,36] Using glycosyltransferases, multivalent polysaccharides can be made.[37] For example, Loos has created hyperbranched polysaccharides off of a modified silicon substrate, an amine functionalized poly(ethylene glycol) macro primer, and a tri-functional tris(2-aminoethyl)amine primer using potato phosphorylase and *Deinococcus geothermalis* branching enzyme.[38,39] Although the use of glycosyltransferases result in high yields and selectivity, the glycosyl donors and enzymes are difficult to acquire.

Glycosidases, which typically hydrolyze polysaccharides, can be used to form glycosidic linkages with an alcohol that is a more efficient nucleophile than water. While both the enzymes and glycosyl donors are relatively inexpensive, reactions that utilize glycosidases are typically low yielding and lack regioselectivity, in spite of maintaining absolute stereoselectivity.[40] In order to form glycosidic bonds using glycosidases, typically thermodynamic or kinetic controls are used. In thermodynamically controlled reactions, an excess of starting materials or increased temperature is used to bias the reaction towards the glycoside product. In kinetically controlled reactions, an activated glycosyl donor is used to favor transfer of itself over water to another sugar. Kinetically controlled reactions, however, need to be carefully monitored and quenched before hydrolysis predominates, but still only produce yields of 10-40%.[40,41] In order to further increase yields, glycosidases have been mutated to allow the formation glycosidic bonds, but not

the hydrolysis of bonds.[42] Although these engineered mutated glycosidases achieve higher yields, the saccharide identity is specific to each enzyme and polysaccharides exceeding 100 repeat units are difficult to attain.[43]

2.1.2. Chemical synthesis

The creation of synthetic polysaccharides via chemical synthesis relies on the anomeric activation of the glycosyl donor and the use of appropriate protecting groups to direct the formation of the desired glycosidic bond.[44] Common glycosyl donor anomeric leaving groups include glycosyl halides,[45,46] glycosyl acetate, thioglycosides,[47] glycosyl trichloroacetimidate,[48] and *n*-pentenyl glycoside.[49] The reactivity of the leaving groups is often further catalyzed by the use of activating agents, usually a Lewis acid such as boron trifluoride or triflic acid which forms an oxocarbenium ion intermediate. The reactivity of the anomeric leaving group can further be affected by the protecting group on the other carbons of the sugar. For example, Mootoo *et al.* reported that a benzyl protected sugar was more reactive as a glycosyl donor compared to an acetyl protected sugar, preventing self-glycosylation of the acetyl protected sugar.[49] This strategy of preferential reactivity using selective protecting groups was termed the armed/disarmed approach, with the intended glycosyl donor protected with arming groups and the intended glycosyl acceptor protected with disarming groups.

In addition to reactivity, the protecting groups can also direct the stereoselectivity and regioselectivity of the glycosidic bond being formed. For example, when an acetyl group is used to protect the alcohol at C-2, an acetoxonium ion is formed which only permits a *trans*-side attack by the glycosyl acceptor.[50] For saccharides with the C-2 alcohol in the equatorial position, such as glucose and galactose, this means that only β linkages are formed, whereas saccharides with the C-2 alcohol in the axial position, such as mannose, only α linkages are formed (Scheme

2.2). When an inert protecting group, such as a benzyl, is used on the alcohol at C-2, the anomeric effect typically dominates, and α linkages are formed.[51]

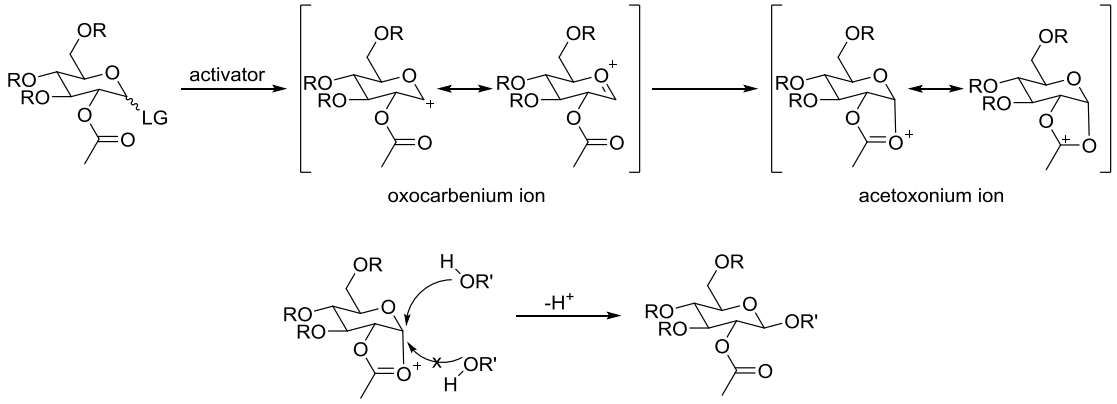

Scheme 2.2. Stereoselectivity using an acetate protecting group at the C-2 alcohol.

In regards to regioselectivity, selective protecting groups are used to block all other free alcohols on the glycosyl acceptor while leaving the alcohol of interest available for glycosylation. For example, the alcohol on C-6 can be selected for glycosylation through protection with triphenylmethyl chloride, protection of all other alcohols with acetic anhydride, and deprotection with hydrobromic acid (Scheme 2.3).[52] Alternatively, the alcohol on C-4 of glucose can be selected for glycosylation by selective protection with benzaldehyde dimethyl acetal, protection of the remaining alcohols with benzyl bromide, and subsequent deprotection with triethylsilane and trifluoroacetic acid (Scheme 2.3).[53,54]

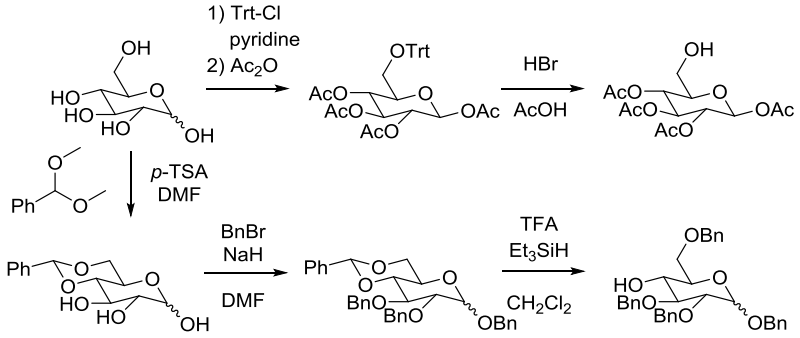

Scheme 2.3. Synthesis of β-D-glucose-1,2,3,4-tetraacetate and benzyl 2,3,6-tri-*O*-benzyl-D-glycopyranoside.

As each saccharide is added to a growing polysaccharide chain, a tedious process of protection and deprotection and purification must be employed. In order to facilitate synthesis of polysaccharides in a more efficient manner, solid-phase synthesis techniques have been employed.[55] Seeberger introduced the first automated solid-phase oligosaccharide synthesizer which utilized an adapted peptide synthesizer with glycosyl phosphate and trichloroacetimidate donors and acceptors either protected with benzyl ethers (deprotected at the end of synthesis) or esters (deprotected before the addition of each additional saccharide).[6,56] Using this technique, a variety of oligosaccharides have been made, including an α-(1,6)-oligomannoside of 30 units[57] and oligosaccharides with complex control of regioselectivity including branching.[58,59] Using a column packed with resin-bound glycosyl acceptor, Stine and Demchenko have also used a standard high-performance liquid chromatography setup to flow solutions of glycosyl donors and activating agents to produce oligosaccharides.[60] This method has the additional advantage of using the in-line UV detector to monitor the consumption of glycosyl donors to determine reaction completion.

Although solid-phase synthesis techniques are attractive due to automation and ease of purification, the reaction is often inefficient due to the insolubility of the resin, requiring multiple repetitions of reaction steps to obtain high yields. Alternatively, techniques (e.g. fluorous-tagging,[4,5,61–65] polymer-support,[66–74] and ionic liquid support[75–80]) have been developed that allow for coupling reactions to occur in solution while purification is conducted using solid-phase techniques. While these alternative techniques afford higher reaction efficiencies and conserves reagents, a number of issues continue to frustrate the widespread use of these techniques (e.g. expensive supports, difficulties with automation, and issues with solubility, especially as the oligosaccharide becomes longer).

2.2. Glycomimetics

In light of the frustrations of isolating or creating polysaccharides, the field of glycomimetics seeks to create synthetic polymers at a lower cost, at a higher molecular weight, or in larger batches while still retaining at least the biological activity exhibited by natural polysaccharides. Unlike polysaccharides that are connected by glycosidic bonds, glycomimetics typically refers to multivalent saccharide-containing polymers that are connected with a synthetic backbone. While abandoning the specific connectivity through glycosidic bonds allows for more flexibility in synthetic design, the biological effect of such a modification is largely unknown.

2.2.1. Considerations in glycomimetic design

As glycomimetics deviate from being an exact replicate of natural polysaccharides, it is important to consider the critical attributes that may affect the functionality of the glycomimetics. The functionality of saccharide-containing molecules is most often evaluated using lectins, the natural binding receptor found on the surface of cells primarily utilized in cell recognition.[81,82] The specificity of lectins comes from the conformation and sequence of the binding site, so that even small amino acid substitutions can have large effects on binding specificity.[83] In designing glycomimetics, typically the following attributes are considered: saccharide identity, length of connectivity, and architecture of the polymer backbone.

2.2.1.1. Saccharide identity

Due to the stereospecificity of lectins, the saccharide identity must be carefully considered.[84] For example, Concanavalin A (ConA),[85,86] one of the first isolated lectins, binds non-reducing terminal α-D-glucose and α-D-mannose, which differ only in the orientation of the hydroxyl functionality on C-2.[87] On the other hand, *Ricinus communis* (castor bean) agglutinin 120 (RCA_{120}) only binds non-reducing terminal β-D-galactose with key interactions with the alcohol

groups at C-2, C-3, and C-4, while modification at C-6 has even exhibited enhanced activity with RCA_{120}.[88,89] In addition, Sakushima has underscored the importance of ring-closed saccharides in maintaining lectin bioactivity.[90]

2.2.1.2. Connectivity and architecture

In addition to saccharide identity, polymer length and architecture has also been observed to play a significant role in saccharide-lectin interactions. In general, increased molecular weights and increased branching enhances lectin interactions.[19,91–93] The enhancement in interaction is attributed to the lectin having multiple carbohydrate recognition domains. For example, ConA has four binding sites, one from each of its subunits,[94] and RCA_{120} is composed of two subunits, each with a carbohydrate recognition domain.[95,96] Multiple carbohydrate recognition domains not only facilitate cellular crosslinking and lectin precipitation, but also allow each lectin to bind multiple saccharides on the same polymer when properly spaced, increasing its avidity. In a binding study of rabbit hepatocytes, divalent oligosaccharides exhibited dissociation constants ranging from 1-40 μM, while trivalent oligosaccharides ranged from 10-100 nM.[97] Lee *et al.* also has reported that an oligosaccharide with three branches presented a 1000-fold increase in binding to hepatic lectin even though it contained only three times as much galactose compared to a similar linear oligosaccharide.[98] The increased interaction due to clusters of saccharides has been termed "the cluster glycoside effect."[91,99]

2.2.2. Glycomimetic synthesis

The design of glycomimetics typically falls into three categories: glycodendrimers, glycoclusters, and glycopolymers (Figure 2.1).[8] Glycodendrimers are of the most complex and difficult to synthesize, but maintain the highest level of saccharide density, fully harnessing the cluster glycoside effect. Glycoclusters utilize small dendritic units to activate the cluster

glycoside effect, allowing more flexibility in synthetic design, but sacrifice the high saccharide density of glycodendrimers. Glycopolymers are typically linear multivalent polymers that present saccharide units as side groups, which activate the cluster glycoside effect due to the high degree of valency presented. Glycopolymers offer a method for facile creation of high molecular weight glycomimetics, but often lack homogeneity and the branched structure offered by glycodendrimers and glycoclusters.

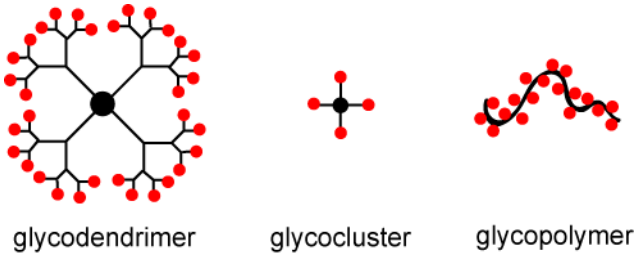

Figure 2.1. Common glycomimetic structures with red circles representing saccharide units.

2.2.2.1. Glycodendrimers and glycoclusters

Glycodendrimers utilize a synthetic dendritic core to display a densely packed saccharide periphery for biological interaction much like the glycocalyx of eukaryotic cells. The dendritic core is created via iterative steps in which a new branch point is added to every terminus. As the dendrimer grows, the molecule becomes increasingly spherical, at which point, molecules can be attached to the periphery of the molecule. As the dendrimer grows, however, termini density increases to the point where steric hindrance prevents high saccharides conjugation efficiency. For example, while up to a generation 2 poly(amidoamine) dendrimer can be fully functionalized with sugar, conjugation efficiency declines to 67% with a generation six dendrimer which would ideally have 256 saccharide residues attached.[100] Some glycodendrimers have been constructed entirely of saccharide units, but are subject to the same drawbacks as synthetic polysaccharides.[101,102] Although glycodendrimers can be used to create nano-sized particles, the

difficulties of creating high molecular weight dendrimers and the limited conjugation efficiency continue to frustrate their potential of being effective glycomimetics.

Glycoclusters are glycomimetics that consist of a small synthetic unit with two to five saccharides attached, typically as an early generation dendrimer.[91] These glycoclusters can be used independently,[103,104] attached to a synthetic core,[105] or polymerized together.[106] Although glycoclusters afford more flexibility in synthetic design compared to dendrimers, they are still limited to low molecular weights due to steric hindrance as with dendrimers. Glycopolymers, consisting of a synthetic backbone with saccharide side groups, have been used as an alternative to produce glycomimetics with control over molecular weight and saccharide identity.[7,8]

2.2.2.2. Glycopolymers

Glycopolymers are primarily created using two methods: post-polymerization conjugation of saccharide groups to a preformed synthetic backbone and direct polymerization of sugar-containing monomers (Scheme 2.4). Using the post-polymerization conjugation method, a synthetic polymer can be created using a variety of techniques without being limited by potential side reactions and the solubility of the saccharide moiety. This method is particularly useful when saccharide identity is varied and an identical polymer architecture is desired or when incorporating saccharides that are incompatible with polymerizations conditions. Due to steric hindrance, however, it is difficult to obtain quantitative conjugation of saccharides to the backbone.[8] The direct polymerization method requires the creation of glycomonomers, which are often created through a tedious series of protection/deprotection reactions, but produces well-defined polymer with saccharide moieties present on every repeat unit.

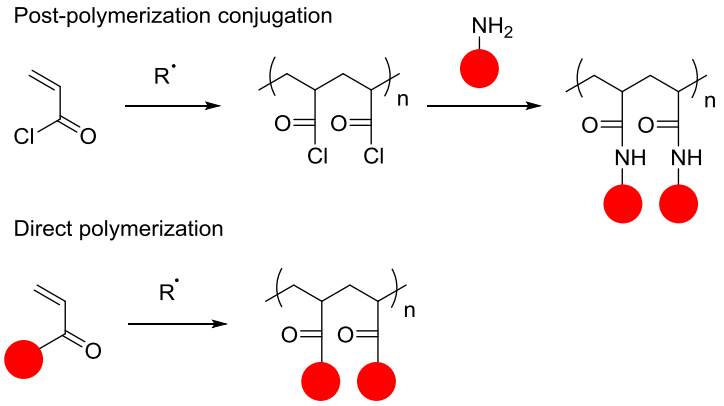

Scheme 2.4. Synthetic scheme demonstrating the difference between post-polymerization conjugation and direct polymerization.

2.2.2.2.1. Post-polymerization conjugation

Saccharides have been conjugated to polymers made through a variety of polymerizations techniques (e.g. free-radical polymerization, anionic polymerization, and ring-opening polymerization) bearing a variety of reactive handles (e.g. activated esters, pyridyl disulfides, alkenes, and alkynes).[107] Amino-sugars are convenient for post-polymerization conjugation, since the amine is more nucleophilic compared to the alcohols. Using commercially available glucosamine and galactosamine, Kodama attached each sugar to a poly(acryloyl chloride) polymer.[108] When compared to similar polymers made via direct polymerization, the glucosamine and galactosamine moieties achieved a conjugation efficiency of only 53.2% and 41.6%, respectively. When using less reactive polymer side chains, activation may be required to achieve high conjugation efficiencies. Using EDC/NHS, glucosamine was conjugated to a polymer with carboxylic acid side chains with an efficiency of 85%.[109] In another instance, poly(vinyl alcohol) was activated with 4-nitrophenyl chloroformate and achieved virtually quantitative conjugation of glucosamine.[110] The resulting polymer showed activity with Concanavalin A (Con A), a glucose-binding lectin.

In addition to amines, thiols[111–115] and azides[116,117] can be synthetically added to saccharides for conjugation to polymers bearing pyridyl disulfides, alkenes, and alkynes. The pyridyl

disulfide group allows for facile quantification of conjugation efficiency though the release of pyridyl-2-thione which absorbs 343 nm light. While polymers with pyridyl disulfide side groups have been synthesized,[118] conjugation efficiency of saccharide moieties have been limited to less than 60%.[119] The conjugation of thiols to alkenes and azides to alkynes is particularly attractive due to the reactions: 1) being modular and wide in scope, 2) being highly efficient, 3) generating inoffensive or no byproducts, 4) being stereospecific, 5) using readily available starting materials, 6) using benign or no solvent, and 7) requiring simple purification techniques.[120] Zhang has quantitatively conjugated 2-mercaptoethyl-β-D-glucoside to a poly(allyl glycidyl ether) backbone using free-radical addition as verified via the disappearance of the alkene protons in ^{1}H NMR.[121] Conjugating azide-containing saccharides to polymers with alkyne side groups using the Cu(I)-catalyzed Huisgen 1,3-cycloaddition, Haddleton[122] and Perrier[24] have created glycopolymers with various architectures. While post-polymerization modification has progressed to obtain high conjugation efficiency through the use of small, highly specific linkers, the use of these linkers increases the distance of the saccharide from the backbone and introduces additional functional groups not found in natural polysaccharide (e.g. triazole rings), moving further away from the compact attribute of natural polysaccharides.

2.2.2.2.2. Direct polymerization

Glycopolymers can also be synthesized through the direct polymerization of glycomonomers, ensuring the presence of a saccharide moiety on every repeat unit. Beginning in 1985,[123] glycopolymers have been created through a number of polymerization techniques including free-radical polymerization, cationic polymerization, anionic polymerization, ring-opening polymerization, and ring-opening metathesis polymerization.[8,9,124] Free-radical polymerization

continues to be a prevailing method for creating glycopolymers due to its tolerance for impurities and flexibility for different initiators, monomers, and solvents.

Due to the influence of regioselectivity and stereoselectivity on biological interactions, protection/deprotection techniques developed for synthetic polysaccharides are adapted to control the attachment of polymerizable groups. Enzymatic techniques are typically utilized in two approaches: conjugation of a polymerizable group containing a free alcohol in a glycosidic bond[125] or the selective removal of a protecting group to expose a single alcohol for attachment of a polymerizable group.[126] The removal of a single acetate protecting group typically occurs at C-6, but other alcohols can be made available through acyl migration under appropriate chemical conditions (e.g. pH 8.5-9.5 at 4 °C).[127] Enzymatic techniques, however, are limited by the specificity and cost of the enzyme.

Chemical techniques, conversely, are often scalable and offer more versatility in saccharide identity. Applying the techniques utilized in the chemical synthesis of polysaccharides, polymerizable groups can be attached through the reaction of a free alcohol at the anomeric position or the conjugation of a polymerizable group to a free alcohol obtained through protecting group selectivity (Scheme 2.5). The Zentel group[128] and Ratner group[129] have separately applied a similar synthetic scheme to four saccharides (glucose, mannose, galactose, and *N*-acetyl glucosamine) and attached a polymerizable group with a free alcohol (2-hydroxyethyl methacrylate) to the anomeric position of each saccharide. Likewise, selective protection and deprotection of the primary alcohol at C-6 using a trityl group[52,130] has been used to attach a polymerizable group irrespective of saccharide identity.[19,131]

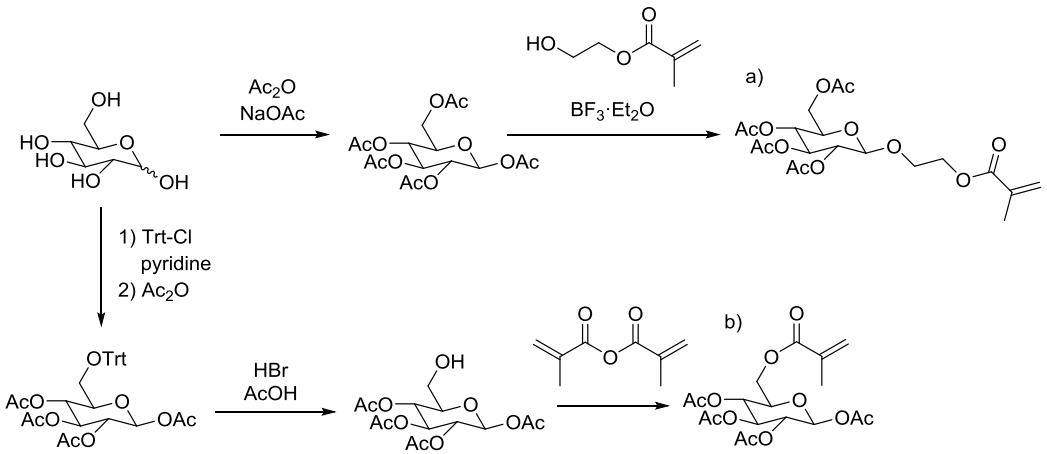

Scheme 2.5. Synthesis of a) 2-*O*-(2,3,4,6-tetraacetyl-β-D-glucosyl)hydroxyethyl methacrylate (polymerizable group attached to the anomeric position) and b) methacryloyl-1,2,3,4-tetraacetate-β-D-glucose (polymerizable group attached to C-6).

Glycomonomers with protected alcohols allow for the polymerization of glycopolymers in organic solvents and with hydrophobic components (e.g. comonomers and initiators).[132–135] Post-polymerization deprotection of these glycopolymers, however, can be non-uniform with partial deprotection or result in cleavage of the saccharide group.[136] In comparing two glycopolymers, one constructed from a deprotected glycomonomer and the other deprotected post-polymerization (Scheme 2.6), Ambrosi observed a fivefold reduction in the binding constant and a sevenfold reduction in interaction with lectin peanut agglutinin for the glycopolymer deprotected post-polymerization.[137]

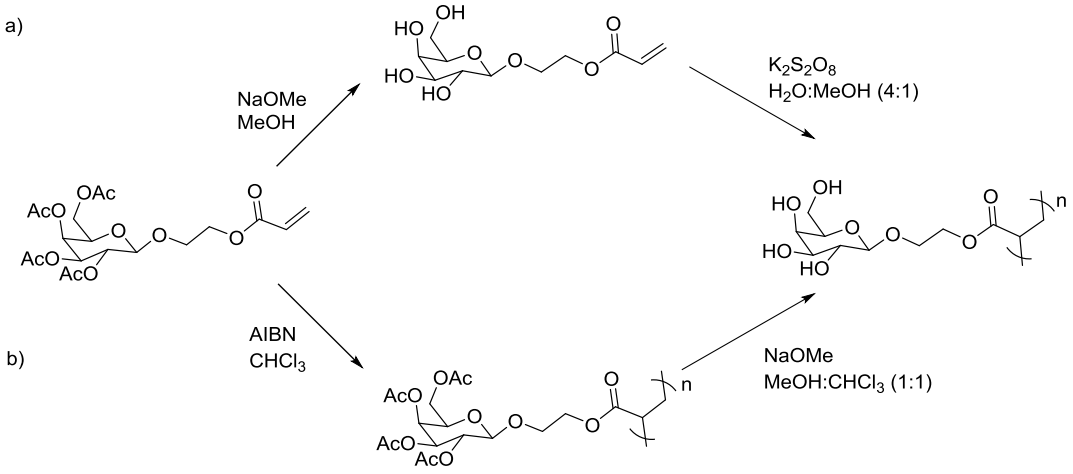

Scheme 2.6. Deprotection of alcohol protecting groups a) prior to polymerization and b) post-polymerization.[137]

2.3. Free-radical polymerization (FRP)

Free-radical polymerization (FRP) is a powerful tool for creating high molecular weight polymers due to its tolerance for impurities and flexibility for different initiators, monomers, and solvents.[138] Initiators for FRP need to be relatively stable under ambient conditions and are categorized into three classes: thermal, photochemical, and redox. Thermal initiators are the most commonly used and consist primarily of peroxides (e.g. benzoyl peroxide) and azo compounds (e.g. 2,2'-azobisisobutyronitrile and 4,4'-azobis(4-cyanovaleric acid)), which produce radicals between 50-100 °C. Monomers for FRP contain a polymerizable vinyl group. Acrylates and methacrylates are particularly useful due to their ease of attachment to amine and alcohol moieties. FRP has been conducted in a wide variety of solvents, ranging from nonpolar solvents (e.g. toluene) to polar, protic solvents (e.g. water).

The process of FRP consists of three stages: initiation, propagation, and termination (Scheme 2.7). During initiation, radicals are formed from the initiator, attached to a monomer, and transferred through the vinyl group. From this initiating species, the polymer begins to propagate to include more monomer until the chain is terminated. Termination can occur in two fashions: 1) the combination of two propagating polymer chains or 2) disproportionation where a hydrogen atom from one polymer chain is abstracted to another, producing one saturated and one unsaturated chain end. In addition, propagating polymers can terminate by chain transfer where the radical is transferred to another species (i.e. solvent, monomer, initiator, or polymer), which can continue to propagate. When chain transfer occurs with a polymer, a branched point is produced.

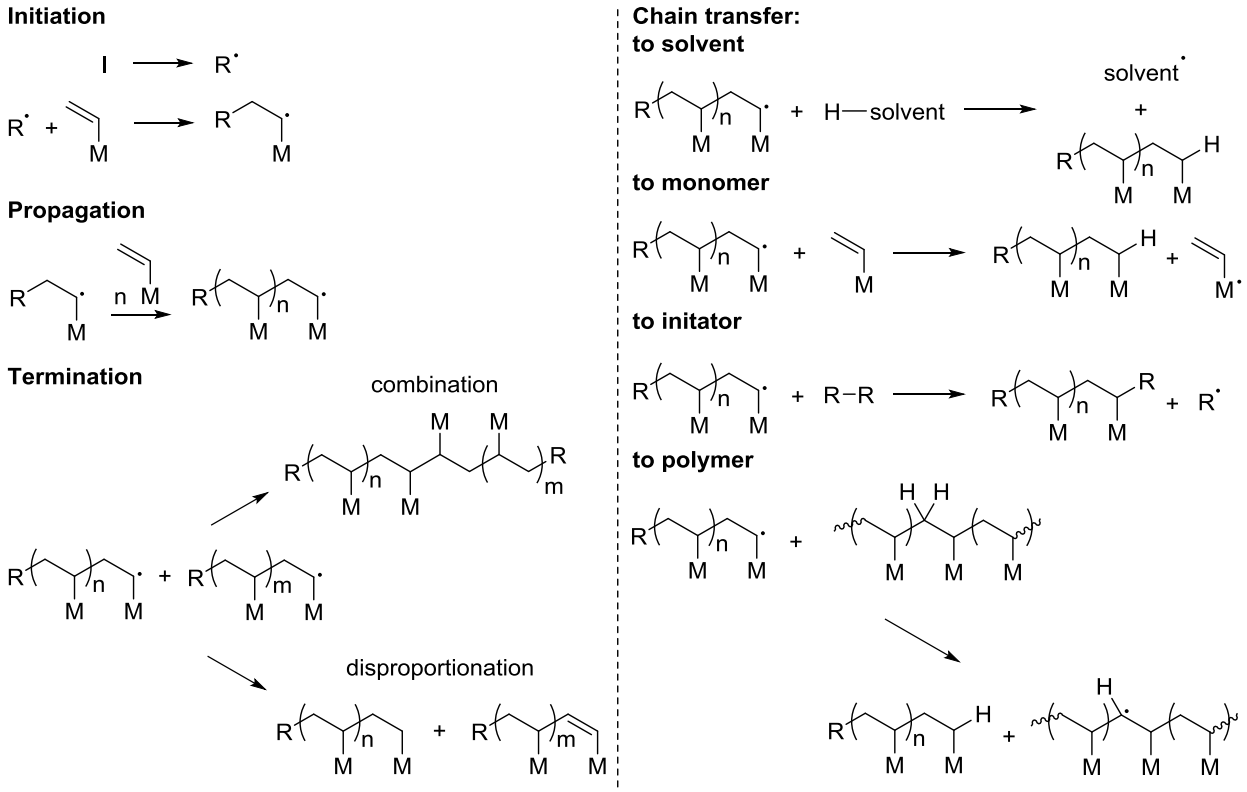

Scheme 2.7. Mechanism of free-radical polymerization.

2.3.1. Molecular weight distribution

The molecular weight of the polymer depends on the model of termination (combination, disproportionation, or chain transfer), the concentration of monomer and initiator, and the rates of propagation and termination. Some of these parameters vary throughout the polymerization and produce a distribution of molecular weights. The number average molecular weight (M_n) is the summation of the product of the number of chains in each i^{th} mass (N_i) and their mass (M_i) divided by the total number of chains (Equation 2.1) and the weight average molecular weight (M_w) is the summation of the product of N_i and M_i squared divided by the summation of the product of N_i and M_i (Equation 2.2). The polymer distribution is described by the dispersity ($Đ = M_w/M_n$). For polymers that terminated by combination or disproportionation, the dispersity is 1.5 or 2.0, respectively. When polymerizations are taken to high conversion, however, the concentration of initiator decreases much faster than the concentration of monomer, and the

dispersity can broaden to 2-5. When branched polymers are created via chain transfer to polymer, the dispersity can increase to as high as 20-50. Highly disperse polymer samples are not ideal, since differences in molecular weight can exhibit different polymer properties.

$$\bar{M}_n = \frac{\sum_i N_i M_i}{\sum_i N_i} \qquad \text{Equation 2.1}$$

$$\bar{M}_w = \frac{\sum_i N_i {M_i}^2}{\sum_i N_i M_i} \qquad \text{Equation 2.2}$$

In order to limit dispersity, controlled radical polymerization techniques have been developed. Controlled radical polymerization techniques, such as nitroxide-mediated polymerization (NMP),[139] atom transfer radical polymerization (ATRP),[140] and reversible addition-fragmentation chain transfer (RAFT) polymerization,[21] prevent termination and chain transfer by limiting the number of actively propagating chains at any given time. RAFT polymerization is particularly useful due to its tolerance for a wide range of reaction conditions and functionalities, in particular aqueous media and biomolecules.[11,141]

2.3.2. Reversible addition-fragmentation chain transfer (RAFT) polymerization

RAFT polymerization (Scheme 2.8) uses typical initiators, monomers, and solvents for free-radical polymerizations, but adds a chain transfer agent (CTA). RAFT CTAs are often composed of a thiocarbonylthio unit attached to an electron rich stabilizing group (referred to as the Z group) and a polymerization reinitiator (referred to as the R group). Throughout polymerization, the CTA maintains the majority of radicals in a dormant adduct intermediate. This limits the number of actively propagating chains avoiding premature termination, which produces less disperse samples.

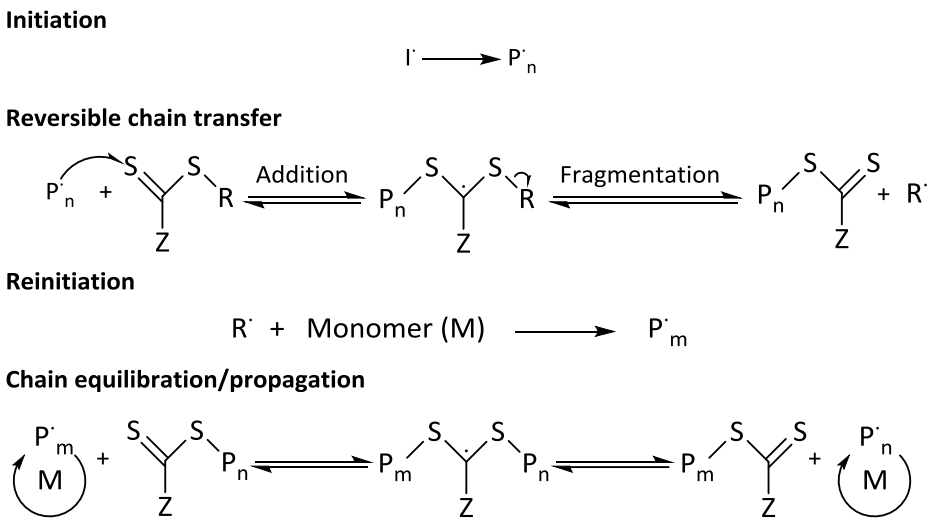

Scheme 2.8. Mechanism of reversible addition-fragmentation chain transfer polymerization.

2.3.2.1. Chain transfer agent synthesis

Due to the reliance of the RAFT polymerization technique on the CTA, a large amount of effort has been dedicated to the design of RAFT CTAs. In RAFT CTA design, careful consideration must be given to the selection of a proper Z group and R group. For controlled polymerization in RAFT, the rate of transfer to the adduct intermediate should be much greater than the rate of propagation, which is evaluated as the transfer coefficient ($C_{tr} = k_{tr}/k_p$, where k_{tr} is the rate of transfer to the adduct and k_p is the rate of propagation). Varying the Z group, which interacts with the carbon-sulfur double bond, allows for modification of the rate of addition of propagating radicals to form the dormant adduct intermediate and the rate of fragmentation from the dormant adduct intermediate to continue as a propagating polymer chain. In general, RAFT CTAs that contain dithioesters (e.g. dithiobenzoate) or trithiocarbonates have high transfer coefficients and are excellent RAFT CTAs, whereas RAFT CTAs with a lone pair of electrons on an oxygen or nitrogen adjacent to the thiocarbonyl have low transfer coefficients and are poor RAFT CTAs.[142] In addition, not only must the R group be a good homolytic leaving group

relative to a propagating polymer chain, so that fragmentation can readily occur, but it must also be capable of reinitiating polymerization effectively upon fragmentation.[143]

RAFT CTAs are generally synthesized through seven methods (Scheme 2.9): 1) thioacylation reactions, 2) thiation of a carboxylic acid or ester, 3) thiol exchange, 4) addition of a dithioic acid across an olefinic double bond, 5) radical-induced R-group exchange, 6) radical substitution of a bis(thioacyl) disulfide, 7) reaction of a carbodithioate salt with an alkylating agent.[144]

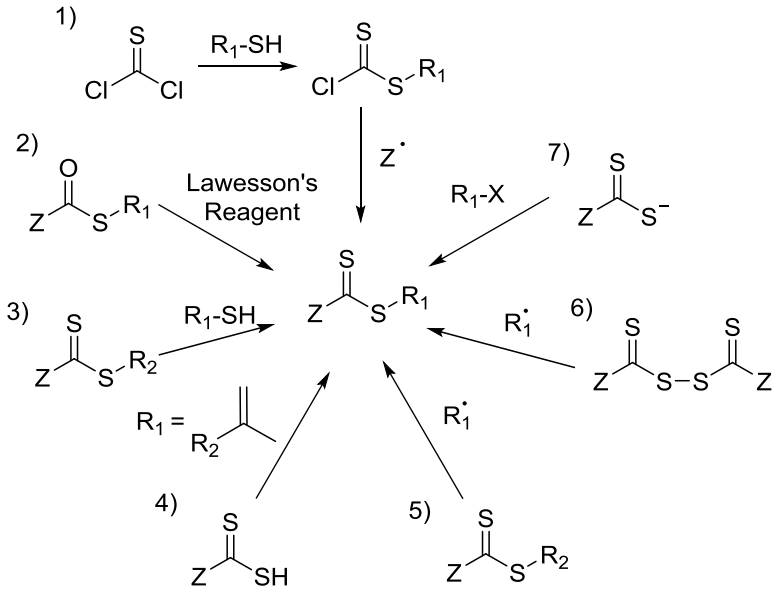

Scheme 2.9. Methods of creating RAFT chain transfer agents via 1) thioacylation reactions, 2) thiation of a carboxylic acid or ester, 3) thiol exchange, 4) addition of a dithioic acid across an olefinic double bond, 5) radical-induced R-group exchange, 6) radical substitution of a bis(thioacyl) disulfide, 7) reaction of a carbodithioate salt with an alkylating agent.

Creation of a RAFT CTA using a radical substitution of a bis(thioacyl) disulfide was reported shortly after the development of RAFT polymerization.[145] This method affords a facile way to create a RAFT CTA bearing an appropriate R group and ensuring that all polymer chains are initiated with the same end group by using the intended radical polymerization initiator in the creation of the RAFT CTA. It is also a convenient method for converting ATRP initiators and polymers into RAFT CTAs.[146] Alternatively, thiocarbonylthio RAFT CTAs are also frequently created utilizing a nucleophilic substitution of a carbodithioate salt (produced via the reaction of

a Grignard reagent with carbon disulfide) to an alkylating agent under milder conditions (e.g. lower temperatures).

2.3.2.2. End group modification

The RAFT CTA chain end has often been associated with increased cytotoxicity[147] and is often removed or modified into useful functional groups for conjugation. A number of end group modifications are available post-polymerizations (Scheme 2.10): nucleophilic substitution at the thiocarbonyl to produce a thiol end group; radical induced oxidation, reduction, and coupling; thermolysis to form an unsaturated chain end; and chain-extension of the polymer through reinitiation or conversion to another form of controlled radical polymerization initiator (ATRP and NMP). Nucleophilic substitution to form a thiol end group is particularly useful for post-polymerization conjugation (e.g. disulfide formation, maleimide conjugation, thiol-acrylate Michael addition, and thiol-ene click reaction) or substrate attachment (e.g. thiol-gold interaction).

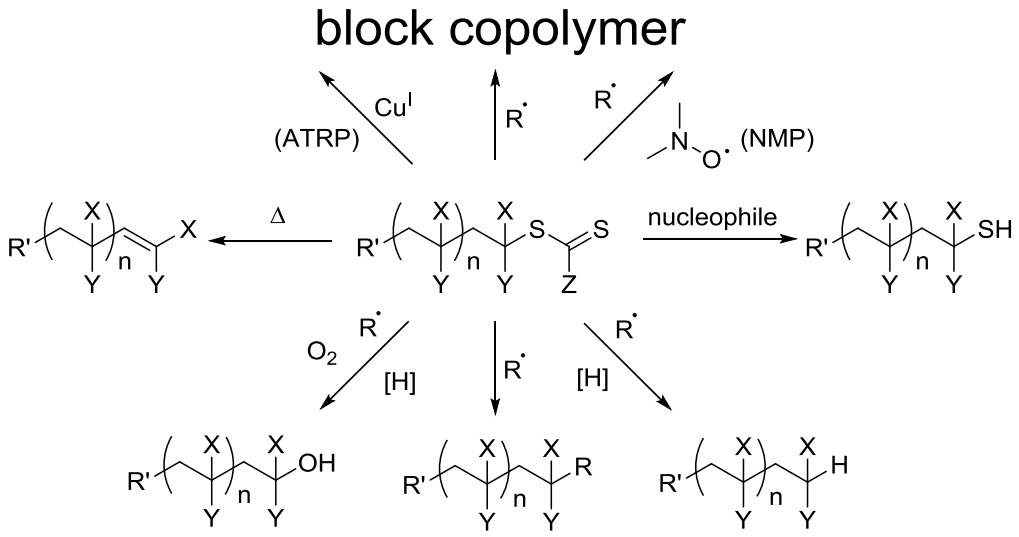

Scheme 2.10. End group modification of RAFT polymers.

2.3.2.3. Glycopolymers via RAFT polymerization

Combining the ease of synthesis and purification of glycomonomers over natural polysaccharides and the control and versatility offered by RAFT polymerization, synthetic glycopolymers can be created with control over monomer identity and connectivity. Glycopolymers can be formed using deprotected glycomonomers or using protected glycomonomers followed by a deprotection step. Forming polymers using deprotected glycomonomers is ideal for ensuring saccharide incorporation which might otherwise be lost due to hydrolysis during removal of the protecting groups. In cases of copolymerization or conjugation with water-insoluble molecules, however, glycopolymers have been formed using protected glycopolymers. When protected glycopolymers are formed, the acid-labile isopropylidene protecting group is often used, which can be deprotected under mild acidic conditions, limiting hydrolysis of other esters.

The first example of a glycopolymer created by RAFT polymerization was by the McCormick group in 2003, which polymerized 2-methacryloxyethyl glucoside using 4-cyano-4-(thiobenzoylthio)pentanoic acid as a chain transfer agent and 4,4′-azobis(4-cyanovaleric acid) as an initiator in a basic aqueous solution necessary for solubility (Scheme 2.11).[148] Since RAFT polymerization was developed following other controlled polymerization techniques, even in this first investigation, the glycomonomer was polymerized in a deprotected form, and the chain was extended by reinitiation to create a block copolymer of 2-methacryloxyethyl glucoside and 3-sulfopropyl methacrylate. While pseudo-first-order kinetics and the ability to reinitiate the chain end are indicative of control polymerization, the order in which the blocks were created affected the dispersity of the resultant copolymer. When poly(2-methacryloxyethyl glucoside) was used as a macro-CTA, the resultant copolymer had a dispersity of 1.63, and when

poly(3-sulfopropyl methacrylate) was used as a macro-CTA, the resultant copolymer had a disperisty of 1.18. The Davis group later discovered that the use of basic aqueous solutions in RAFT polymerization led to a loss of control at high conversion which could be circumvented by using a 10% ethanol solution.[149] Since then, many glycopolymers have been created by RAFT polymerization for biomedical applications, but several synthetic tools are still absent that allow for systematic control of highly branched structures and incorporation of charged glycomonomers.[150,151]

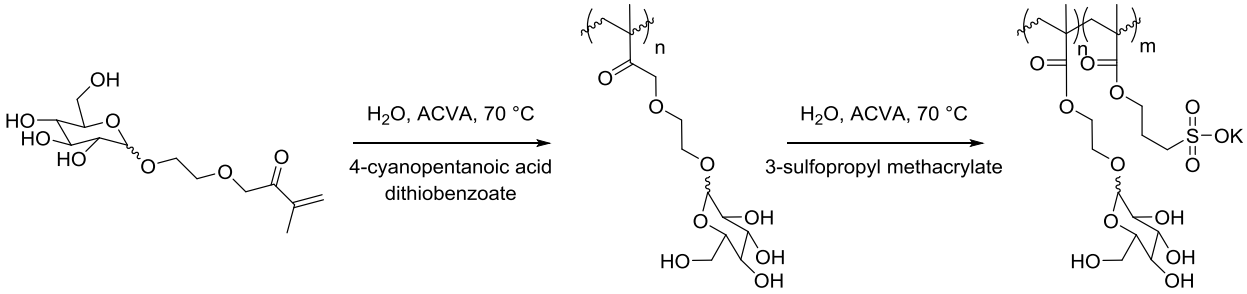

Scheme 2.11. First glycopolymer and block copolymer synthesized via RAFT polymerization by the McCormick group.[148]

2.4. Applications of glycopolymers

As a powerful alternative to natural polysaccharides, glycopolymers have been used in a number of biomedical applications. Some of the current applications include studying bacterial attachment, delivering therapeutics, and investigating cellular interactions.

2.4.1. Bacterial attachment

Bacteria utilize lectins to mediate adhesion to host cells and facilitate infection.[152] This behavior can be utilized for bacterial detection and isolation. The Seeberger group synthesized a mannose-functionalized fluorescent polymer by conjugation of 2-aminoethyl mannoside to poly(*p*-phenylene ethynylene).[153] Addition of the glycopolymer to *E. coli* formed fluorescent aggregates detectable within 15 minutes and with as little at 10,000 bacteria cells, similar to the detection limit of fluorescently labeled antibodies. The Ulbricht group grafted

2-lactobionamidoethyl methacrylate to a polypropylene microfiltration membrane using an entrapped photoinitiator.[154] *E. faecalis*, which has galactose-binding lectin on the cell surface, exhibited a 40-fold enhancement in adhesion compared to an unmodified polypropylene microfiltration membrane, while *S. matolphilia*, which lacks galactose-binding lectin, saw similar adhesion to the unmodified membrane. Utilizing the synthetic techniques of the Narain group, Wang *et al.* synthesized galactose-bearing glycopolymers via RAFT polymerization and immobilized them on a gold-coated 2-D substrate for analysis of the adhesion mechanism of *P. aeruginosa* via quartz crystal microbalance with dissipation.[155] They observed that *P. aeruginosa* in 10 mM $CaCl_2$ exhibited a significantly higher contact point stiffness on the galactose-bearing surfaces compared to *E. coli*, indicating that galactose-binding lectin on the bacterial membrane were involved in adhesion to the surfaces.

2.4.2. Therapeutic delivery

Many therapeutics are limited in their efficacy due to poor solubility, protection from degradation, or specificity of target. Glycopolymers are an attractive solution due to saccharide involvement in cellular recognition within the body and their amplified efficiency due to their multivalency.

2.4.2.1. Bioconjugates

Many polysaccharide-drug conjugates have been created,[156] but polysaccharides have recently been substituted with glycopolymers. The Li group takes advantage of RAFT chain end modification of a glucose glycopolymer to introduce a pyridyl disulfide moiety which is used to conjugate glutathione.[132] Their peptide-glycopolymer bioconjugate exhibited antioxidant activity, clearing 50% of radicals from a solution after 24 hours at 37 °C. The Stenzel group, utilizing the RAFT chain-extension, synthesized a block-glycopolymer and self-assembled it into

micelles presenting auranofin moieties conjugated to glucose on its surface.[157] These micelles displayed high activity as a chemotherapeutic agent against ovarian carcinoma cells. The Stenzel group created a thermosresponsive block copolymer containing poly(acryloyl glucosamine)-block-poly(*N*-isopropylacryamide) via RAFT polymerization.[158] When heated above the lower critical solution temperature (LCST), micelles are formed and stabilized using an acid-sensitive crosslinker incorporated through reinitiation of the RAFT polymerization. While stable at basic and slightly acid pH, the micelles degraded at pH 4 in approximately 12 hours and rapidly degraded at pH 2 within 30 minutes, making it a viable delivery system for selective targeting of carcinoma which tends to create a low pH environment due to high metabolic activity.

In addition, many groups have looked at using saccharides as a ligand to target cell receptors for selective delivery of therapeutics. Suriano *et al*. designed self-assembled micelles presenting different saccharide identities on the surface and demonstrated selectivity of galactose-presenting micelles for asialoglycoprotein receptors (ASGPR) on HepG2 liver cancer cells over HEK293 cells.[159] Doxorubicin (DOX), a common chemotherapeutic, was loaded into the micelles and increased cytotoxicity was observed in HepG2. Furthermore, the Lu group created a degradable and biocompatible aldehyde-functionalized galactose glycopolymer via RAFT polymerization and attached DOX via an acid-labile Schiff base linkage, which allowed for selective delivery in low pH environments.[160] Using hyperbranched galactose-containing glycopolymers created via RAFT polymerization, the Narain group found that galactose glycopolymers are highly hemocompatible (not inducing clot formation, red blood cell aggregation, or immune response).[161]

2.4.2.2. Gene Delivery

Glycopolymers have also been utilized in the delivery of nucleic acids. In order for a polymer to be used as a gene delivery vehicle, it must complex with the genetic material and deliver the payload.[162] One of the most extensively studied synthetic polymers for gene delivery purposes is poly(ethyleneimine) (PEI), due to its ability to avoid lysosomal degradation and complex/release DNA efficiently.[163–165] However, PEI is toxic, has non-specific interactions, and elicits an immune response.[166–168] The toxic effects of PEI are dependent on a number of parameters including molecular weight and branching, which affect charge density.[166,169–173] In general, higher molecular weight[174] and branching[173] are correlated with higher transfection efficiency but also higher cytotoxicity.[167,168] Godbey *et al.* report that cytotoxicity comes primarily from free PEI that interacts with negatively charged biomolecules and perturbs membranes after the release of genetic material.[165,175,176]

To address the toxicity of PEI, many groups have developed PEI-derivatives that seek to maintain transfection efficiency while reducing toxicity.[177–180] The Reineke group saw decreased cytotoxicity while maintaining high transfection efficiency when a ring-opened glucose derivative was used to interspace short oligo-ethylenimines.[181] Shortly afterwards, they expanded the work using other ring-opened sugars and saw particular promise with galactose targeting HepG2 cells.[182] Optimal transfection was observed at a nitrogen/phosphate (N/P) ratio between 20 and 30,[182] while polyplexes with an N/P ratio higher than 40 exhibited significant cytotoxicity.[183] The presence of alcohols from the polysaccharides is believed to assist in strengthening the association of genetic material with the cationic polymer through hydrogen bonding,[184] while longer cationic blocks were seen to prevent the release of genetic material after transfection.[185] With the advantages of using glycopolymers to target ASGPR in mind, Zhang *et*

al. modified polyphosphoramidate polymers with galactose residues and observed decreased cytotoxicity and affinity for galactose-binding lectin.[186] Transfection efficiency, however, also diminished due to decreased DNA-binding capacity and particle stability. The Narain group has utilized RAFT polymerization to make copolymers of cationic monomers (2-amino ethyl methacrylamide or 3-aminopropyl methacrylamide) and a ring-opened glycomonomer (3-gluconamidopropyl methacrylamide) and formed polyplexes with an N/P ratio between 40 to 60 and saw similar gene expression compared to PEI with significantly lower toxicity.[187] In order to utilize the ASGPR on HepG2 cells, they followed with a study using a galactose-containing monomer (2-lactobionamidoethyl methacrylamide) to form hyperbranched copolymers with 2-aminoethyl methacrylamide via RAFT polymerization and achieved efficient transfection of hepatocytes at lower N/P ratios.[188] Since then, many groups have used glycopolymers to mitigate the cytotoxic effects of cationic monomers, such as a L-lysine monomer[135] and a spermine-like monomer,[189] for gene delivery.

2.4.3. Cellular interactions

A dense layer of glycolipids and glycoproteins, the glycocalyx, is often found surrounding cell membranes and is important in recognition by the immune system and in other cell-cell interactions.[190] An intact glycocalyx, for example, is essential in preventing leukocyte adhesion and preventing an inflammatory response.[191] Glycopolymers are an attractive way to coat a surface with saccharide residues and create a layer similar to a glycocalyx for preventing non-specific activity and for investigating interactions with lectins, saccharide-binding proteins. The Ulbricht group created a glycocalyx mimic through surface-initiated atom transfer radical polymerization of D-gluconamindoethyl methacrylate from a surface plasmon resonance chip and showed resistance to non-specific protein adsorption, using bovine serum albumin (BSA),

lysozyme, and fibrinogen as model proteins.[192] The glycopolymer coating prevented up to 99.83% of BSA adsorption and up to 99.97% irreversible adsorption.

Inspired by the properties of mucin, a major constituent of the glycocalyx of mucosal tissue,[193] the Bertozzi group created an α-*N*-acetyl galactosamine glycopolymer to coat carbon nanotubes.[194] Poly(methyl vinyl ketone) was polymerized using a lipophilic radical initiator and α-aminooxy-*N*-acetyl galactosamine was conjugated to the backbone through an oxime bond. These polymers were inserted into carbon nanotubes in order to prevent biofouling. Expanding on this work, glycolipids were created that contained *N*-acetyl galactosamine or *N*-acetyl lactosamine that could be inserted into lipid bilayers[195] and eventually cellular membranes.[196] Using this technique, the Godula group remodeled the plasma membrane of embryonic stem cells deficient in heparin sulfate biosynthesis with a synthetic neoproteoglycan synthesized via RAFT polymerization.[197] The neoproteoglycans assumed the function of the deficient heparin sulfate proteoglycans and sequestered fibroblast growth factor 2 promoting neural differentiation. These glycopolymers provide a powerful tool for understanding the role of glycolipids and glycoproteins in the glycocalyx through direct incorporation into the glycocalyx of live cells.

To further understand the role of polysaccharides in the glycocalyx, nanoparticles and their interaction with lectins have been instrumental. Since cells are three-dimensional constructs, nanoparticles afford a similar presentation of saccharide residues to lectin to better mimic the natural presentation. The Akashi group has seen that even the conjugation of saccharides to the surface of a nanoparticle amplifies the interaction with lectin 100-fold.[198] Utilizing RAFT polymerization, the Miura group conjugated a 2.5 nm layer of glycopolymer onto the surface of gold nanoparticles[199] and the Jiang group created glucose-containing and galactose-containing

nanoparticles utilizing the LCST behavior of conjugated poly(*N*-isopropylacrylamide) blocks to create a glycocalyx mimic.[200]

2.5. Conclusion

Although polysaccharides are ubiquitous in nature, there are only limited tools for examining their roles, especially compared to peptides and nucleic acids. The primary limiting factor is the complexity of synthetic polysaccharide synthesis due to the abundance of alcohols available for modification and the specificity of these modifications in biological activity. In order to create well-defined polysaccharides, an arduous process of selective protection and deprotection must be performed with the addition of each saccharide unit, making the creation of high molecular weight polysaccharides impractical. In order to facilitate the creation of higher molecular saccharide-bearing polymers, glycopolymers can be created via free-radical polymerization and used in a variety of biomedical applications, such as investigating bacterial attachment, therapeutic delivery, and cellular interactions.

In order to develop new glycopolymer tools, the investigations of this dissertation seek to develop new cationic glycomonomers and RAFT branching agents to: 1) create patterned substrates with various glycopolymers for directing bacteria, 2) develop 3D constructs of various saccharide density for investigating cellular interactions with saccharides as naturally presented, and 3) investigate the usage of cationic glycopolymers in biomedical applications.

CHAPTER 3

Synthetic tools for glycopolymer synthesis

3.1. Introduction

Glycopolymer have been synthesized by numerous groups[7–14] and have been used to investigate several structural property relationships, such as monomer identity and chain length,[15–18] but the inclusion of cationic charge and branching is still not fully understood with few examples reported.

3.1.1. Cationic charge

Naturally-derived cationic polymers are limited to gelatin and chitosan. Gelatin is a protein obtained for chemical denaturation of collagen, and chitosan is a polysaccharide consisting of β-(1,4)-linked-D-glucosamine obtained from the alkaline deacetylation of chitin (Figure 3.1). Chitin is commonly isolated from the exoskeleton of insects and crustaceans or the cell wall of fungi.[201] Upon deacetylation, the amines can adopt a cationic charge at low pH increasing the solubility of the polysaccharide. Due to its biocompatible, biodegradable, and cationic properties, chitosan has been used in a variety of applications including food, medicine, and cosmetics.

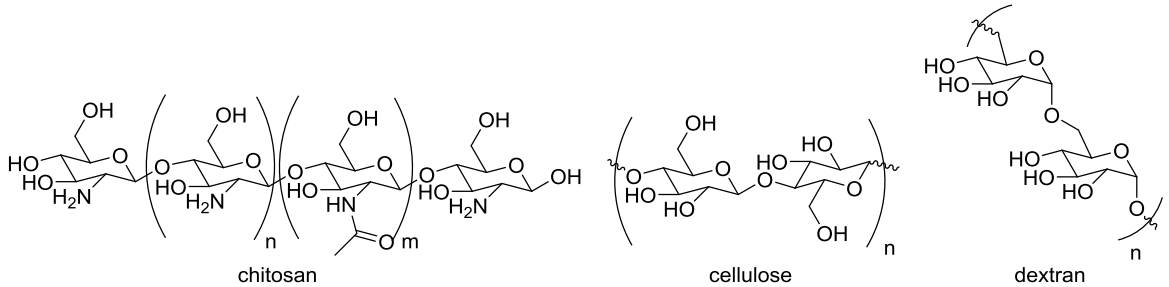

Figure 3.1. Structure of natural polysaccharides.

In an effort to replicate the cationic properties of chitosan, cellulose[202] and dextran[203] (Figure 3.1) have been modified with glycidyltrimethyl ammonium chloride to introduce a cationic

charge. Cellulose, consisting of β-(1,4)-linked-D-glucose, is both renewable and widely abundant, but has limited solubility in most solvents. Dextran, consisting of α-(1,6)-linked-D-glucose, is highly soluble irrespective of pH. While these chitosan-mimics have been useful as therapeutic delivery agents, they still maintain the inherent limitations of naturally-derived materials, such as immunogenicity and batch-to-batch variation.

Synthetic cationic polymers can be constructed from small-molecule monomers that ensure high purity and enable control of molecular weight. Common cationic polymers include polyethylenimine, poly(L-lysine), polyamidoamine, poly(amino-*co*-ester)s, and poly(2-(*N*,*N*-dimethylamino)ethyl methacrylate (Figure 3.2). The main limitations of synthetic cationic polymers are their cytotoxicity[167,168] and lack of biodegradability,[204] which can lead to accumulation.

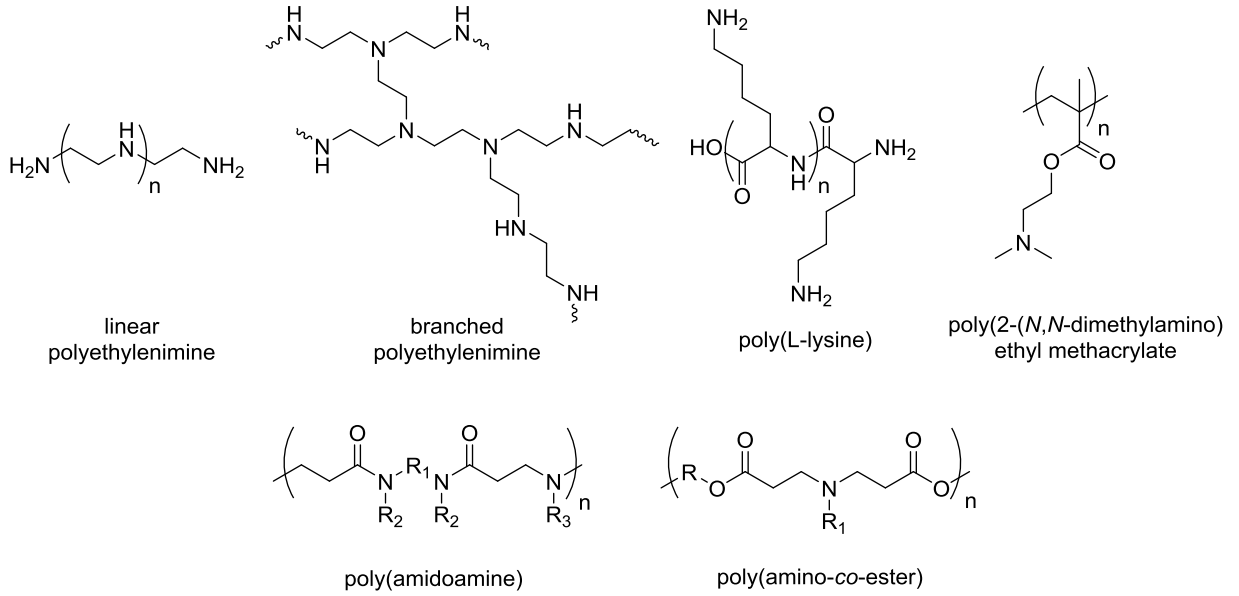

Figure 3.2. Structure of synthetic cationic polymers.

In order to retain the biocompatibility and biodegradability of natural polysaccharides without sacrificing synthetic control, monomers can be designed to more closely resemble their natural counterparts and polymerized into glycomimetics. Glucose, galactose, mannose, and

N-acetyl glucosamine have previously been transformed into glycomonomers.[19,128,129,131] Primary amine containing saccharides, such as glucosamine and galactosamine, have also been used to create glycopolymers, but the amine moiety was used as a facile attachment site for a polymerizable group, such as with acryloyl chloride.[108] The formation of an amide linkage eliminates the capability of the amine to adopt a cationic charge. In order to produce a cationic monomer using glucosamine, a polymerizable group must be incorporated while maintaining the primary amine moiety. This is particularly difficult due to the high reactivity of the amine compared to the alcohol moieties and the exceptional stability of amide bonds preventing deprotection. In this chapter, a series of amine-protected glycomonomers with differing connectivity to the polymerizable group were synthesized that allow for restoration of their cationic charge post-polymerization.

3.1.2. Branching

Initially, our group investigated hyperbranched glycopolymers made via atom-transfer radical polymerization (ATRP) and saw increase lectin interactions with increased branching density.[19] However, ATRP is limited by the inability to polymerize amine-containing monomers due to competitive complex formation with the copper catalyst and the need to remove the copper catalyst post-polymerization.[20] Therefore, we looked to reversible addition-fragmentation chain transfer (RAFT) polymerization as an alternative method for creating hyperbranched glycopolymers.

RAFT polymerization is one of many controlled radical polymerization techniques developed to synthesize polymers with well-defined molecular weights and is compatible with a wide variety of initiators, monomers, and solvents.[21] RAFT polymerization is dependent on the use of a chain transfer agent (CTA) which is often composed of a thiocarbonylthio unit attached

to an electron-rich stabilizing group (referred to as the Z group) and a polymerization reinitiator (referred to as the R group). During polymerization, the CTA maintains the majority of radicals in a dormant adduct intermediate. This limits the number of actively propagating chains and avoids premature termination.

Branching can be introduced in RAFT polymerizations using bifunctional monomers. Typically, branching is introduced using a homobifunctional branching unit containing two identical polymerizable units, such as ethylene glycol dimethacrylate (EGDMA).[23] Since the branching unit is also a crosslinker, gelation has been observed at high degrees of branching.[24–26] In order to address this issue, heterofunctional polymerizable CTAs have been developed, which contain a polymerizable unit and a chain transfer unit.[205–207] The polymerizable unit allows for incorporation of the branching unit into a propagating polymer chain whereas the chain transfer unit can only begin a new chain (Scheme 3.1). The polymerizable unit should have similar reactivity to the monomer and the chain transfer unit should have similar reactivity to the CTA used in the polymerization. In this chapter two RAFT CTAs are synthesized with an alcohol moiety available for attachment of a polymerizable unit. Using one of these RAFT CTAs, we attach a polymerizable acrylate or a glycomonomer.

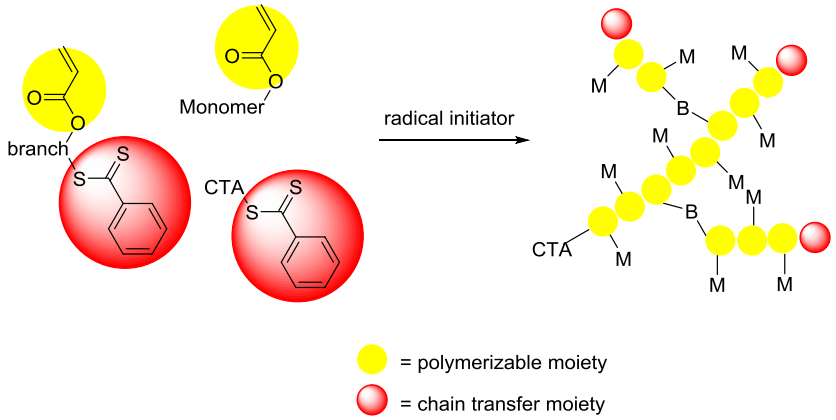

Scheme 3.1. Hyperbranched polymer created with polymerizable CTA.

3.2. Synthesis of glycomonomers

In order to create a variety of glycopolymers, a library of glycomonomers was created using glucose, galactose, mannose, *N*-acetyl glucosamine, and glucosamine. The first set of glycomonomers was designed with the polymerizable group attached through a glycosidic bond, which tends to have increased biological activity compared to reducing saccharides.[88] In addition, an acrylate polymerizable group was selected over the more hydrophobic methacrylate group to minimize poor solvent interactions with the glycopolymer. In general, the monomers were synthesized through the acetate protection of all the alcohols, Lewis acid-catalyzed glycosidic linkage of hydroxyethyl acrylate, and deprotection of the acetate protecting groups with sodium methoxide. Each saccharide, however, possessed subtle differences in the isolation of isomers and the optimization of acetate deprotection conditions. The *N*-acetyl glucosamine monomer, in particular, required stronger acid and elevated temperatures to form the oxazoline intermediate and facilitate the backside nucleophilic attack to form the glycosidic bond. In this fashion, four monomers were created: 2-*O*-(β-D-glucosyl)hydroxyethyl acrylate, 2-*O*-(β-D-galactosyl)hydroxyethyl acrylate, 2-*O*-(α-D-mannosyl)hydroxyethyl acrylate, and 2-*O*-(2-acetamido-2-deoxy-β-D-glucosyl)hydroxyethyl acrylate (Scheme 3.2).

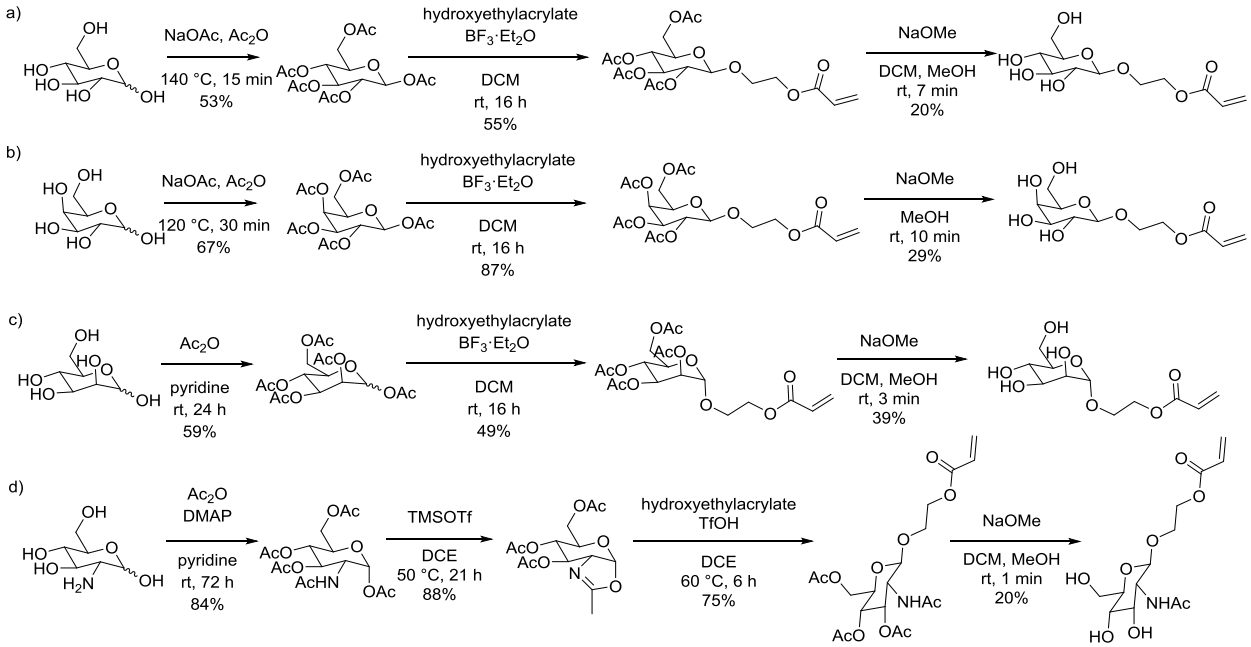

Scheme 3.2. Synthesis of a) glucose, b) galactose, c) mannose, and d) *N*-acetyl glucosamine glycomonomers through the conjugation of hydroxyethyl acrylate through a glycosidic bond.

A second set of glycomonomers was synthesized to contain a polymerizable group attached to the primary alcohol of the saccharide to diminish biological activity so that the cluster glycoside effect would be more pronounce. A galactose-based glycomonomer was synthesized through the selective protection of the secondary alcohols of D-galactose with isopropylidene protecting groups which can be deprotected under milder conditions than acetate protecting groups. An acrylate moiety was attached to the unprotected primary alcohol by base-catalyzed esterification with acryloyl chloride to obtain acryloyl-1,2:3,4-di-*O*-isopropylidene-α-D-galactose (Scheme 3.3a).

A glucose-based glycomonomer was synthesized through selective protection of the primary alcohol of D-glucose with triphenylmethyl chloride followed by acetate protection of the secondary alcohols to facilitate the formation of a glycosidic linkage. The α-isomer undergoes acetyl migration upon deprotection of the primary alcohol and was removed by solvation in

diethyl ether. The primary alcohol of the β-isomer was deprotected with hydrobromic acid and a methacrylate moiety was attached by base-catalyzed esterification with methacrylic anhydride to obtain methacryloyl-1,2,3,4-tetraacetate-β-D-glucose (Scheme 3.3b).

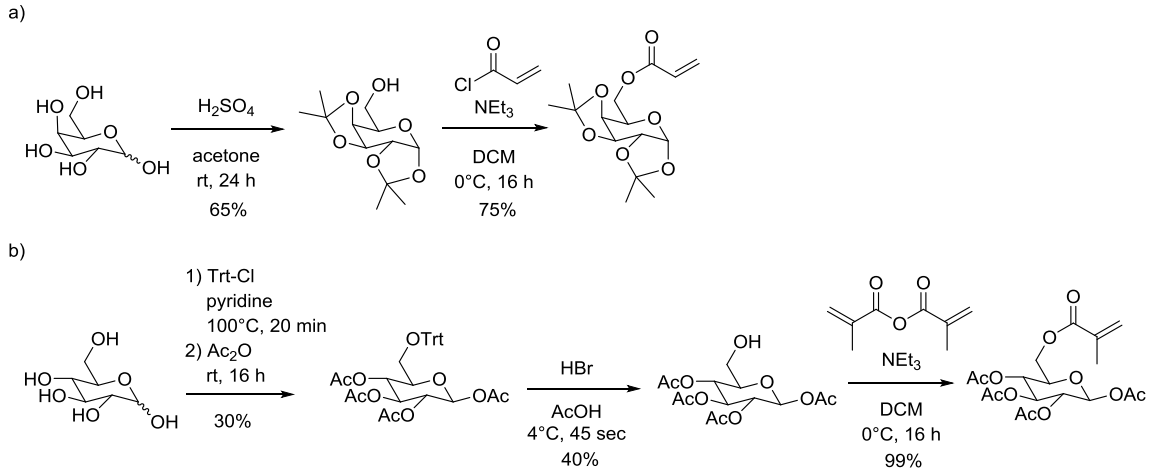

Scheme 3.3. Synthesis of a) acryloyl-1,2:3,4-di-*O*-isopropylidene-α-D-galactose b) methacryloyl-1,2,3,4-tetraacetate-β-D-glucose.

A third set of glycomonomers was created based on glucosamine to produce cationic glycopolymers. While the amine moiety of glucosamine is a poor nucleophile in acidic conditions, basic conditions are often necessary for the attachment and removal of alcohol protecting groups and the attachment of polymerizable groups. In order to prevent the formation of an amide bond or a Michael addition with a polymerizable acrylate, the primary amine was protected with 9-fluorenylmethoxycarbonyl chloride (Fmoc-Cl). A total of three cationic monomers were synthesized: 1) with a polymerizable group attached to the primary alcohol, 2) with a polymerizable group attached to the primary alcohol and bearing a methyl glycoside, and 3) with a polymerizable group attached through a glycosidic bond (Scheme 3.4).

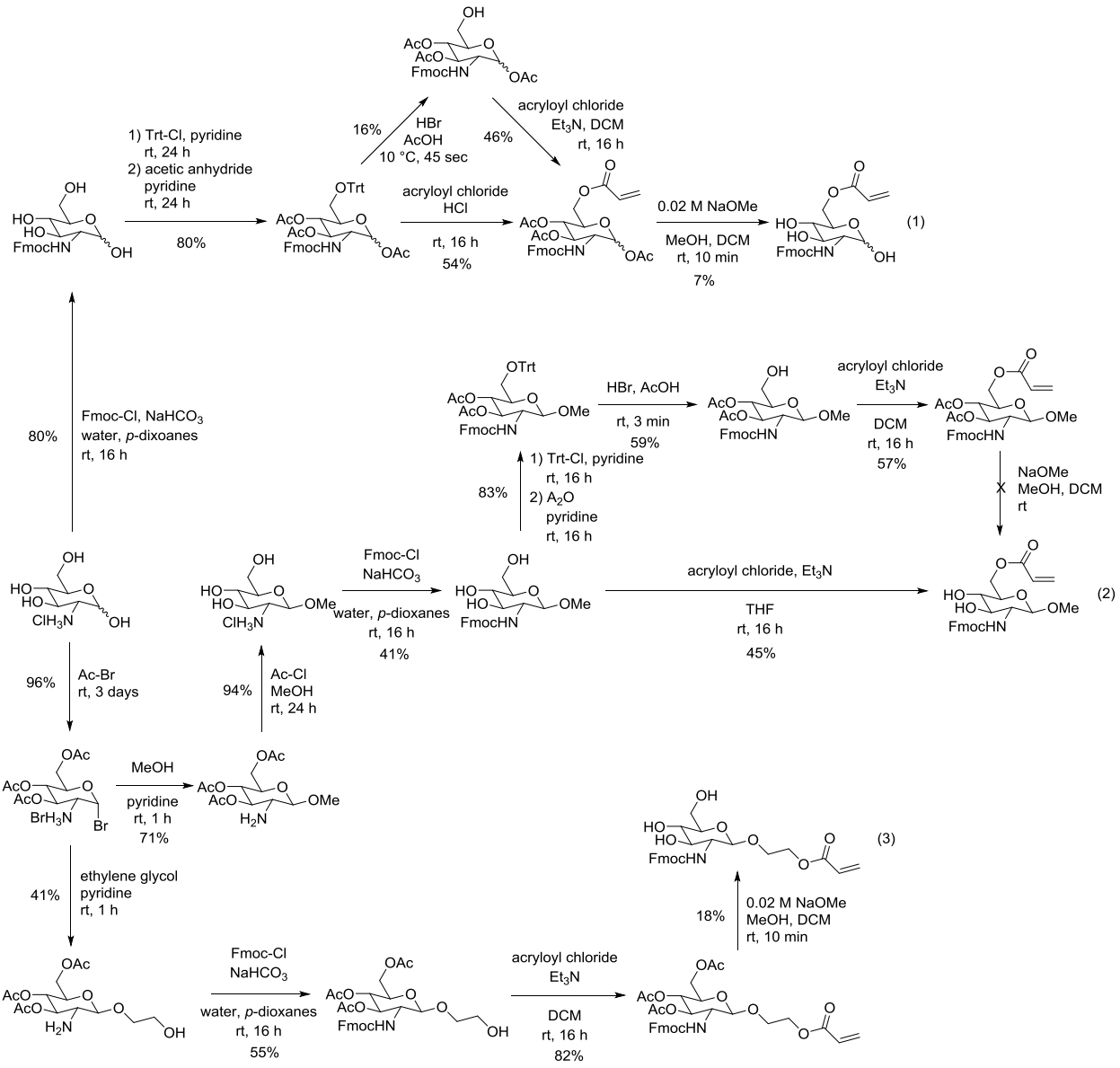

Scheme 3.4. Synthesis of Fmoc-protected glycomonomers: 1) *N*-Fmoc-6-acryloyl-D-glucosamine, 2) methyl *N*-Fmoc-6-acryloyl-β-D-glucosaminoside, and 3) 2-*O*-(*N*-Fmoc-β-D-glucosaminosyl)hydroxyethyl acrylate.

N-Fmoc-6-acryloyl-D-glucosamine was synthesized via four steps. First, the amine was protected with Fmoc-Cl followed by the selective protection of the primary alcohol with triphenylmethyl chloride and the secondary alcohols with acetic anhydride. The primary alcohol was initially deprotected using hydrobromic acid followed by base-catalyzed esterification with acryloyl chloride, but transesterification of the acetate protecting groups resulted in a mixture of products which produced an impractically low yield of 7%. Instead, a one-pot trityl

deprotection/acrylation method[208] was employed using neat acryloyl chloride and a catalytic amount of hydrogen chloride, resulting in an improved yield of 54%. Finally, the secondary alcohols were deprotected using a sodium methoxide solution optimized for concentration and duration. The resultant glycomonomer was characterized via nuclear magnetic resonance (NMR) (Figure 3.3 and Figure 3.4) and electrospray ionization (ESI) spectrometry (Figure 3.5).

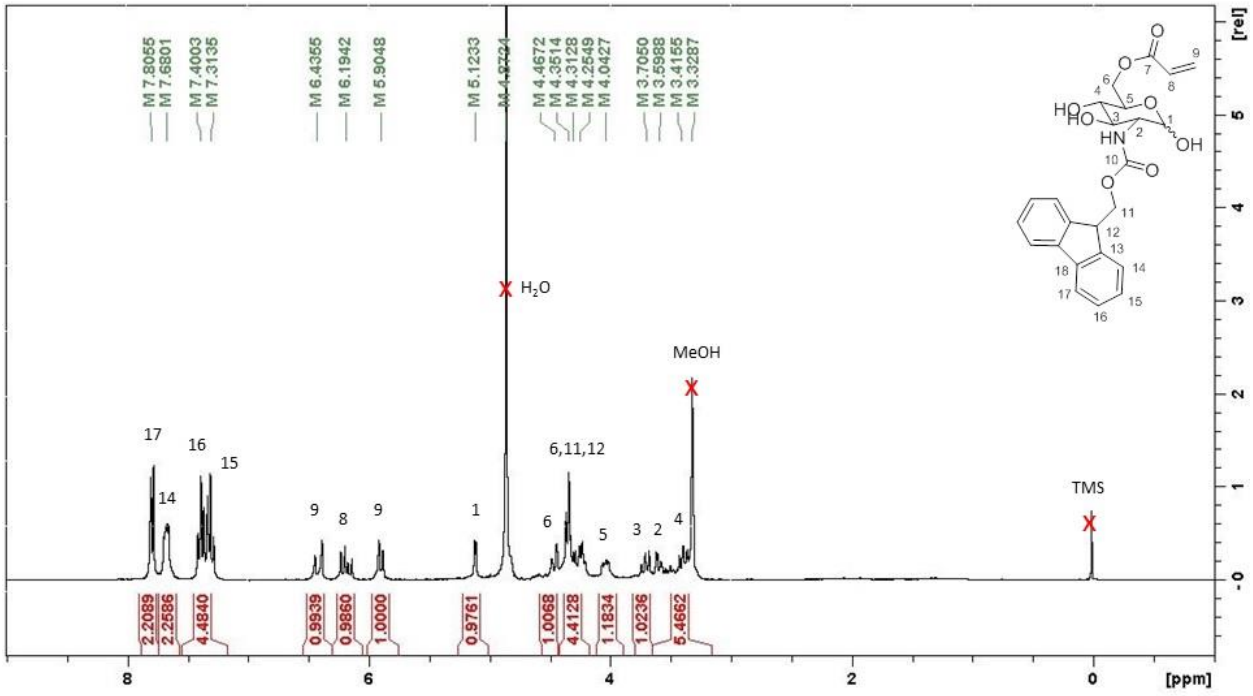

Figure 3.3. [1]H NMR of *N*-Fmoc-6-acryloyl-D-glucosamine taken in MeOD.

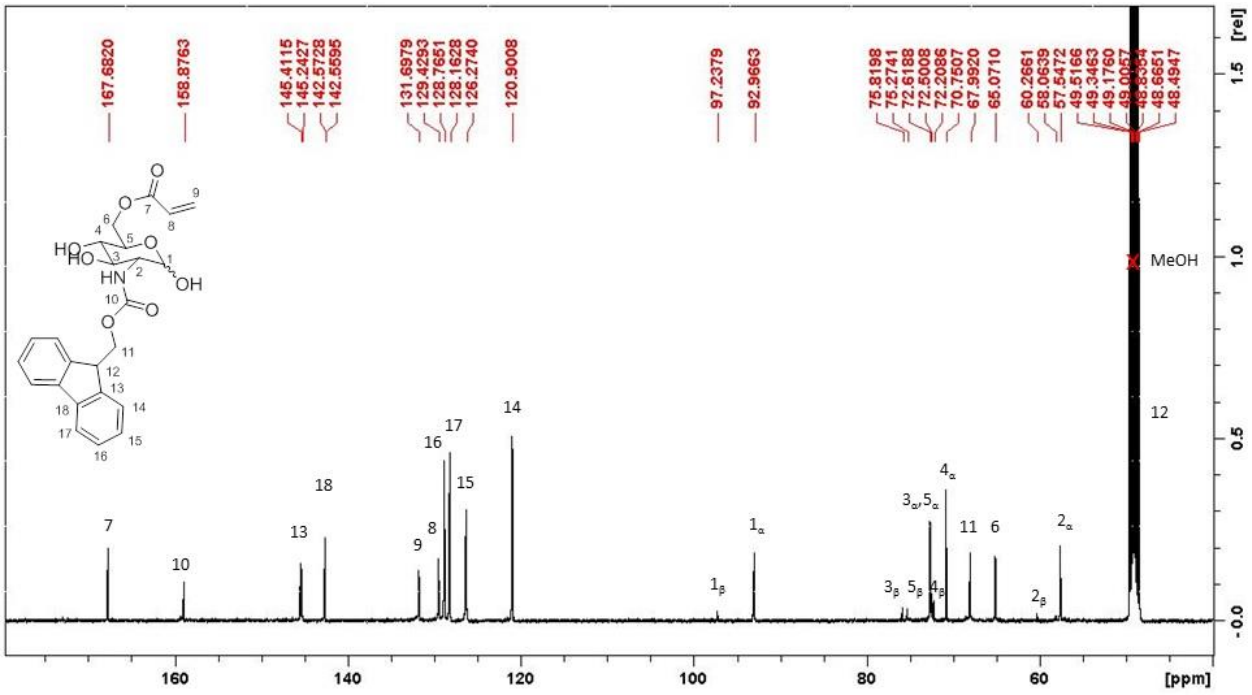

Figure 3.4. ^{13}C NMR of *N*-Fmoc-6-acryloyl-D-glucosamine taken in MeOD.

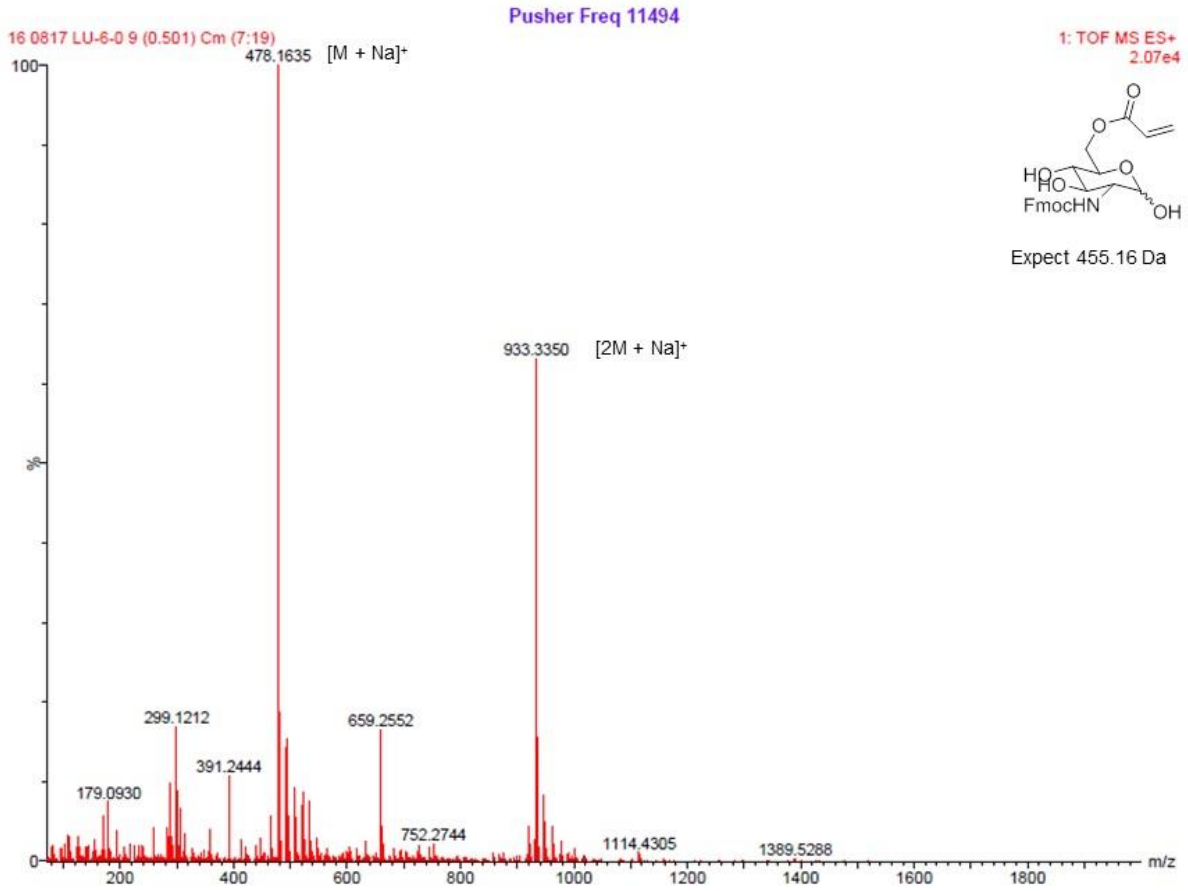

Figure 3.5. ESI of *N*-Fmoc-6-acryloyl-D-glucosamine taken in methanol.

Methyl *N*-Fmoc-6-acryloyl-β-D-glucosaminoside was synthesized in five steps beginning with the bromination of the anomic position and the acetylation at C-3, C-4, and C-6 with neat acetyl bromide. The amine was unaffected due to protonation from the acidic conditions. The methyl glycoside was formed using pyridine in methanol followed by acid hydrolysis of the acetate protecting groups using a solution of acetyl chloride in methanol, and the amine was protected with Fmoc-Cl. Initially, selective protection and deprotection of the primary alcohol was attempted as in the synthesis of *N*-Fmoc-6-acryloyl-D-glucosamine, but the deprotection conditions for removing the acetate groups also removed the acrylate moiety at a similar rate, resulting in no isolatable amount of the desired glycomonomer. Instead, the polymerizable group was attached to the primary alcohol by base-catalyzed esterification using acryloyl chloride as a limiting reagent and selectively esterifying the primary alcohol by utilizing the difference in reactivity of the alcohols due to steric hindrance. The resultant glycomonomer was characterized via NMR (Figure 3.6 and Figure 3.7) and ESI spectrometry (Figure 3.8).

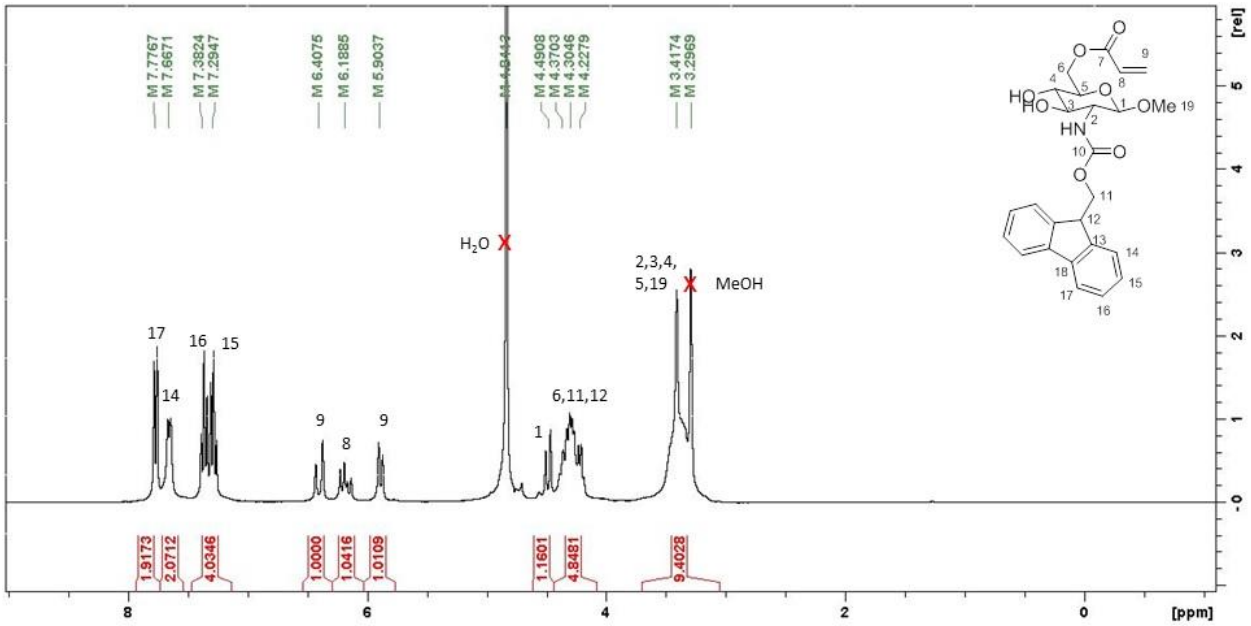

Figure 3.6. ^{1}H NMR of methyl *N*-Fmoc-6-acryloyl-β-D-glucosaminoside taken in MeOD.

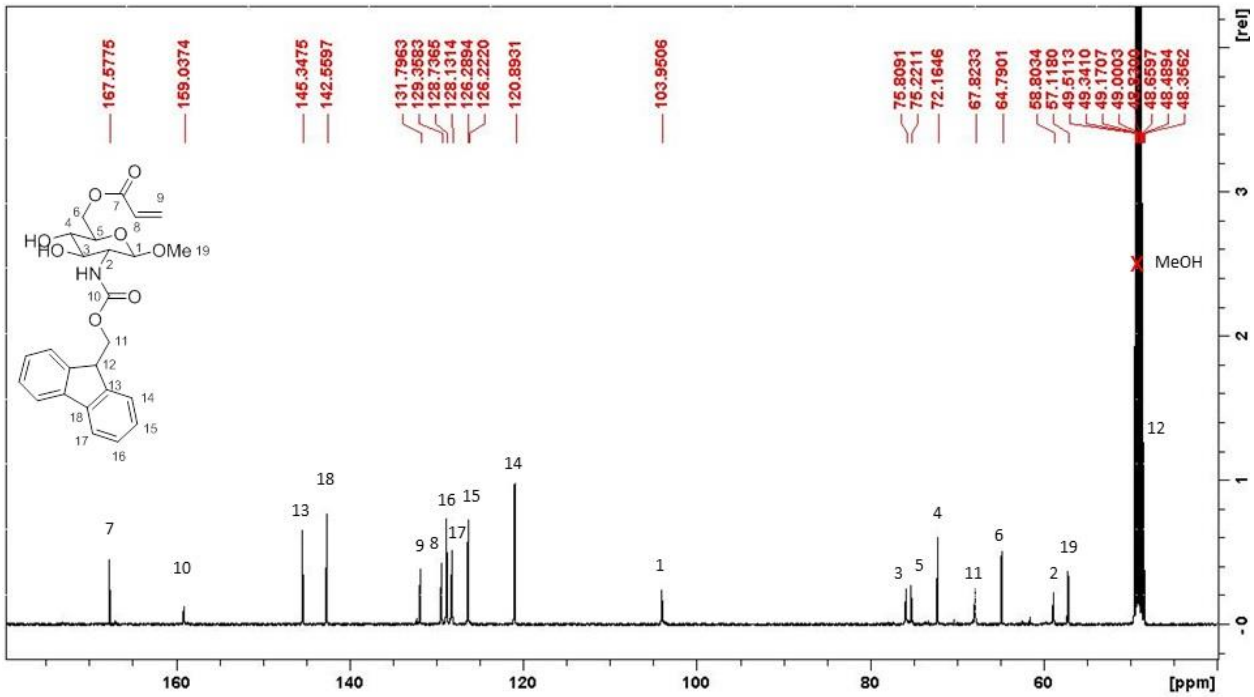

Figure 3.7. ^{13}C NMR of methyl *N*-Fmoc-6-acryloyl-β-D-glucosaminoside taken in MeOD.

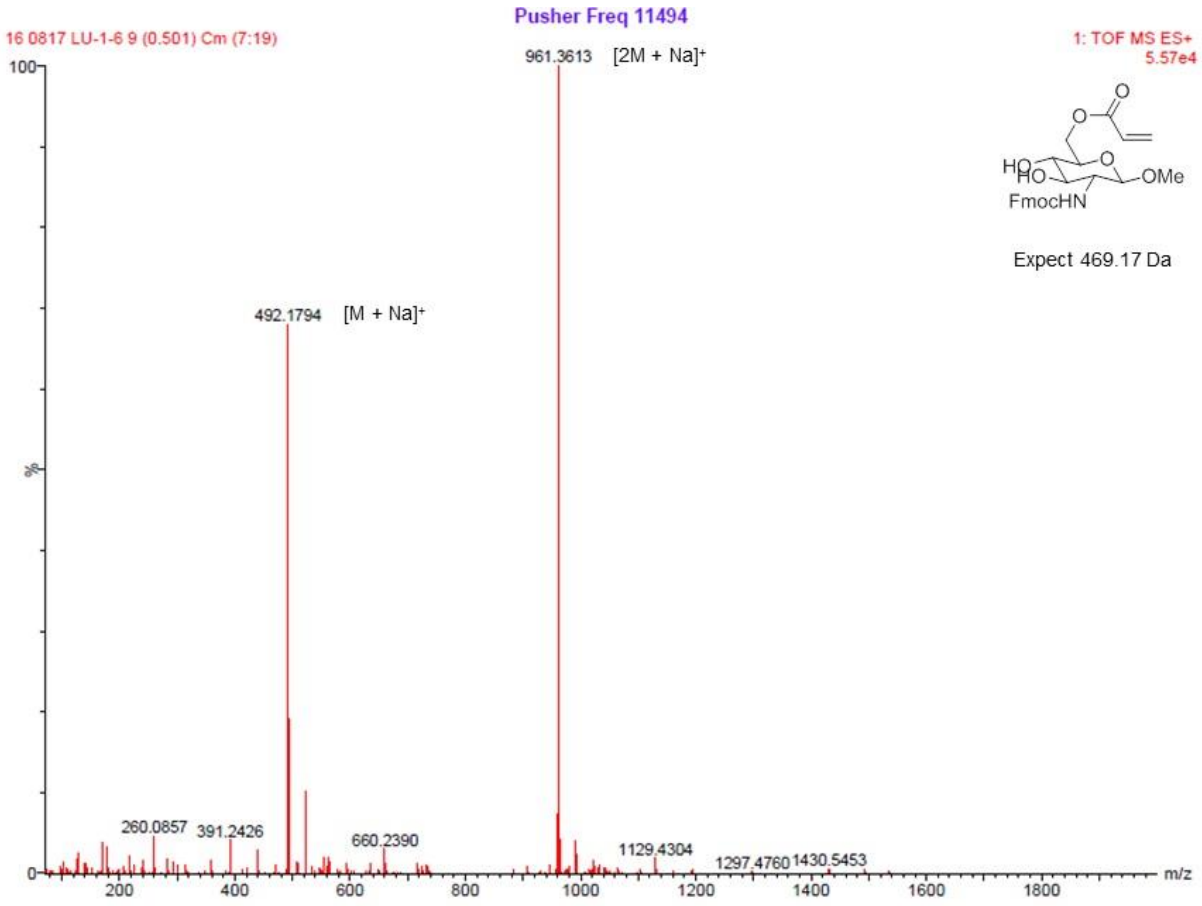

Figure 3.8. ESI of methyl *N*-Fmoc-6-acryloyl-β-D-glucosaminosidetaken in methanol.

2-*O*-(*N*-Fmoc-β-D-glucosaminosyl)hydroxyethyl acrylate was synthesized in five steps beginning with the bromination of the anomic position and the acetylation at C-3, C-4, and C-6 with neat acetyl bromide. Instead of methanol, ethylene glycol was used as a solvent and attached in a glycosidic bond. Following Fmoc protection of the amine, an acrylation was conducted on the exposed primary alcohol using acryloyl chloride. Finally, the secondary alcohols were deprotected using a sodium methoxide solution optimized for concentration and duration. The resultant glycomonomer was characterized via NMR (Figure 3.9 and Figure 3.10) and ESI spectrometry (Figure 3.11).

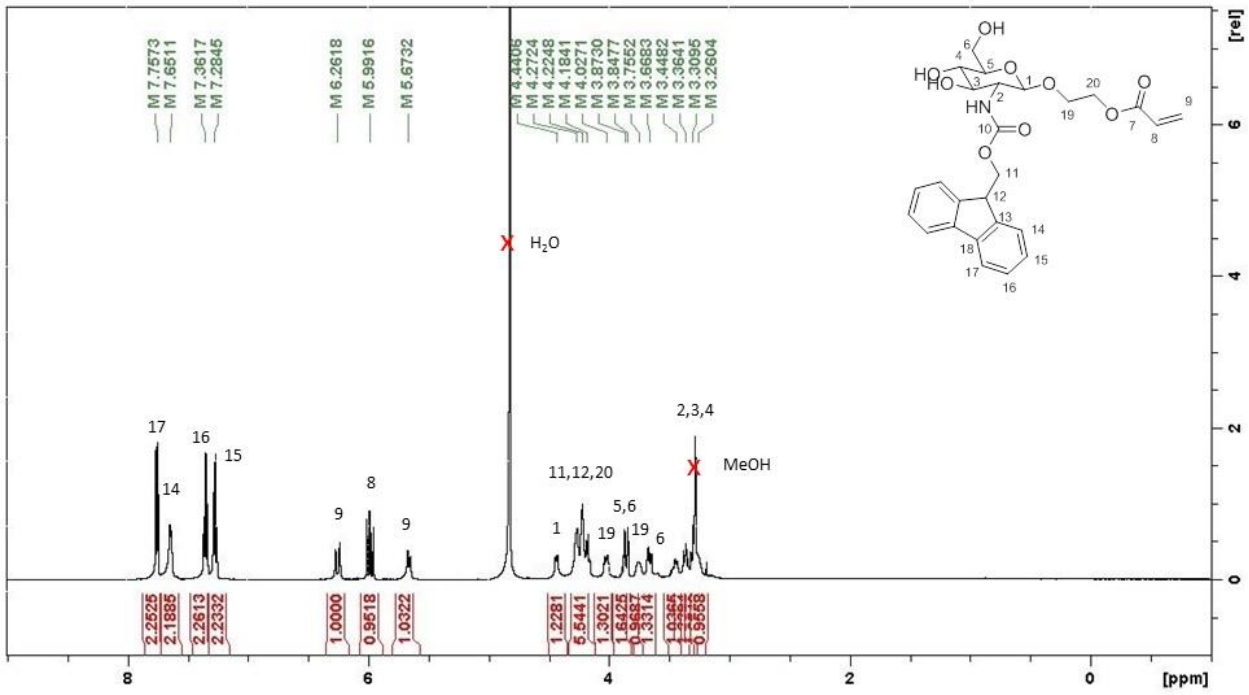

Figure 3.9. ^{1}H NMR of 2-*O*-(*N*-Fmoc-β-D-glucosaminosyl)hydroxyethyl acrylate taken in MeOD.

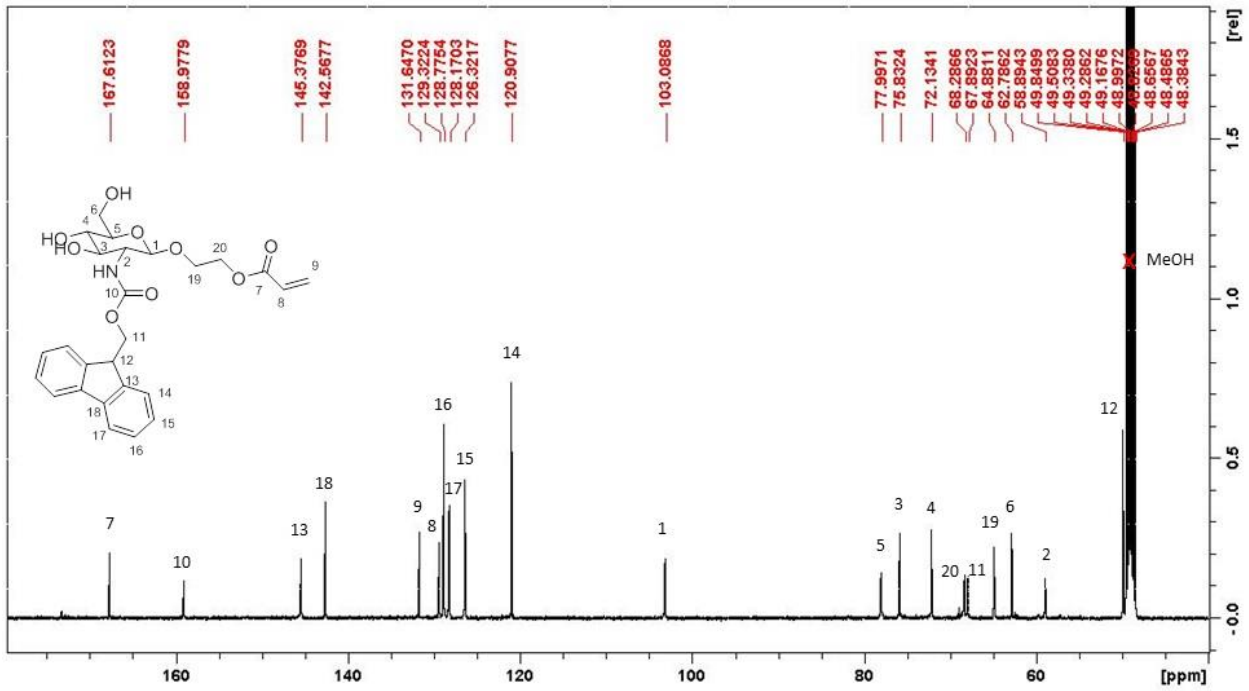

Figure 3.10. ^{13}C NMR of 2-*O*-(*N*-Fmoc-β-D-glucosaminosyl)hydroxyethyl acrylate taken in MeOD.

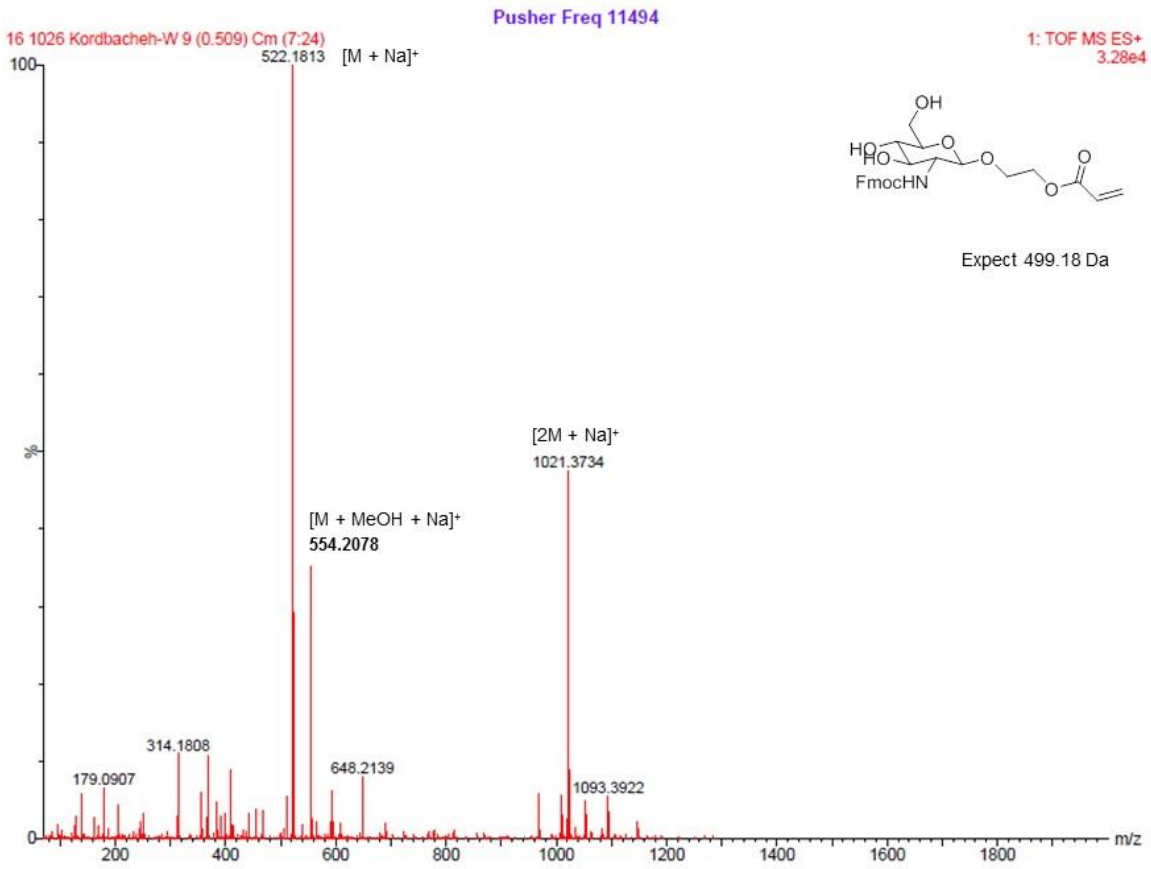

Figure 3.11. ESI of 2-*O*-(*N*-Fmoc-β-D-glucosaminosyl)hydroxyethyl acrylate taken in methanol.

3.3. Synthesis of polymerizable chain transfer agents

In order to produce polymerizable chain transfer agents, a CTA was synthesized that contained a free alcohol available for attachment of polymerizable groups. Initially, an alcohol bearing CTA was synthesized from the nucleophilic substitution of methyl 2-bromo-3-hydroxypropionate[209] with a carbodithioate salt (Scheme 3.5). Decomposition of the CTA was observed in mild acid, mild base, and high temperatures, making modification the alcohol difficult and polymerization with thermal initiators impractical.

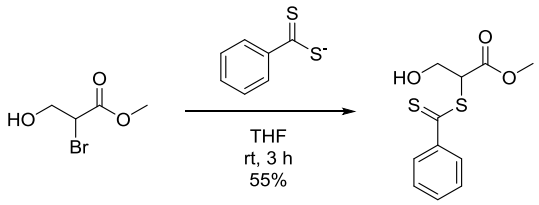

Scheme 3.5. Initial synthesis of alcohol-bearing RAFT CTA from methyl 2-bromo-3-hydroxypropionate.

Alternatively, an alcohol-bearing CTA was synthesized by base-catalyzed esterification of 2-bromopropionyl bromide with ethylene glycol followed by radical substitution of a bis(thioacryl) disulfide (Scheme 3.6a). Two polymerizable CTAs were created from this alcohol-bearing CTA. Initially, base-catalyzed esterification of acryloyl chloride was attempted, but triethylamine was observed to cause aminolysis of the dithioester. Instead, a polymerizable CTA was created by esterification of acrylic acid with the alcohol-bearing CTA via a carbodiimide intermediate (Scheme 3.6b). A second polymerizable CTA was synthesized, which would incorporate a saccharide unit into the branch point of the polymer, through the Lewis acid-catalyzed glycosylation of an acetate protected glycomonomer with the alcohol-bearing CTA (Scheme 3.6c).

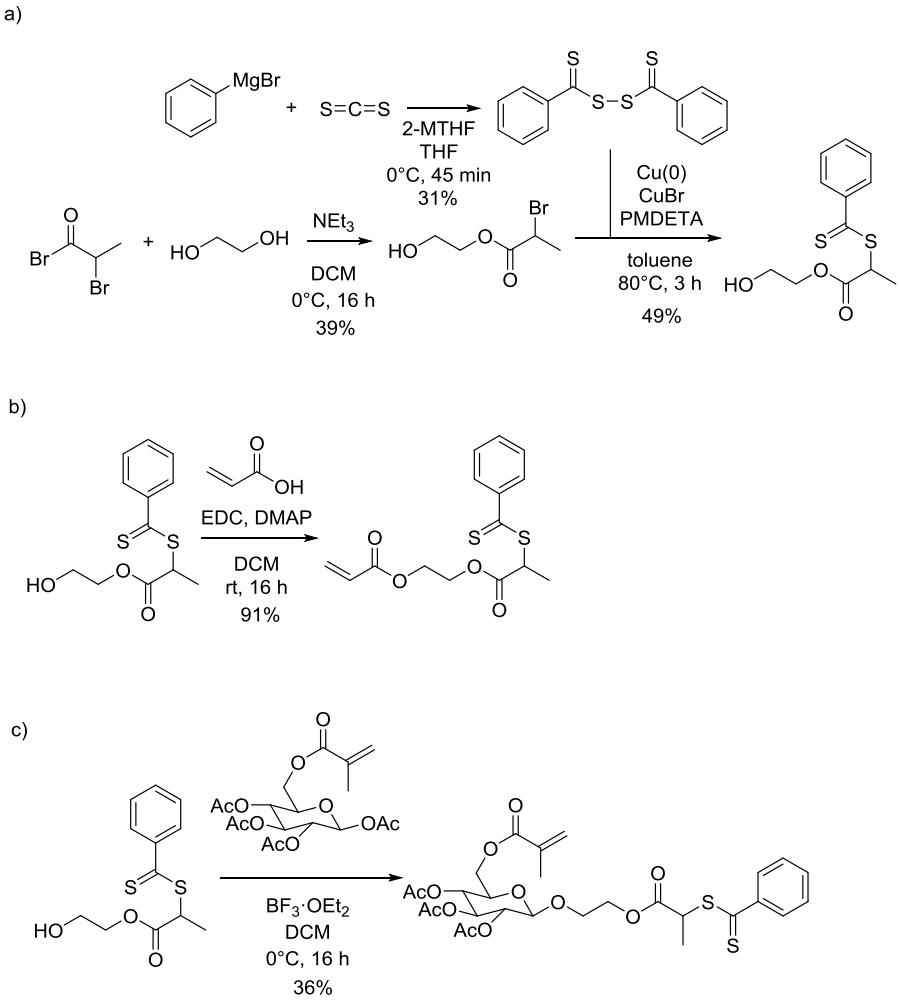

Scheme 3.6. Synthesis of a a) RAFT CTA bearing a primary alcohol b) PCTA c) PCTA incorporating a saccharide into the branch point.

3.4. Conclusions

In this chapter, a library of tools was created for polymerizing glycopolymers (Figure 3.12). A total of nine glycomonomers and two polymerizable CTAs were created. The glycomonomers can be divided into three categories. The first category contains four deprotected glycomonomers based on glucose, galactose, mannose, and *N*-acetyl glucosamine that all have a polymerizable group attached through a glycosidic bond. The second category contains an isopropylidene-protected galactose glycomonomer and an acetate-protected glucose glycomonomer both with a polymerizable group attached to the primary alcohol. The isopropylidene groups allow for post-polymerization deprotection without the cleavage of the saccharide form the polymer backbone, and the acetate protecting groups allow for the attachment of alcohols in a glycosidic bond. The third category of glycomonomers consist of three Fmoc-protected glycomonomers based on glucosamine with a polymerizable group attached at the primary alcohol, with a polymerizable group attached at the primary alcohol and a methyl glycosidic bond, and with a polymerizable group attached through a glycosidic bond. In addition, two polymerizable CTAs were synthesized through the attachment of a polymerizable group to an alcohol-bearing CTA or through the attachment of the same alcohol-bearing CTA to a glycomonomer through a glycosidic bond. Using these tools, a variety of glycopolymers can be created.

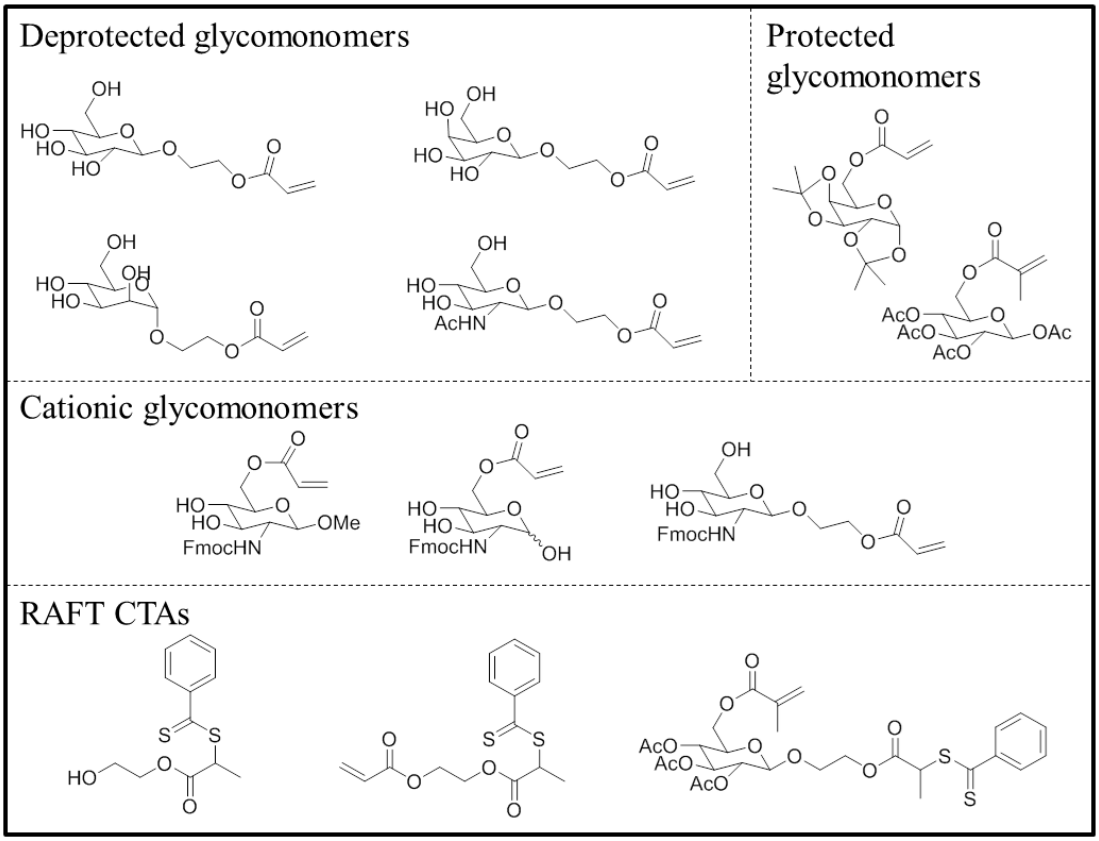

Figure 3.12. Summary of synthesized glycopolymer tools.

3.5. Experimentals

3.5.1. Materials

D-Glucose (ACROS, ACS grade), D-galactose (Fisher, off white to white powder), D-mannose (Amresco, high purity grade), D-glucosamine hydrochloride (ACROS, 98+%), 9-fluorenylmethoxycarbonyl chloride (Fmoc-Cl) (Oakwood Products, 97%), triphenylmethyl chloride (ACROS, 98%), acetic anhydride (Fisher, ACS grade), boron trifluoride etherate (ACROS, 48%), trimethylsilyl trifluoromethanesulfonate (ACROS, 99%), trifluoromethanesulfonic acid (ACROS, 99%), hydrochloric acid (Fisher, ACS grade), sulfuric acid (Fisher, ACS grade), hydrobromic acid in acetic acid (ACROS, 33 wt%), 2-bromopropionyl bromide (Alfa Aesar, 97%), acetyl bromide (Alfa Aesar, 98+%), acetyl chloride (ACROS, ACS grade), acetic acid (Macron Chemicals, ACS grade), sodium acetate trihydrate (Fisher, ACS grade), 4-dimethylaminopyridine (DMAP) (Alfa Aesar, 99%), 1-ethyl-3-(3-dimethylaminopropyl) carbodiimide (CreoSalus), triethylamine (Alfa Aesar, 99%), sodium bicarbonate (Fisher, USP/FCC), sodium carbonate (Fisher, ACS), sodium methoxide in methanol (ACROS, 5.4 M), phenylmagnesium bromide in THF (ACROS, 1 M), phenylmagnesium bromide in 2-methyltetrahydrofuran (Strem, Chemicals, 2.9 M), carbon disulfide (Fisher, ACS grade), Cu(0) (ACROS, 99%), iodine (ACROS, resublimed), ethylene glycol (MP Biomedicals, 99%), methanol (EMD DriSolv, 99.8%), ethanol (Decon Labs, 200 proof), acetone (Fisher, ACS grade), diethyl ether (Macron Chemicals, ACS grade), tetrahydrofuran (EMD DriSolv, 99.9%), *p*-dioxane (ACROS, 99.8% extra dry), chloroform (Fisher, ACS grade), dichloroethane (ACROS, ACS grade), dimethyl sulfoxide (DMSO) (Fisher, ACS grade), ethyl acetate (Fisher, ACS grade), hexanes (Fisher, ACS grade), and DOWEX 50WX8 ion-exchange resin (ACROS, 200-400 mesh) were used as received. *N,N,N′,N′,N″*-Pentamethyldiethylenetriamine (Pfaltz &

Bauer Inc., 99%), hydroxyethyl acrylate (HEA) (Sigma-Aldrich, 96%), acryloyl chloride (Alfa Aesar, 96%), methacrylic anhydride (Sigma-Aldrich, 94%), toluene (Fisher, ACS grade), dichloromethane (DCM) (Fisher, ACS grade), pyridine (JT Baker, ACS grade), and water (Fisher, HPLC) were distilled. Acrylic acid (ACROS, 99.5%) was passed through basic alumina. CuBr (ACROS, 98%) was purified with acetic acid and washed with ethanol. Methyl 2-bromo-3-hydroxypropionate was synthesized as reported by Pugh *et al*.[209]

3.5.2. Analytical techniques

^{1}H NMR spectra were recorded with a Bruker Avance 300. ^{13}C NMR spectra were recorded on a Bruker Avance 500 equipped with a 5 mm dual cryoprobe. Electrospray ionization (ESI) was conducted on a Waters LCT Premier with ACQUITY UPLC with autosampler.

3.5.3. 1,2,3,4,6-Pentaacetyl-β-D-glucose

D-Glucose (6 g, 33 mmol) was added gradually to a solution of sodium acetate trihydrate (3 g, 22 mmol) dissolved in acetic anhydride (42 mL, 0.45 mol) previously heated at 140 °C for 20 minutes. The reaction was removed from heat after 15 minutes and allowed to cool to room temperature before gradually pouring into ice water and allowed to precipitate at 4 °C overnight. The solid was collected by vacuum filtration and recrystallized in ethanol (6.9 g, 53%).

^{1}H NMR (300 MHz, $CDCl_3$): δ5.73 (d, H-1), 5.10-5.30 (m, H-2,3,4), 4.10-4.30 (m, 2H, H_2-6), 3.85 (m, H-5), 2.01-2.11 (s, 15H, 5 CH_3).

3.5.4. 2-*O*-(2,3,4,6-Tetraacetyl-β-D-glucosyl)hydroxyethyl acrylate

Boron trifluoride etherate (2.7 mL, 21 mmol) was added dropwise to a stirring solution of 1,2,3,4,6-pentaacetyl-β-D-glucose (2.7 g, 7 mmol) and hydroxyethyl acrylate (1.2 mL, 10.4 mmol) dissolved in DCM (25 mL) cooled in an ice bath. The solution was allowed to warm to room temperature after the addition was completed and stirred for 16 hours. The reaction was

washed with DI water (2×), a saturated solution of sodium bicarbonate (2×), and brine. The organic solution was dried with sodium sulfate, concentrated, and isolated by silica column chromatography using 1:1 ethyl acetate in hexanes as an eluent (1.7 g, 55%).

^{1}H NMR (300 MHz, $CDCl_3$): δ6.42 (d, 1H, C*H*$_2$═CH), 6.11 (m, CH_2═C*H*), 5.85 (d, 1H, C*H*$_2$═CH), 5.00-5.20 (m, H-2,3,4), 4.55 (d, H-1), 4.10-4.30 (m, 4H, H_2-6, OCH_2CH_2OC═O), 4.01 (m, 1H, OCH_2CH_2OC═O), 3.80 (m, 1H, OCH_2CH_2OC═O), 3.70 (m, H-5), 2.00-2.10 (s, 12H, 4 CH_3).

3.5.5. 2-*O*-(β-D-Glucosyl)hydroxyethyl acrylate

Sodium methoxide (2 mL, 0.2 M) was added to a solution of 2-*O*-(2,3,4,6-tetraacetyl-β-D-glucosyl)hydroxyethyl acrylate (1.7 g, 4 mmol) dissolved in DCM (8 mL) and methanol (10 mL) and stirred for 7 minutes before quenching with DOWEX 50WX8 ion-exchange resin for 30 minutes. The glycomonomer was isolated by silica column chromatography using 2:8 methanol in DCM as an eluent (207 mg, 20%).

^{1}H NMR (300 MHz, MeOD): δ6.42 (d, 1H, C*H*$_2$═CH), 6.19 (m, CH_2═C*H*), 5.91 (d, 1H, C*H*$_2$═CH), 4.35 (m, 3H, H-1, OCH_2CH_2OC═O), 4.12 (m, 1H, OCH_2CH_2OC═O), 3.88 (m, 2H, H_2-6, OCH_2CH_2OC═O), 3.69 (dd, 1H, H_2-6), 3.31 (m, H-3,4,5), 3.19 (t, H-2).

3.5.6. 1,2,3,4,6-Pentaacetyl-β-D-galactose

D-Galactose (20 g, 111 mmol) was added gradually to a solution of sodium acetate trihydrate (10 g, 74.5 mmol) dissolved in acetic anhydride (200 mL, 2.1 mol) previously heated at 120 °C for 30 minutes. The reaction was removed from heat after an hour and allowed to cool to room temperature before gradually pouring into a solution of sodium bicarbonate. Additional sodium bicarbonate was added until no gas was produced upon addition. The solid was taken up in DCM and washed with saturated sodium bicarbonate (4×), DI water, and brine. The organic solution

was dried with sodium sulfate, concentrated, and covered with diethyl ether at -20 °C. The white crystals were collected by vacuum filtration (24.84 g, 67%).

^{1}H NMR (300 MHz, $CDCl_3$): δ5.71 (d, H-1), 5.43 (d, H-4), 5.34 (dd, H-2), 5.09 (dd, H-3), 4.15 (m, 2H, H_2-6), 4.05 (t, H-5), 2.00-2.17 (s, 15H, 5 CH_3).

3.5.7. 2-*O*-(2,3,4,6-Tetraacetyl-β-D-galactosyl)hydroxyethyl acrylate

Boron trifluoride etherate (2.0 mL, 16 mmol) was added dropwise to a stirring solution of 1,2,3,4,6-pentaacetyl-β-D-galactose (2.0 g, 5.1 mmol) and hydroxyethyl acrylate (1.2 mL, 10.4 mmol) dissolved in DCM (25 mL) cooled in an ice bath. The solution was allowed to warm to room temperature after the addition was completed and stirred for 16 hours. The reaction was washed with DI water (3×), a saturated solution of sodium bicarbonate, and brine. The organic solution was dried with sodium sulfate, concentrated, and isolated by silica column chromatography using 7:3 ethyl acetate in hexanes as an eluent (2.0 g, 87%).

^{1}H NMR (300 MHz, $CDCl_3$): δ6.44 (d, 1H, C*H*$_2$═CH), 6.13 (m, CH_2═C*H*), 5.87 (d, 1H, C*H*$_2$═CH), 5.39 (d, H-4), 5.21 (dd, H-2), 5.03 (dd, H-3), 4.54 (d, H-1), 4.32 (m, 2H, OCH$_2$C*H*$_2$OC═O), 4.15 (m, 3H, H_2-6, OC*H*$_2$CH$_2$OC═O), 3.93 (t, H-5), 3.83 (m, 1H, OC*H*$_2$CH$_2$OC═O), 1.99-2.16 (s, 12H, 4 CH_3).

3.5.8. 2-*O*-(β-D-Galactosyl)hydroxyethyl acrylate

Sodium methoxide (300 µL, 0.2 M) was added to a solution of 2-*O*-(2,3,4,6-tetraacetyl-β-D-galactosyl)hydroxyethyl acrylate (2.0 g, 4.5 mmol) dissolved in methanol (20 mL) and stirred for 10 minutes before quenching with DOWEX 50WX8 ion-exchange resin for 30 minutes. The glycomonomer was isolated by silica column chromatography using 2:8 methanol in DCM as an eluent (357 mg, 29%).

^{1}H NMR (300 MHz, MeOD): δ6.39 (d, 1H, C*H*$_2$═CH), 6.17 (m, CH$_2$═C*H*), 5.87 (d, 1H, C*H*$_2$═CH), 4.33 (m, 2H, OCH$_2$C*H*$_2$OC═O), 4.26 (d, H-1), 4.09 (m, 1H, OC*H*$_2$CH$_2$OC═O), 3.60-3.80 (m, 4H, H-4, H$_2$-6, OC*H*$_2$CH$_2$OC═O), 3.50 (m, H-2,3,5).

3.5.9. 1,2,3,4,6-Pentaacetyl-α,β-D-mannose

Acetic anhydride (50 mL, 0.53 mol) was added to a solution of D-mannose (10 g, 55 mmol) dissolved in pyridine (100 mL) and stirred for 24 hours. The solution was concentrated in vacuo and added to cold DI water. The product was taken up in DCM and washed with a saturated sodium bicarbonate solution (2×), washed with brine, dried with sodium sulfate, and concentrated in vacuo (12.7 g, 59%).

^{1}H NMR (300 MHz, CDCl$_3$): δ6.10 (d, H-1$_\alpha$), 5.89 (d, H-1$_\beta$), 5.10-5.50 (m, H-2,3,4), 3.71-4.30 (m, H-5$_\alpha$, H$_2$-6), 3.83 (m, H-5$_\beta$), 2.00-2.19 (s, 15H, 5 CH$_3$).

3.5.10. 2-*O*-(2,3,4,6-Tetraacetyl-α-D-mannosyl)hydroxyethyl acrylate

Boron trifluoride etherate (2.7 mL, 21 mmol) was added dropwise to a stirring solution of 1,2,3,4,6-pentaacetyl-α,β-D-mannose (2.7 g, 6.9 mmol) and hydroxyethyl acrylate (1.0 mL, 8.7 mmol) dissolved in DCM (25 mL) cooled in an ice bath. The solution was allowed to warm to room temperature after the addition was completed and stirred for 96 hours. The reaction was washed with DI water (3×), a saturated solution of sodium bicarbonate, and brine. The organic solution was dried with sodium sulfate, concentrated, and isolated by silica column chromatography using 11:9 ethyl acetate in hexanes as an eluent (1.5 g, 49%).

^{1}H NMR (300 MHz, CDCl$_3$): δ6.43 (d, 1H, C*H*$_2$═CH), 6.15 (m, CH$_2$═C*H*), 5.87 (d, 1H, C*H*$_2$═CH), 5.20-5.40 (m, H-2,3,4), 4.87 (d, H-1), 4.34 (m, 2H, OCH$_2$C*H*$_2$OC═O), 4.03-4.27 (m, 3H, H-5, H$_2$-6), 3.78-3.90 (m, 2H, OC*H*$_2$CH$_2$OC═O), 1.99-2.17 (s, 12H, 4 CH$_3$).

3.5.11. 2-*O*-(α-D-Mannosyl)hydroxyethyl acrylate

Sodium methoxide (1 mL, 0.2 M) was added to a solution of 2-*O*-(2,3,4,6-tetraacetyl-α-D-mannosyl)hydroxyethyl acrylate (1.5 g, 3.4 mmol) dissolved in DCM (5 mL) and methanol (4 mL) and stirred for 3 minutes before quenching with DOWEX 50WX8 ion-exchange resin for 30 minutes. The glycomonomer was isolated by silica column chromatography using 2:8 methanol in DCM as an eluent (368 mg, 39%).

^{1}H NMR (300 MHz, MeOD): δ6.40 (d, 1H, C*H*$_2$═CH), 6.19 (m, CH$_2$═C*H*), 5.90 (d, 1H, C*H*$_2$═CH), 4.80 (d, H-1), 4.34 (m, 2H, OCH$_2$C*H*$_2$OC═O), 3.94 (m, 1H, OC*H*$_2$CH$_2$OC═O), 3.58-3.81 (m, 7H, H-2,3,4,5, H$_2$-6, OC*H*$_2$CH$_2$OC═O).

3.5.12. 2-Acetamido-1,3,4,6-tetraacetyl-2-deoxy-α-D-glucose

Acetic anhydride (47 mL, 0.5 mol) was added to a solution of D-glucosamine hydrochloride (10 g, 46 mmol) and 4-dimethylaminopyridine (10 mg) dissolved in pyridine (50 mL) and stirred for 72 hours. The reaction was chilled in an ice bath and sodium bicarbonate was gradually added until no gas evolved. The product was extracted with ethyl acetate, washed with brine, concentrated in vacuo, and crystallized with ethanol (15 g, 84%).

^{1}H NMR (300 MHz, CDCl$_3$): δ6.18 (d, H-1), 5.61 (d, H-4), 5.24 (m, H-2,3), 4.52 (m, -NH), 4.27 (dd, 1H, H$_2$-6), 4.09 (dd, 1H, H$_2$-6), 4.02 (m, H-5), 1.95-2.21 (s, 15H, 5 CH$_3$).

3.5.13. 2-Methyl-2-(3,4,6-triacetyl-1,2-dideoxy-α-D-glucosyl)-[2,1-d]-2-oxazoline

Trimethylsilyl trifluoromethanesulfonate (1 mL, 5.5 mmol) was added to a solution of 2-acetamido-1,3,4,6-tetraacetyl-2-deoxy-α-D-glucose (2.0 g, 5.1 mmol) dissolved in dichloroethane (9 mL) and heated at 50 °C for 21 hours before quenching with triethylamine (1 mL). The reaction was washed with DI water (4×) and dried with sodium sulfate. The product

was isolated by silica column chromatography using 9:1 ethyl acetate in hexanes as an eluent (1.5 g, 88%).

^{1}H NMR (300 MHz, $CDCl_3$): δ5.94 (d, H-1), 5.24 (t, H-3), 4.91 (d, H-4), 4.16 (m, H-5, H_2-6), 3.60 (m, H-2), 2.07 (s, 12H, 4 CH_3).

3.5.14. 2-*O*-(2-Acetamido-3,4,6-triacetyl-2-deoxy-β-D-glucosyl)hydroxyethyl acrylate

Trifluoromethanesulfonic acid (25 µL, 0.3 mmol) was added to a solution of 2-methyl-2-(3,4,6-triacetyl-1,2-dideoxy-α-D-glucosyl)-[2,1-d]-2-oxazoline (1.0 g, 3 mmol) and hydroxyethyl acrylate (0.54 mL, 4.7 mmol) dissolved in dichloroethane (8.3 mL) and heated at 60 °C for 6 hours before quenching with triethylamine and diluting with DCM. The reaction was washed with DI water (2×), washed with brine, dried with sodium sulfate, and crystallized from diethyl ether (1.0 g, 75%).

^{1}H NMR (300 MHz, $CDCl_3$): δ6.44 (d, 1H, C*H*$_2$═CH), 6.14 (m, CH_2═C*H*), 5.87 (d, 1H, C*H*$_2$═CH), 5.67 (d, H-4), 5.30 (t, H-2), 5.04 (t, H-3), 4.78 (d, H-1), 4.43 (m, -NH), 4.25 (m, 2H, OCH_2CH_2OC═O), 4.15 (dd, 1H, H_2-6), 4.02 (m, 1H, O*CH*$_2$$CH_2OC$═O), 3.86 (m, 2H, H_2-6, O*CH*$_2$$CH_2OC$═O), 1.91-2.08 (s, 12H, 4 CH_3).

3.5.15. 2-*O*-(2-Acetamido-2-deoxy-β-D-glucosyl)hydroxyethyl acrylate

Sodium methoxide (1 mL, 0.2 M) was added to a solution of 2-*O*-(2-acetamido-3,4,6-triacetyl-2-deoxy-β-D-glucosyl)hydroxyethyl acrylate (511 mg g, 1.1 mmol) dissolved in DCM (2.5 mL) and methanol (1.5 mL) and stirred for 1 minutes before quenching with DOWEX 50WX8 ion-exchange resin for 30 minutes. The glycomonomer was isolated by silica column chromatography using 2:8 methanol in DCM as an eluent (106 mg, 29%).

^{1}H NMR (300 MHz, MeOD): δ6.40 (d, 1H, C*H*$_2$═CH), 6.16 (m, CH_2═C*H*), 5.88 (d, 1H, C*H*$_2$═CH), 4.47 (d, H-1), 4.28 (m, 2H, OCH_2CH_2OC═O), 4.04 (m, 1H, O*CH*$_2$$CH_2OC$═O), 3.88

(dd, 1H, H_2-6), 3.78 (m, 1H, OC*H*$_2$CH$_2$OC═O), 3.65 (m, 3H, H-3,4, H_2-6), 3.46 (t, H-2), 3.32 (m, H-5).

3.5.16. 1,2:3,4-Di-*O*-isopropylidene-α-D-galactose

D-Galactose (20 g, 111 mmol) was dissolved in acetone (300 mL, 4.1 mol), and sulfuric acid (1.5 mL, 28 mmol) was added at room temperature for 24 hours. The insoluble galactose was filtered and recycled. The filtrate was neutralized with sodium bicarbonate, and the solvent was removed in vacuo. The resultant syrup was dissolved in DCM and washed with brine (3×). The DCM was removed in vacuo and the product was distilled (19 g, 65%).

^{1}H NMR (300 MHz, $CDCl_3$): δ5.56 (d, H-1), 4.61 (dd, H-3), 4.34 (dd, H-2), 4.28 (dd, H-4), 3.87 (m, 2H, H_2-6), 3.73 (m, H-5), 1.52, 1.46, 1.33 (s, 12H, 4 CH_3).

3.5.17. Acryloyl-1,2:3,4-di-*O*-isopropylidene-α-D-galactose

Acryloyl chloride (0.63 mL, 7.8 mmol) in DCM (2.26 mL) was added dropwise to a solution of 1,2:3,4-di-*O*-isopropylidene-α-D-galactose (1 g, 4.2 mmol) and triethylamine (1.34 mL, 9.6 mmol) in DCM (10 mL) at 0°C and allowed to warm to room temperature and stir for 16 hours. The solution was washed with brine (3×), dried with sodium sulfate, and purified by silica dry vacuum column chromatography (0-50% EtOAc, hexanes). Fractions with R_f = 0.80 in 50% EtOAc/hexanes were combined and concentrated to yield a pale yellow syrup that was passed through basic alumina with DCM (0.89 g, 74%).

^{1}H NMR (300 MHz, $CDCl_3$): δ6.44 (d, 1H, C*H*$_2$=CH), 6.17 (m, CH$_2$=C*H*), 5.84 (d, 1H, C*H*$_2$=CH), 5.55 (d, H-1), 4.63 (dd, H-3), 4.24-4.41 (m, 4H, H-2, H-4, H_2-6), 4.07 (m, H-5), 1.52, 1.46, 1.34 (s, 12H, 4 CH_3).

3.5.18. Trityl-1,2,3,4-tetraacetate-β-D-glucose

D(+)-glucose (20 g, 111 mmol), triphenylmethyl chloride (34 g, 122 mmol) and pyridine (80 mL) were combined and heated to 100°C for 20 minutes, after which acetic anhydride (60 mL, 636 mmol) was added and stirred overnight at room temperature. The solution was precipitated in vigorously stirred acetic acid (1.5 L, 3%) at 0°C for three hours. The precipitate was crystallized in diethyl ether (300 mL) and recrystallized in ethanol yielding fine crystals (20 g, 30%).

^{1}H NMR (300 MHz, $CDCl_3$): δ7.20-7.50 (m, 15H, φ), 5.73 (d, H-1), 5.1-5.3 (m, H-2,3,4), 3.70 (m, H-5), 3.00-3.40 (m, 2H, H_2-6), 1.76, 2.00, 2.06, 2.18 (s, 12H, 4 CH_3).

3.5.19. 1,2,3,4-Tetraacetate-β-D-glucose

6-trityl-β-D-glucose-1,2,3,4-tetraacetate (19.26 g, 32.6 mmol) was heated in acetic acid (100 mL, glacial) until dissolved. Hydrobromic acid in acetic acid (10 mL, 33 wt%) was added at 10°C and shaken vigorously for 45 seconds. The solution was filtered into DI water (500 mL) at 4°C. The product was extracted with DCM, washed with cold water, dried with sodium sulfate, and crystallized from diethyl ether, yielding white crystals (4.5 g, 40%).

^{1}H NMR (300 MHz, $CDCl_3$): δ5.73 (d, H-1), 5.28 (t, H-3), 5.1 (m, H-2,4), 3.78 (m, H-5), 3.61 (m, 2H, H_2-6), 2.00-2.15 (s, 12H, 4 CH_3).

3.5.20. Methacryloyl-1,2,3,4-tetraacetate-β-D-glucose

Methacrylic anhydride (1.1 mL, 7.4 mmol) in DCM (11 mL) was added dropwise to β-D-glucose-1,2,3,4-tetraacetate (1.6 g, 4.7 mmol) and triethylamine (1 mL, 7.5 mmol) in DCM (33 mL) at 0°C overnight. The reaction was wash with water (5×), dried with sodium sulfate, and purified by silica gradient column chromatography with a 1:1 ethyl acetate:hexanes mixture (1.9 g, 99%).

^{1}H NMR (300 MHz, $CDCl_3$): δ6.15 (s, 1H, C*H*$_2$═CCH$_3$), 5.73 (d, H-1), 5.61 (s, 1H, C*H*$_2$═CCH$_3$), 5.26 (m, H-3), 5.14 (m, H-2,4), 4.26 (m, 2H, H$_2$-6), 3.90 (m, H-5), 2.00-2.15 (s, 12H, 4 CH$_3$), 1.96 (s, CH$_2$═CC*H*$_3$).

3.5.21. *N*-Fmoc-6-trityl-1,3,4-triacetyl-D-glucosamine

9-Fluorenylmethoxycarbonyl chloride (Fmoc-Cl) (23 g, 89 mmol) was dissolved in *p*-dioxane (130 mL) and added to a solution of D-glucosamine hydrochloride (19 g, 88 mmol) and sodium bicarbonate (21 g, 250 mmol) dissolved in water (250 mL) cooled to 0°C and stirred for 16 hours. The precipitate was filtered, washed with toluene and water, dried, and used without further purification (28 g, 80%). Triphenylmethyl chloride (22 g, 78 mmol) was added to the Fmoc-protected glucosamine (28 g, 71 mmol) dissolved in pyridine (300 mL) at room temperature for 24 hours before the addition of acetic anhydride (150 mL, 1.6 mol). The solution was stirred for 24 hours and precipitated in water. The solid was collected and purified via silica gel column chromatography using 2:3 ethyl acetate in hexanes as an eluent (43 g, 80%).

^{1}H NMR (300 MHz, $CDCl_3$): δ7.00-8.00 (m, 24H, Fmoc, Trt, NH), 6.33 (d, H-1), 5.10-5.40 (m, H-2,3,4), 4.20-4.50 (m, 3H, Fmoc), 3.91 (m, H-5), 3.06-3.32 (dd, 2H, H$_2$-6), 1.80-2.20 (s, 9H, 3 CH$_3$).

3.5.22. *N*-Fmoc-1,3,4-triacetyl-D-glucosamine

N-Fmoc-6-trityl-1,3,4-triacetyl-D-glucosamine (2 g, 2.60 mmol) was dissolved in acetic acid (10 mL) and chilled to 10 °C. Hydrobromic acid in acetic acid (1 mL, 33%) was added and the mixture was shaken vigorously for 45 seconds and filtered into cold DI water (200 mL). The precipitate that formed in the water was collected by filtration and the product was isolated by silica column chromatography using 4:1 ethyl acetate in hexanes (215 mg, 16%).

^{1}H NMR (300 MHz, $CDCl_3$): δ7.00-8.00 (m, 8H, Fmoc), 6.24 (d, H-1), 5.32 (t, H-3), 5.17 (m, H-2,4), 4.20-4.50 (m, 3H, Fmoc), 3.85 (m, H-5), 3.65 (m, 2H, H_2-6), 1.80-2.25 (s, 9H, 3 CH_3).

3.5.23. *N*-Fmoc-6-acryloyl-1,3,4-triacetyl-D-glucosamine

Method 1

Acryloyl chloride (100 µL, 1.2 mmol) dissolved in DCM (1.4 mL) was added dropwise to a solution of *N*-Fmoc-1,3,4-triacetyl-D-glucosamine (215 mg, 0.41 mmol) and triethylamine (185 µL, 1.3 mmol) dissolved in DCM (4.3 mL) at 0 °C and stirred at room temperature for 16 hours. The solution was washed with water, washed with a saturated sodium bicarbonate solution (3×), washed brine, dried with sodium sulfate, and purified via silica gel column chromatography using 1:1 ethyl acetate in hexanes as an eluent (108 mg, 46%).

Method 2

Hydrochloric acid (1 mL) was added dropwise to *N*-Fmoc-6-trityl-1,3,4-acetyl-D-glucosamine (43 g, 56 mmol) dissolved in acryloyl chloride (160 mL, 2 mol) and stirred for 16 hours at room temperature. The reaction was quenched by dropwise addition into an ice-cold sodium bicarbonate solution. The compound was extracted with DCM, washed with a saturated sodium bicarbonate solution (3×) and brine, dried with sodium sulfate, and purified via silica gel column chromatography using 1:1 ethyl acetate in hexanes as an eluent (17.5 g, 54%).

^{1}H NMR (300 MHz, $CDCl_3$): δ7.30-7.80 (m, 9H, Fmoc, NH), 6.44 (d, 1H, C*H*$_2$═CH), 6.18 (m, H-1, CH_2═C*H*), 5.89 (d, 1H, C*H*$_2$═CH), 5.23 (m, H-3,4), 5.03 (d, H-2), 4.11-4.52 (m, 5H, Fmoc, H_2-6), 4.06 (m, H-5), 2.00-2.19 (s, 9H, 3 CH_3).

3.5.24. *N*-Fmoc-6-acryloyl-D-glucosamine (1)

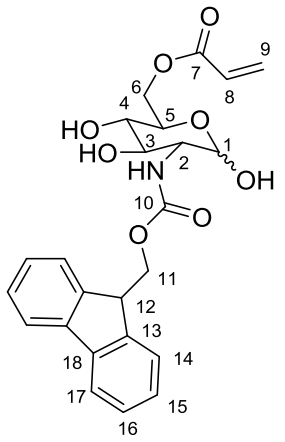

Sodium methoxide (4 mL, 0.2 M) was added to *N*-Fmoc-6-acryloyl-1,3,4-acetyl-D-glucosamine (1 g, 1.7 mmol) dissolved in DCM (20 mL) and methanol (16 mL) and stirred for 10 minutes and quenched with DOWEX 50WX8 ion-exchange resin for 30 minutes. The compound was purified via silica gel column chromatography using 9:1 ethyl acetate in hexanes as an eluent (62 mg, 7%).

^{1}H NMR (300 MHz, MeOD): δ7.31-7.82 (m, 8H, Fmoc), 6.42 (d, 1H, C*H*$_2$═CH), 6.21 (m, CH$_2$═C*H*), 5.90 (d, 1H, C*H*$_2$═CH), 5.13 (d, H-1), 4.20-4.47 (m, 5H, H$_2$-6, Fmoc), 4.05 (m, H-5), 3.71 (d, H-3), 3.62 (dd, H-2), 3.37 (m, H-4). ^{13}C NMR (400 MHz, MeOD): δ167.68 (C$_7$), 158.88 (C$_{10}$), 145.41 (C$_{13}$), 142.56 (C$_{18}$), 131.70 (C$_9$), 129.43 (C$_8$), 128.77 (C$_{16}$), 128.16 (C$_{17}$), 126.27 (C$_{15}$), 120.90 (C$_{14}$), 97.24 (C$_{β-1}$), 92.97 (C$_{α-1}$), 75.82 (C$_{β-3}$), 75.27 (C$_{β-5}$), 72.62 (C$_{α-5}$), 72.50 (C$_{α-3}$), 72.21 (C$_{β-4}$), 70.75 (C$_{α-4}$), 67.99 (C$_{11}$), 65.07 (C$_6$), 60.27 (C$_{β-2}$), 57.55 (C$_{α-2}$), 48.49 (C$_{12}$).

3.5.25. Methyl *N*-Fmoc-6-trityl-3,4-diacetyl-β-D-glucosaminoside

Methyl *N*-Fmoc-β-D-glucosaminoside (2.64 g, 6.4 mmol) was synthesized as reported[210] and was dissolved in pyridine (140 mL). Triphenylmethyl chloride (8.9 g, 32 mmol) was added at room temperature and stirred for 16 hours followed by the addition of acetic anhydride (15 mL, 159 mmol) and stirred for an additional 16 hours. The reaction was precipitated in ice water,

filtered, dissolved in DCM, washed with brine, and concentrated. The product was purified by a silica plug eluting a trityl byproduct with 20% ethyl acetate in hexanes and eluting the product with 50% ethyl acetate in hexanes. The product was crystallized in ethyl acetate to produce fine white crystals (3.9 g, 83%).

^{1}H NMR (300 MHz, $CDCl_3$): δ7.20-7.90 (m, 24H, Fmoc, Trt), 5.21 (br, H-3), 5.4.92 (br, H-4), 4.20-4.60 (br, 4H, H-5, Fmoc), 3.50-3.90 (br, 4H, H-2, OMe), 3.28 (br, H-1), 3.16 (br, H_2-6), 1.81-2.03 (s, 6H, 2 CH_3).

3.5.26. Methyl *N*-Fmoc-3,4-diacetyl-β-D-glucosaminoside

Hydrobromic acid in acetic acid (2.5 mL, 33 wt%) was added to methyl 6-trityl-3,4-diacetyl-2-*N*-Fmoc glycosaminoside (3.9 g, 5.3 mmol) dissolved in glacial acetic acid (180 mL) at room temperature for 3 minutes before quenching by pouring the reaction into ice water. The product was extract with DCM, dried with sodium sulfate, concentrated, and crystallized in diethyl ether to produce white crystals (1.56 g, 59%).

^{1}H NMR (300 MHz, $CDCl_3$): δ7.20-7.80 (m, 8H, Fmoc), 5.31 (br, H-3), 5.03 (br, H-4), 4.10-4.60 (br, 4H, H-5, Fmoc), 3.27-3.92 (br, 6H, H-2, H_2-6, OMe), 3.16 (br, H-1), 1.77-2.18 (s, 6H, 2 CH_3).

3.5.27. Methyl *N*-Fmoc-6-acryloyl-3,4-diacetyl-β-D-glucosaminoside

Acryloyl chloride (55 µL, 0.68 mmol) dissolved in DCM (5 mL) was added dropwise to methyl *N*-Fmoc-3,4-diacetyl-β-D-glucosaminoside (189 mg, 0.38 mmol) and triethylamine (105 µL, 0.76 mmol) dissolved in DCM (20 mL) chilled in an ice bath. The reaction was warmed to room temperature and stirred for 16 hours followed by washing with water, saturated sodium bicarbonate solution (3×), brine, and drying with sodium sulfate. The solution was concentrated and crystallized in methanol (120 mg, 57%).

^{1}H NMR (300 MHz, $CDCl_3$): δ7.20-7.80 (m, 8H, Fmoc), 6.45 (d, 1H, C*H*$_2$═CH), 6.17 (m, CH_2═C*H*), 5.87 (d, 1H, C*H*$_2$═CH), 5.09 (br, H-3,4), 4.10-4.60 (br, 6H, H-5, H_2-6, Fmoc), 3.27-3.92 (br, 4H, H-2, OMe), 3.08 (br, H-1), 1.77-2.18 (s, 6H, 2 CH_3).

3.5.28. Methyl *N*-Fmoc-6-acryloyl-β-D-glucosaminoside (2)

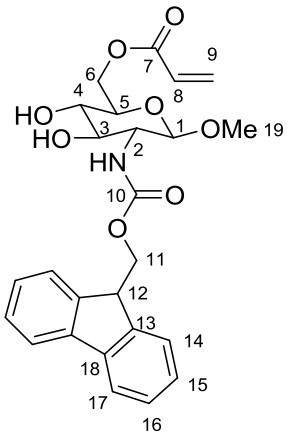

Methyl *N*-Fmoc-β-D-glucosaminoside (1.5 g, 3.6 mmol) was synthesized as reported[210] and dissolved in THF (60 mL) with triethylamine (625 µL, 4.5 mmol) in an ice bath. Acryloyl chloride (300 µL, 3.6 mmol) was dissolved in THF (15 mL) and added dropwise with vigorous stirring for 16 hours. The compound was precipitated into cold water, extracted with ethyl acetate, washed with a saturated solution of sodium bicarbonate (3×) and brine, dried with sodium sulfate, and purified via silica gel column chromatography using ethyl acetate as an eluent. The white solid was recrystallized from methanol (756 mg, 45%).

^{1}H NMR (300 MHz, MeOD): δ7.20-7.71 (m, 8H, Fmoc), 6.34 (d, 1H, C*H*$_2$═CH), 6.14 (m, CH_2═C*H*), 5.85 (d, 1H, C*H*$_2$═CH), 4.46 (m, H-1), 4.00-4.40 (m, 5H, H_2-6, Fmoc), 3.25-3.60 (m, 7H, H-2, H-3, H-4, H-5, -OMe). ^{13}C NMR (400 MHz, MeOD): δ167.58 (C_7), 159.04 (C_{10}), 145.35 (C_{13}), 142.56 (C_{18}), 131.80 (C_9), 129.36 (C_8), 128.74 (C_{16}), 128.13 (C_{17}), 126.29 (C_{15}), 120.89 (C_{14}), 103.95 (C_1), 75.81 (C_3), 75.22 (C_5), 72.16 (C_4), 67.82 (C_{11}), 64.79 (C_6), 58.80 (C_2), 57.12 (C_{19}), 48.66 (C_{12}).

3.5.29. Hydroxyethyl 3,4,6-triacetyl-β-D-glucosaminoside

Tri-*O*-acetyl-2-amino-2-deoxy-α-glucopyranosyl bromide hydrobromide (12.5 g, 27.5 mmol) was synthesized as report[210] and dissolved in ethylene glycol (250 mL, 4.4 mol). Pyridine (2.5 mL, 31 mmol) was added and stirred at room temperature for 4 days. The solution was diluted with sodium carbonate (aq) (250 mL, 5%), extracted with chloroform (3×), concentrated, and crystallized by adding hexanes (4.0 g, 41%).

^{1}H NMR (300 MHz, $CDCl_3$): δ5.02 (m, H-3,4), 4.36 (d, H_2-6), 4.23 (m, H-5, H_2-6), 3.93 (m, OCH_2CH_2OH), 3.78 (m, H-2, OCH_2CH_2OH), 2.95 (td, H-1), 2.00-2.12 (s, 9H, 3 CH_3).

3.5.30. Hydroxyethyl β-D-glucosaminoside

Hydroxyethyl 3,4,6-triacetyl-β-D-glucosaminoside (303 mg, 0.87 mmol) was dissolved in a solution of acetyl chloride (1.66 mL) and methanol (8 mL) and stirred for 24 hours. The solution was concentrated in vacuo, and the product was crystallized by adding ethyl acetate (120 mg, 54%).

^{1}H NMR (300 MHz, MeOD): δ4.59 (d, H-1), 4.02 (H-5), 3.89 (dd, 1H, H_2-6), 3.75 (m, 3H, H_2-6, OCH_2CH_2OH), 3.69 (m, 1H, OCH_2CH_2OH), 3.51 (m, 1H, OCH_2CH_2OH), 3.35 (m, H-3, H-4), 2.88 (dd, H-2).

3.5.31. (*N*-Fmoc-3,4,6-triacetyl-β-D-glucosaminosyl)hydroxyethanol

9-Fluorenylmethoxycarbonyl chloride (3.0 g, 12 mmol) was dissolved in *p*-dioxanes (50 mL) and added gradually to a solution of hydroxyethyl 3,4,6-triacetyl-β-D-glucosaminoside (4.0 g, 12 mmol) and sodium bicarbonate (3.0 g, 36 mmol) dissolved in water (50 mL) submerged in an ice bath and stirred for 16 hours. The precipitate was filtered, dissolved in DCM, dried with sodium sulfate, concentrated, and crystallized in diethyl ether (3.6 g, 55%).

^{1}H NMR (300 MHz, $CDCl_3$): δ7.29-7.83 (m, 8H, Fmoc), 5.00 (br, H-3,4), 4.00-4.84 (br, 6H, Fmoc, H-5, H_2-6), 3.35-4.00 (br, 5H, H-2, OC*H*$_2$C*H*$_2$OH), 2.53 (br, H-1), 2.00-2.12 (s, 9H, 3 CH_3).

3.5.32. 2-*O*-(*N*-Fmoc-3,4,6-triacetyl-β-D-glucosaminosyl)hydroxyethyl acrylate

Acryloyl chloride (0.92 mL, 11.3 mmol) dissolved in DCM (25 mL) was added dropwise to (*N*-Fmoc-3,4,6-triacetyl-β-D-glucosaminosyl)hydroxyethanol (3.6 g, 6.3 mmol) and triethylamine (1.14 mL, 8.2 mmol) dissolved in DCM (125 mL) submerged in an ice bath and stirred for 16 hours. The solution was washed with water, washed with a saturated sodium bicarbonate solution (3×), washed brine, dried with sodium sulfate, concentrated, and crystallized in methanol (3.2 g, 82%).

^{1}H NMR (300 MHz, $CDCl_3$): δ7.27-7.88 (m, 8H, Fmoc), 6.37 (d, 1H, C*H*$_2$═CH), 6.05 (m, CH_2═C*H*), 5.76 (br, 1H, C*H*$_2$═CH), 2.55-5.53 (br, 14H, H-1,2,3,4,5, H_2-6, Fmoc, OC*H*$_2$C*H*$_2$OC═O), 1.80-2.18 (s, 9H, 3 CH_3).

3.5.33. 2-*O*-(*N*-Fmoc-β-D-glucosaminosyl)hydroxyethyl acrylate (3)

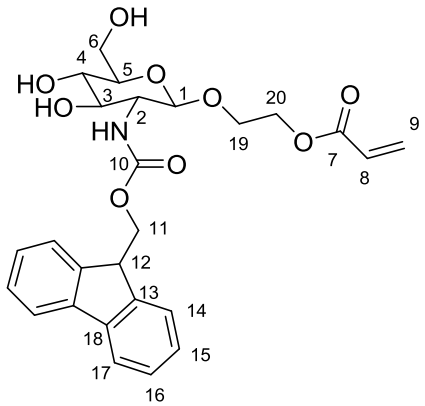

Sodium methoxide (1 mL, 0.2 M) was added to 2-*O*-(*N*-Fmoc-3,4,6-triacetyl-β-D-glucosaminosyl)hydroxyethyl acrylate (1 g, 1.6 mmol) dissolved in DCM (10 mL) and methanol (9 mL) and stirred for 10 minutes and quenched with DOWEX 50WX8 ion-exchange

resin for 30 minutes. The compound was purified via silica gel column chromatography using 1:19 methanol in ethyl acetate as an eluent and crystallized from ethyl acetate (144 mg, 18%).

^{1}H NMR (300 MHz, MeOD): δ7.31-7.82 (m, 8H, Fmoc), 6.31 (d, 1H, C*H*$_2$═CH), 6.04 (m, CH$_2$═C*H*), 5.73 (d, 1H, C*H*$_2$═CH), 4.48 (d, H-1), 4.27 (m, 5H, OCH$_2$C*H*$_2$OC═O, Fmoc), 4.08 (m, 1H, OC*H*$_2$CH$_2$OC═O), 3.91 (m, 2H, H-5, H$_2$-6), 3.82 (br, 1H, OC*H*$_2$CH$_2$OC═O), 3.72 (m, 1H, H$_2$-6), 3.48 (m, H-2), 3.41 (m, H-3), 3.36 (m, H-4). ^{13}C NMR (400 MHz, MeOD): δ167.61 (C$_7$), 158.98 (C$_{10}$), 145.38 (C$_{13}$), 142.57 (C$_{18}$), 131.65 (C$_9$), 129.32 (C$_8$), 128.78 (C$_{16}$), 128.17 (C$_{17}$), 126.32 (C$_{15}$), 120.91 (C$_{14}$), 103.09 (C$_1$), 78.00 (C$_5$), 75.83 (C$_3$), 72.13 (C$_4$), 68.29 (C$_{20}$), 67.89 (C$_{11}$), 64.88 (C$_{19}$), 62.79 (C$_6$), 58.89 (C$_2$), 49.85 (C$_{12}$).

3.5.34. Methyl 2-(phenylcarbonothioylthio)-3-hydroxypropionate

Carbon disulfide (280 μL, 4.6 mmol) was added to phenyl magnesium bromide in THF (4.08 mL, 1 M) and heated at 40 °C for 30 minutes. Methyl 2-bromo-3-hydroxypropionate (300 μL, 2.7 mmol) was added at room temperature and stirred for three hours before quenching by the addition of water. The compound was extracted with ether (5×), washed with water (5×), dried with sodium sulfate, concentrated in vacuo, and isolated by silica column chromatography using a 3:2 ethyl acetate:hexanes mixture as an eluent. R_f = 0.45 in 1:1 ethyl acetate:hexanes (386 mg, 55%).

^{1}H NMR (300 MHz, CDCl$_3$): δ7.40-8.05 (m, 5H, φ), 5.13 (dd, C*H*CH$_2$OH), 4.11 (m, CHC*H*$_2$OH), 3.81 (s, CH$_3$), 2.45 (br, OH).

3.5.35. Bis(thiobenzyl) disulfide (BTBD)

Carbon disulfide (5.25 mL, 87 mmol) was added dropwise to a phenylmagnesium bromide solution in 2-methyltetrahydrofuran (30 mL, 2.9M) diluted with THF (15 mL) at 0°C and stirred under argon. The solution was stirred for 45 minutes and quenched by the addition of water

dropwise. The THF was removed in vacuo and the solution was filtered. The product was extracted with DCM as hydrochloric acid was added until the aqueous layer was colorless. The organic layer was washed with brine (2×) and reduced to a red oil in vacuo. The oil was crystallized with ethanol (10 mL), dimethyl sulfoxide (DMSO) (2 mL), and catalytic amounts of crystalline iodine at 0 °C. The magenta crystals were filtered and washed with water (4.18 g, 31%).

^{1}H NMR (300 MHz, $CDCl_3$): δ7.40-8.10 (m, 10H, ϕ).

3.5.36. 2-Hydroxyethyl 2-bromo propionate

A solution of 2-bromopropionyl bromide (2.1 mL, 20 mmol) in DCM (30 mL) was added dropwise to a solution of ethylene glycol (22.4 mL, 400 mmol) and triethylamine (3 mL, 21 mmol) in DCM (30 mL) at 0°C and allowed to warm to room temperature and stir for 16 hours. The solution was washed with brine (3×), dried with sodium sulfate, and purified by silica dry vacuum column chromatography (0-80% EtOAc, hexanes). Fractions with R_f = 0.33 in 50% EtOAc/hexanes were combined and concentrated to yield a clear viscous liquid (1.5 g, 39%).

^{1}H NMR (300 MHz, $CDCl_3$): δ4.41 (q, 1H, BrC*H*CH_3), 4.31 (m, 2H, C*H*$_2$$CH_2OH$), 3.87 (m, 2H, CH_2C*H*$_2$OH), 1.85 (d, 3H, BrCHC*H*$_3$).

3.5.37. 2-Hydroxyethyl 2-(phenylcarbonothioylthio) propionate

2-Hydroxyethyl 2-bromo propionate (677 µL, 5.0 mmol), BTBD (1.03 g, 3.4 mmol), Cu(0) (400 mg, 6.3 mmol), and CuBr (361 mg, 2.5 mmol) were combine in toluene (20 mL). The solution was degassed by freeze-pump-thaw cycles (5×) and backfilled with argon. *N,N,N′,N′,N″*-Pentamethyldiethylenetriamine (526 µL, 2.5 mmol) was added, and the solution was degassed (3×), backfilled with argon, and heated to 80°C for 3 hours. The solution was

passed through neutral alumina with DCM, and the solvent was removed in vacuo (705 mg, 49%).

^{1}H NMR (300 MHz, $CDCl_3$): δ7.40-8.00 (m, 5H, φ), 4.78 (q, 1H, C*H*CH_3), 4.32 (m, 2H, C*H*$_2$$CH_2OH$), 3.86 (m, 2H, CH_2C*H*$_2$OH), 1.72 (d, 3H, CHC*H*$_3$).

3.5.38. 2-Acryloylethyl 2-(phenylcarbonothioylthio) propionate

Acrylic acid (400 µL, 5.9 mmol), 4-dimethylaminopyridine (36 mg, 0.3 mmol), and 1-ethyl-3-(3-dimethylaminopropyl)carbodiimide hydrochloride (567 mg, 3.0 mmol) were combined in DCM (40 mL) and stirred at room temperature for 15 minutes. 2-Hydroxyethyl 2-(phenylcarbonothioylthio) propionate (400 mg, 1.48 mmol) was added and stirred for 16 hours. The solution was washed with a saturated sodium bicarbonate solution, dried with sodium sulfate, and the solvent was removed in vacuo (356 mg, 91%).

^{1}H NMR (300 MHz, $CDCl_3$): δ7.40-8.00 (m, 5H, φ), 6.42 (d, 1H, C*H*$_2$=CH), 6.12 (m, 1H, CH_2=C*H*), 5.85 (d, 1H, C*H*$_2$=CH), 4.77 (q, 1H, C*H*CH_3), 4.42 (m, 4H, CH_2), 1.69 (d, 3H, CHC*H*$_3$).

3.5.39. 2-(Methacryloyl-2,3,4-triacetate glucopyranosyl)ethyl 2-(phenylcarbonothioylthio) propionate.

Boron trifluoride etherate (193 µL, 1.53 mmol) was added to methacryloyl-1,2,3,4-tetraacetate-β-D-glucose (138 mg, 0.51 mmol) and 2-hydroxyethyl 2-(phenylcarbonothioylthio) propionate (193 mg, 0.46 mmol) in DCM (2 mL) at 0°C overnight. The reaction was wash with water (5×), dried with sodium sulfate, and purified by silica gradient column chromatography with an ethyl acetate/hexanes mixture (102 mg, 36%).

^{1}H NMR (300 MHz, $CDCl_3$): δ7.40-8.00 (m, 5H, φ), 6.14 (s, 1H, C*H*$_2$═CCH_3), 5.60 (s, 1H, C*H*$_2$═CCH_3), 5.18 (m, H-3), 5.07 (m, H-4), 4.96 (m, H-2), 4.74 (q, 1H, C*H*CH_3), 4.56 (m, H-1),

4.26 (m, 2H, H_2-6), 4.42 (m, 4H, C*H*$_2$), 3.91 (m, H-5), 2.00-2.15 (s, 12H, 4 CH_3), 1.96 (s, CH_2═CC*H*$_3$), 1.69 (d, 3H, CHC*H*$_3$).

CHAPTER 4

Polymerization and characterization of glycopolymers

4.1. Introduction

Free-radical polymerization (FRP) continues to be the most prevalent method for creating glycopolymers via direct polymerization due to its flexibility for different initiators, monomers, and solvents.[138] In FRP, however, the molecular weight is difficult to control since polymers propagate and terminate quickly after radical initiation leading to dispersity values ($Đ = M_w/M_n$) ranging from 1.5 to 2 depending on the mode of termination. As polymerizations are taken to high conversion, dispersity values increase to as high as 50 from changes in concentrations and chain transfer. For biomedical applications, however, high dispersity values are undesirable due to the effect of molecular weight on the biological properties of the polymer, such as cytotoxicity.

In order to maintain low dispersity, controlled radical polymerization techniques have been developed. One of these controlled radical polymerization techniques is reversible addition-fragmentation chain transfer (RAFT) polymerization,[21] which is particularly useful due to its tolerance for a wide range of reaction conditions and functionalities, in particular aqueous media and biomolecules.[11,141] RAFT polymerization limits dispersity using a chain transfer agent (CTA) that reversibly limits the number of actively propagating chains, avoiding premature termination. By keeping most of the polymer chains in a dormant state and quickly transferring the radical among all the chains, the polymers grow in a uniform fashion throughout the entire course of the polymerization with molecular weight increasing proportionally with conversion.

At the completion of the polymerization, the RAFT CTA is still attached to the chain end and allows for continued polymerization by the addition of the same monomer or allows for the creation of block copolymers by the addition of a different monomer. Transformation of the RAFT CTA chain end into a free thiol can be facilitated with the addition of ethanolamine. Due to these attributes, RAFT polymerization is a particularly powerful technique for the creation of glycopolymers. In this chapter, three sets of glycopolymers are created using the glycopolymer tools synthesized in Chapter 3: 1) glycopolymers with a variety of saccharide identities linked to the polymer backbone through a glycosidic bond, 2) linear and branched glycopolymers and linear and branched amphiphilic glycopolymers of various molecular weights with galactose linked through the primary alcohol to the polymer backbone, and 3) a cationic methyl glucosaminoside glycopolymer with various molecular weights isolated via fractional precipitation.

4.2. Aqueous RAFT polymerization of glycopolymers

The glycomonomers in the first set produced in Chapter 3 (Figure 4.1) were each polymerized via RAFT polymerization using 4,4'-azobis(4-cyanovaleric acid) (ACVA) and 4-cyano-4-(thiobenzoylthio)pentanoic acid as an initiator and chain transfer agent, respectively, at 70 °C in 25% ethanolic water for 16 hours with a target degree of polymerization (DP) of 100 repeat units (Scheme 4.1). In addition, poly(2-*O*-(α-D-mannosyl)hydroxyethyl acrylate) was also polymerized with a target degree of polymerization of 250. After the polymerization was complete, the polymerization solution was extensively dialyzed to remove any residual monomer, and the DP was determined from ^{1}H NMR by comparing the saccharide proton to the CTA chain end protons (7.40-8.00 ppm). The resultant glycopolymers were lyophilized and analyzed for their molecular weight and dispersity via aqueous GPC relative to pullulan standards (Figure 4.2, Table 4.1).

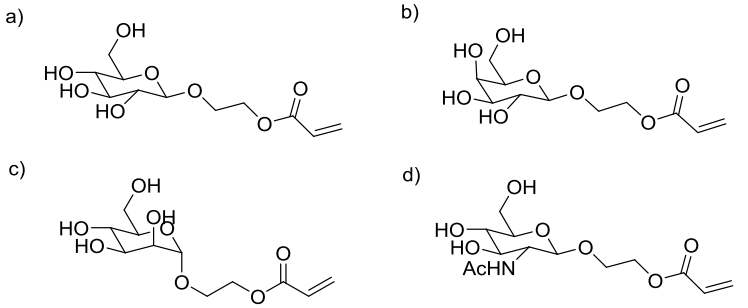

Figure 4.1. Set of deprotected glycomonomers based on a) glucose, b) galactose, c) mannose, and d) *N*-acetyl glucosamine.

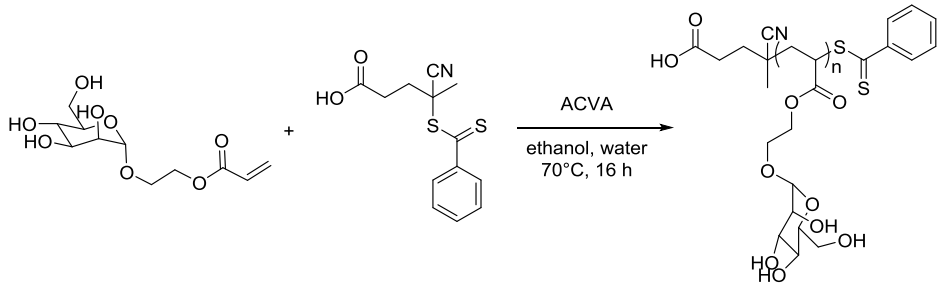

Scheme 4.1. Aqueous RAFT polymerization of deprotected glycomonomer.

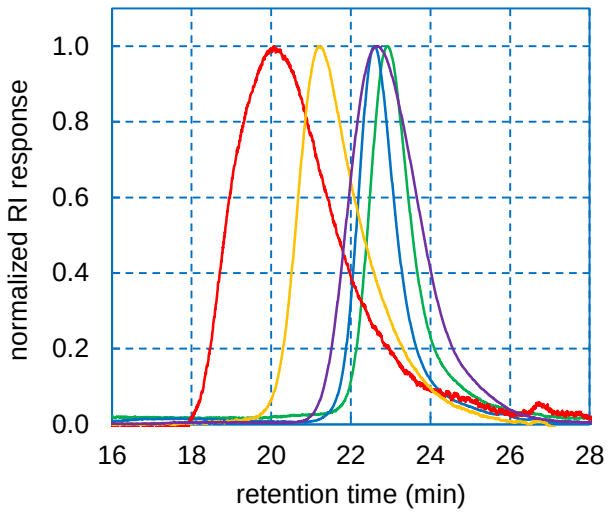

Figure 4.2. Aqueous GPC trace of mannose DP 215 polymer (red), mannose DP 108 polymer (orange), *N*-acetyl glucosamine DP 76 polymer (purple), galactose DP 76 polymer (blue), and glucose DP 65 polymer (green) relative to pullulan standards.

Table 4.1. Characterization of glucose, galactose, mannose, and *N*-acetyl glucosamine glycopolymers via ^{1}H NMR and GPC.

saccharide	DP_n[a]	M_w[b]	M_n[b]	$Đ$[b]	DP_n[c]
glucose	65	9600	6800	1.42	24
galactose	76	12000	8500	1.41	31
mannose	215	72600	37200	1.95	134
mannose	108	28700	16400	1.75	59
N-acetyl glucosamine	76	14200	8400	1.68	27

[a] Determined via ^{1}H NMR comparison of the chain end and saccharide protons.
[b] Determined via aqueous GPC relative to pullulan standards.
[c] Determined from M_n divided by the molecular weight of the monomer.

The degrees of polymerization determined via GPC were consistently lower than the degree of polymerization determined via ^{1}H NMR. Figure 4.3 shows the linear relationship between the molecular weights obtained via GPC and ^{1}H NMR. GPC separates polymers according to their hydrodynamic volume. The underestimation of molecular weight from GPC is likely due to the

hydrophobic characteristic of the glycopolymer backbone and the hydrophobic RAFT chain end, which are absent in pullulan (Figure 4.4). When dissolved in water, the glycopolymers adopt a more compact conformation to reduce the thermodynamically unfavorable interactions between the backbone and the solvent, resulting in smaller hydrodynamic volumes compared to pullulan of equivalent molecular weights.

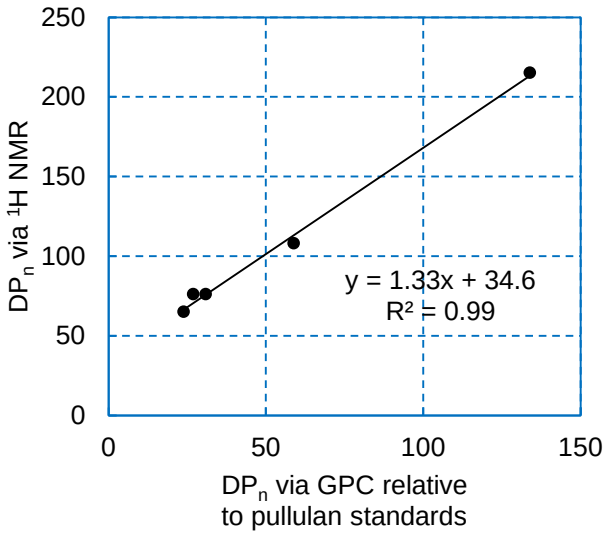

Figure 4.3. Plot and linear curve fit of the degree of polymerization (DP_n) as determined from ^1H NMR versus as determined via aqueous GPC relative to pullulan standards.

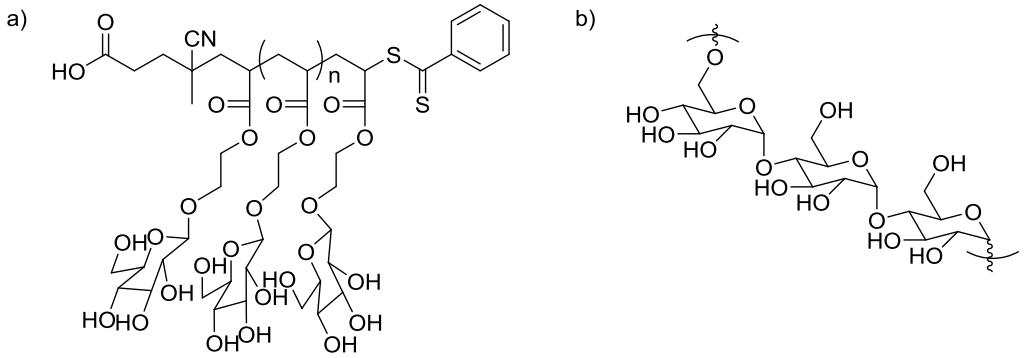

Figure 4.4. Structure of a) a glycopolymer and b) pullulan.

4.3. Polymerization of linear and branched glycopolymers

Linear and branched glycopolymers of various molecular weights were synthesized via RAFT polymerization using azobisisobutyronitrile (AIBN) as an initiator, ethyl 2-(phenylcarbonothioylthio) propionate as a CTA, 2-acryloylethyl 2-(phenylcarbonothioylthio)

propionate as a polymerizable CTA (PCTA) branching agent, acryloyl-1,2:3,4-di-*O*-isopropylidene-α-D-galactose as a monomer, and toluene as a solvent at 80°C for 72 hours. The PCTA has a polymerizable acrylate unit and a chain transfer unit, analogous to ethyl 2-(phenylcarbonothioylthio) propionate. This expected similarity in reactivity with the CTA and monomer promotes random incorporation of branching units into the glycopolymer. The isopropylidene protecting groups were removed via acidolysis with formic acid, and the RAFT chain ends were removed via aminolysis with ethanolamine (Scheme 4.2).

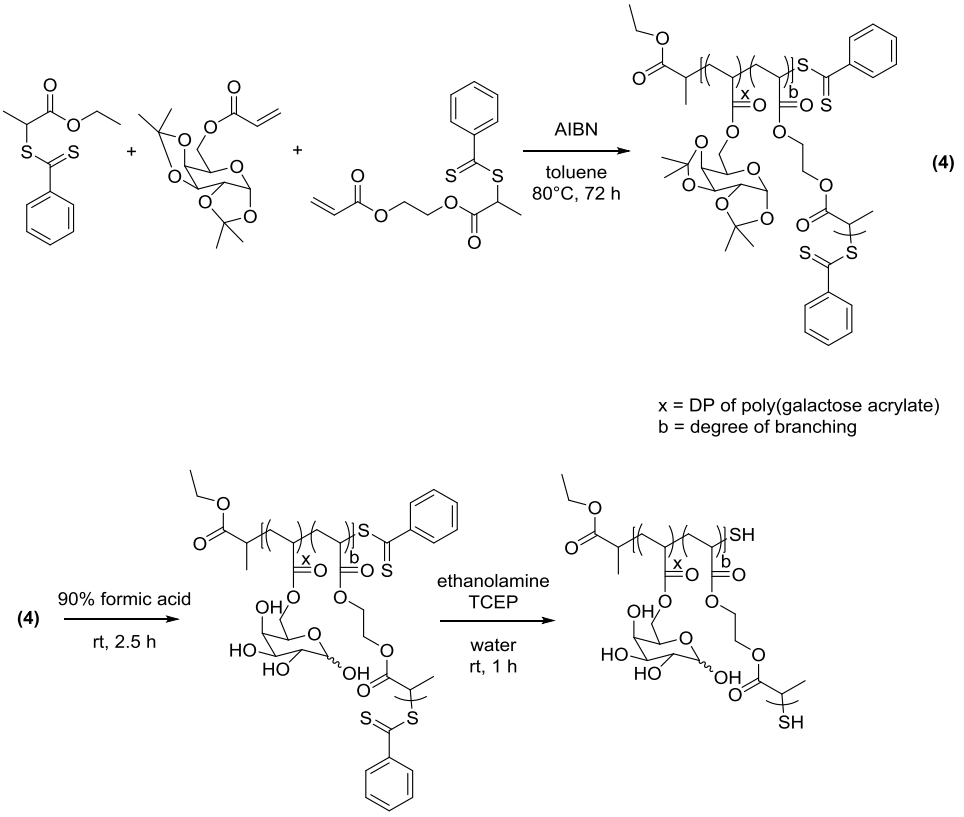

Scheme 4.2. Polymerization and deprotection of hyperbranched poly(6-acryloyl-D-galactose).

Different molecular weights of polymer were prepared by varying the $[M]_0$:$[CTA]_0$ from 12:1 to 50:1, and polymers with different degrees of branching were prepared by varying the $[PCTA]_0$:$[CTA]_0$ from 0:1 to 5:1. Polymer characterization was conducted prior to deprotection

by ^{1}H NMR and GPC in THF (Table 4.2). The DP was calculated from ^{1}H NMR by comparing the anomeric proton of the saccharide (5.56 ppm) to the CTA chain ends (7.40-8.00 ppm). By GPC, branched polymers exhibited the characteristic drop in apparent molecular weight and increase in dispersity associated with branching. GPC measures molecular weight relative to the hydrodynamic volume of known linear standards. Branched polymers are more compact and thus have smaller hydrodynamic volumes, resulting in lower molecular weights being reported by GPC.[211] The increase in dispersity is theorized to be caused by the difference in reactivity between the polymerizable unit and chain transfer unit on the PCTA.[212]

Table 4.2. Summary of glycopolymers characterization via NMR[†] and GPC[‡].

	target degree of polymerization								
	DP = 12			DP = 25			DP = 50		
degree of branching	DP[†]	M_n[‡]	$Đ$[‡]	DP[†]	M_n[‡]	$Đ$[‡]	DP[†]	M_n[‡]	$Đ$[‡]
0	9	2630	1.01	32	5410	1.02	41	7600	1.04
1	15	1530	1.17	20	2340	1.06	46	4530	1.13
5	10	1060	1.24	32	1750	1.36	58	2600	1.39

[†] Determined via ^{1}H NMR conducted in chloroform and calculated from the comparison of the chain end and saccharide protons.
[‡] Determined via GPC performed in THF and calibrated using linear poly(methyl methacrylate) standards.

4.4. Polymerization of amphiphilic glycopolymers

Taking advantage of the ability to chain-extend polymers in RAFT polymerization, amphiphilic polymers can be created. First, methyl acrylate was polymerized using ethyl 2-(phenylcarbonothioylthio) propionate as a CTA and AIBN as an initiator. The polymer then underwent chain-extension with acryloyl-1,2:3,4-di-*O*-isopropylidene-α-D-galactose (Scheme 4.3) or with acryloyl-1,2:3,4-di-*O*-isopropylidene-α-D-galactose and a PCTA to introduce a branched architecture (Scheme 4.4). The saccharide moieties were subsequently deprotected using a formic acid solution. Each copolymer was named according to the ratio of the degree of polymerization of methyl acrylate, the expected degree of polymerization of acryloyl-1,2:3,4-di-

O-isopropylidene-α-D-galactose, and the expected number of branches per chain. For example, a copolymer with poly(methyl acrylate) with a degree of polymerization of 25, poly(acryloyl-1,2:3,4-di-*O*-isopropylidene-α-D-galactose) with a target degree of polymerization of 50, and a target of five branches per chain would be named 25:50 5 branch.

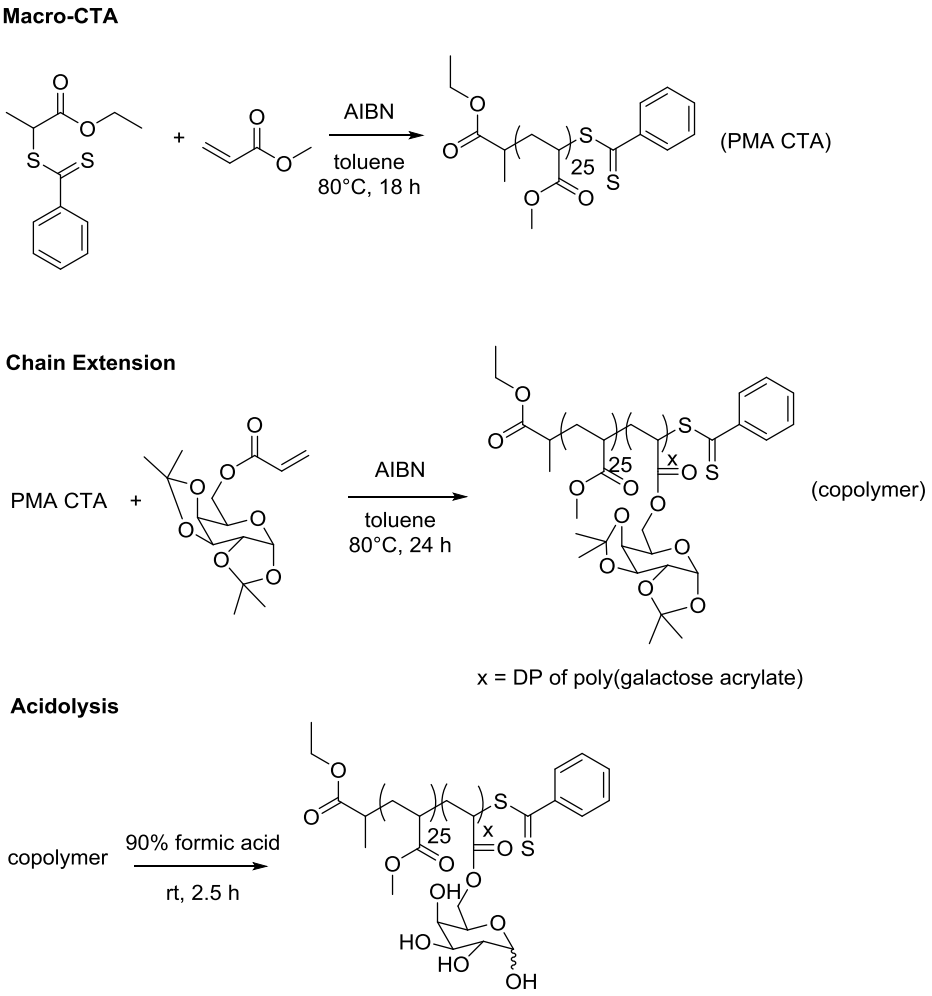

Scheme 4.3. Synthesis of linear poly(methyl acrylate-co-acryloyl-1,2:3,4-di-*O*-isopropylidene-α-D-galactose).

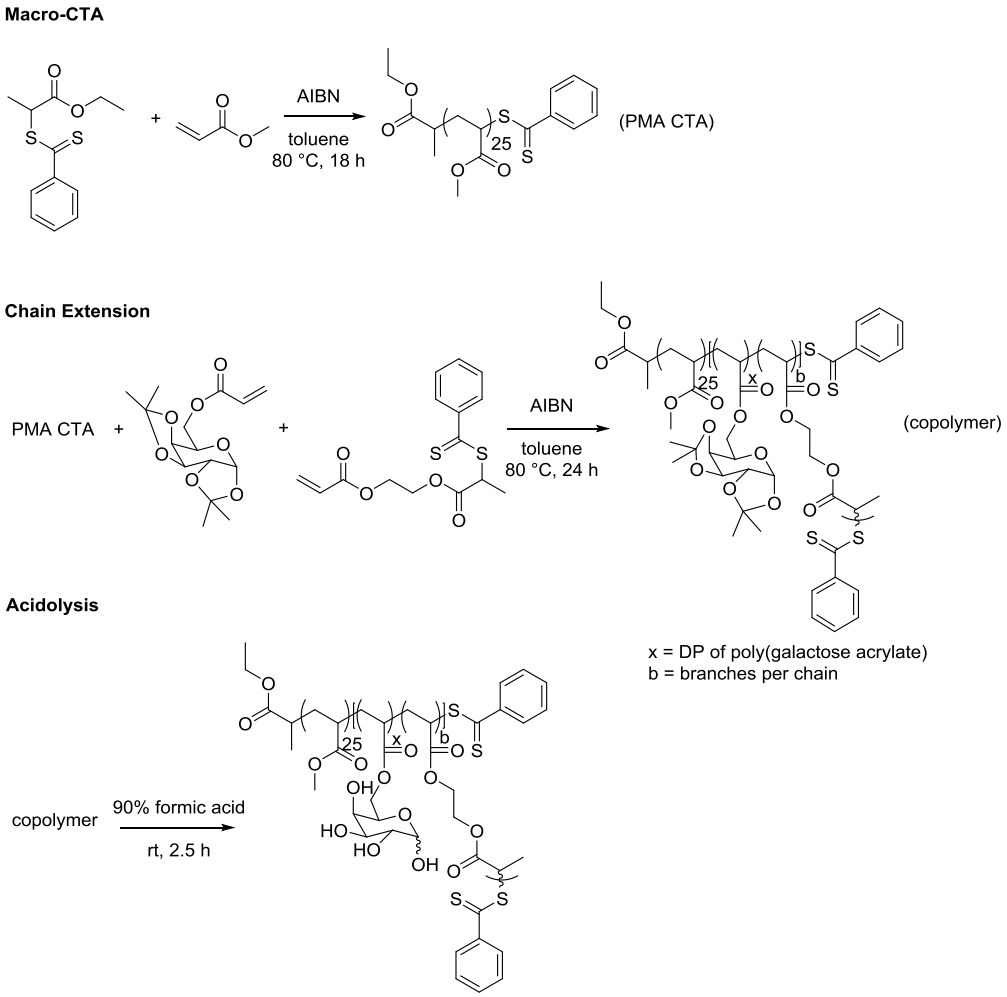

Scheme 4.4. Synthesis of branched poly(methyl acrylate-co-acryloyl-1,2:3,4-di-*O*-isopropylidene-α-D-galactose).

Copolymer chain-extension polymerization conversion was determined by ^{1}H NMR and was used to calculate the degree of polymerization of the saccharide monomer, while M_n and M_w were determined by GPC relative to poly(methyl methacrylate) standards (Figure 4.5) and used to calculate molecular weight distribution ($Đ = M_w/M_n$) (Table 4.3). As expected for copolymers with similar degrees of polymerization, as branching increased, a greater discrepancy is seen between relative molecular weights obtained by GPC and those calculated from ^{1}H NMR.

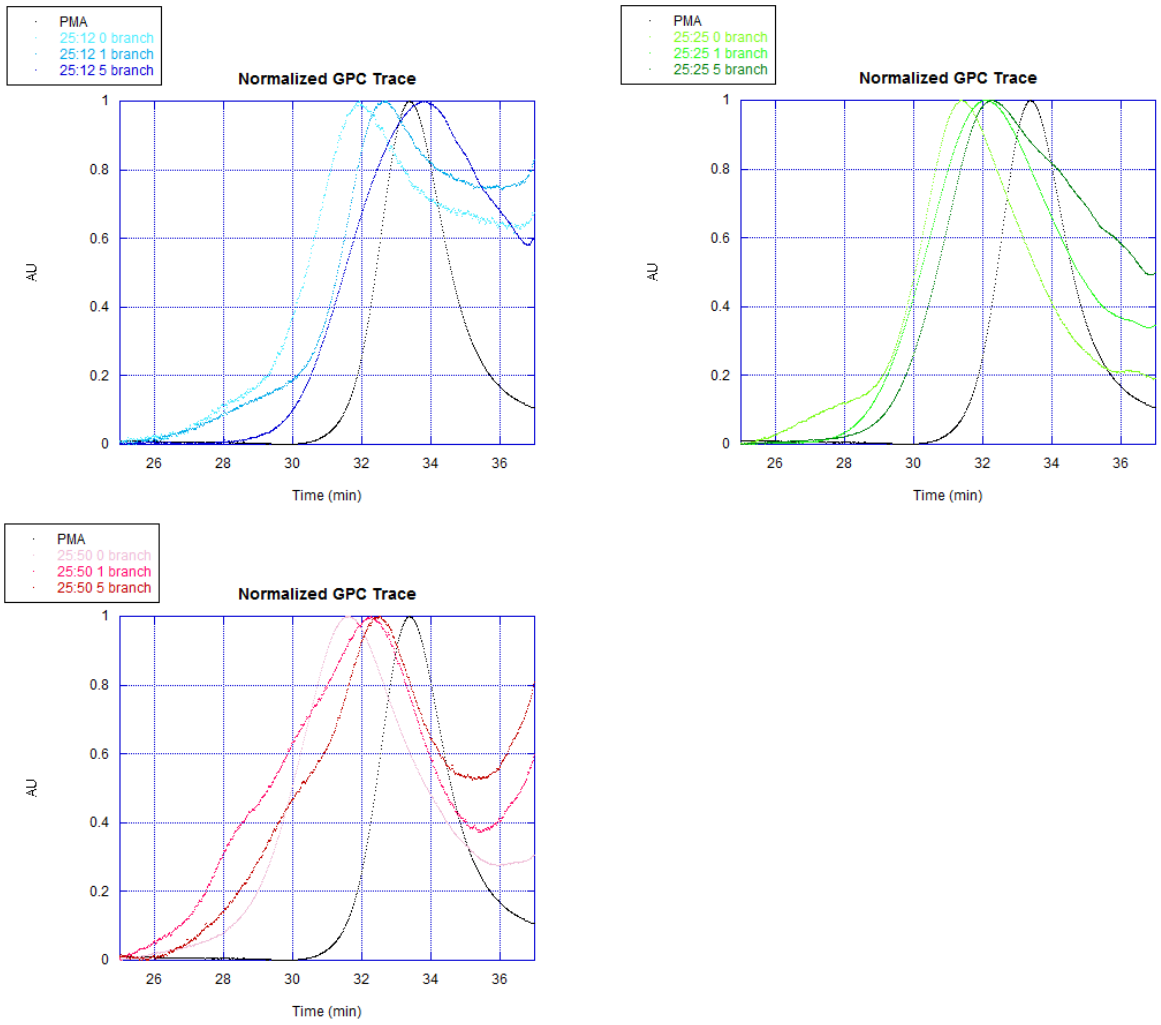

Figure 4.5. Normalized GPC traces for each copolymer in THF relative to the poly(methyl acrylate) macro-CTA (black).

Table 4.3. Summary of the characterization via NMR and GPC for each chain-extension polymerization of poly(methyl acrylate) with acryloyl-1,2:3,4-di-*O*-isopropylidene-α-D-galactose with a specified number of branches per chain.

	^{1}H NMR			GPC†		
copolymer	conversion of chain-extension	DP of sugar	M_n	M_w	M_n	$Đ$
25:50 0 branch	88%	44	16190	10270	6480	1.58
25:50 1 branch	86%	43	16170	7790	5610	1.39
25:50 5 branch	92%	46	18290	7700	5830	1.32
25:25 0 branch	90%	23	9480	7580	5870	1.29
25:25 1 branch	71%	18	8220	6790	4980	1.36
25:25 5 branch	78%	20	9800	5420	3920	1.38
25:12 0 branch	42%	5	4060	6310	4800	1.31
25:12 1 branch	30%	4	3680	4820	4130	1.17
25:12 5 branch	80%	10	6850	4230	3350	1.26

†Gel permeation chromatography (GPC) was performed in THF and calibrated using linear poly(methyl methacrylate) standards.

The incorporation of branching units was verified via ^{1}H NMR. Although the ethylene peaks corresponding to the branching unit overlap with the saccharide peaks at 4 ppm, it is possible to quantify the amount of polymerizable CTA units incorporated from the increase of the integration of the peaks at 4 ppm and also the aromatic peak at 7.9 ppm from the chain transfer unit. For example, using both integrations, the 25:50 5 branch copolymer was determined to have approximately seven branching units incorporated (Figure 4.6).

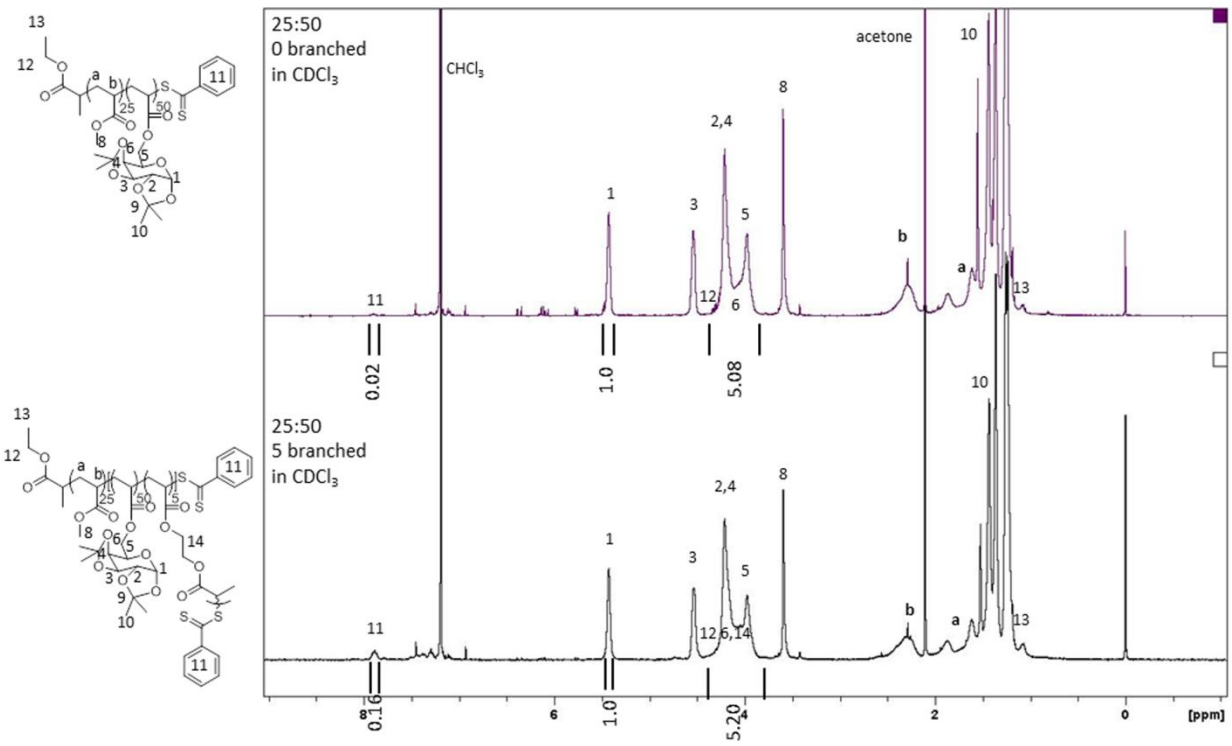

Figure 4.6. ^{1}H NMR taken in $CDCl_3$ used to quantify the incorporation of the polymerizable CTA.

After deprotection with formic acid, the amount of deprotected saccharide was determined by comparing the integration of the residual protected anomeric protons (5.5 ppm) relative to the methyl acrylate protons (3.6 ppm) (Figure 4.7). It was not possible to quantify the deprotected saccharide directly due to the overlapping peaks from the isomerization of the saccharide in DMSO-d_6 as confirmed by the ^{13}C NMR (Figure 4.8).[213] Even though the deprotected saccharide cannot be quantified, NMR does confirm that the saccharide moieties are present and retain their natural ability to isomerize while connected to the polymer backbone.

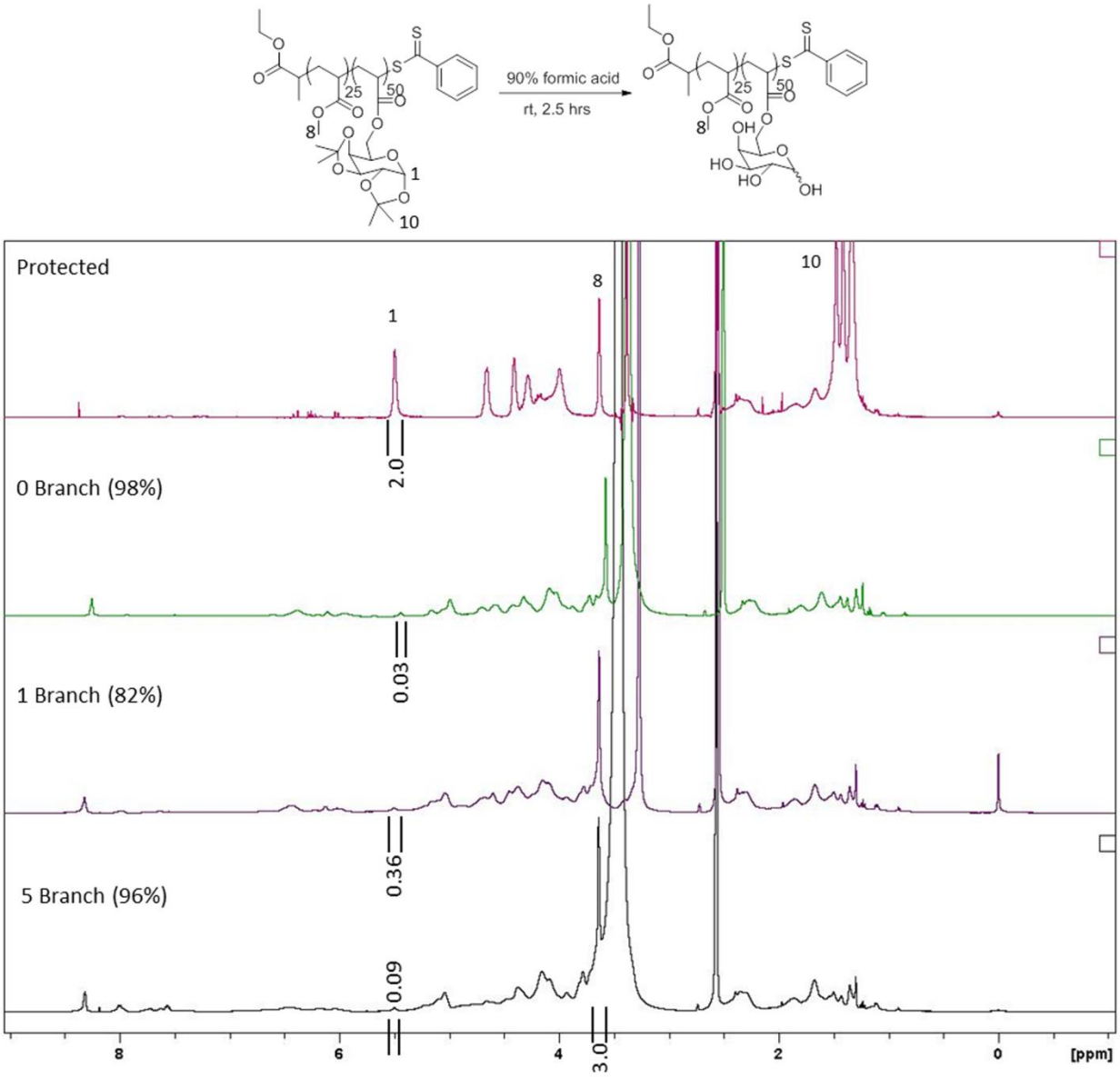

Figure 4.7. ^{1}H NMR of 25:50 0 branch protected copolymer overlaid with ^{1}H NMRs of deprotected 0, 1, and 5 branch copolymers of the same molecular weight. Percent deprotection was calculated by using the methyl acrylate peak (8) as a reference and comparing the residual integration of the protected anomeric peak (1). All NMRs were taken in DMSO-d_6.

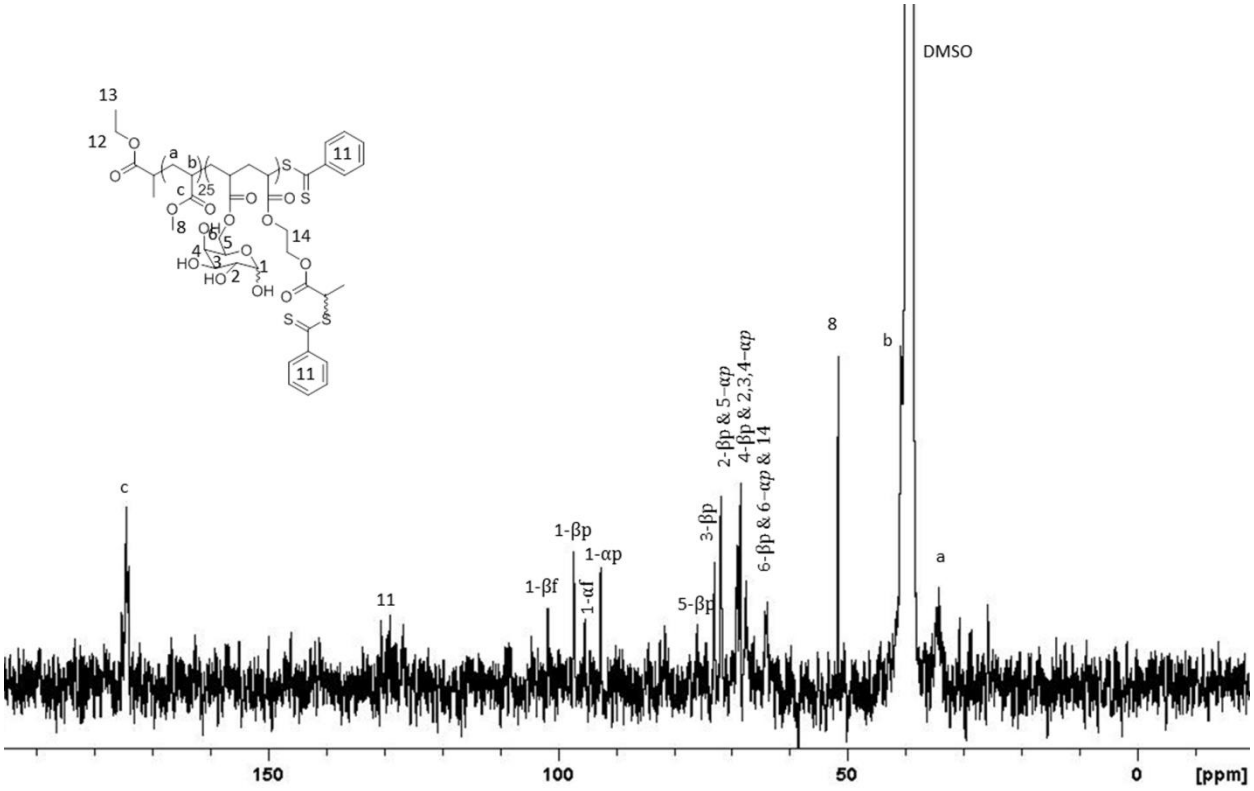

Figure 4.8. ^{13}C NMR in DMSO-d_6 of 25:50 5 branch deprotected copolymer showing the isomerization of the deprotected saccharide unit. All four isomers (α-pyranose, β-pyranose, α-furanose, β-furanose) are observed.

4.5. Polymerization of Fmoc-protected cationic glycopolymers

For the polymerization of the Fmoc-protected cationic glycopolymers, methyl *N*-Fmoc-6-acryloyl-β-D-glucosaminoside was used as a model monomer due to its relatively high yield. A number of free-radical polymerization techniques and conditions were explored. Initial investigations using RAFT polymerization failed to produce any evidence of monomer conversion via ^{1}H NMR. Based on the structural differences between methyl *N*-Fmoc-6-acryloyl-β-D-glucosaminoside and 2-*O*-(2-acetamido-2-deoxy-β-D-glucosyl)hydroxyethyl acrylate, which was polymerized by RAFT polymerization, the Fmoc group was suspected to be interfering with polymerization. A series of amine-protected monomers was synthesized (Scheme 4.5) and used to investigate the effect of incorporating Fmoc into a monomer utilized in RAFT polymerization.

Each monomer was polymerized using ethyl 2-(phenylcarbonothioylthio) propionate as a RAFT CTA and AIBN as an thermal initiator in toluene or a mixture of tetrahydrofuran/toluene at 80 °C for 70 hours after which monomer conversion was evaluated using ^{1}H NMR (Table 4.4).

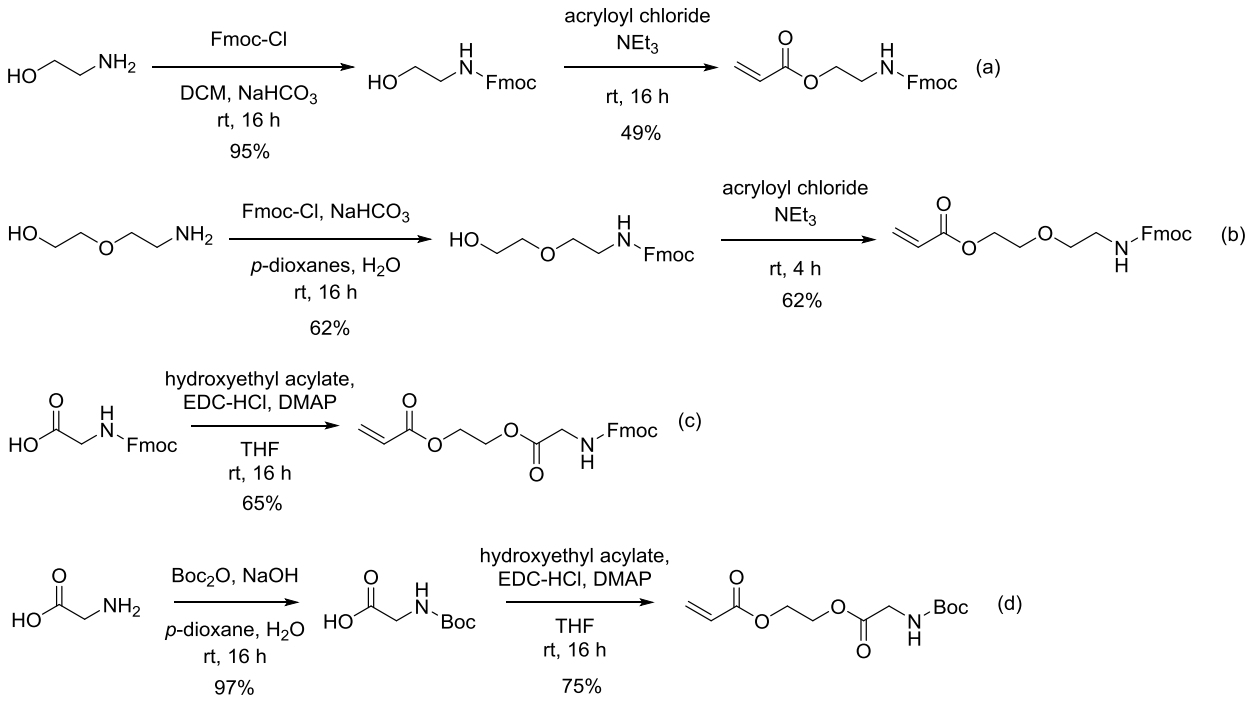

Scheme 4.5. Series of amine-protected monomers: a) *N*-Fmoc-2-aminoethyl acrylate, b) 2-(*N*-Fmoc-2-aminoethoxy)ethyl acrylate, c) Fmoc-glycine-HEA, and d) Boc-glycine-HEA.

Table 4.4. Monomer conversion of RAFT polymerizations of amine-protected monomers.

monomer	conversion[†]
N-Fmoc-2-aminoethyl acrylate	<10%
2-(*N*-Fmoc-2-aminoethoxy)ethyl acrylate	31%
Fmoc-glycine-HEA	41%
Boc-glycine-HEA	74%

[†] Determined by ^{1}H NMR in $CDCl_3$.

From the series of amine-protected monomers, monomer conversion increased as the Fmoc protecting group was distanced from the polymerizable group, and typical RAFT polymerization conversion was recovered when a *tert*-butyloxycarbonyl protecting group[214] was substituted for the Fmoc protecting group. These results suggest that the Fmoc moiety has an inhibitory effect

on free-radical polymerization, preventing the creation of high molecular weight polymers through controlled radical polymerization techniques.

Since glycopolymers via RAFT polymerization were not achievable, conventional free-radical polymerization techniques were explored. Initial investigations focused on determining a suitable polymerization solvent. Due to the amphiphilic characteristic of the glycomonomers from the deprotected alcohols and the Fmoc protecting group, glycomonomer solubility was limited to polar, organic solvents. Many of these solvents, however, facilitate the removal of the Fmoc protecting group at elevated temperatures,[215] which are necessary for thermal initiators, leading to polymerization of the monomer via a Michael addition (Scheme 4.6). Tetrahydrofuran (THF) was found to dissolve the glycomonomers while preserving the Fmoc protecting group at elevated temperatures. Employing ACVA as an initiator, glycopolymers were created in THF at 70 °C for 90 hours. Under these conditions, however, only relatively low molecular weight polymers were produced (Table 4.5). In an effort to generate higher molecular weight polymers, the monomer concentration, initiator concentration, temperature, and the type of initiator were adjusted (Table 4.6).

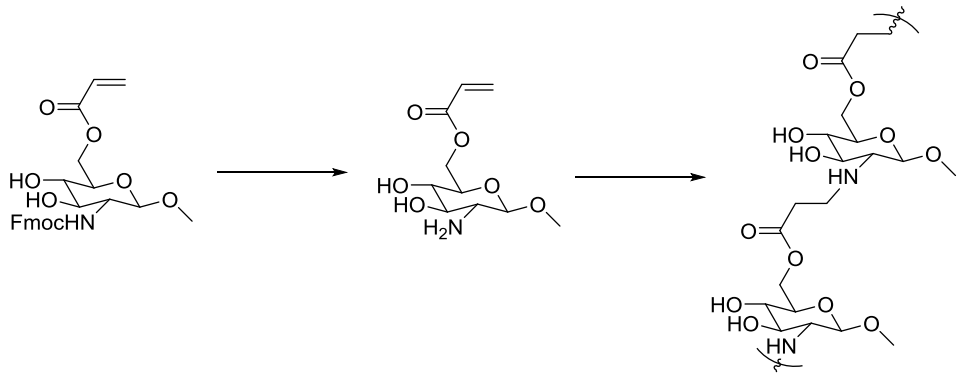

Scheme 4.6. Polymerization from the Michael addition of methyl 6-acryloyl-β-D-glucosaminoside.

For a polymerization initiated by the homolytic cleavage of a thermal initiator, the kinetic chain length (ν) is governed by Equation 4.1, where k_p is the rate constant of propagation, [*M*] is

the monomer concentration, f is the initiator efficiency, k_d is the rate constant of initiator disassociation, k_t is the rate constant of termination, and $[I]$ is the initiator concentration. For polymers that terminate via combination, the molecular weight will be equal to 2ν, whereas for polymers than terminate via disproportionation, the molecular weight will be equal to ν. Since the kinetic chain length scales with $[M]/[I]^{1/2}$, increasing monomer concentration while decreasing initiator concentration should produce polymers of higher molecular weight.

$$\nu = \frac{k_p[M]}{2(fk_dk_t[I])^{\frac{1}{2}}} \qquad \text{Equation 4.1}$$

In considering the effect of temperature on molecular weight, the energetic effect on each rate constant needs to be taken into account. In general, the rate of propagation and the molecular weight are governed by Equation 4.2 and Equation 4.3, respectively, where A is the collision frequency factor, E is the Arrhenius activation energy, and T is the Kelvin temperature. For a thermally initiated polymerization, E_R is about 80-90 kJ/mol and $E_{\bar{X}_n}$ is about -60 kJ/mol. With decreasing temperature, the molecular weight will increase while rate of propagation will decrease. In addition, a decrease in temperature also promotes higher molecular weights by reducing chain transfer.[216]

$$ln\, R_p = ln\left[A_p\left(\frac{A_d}{A_t}\right)^{\frac{1}{2}}\right] + ln\left[\left(f[I]^{\frac{1}{2}}[M]\right)\right] - \frac{E_R}{RT} \qquad \text{Equation 4.2}$$

$$ln\, \bar{X}_n = ln\left[A_p(A_dA_t)^{-\frac{1}{2}}\right] + ln\left[(f[I])^{-\frac{1}{2}}[M]\right] - \frac{E_{\bar{X}_n}}{RT} \qquad \text{Equation 4.3}$$

In addition to thermal initiators, photoinitiated polymerization was also investigated. For a pure photochemical polymerization, E_R and $E_{\bar{X}_n}$ are both approximately 20 kJ/mol indicating that both the rate of propagation and the molecular weight will increase with increasing temperature. At higher temperatures, however, photoinitiators may also initiate thermally, which would complicate the molecular weight prediction.

Table 4.5. ^{1}H NMR and GPC characterization of *N*-Fmoc-6-acryloyl-D-glucosamine, methyl *N*-Fmoc-6-acryloyl-β-D-glucosaminoside, and 2-*O*-(*N*-Fmoc-β-D-glucosaminosyl) hydroxyethyl acrylate polymerized using 4,4'-azobis(4-cyanovaleric acid) in THF at 70 °C for 90 hours.

polymer	conversion[a] (%)	M_w[b] (Da)	M_n[b] (Da)	$Đ$[b]	DP_n[c]
poly(*N*-Fmoc-6-acryloyl-D-glucosamine)	73	4042	2197	1.84	5
poly(methyl *N*-Fmoc-6-acryloyl-β-D-glucosaminoside)	55	3369	1545	2.18	3
poly(2-*O*-(*N*-Fmoc-β-D-glucosaminosyl)hydroxyethyl acrylate)	95	491	445	1.10	1

[a] Determined via ^{1}H NMR comparing the Fmoc aromatic peaks to the acrylate peaks.
[b] Determined via GPC in THF relative to polystyrene standards.
[c] Determined from M_n divided by the molecular weight of the monomer.

Table 4.6. Polymerization of methyl *N*-Fmoc-6-acryloyl-β-D-glucosaminoside with various free-radical polymerization conditions with characterization via ^{1}H NMR and GPC.

initiator	temperature (°C)	[*M*] (mM)	[*I*] (mM)	conversion[a] (%)	M_w[b] (Da)	M_n[b] (Da)	$Đ$[b]	DP_n[c]
ACVA	70	210	1.05	55	3370	1550	2.18	3
ACVA	70	790	1.43	98	3940	2760	1.43	6
ACVA	70	790	0.71	94	3980	2790	1.42	6
ACVA	50	790	0.71	47	6690	4830	1.38	10
ACVA	40	790	0.71	38	4750	3580	1.33	8
AIBN	40	790	0.71	40	4360	3290	1.32	7
Irgacure 2959	RT	833	0.83	100	7370	5250	1.40	11

[a] Determined via ^{1}H NMR comparing the Fmoc aromatic peaks to the acrylate peaks.
[b] Determined via GPC in THF relative to polystyrene standards.
[c] Determined from M_n divided by the molecular weight of the monomer.

As expected from Equation 4.1, as monomer concentration was increased, conversion and molecular weight increased, and as initiator concentration was decreased, conversion slightly decrease and molecular weight slightly increased. As temperature was decreased, there was a

drop in conversion and an increase in molecular weight as expected from Equation 4.2 and Equation 4.3. As temperature was decreased further to 40 °C, the molecular weight began to decrease, suggesting that the optimal temperature for creating high molecular weight polymer was approximately 50 °C. The use of Irgacure 2959 at room temperature produced the highest molecular weight polymer with close to quantitative conversion, making this the optimal conditions for producing high molecular weight polymer (Table 4.6). RAFT polymerization was investigated using Irgacure 2959 as an initiator, but the polymerization lost its characteristic magenta color, exhibited a decrease in conversion, and produced a bimodal distribution by GPC indicative of degradation of the RAFT CTA by UV irradiation as has been previously reported in literature.[217–219] Recent advancements in the use of visible light for initiating RAFT polymerizations[220,221] may be a viable option for creating glycopolymers via controlled radical polymerization but were not investigated herein.

The conditions used to polymerize methyl *N*-Fmoc-6-acryloyl-β-D-glucosaminoside were applied to *N*-Fmoc-6-acryloyl-D-glucosamine, and likewise, higher molecular weight polymer was produced (Table 4.7). When the same conditions were applied to 2-*O*-(*N*-Fmoc-β-D-glucosaminosyl)hydroxyethyl acrylate, however, precipitate formed during the polymerization with a conversion of only about 17%. Similar conversions were observed in other solvent systems, including mixtures of THF and methanol, dimethyl sulfoxide, and dimethylformamide, while the monomer was insoluble in water, anisole, toluene, and dichloromethane. A conversion of 40% was achieved using ammonium persulfate catalyzed with tetramethylethylenediamine, but only low molecular weight oligomers were produced similar to the size of the glycopolymer produced using thermo-initiated radical polymerization.

Table 4.7. Analysis of 1) poly(*N*-Fmoc-6-acryloyl-D-glucosamine) and 2)poly(*N*-Fmoc-6-acryloyl-D-glucosamine) (2) polymerized using Irgacure 2959 in THF.

polymer	conversion[a] (%)	M_w[b] (Da)	M_n[b] (Da)	$Đ$[b]	DP_n[c]
1	92	4650	3420	1.36	8
2	100	7370	5250	1.40	11

[a] Determined via ^{1}H NMR comparing the Fmoc aromatic peaks to the acrylate peaks.
[b] Determined via GPC in THF relative to polystyrene standards.
[c] Determined from M_n divided by the molecular weight of the monomer.

In order to obtain a series of glycopolymers with various molecular weights and reduced dispersity of each sample produced by photoinitiated polymerization, the glycopolymers were dissolved in THF and subjected to fractional precipitation using methanol as a nonsolvent (Figure 4.9, Table 4.8, Figure 4.10, Table 4.9).

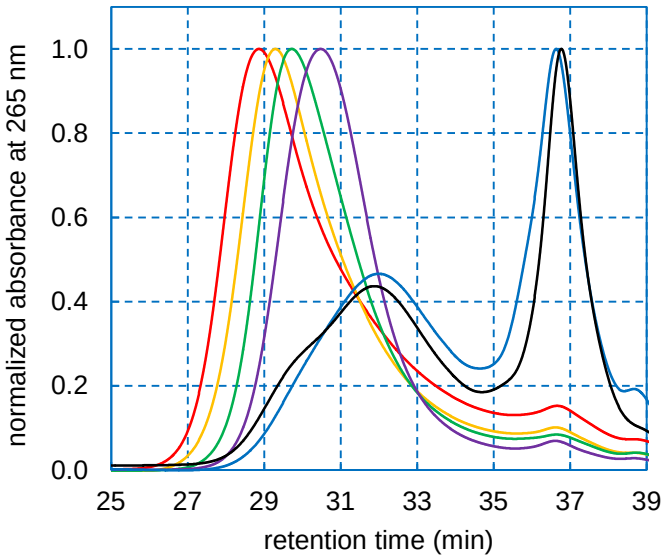

Figure 4.9. GPC plot of the absorbance at 254 nm of poly(*N*-Fmoc-6-acryloyl-D-glucosamine) prior to fractional precipitation (black) and fraction 1 (red), fraction 2 (orange), fraction 3 (green), fraction 4 (purple), and filtrate (blue) from fractional precipitation in THF relative to polystyrene standards.

Table 4.8. GPC analysis of the fractional precipitation of poly(*N*-Fmoc-6-acryloyl-D-glucosamine).

fraction	solvent (mL THF/mL methanol)	M_w[†] (Da)	M_n[†] (Da)	$Đ$[†]	DP_n[‡]
1	5/20	9430	5930	1.65	13
2	5/27.5	8610	5910	1.65	13
3	5/42.5	7480	5550	1.56	12
4	2/15	6450	5150	1.38	11
filtrate		4610	3120	1.29	7

[†] Determined via GPC in THF relative to polystyrene standards.
[‡] Determined from M_n divided by the molecular weight of the monomer.

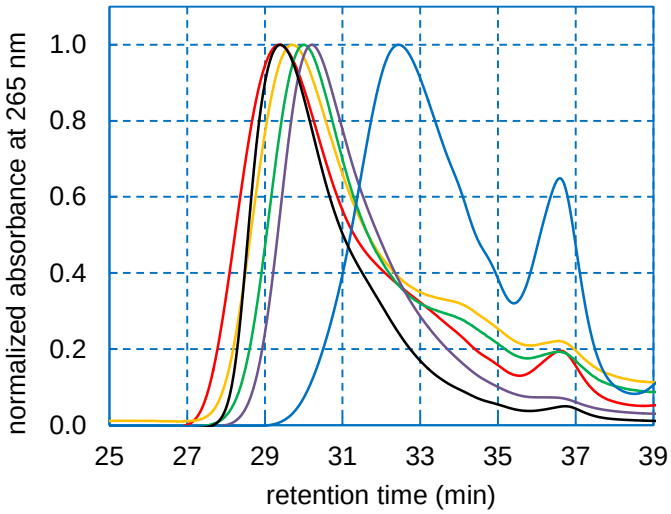

Figure 4.10. GPC plot of the absorbance at 254 nm of poly(methyl *N*-Fmoc-6-acryloyl-β-D-glucosaminoside) prior to fractional precipitation (black) and fraction 1 (red), fraction 2 (orange), fraction 3 (green), fraction 4 (purple), and filtrate (blue) from fractional precipitation in THF relative to polystyrene standards.

Table 4.9. GPC analysis of the fractional precipitation of poly(methyl *N*-Fmoc-6-acryloyl-β-D-glucosaminoside).

fraction	Solvent (mL THF/mL methanol)	M_w[†] (Da)	M_n[†] (Da)	$Đ$[†]	DP_n[‡]
1	5/5.42	7670	4630	1.66	10
2	5/7.42	6570	3970	1.65	8
3	5/8.92	6050	3880	1.56	8
4	5/12.92	5880	4270	1.38	9
filtrate		3080	2400	1.29	5

[†] Determined via GPC in THF relative to polystyrene standards.
[‡] Determined from M_n divided by the molecular weight of the monomer.

The reported molecular weights via GPC in THF relative to polystyrene standards were smaller than expected, and the polymers were observed to be sparingly soluble in THF. These observations were indicative that THF may be a poor solvent for these glycopolymers. A poor solvent would cause the polymer to adopt a collapsed chain conformation resulting in a smaller hydrodynamic volume. Since GPC separates polymers according to their hydrodynamic volume, the reported molecular weights would be smaller than expected. Select samples were analyzed by GPC in DMF with 0.01 M LiBr and significantly higher molecular weights were observed due to the difference in solvent quality (Table 4.10).

Table 4.10. GPC analysis of select samples of poly(methyl *N*-Fmoc-6-acryloyl-β-D-glucosaminoside) in DMF with 0.01 M LiBr.

initiator	temp (°C)	[*M*] (mM)	[*I*] (mM)	M_w[†] (Da)	M_n[†] (Da)	*Đ*[†]	DP_n[‡]
ACVA	70	210	1.05	22500	20400	1.10	43
ACVA	70	790	0.71	26900	21300	1.26	45
ACVA	50	790	0.71	43400	33100	1.31	71

[†] Determined via GPC in DMF with 0.01 M LiBr relative to polystyrene standards.
[‡] Determined from M_n divided by the molecular weight of the monomer.

Due to the discrepancies between the two GPC solvent systems, the poly(methyl *N*-Fmoc-6-acryloyl-β-D-glucosaminoside) series obtained from fractional precipitation was further analyzed via gel permeation chromatography with multi-angle light scattering (GPC-MALS) to determine the absolute molecular weights of each fraction. In order to obtain accurate molecular weights via multi-angle light scattering (MALS), the change in refractive index with respect to a change in concentration (dn/dc) must be accurately determined via batch injection of increasing concentrations into the differential refractive index (dRI) detector (Figure 4.11). The dn/dc for poly(methyl *N*-Fmoc-6-acryloyl-β-D-glucosaminoside) in THF was determined to be 0.143 mL/g. When the series of fractionally precipitated poly(methyl *N*-Fmoc-6-acryloyl-β-D-glucosaminoside) was analyzed by GPC-MALS (Figure 4.12), the higher molecular weight fractions were observed to form aggregates at a concentration of 4 mg/mL. These aggregates were seen to scatter a large amount of light but have little effect on the index of refraction (Figure 4.12a & b). When molecular weights were calculated, the extremities of the dRI peaks were avoided to not include aggregates, but the molecular weights may still be skewed towards higher molecular weights (Figure 4.13). Even in fractions where no aggregation was observed, a sharp increase in molecular weight was observed at earlier elution times characteristic of branched structures (Figure 4.12c). Branched polymers are more density packed and thus have a higher molecular weight compared to a linear polymer of identical hydrodynamic volume. Branched structures can form at high conversion due to chain transfer to polymer.[138]

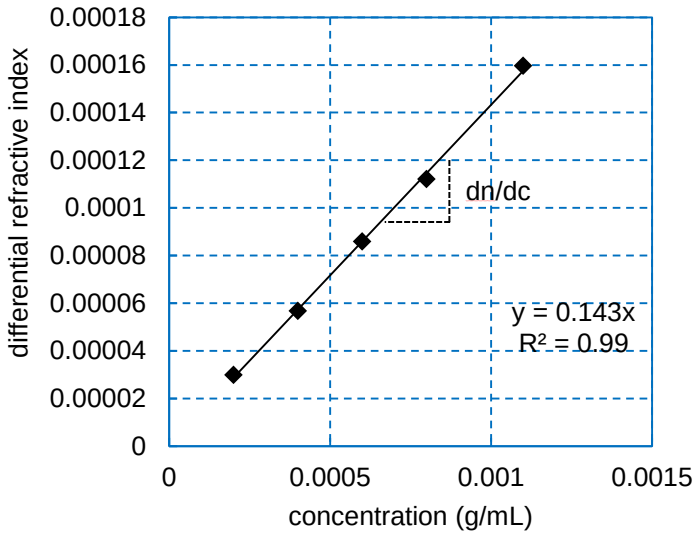

Figure 4.11. Determining change in refractive index per unit concentration (dn/dc) of poly(methyl *N*-Fmoc-6-acryloyl-β-D-glucosaminoside) dissolved in THF via batch injection of increasing concentrations into the differential refractive index detector.

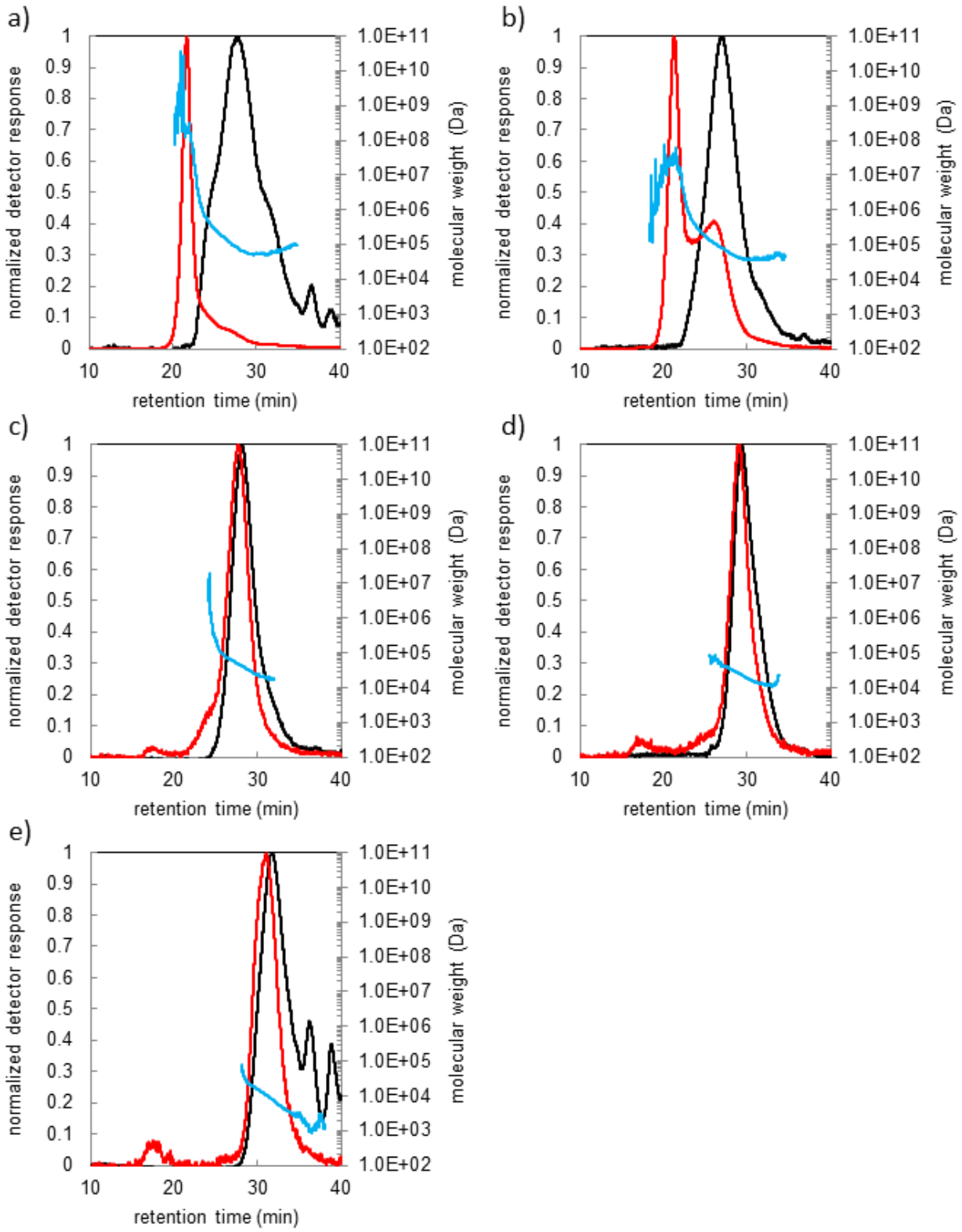

Figure 4.12. GPC-MALS plot of the differential refractive index response (black), MALS response at 90° (red), and molecular weight (light blue) of poly(methyl *N*-Fmoc-6-acryloyl-β-D-glucosaminoside) a) fraction 1, b) fraction 2, c) fraction 3, d) fraction 4, and e) filtrate from fractional precipitation in THF.

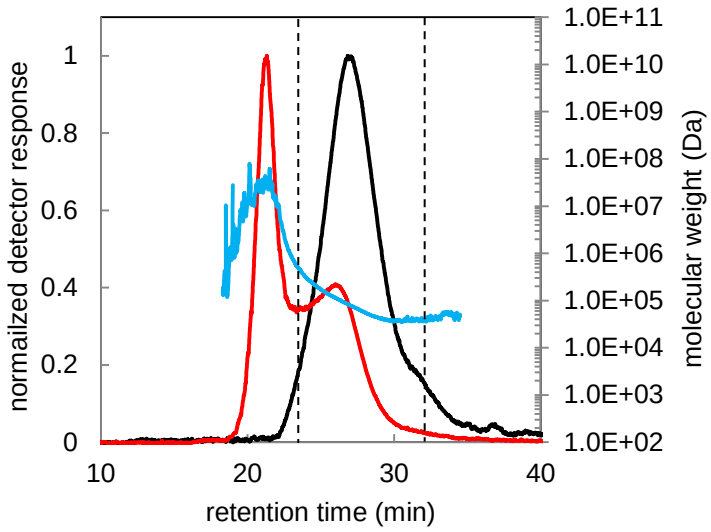

Figure 4.13. GPC-MALS plot of the differential refractive index (dRI) (black), MALS response at 90° (red), and molecular weight (light blue) of fraction 2 of poly(methyl *N*-Fmoc-6-acryloyl-β-D-glucosaminoside) in THF with the range of molecular weight calculation (- - -).

Each fraction of poly(methyl *N*-Fmoc-6-acryloyl-β-D-glucosaminoside) was evaluated by GPC-MALS, and the molecular weight information was compared to those determined by GPC relative to polystyrene standards (Table 4.11). In general, the polystyrene standards underestimated the molecular weight of the polymers in an exponential manner as the polymer fractions increased in molecular weight (Figure 4.14). The higher molecular weight fraction, however, may have skewed higher molecular weights due to the presence of aggregation and branched architectures.

Table 4.11. Molecular weights of the fractional precipitation of poly(methyl *N*-Fmoc-6-acryloyl-β-D-glucosaminoside) in THF relative to polystyrene standards and via multi-angle light scattering (MALS).

	relative to polystyrene				MALS			
fraction	M_w (kDa)	M_n (kDa)	M_p (kDa)	$Đ$	M_w (kDa)	M_n (kDa)	M_p (kDa)	$Đ$
1	7.67	4.63	9.97	1.65	151	84.0	83.2	1.80
2	6.57	3.97	8.80	1.65	108	70.2	83.5	1.53
3	6.05	3.88	7.89	1.56	43.6	38.2	41.1	1.14
4	5.88	4.27	7.36	1.38	22.1	19.2	23.1	1.15
filtrate	3.08	2.39	3.29	1.29	8.56	6.49	7.94	1.32

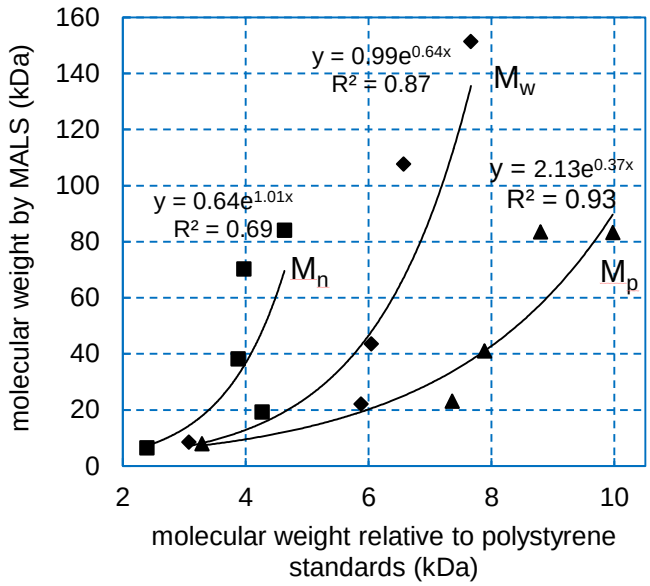

Figure 4.14. Weight-average molecular weight (M_w) (♦), number-average molecular weight (M_n) (■), and peak molecular weight (M_p) (▲) of the fractional precipitation of poly(methyl *N*-Fmoc-6-acryloyl-β-D-glucosaminoside) in THF via multi-angle light scattering (MALS) versus relative to polystyrene standards.

The difference in molecular weights determined by GPC using polystyrene standards versus GPC-MALS comes from the difference in the solvent quality of THF for poly(methyl *N*-Fmoc-6-acryloyl-β-D-glucosaminoside) compared to polystyrene. The relationship between the radius of gyration (R_g) and molecular weight (M) is defined by $R_g = KM^{\nu}$. A Mark-Houwink equation exponent (ν) of 1/3, 1/2, and 3/5 corresponds to a poor solvent (collapsed chains that minimize polymer-solvent interaction), theta solvent (unperturbed, ideal chain), and good solvent (swollen chain that maximizes polymer-solvent interaction), respectively. From the log-log plot of the root mean square radius of gyration versus the molecular weight determined by MALS, the slope of the linear region is equal to the Mark-Houwink equation exponent, representing the solvent quality of poly(methyl *N*-Fmoc-6-acryloyl-β-D-glucosaminoside) in THF (Figure 4.15). With ν = 0.299, poly(methyl *N*-Fmoc-6-acryloyl-β-D-glucosaminoside) exists as a collapsed chain in THF as opposed to polystyrene (ν = 0.725), which exists as a swollen chain in THF.[222] Since

GPC separates polymers based on hydrodynamic volume, poly(methyl *N*-Fmoc-6-acryloyl-β-D-glucosaminoside) will appear to be a much smaller polymer due to the poor solvent quality.

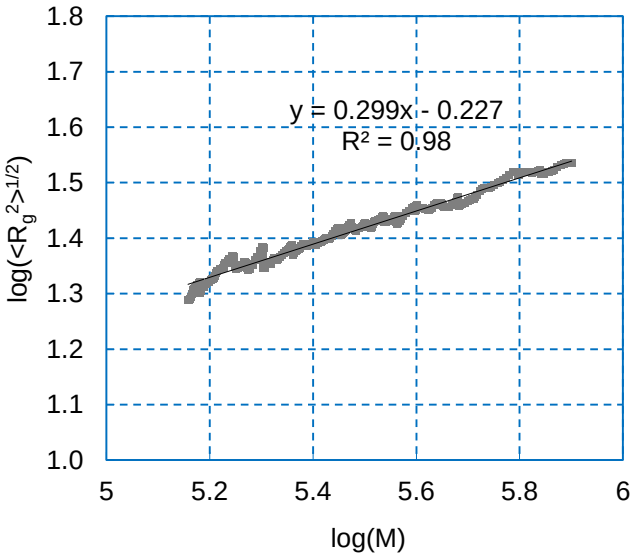

Figure 4.15. Log-log plot of root mean square radius of gyration (R_g) versus molecular weight (M) determined by multi-angle light scattering with the slope of the linear region equal to the Mark-Houwink equation exponent, representing solvent quality of poly(methyl *N*-Fmoc-6-acryloyl-β-D-glucosaminoside) in tetrahydrofuran.

Using poly(methyl *N*-Fmoc-6-acryloyl-β-D-glucosaminoside) as molecular weight standards, more accurate molecular weight estimates were determined for poly(*N*-Fmoc-6-acryloyl-D-glucosamine) (Table 4.12).

Table 4.12. Molecular weights of the fractional precipitation of poly(*N*-Fmoc-6-acryloyl-D-glucosamine) in THF relative to polystyrene standards and to relative poly(methyl *N*-Fmoc-6-acryloyl-β-D-glucosaminoside).

	relative to polystyrene			relative to poly(methyl *N*-Fmoc-6-acryloyl-β-D-glucosaminoside)		
fraction	M_w (kDa)	M_n (kDa)	*Đ*	M_w (kDa)	M_n (kDa)	*Đ*
1	9.43	5.93	1.59	120	56.1	2.13
2	8.61	5.91	1.46	93.0	49.1	1.90
3	7.48	5.55	1.35	66.7	40.4	1.65
4	6.45	5.15	1.25	47.8	32.1	1.49
filtrate	4.61	3.12	1.48	12.0	5.44	3.67

4.6. Characterization of cationic glycopolymers

The Fmoc protecting group on the glycopolymers was removed using typical deprotection conditions from peptide synthesis (20% piperidine in DCM). When the deprotection conditions were applied to poly(*N*-Fmoc-6-acryloyl-D-glucosamine) the polymer developed a brown color, would not dissolve in aqueous solution of any pH, swelled in dimethyl sulfoxide, and collapsed in acetone and DCM. Based on these observations, polymer crosslinking was suspected through a Maillard reaction, typically seen when reducing sugars (alcohol functionality at the anomeric carbon) are in the presence of amines (Scheme 4.7).[223] In a model reaction in which the deprotection conditions were applied to *N*-Fmoc glucosamine, the ^{1}H and ^{13}C NMR showed that glucosamine was not the product of the reaction, and the ESI showed higher molecular weight products that are consistent with polymerization via a Maillard reaction that results in the loss of a molecule of water. When ethanolamine was added to compete with the amine on glucosamine in the Maillard reaction, the polymer likewise developed a brown color, but was soluble in water. The ^{1}H NMR of the deprotected polymer showed the persistence of peaks characteristic of ethanolamine even after exhaustive dialysis. While water-soluble polymer can be produced using ethanolamine, it is difficult to properly characterize the saccharide side groups of the polymer.

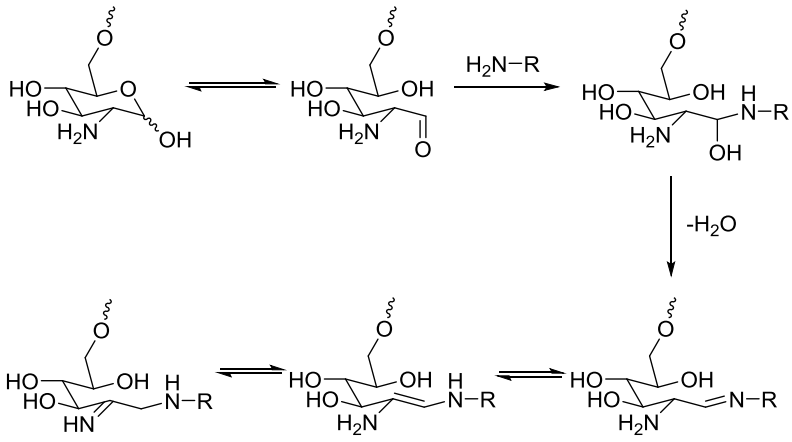

Scheme 4.7. Maillard reaction with poly(6-acryloyl-D-glucosamine).

When the deprotection conditions were applied to poly(methyl *N*-Fmoc-6-acryloyl-β-D-glucosaminoside), which contains a methyl glycoside instead of the reducing sugar, the polymer remained white after lyophilization and dissolved easily in water. Using the difference in molecular weights of the repeat unit with and without the Fmoc protecting group, molecular weights were calculated for the cationic glycopolymers from the molecular weights obtained from MALS (Table 4.13).

Table 4.13. Calculated molecular weights of poly(methyl 6-acryloyl-β-D-glucosaminoside) from the ratio of the molecular weight of methyl 6-acryloyl-β-D-glucosaminoside and methyl *N*-Fmoc-6-acryloyl-β-D-glucosaminoside.

fraction	M_w (kDa)	M_n (kDa)	DP_n †
1	79.7	44.2	179
2	56.7	37.0	149
3	22.9	20.1	81
4	11.6	10.1	41
filtrate	4.51	3.42	14

† calculated from M_n divided by the molecular weight of the monomer.

Following deprotection of the Fmoc group with 20% piperidine in DCM, the polymers were analyzed for amine content using the CBQCA Protein Quantification Kit and pKa by potentiometric titration (Table 4.14). The glycopolymers contain between 85-95% of the expected amines. Previously, post-polymerization deprotection of the acetate groups was employed and only 60% of the expected amines were detected, underscoring the importance of deprotecting glycomonomers prior to polymerization. The potentiometric titration of the polymers revealed the pKa of poly(6-acryloyl-D-glucosamine), poly(methyl 6-acryloyl-β-D-glucosaminoside), and poly(2-*O*-(β-D-glucosaminosyl) hydroxyethyl acrylate) to be 7.20, 6.61, and 6.46, respectively. The pKa of the glycosides are approximately 6.5, the pKa of chitosan,[224] whereas poly(6-acryloyl-D-glucosamine) is closer to 7.58, the pKa of glucosamine.[225] Upon hydrolysis of the ester linkage to release the saccharide moiety from the

polymer backbone, the pKa of the amine increases, which could be a useful characteristic for shielding the anionic charge from the resultant carboxylic acid on the polymer backbone or for facilitating an enhanced proton sponge effect by increasing cationic charge within a lysosome.

Table 4.14. Amine quantification and pKa of cationic glycopolymers.

polymer	amine content[†]	pKa[‡]	pKa of expected saccharide product from hydrolysis[‡]
poly(6-acryloyl-D-glucosamine)	85%	7.20	7.51
poly(methyl 6-acryloyl-β-D-glucosaminoside)	95%	6.61	7.15
poly(2-*O*-(β-D-glucosaminosyl) hydroxyethyl acrylate)	89%	6.46	7.08

[†] Determined via CBQCA protein quantification assay.
[‡] Determined via potentiometric titration.

4.7. Conclusion

In this chapter, three sets of glycopolymers were created: 1) glycopolymers with a variety of saccharide identities linked to the polymer backbone through a glycosidic bond, 2) linear and branched glycopolymers and linear and branched amphiphilic glycopolymers of various molecular weights with galactose linked through the primary alcohol to the polymer backbone, and 3) a cationic methyl glucosaminoside glycopolymer with various molecular weights isolated via fractional precipitation. Using the four glycomonomers with the polymerizable group attached through a glycosidic bond, the first set of glycopolymers was synthesized via RAFT polymerization. Using a galactose glycomonomer with a polymerizable group attached at the primary alcohol and one of polymerizable CTAs developed in Section 3.3, a second set of glycopolymers was synthesized with varying molecular weights and degrees of branching. Using methyl acrylate as a hydrophobic monomer and the galactose glycomonomer as a hydrophilic monomer, we created amphiphilic block copolymers of various molecular weights and degrees of branching in the hydrophilic domain. The saccharide moieties were observed to retain their natural ability to isomerize even though connected to the polymer backbone.

A final set of Fmoc-protected glycopolymers was created using free-radical polymerization. Initially, RAFT polymerization was attempted, but an inhibitory effect was observed, which prevented high conversion. Even using conventional free-radical polymerization techniques with a thermo-initiator, only glycooligomers could be formed. By increasing monomer concentration and lowering the polymerization temperature, higher molecular weights were produced, but with lower conversions. When a UV-photoinitiator was substituted for the thermo-initiator, high molecular weight polymers were produced with high conversion at room temperature with *N*-Fmoc-6-acryloyl-D-glucosamine and methyl *N*-Fmoc-6-acryloyl-β-D-glucosaminoside.

UV light, however, is incompatible with RAFT polymerizations due to the degradation of the RAFT CTA. Low dispersity glycopolymers were obtained through fractional precipitation and were analyzed by GPC. After deprotection of the Fmoc protecting group, poly(*N*-Fmoc-6-acryloyl-D-glucosamine) exhibited evidence of side reactions involving the reducing saccharide that resulted in crosslinking, which can be avoided by including ethanolamine but are difficult to characterize. Poly(methyl *N*-Fmoc-6-acryloyl-β-D-glucosaminoside) was deprotected without signs of side reactions. The deprotected glycopolymers were characterized by an amine quantification assay for amine content and potentiometric titration for pKa.

4.8. Experimental

4.8.1. Materials

Phenylmagnesium bromide in 2-methyltetrahydrofuran (Strem, Chemicals, 2.9 M), carbon disulfide (Fisher, ACS grade), iodine (ACROS, resublimed), ethyl 2-(phenylcarbonothioylthio) propionate (Sigma-Aldrich, 97%), Irgacure 2959 (Ciba), ethanolamine (Sigma-Aldrich, 98%), 2-(2-aminoethoxy)ethanol (ACROS, 98%), glycine (Fisher, white crystals), Fmoc-glycine-OH (Anaspec), 9-fluorenylmethoxycarbonyl chloride (Fmoc-Cl) (Oakwood Products, 97%), di-*tert*-butyl dicarbonate (Alfa Aesar, 97+%), immobilized TCEP disulfide reducing gel (Pierce), hydrochloric acid (Fisher, ACS grade), formic acid (Fluka, 98%), sodium phosphate dibasic heptahydrate (Fisher, USP grade), *N*-(3-dimethylaminopropyl)-*N′*-ethylcarbodiimide hydrochloride (EDC•HCl) (CreoSalus), 4-dimethylaminopyridine (DMAP) (Alfa Aesar, 99%), triethylamine (Alfa Aesar, 99%), sodium bicarbonate (Fisher, USP/FCC), sodium hydroxide (Fisher, ACS grade), tetrahydrofuran (THF) (Fisher, HPLC), *p*-dioxane (ACROS, 99.8% extra dry), acetone (Fisher, ACS grade), diethyl ether (Macron Chemicals, ACS grade), dimethyl sulfoxide (DMSO) (Scharlau, HPLC grade), ethanol (Decon Labs, 200 proof), methanol (EMD DriSolv, 99.8%), hexanes (Fisher, ACS grade), and petroleum ether 40/60 (Alfa Aesar) were used as received. Methyl acrylate (Alfa Aesar, 99%) was passed through basic alumina. Azobisisobutyronitrile (AIBN) (Sigma-Aldrich, 98%) and 4,4’-azobis(4-cyanovaleric acid) (ACVA) (Pfaltz & Bauer, 98%) was recrystallized in methanol. Piperidine (Alfa Aesar, 99%), hydroxyethyl acrylate (HEA) (Sigma-Aldrich, 96%), acryloyl chloride (Alfa Aesar, 96%), toluene (Fisher, ACS grade), dichloromethane (DCM) (Fisher, ACS grade), and ethyl acetate (Fisher, ACS grade) were distilled. Water was distilled or purified using an ELGA PURELAB Classic. Photopolymerizations were irradiated with 365 nm light using a UVP XX-15L

Black-Ray UV bench lamp. Dialysis was conducted using a Spectra/Por® dialysis membrane (1000 Da).

4.8.2. Analytical techniques

Lyophilization was conducted on a Labconco FreeZone 4.5 freeze dryer or a Christ Alpha 1-2 LD plus freeze dryer. NMR spectra were recorded with a Bruker Avance 300, except for the copolymers that were recorded with a Bruker Avance 400. Aqueous gel permeation chromatography (GPC) was conducted on a Jasco system equipped with a UV detector, a refractive index detector, and four Waters ultrahydrogel columns (100-5K, 1K-80K, 10K-400K, 2K-4M, 500-10M) using 10 mM PBS with 0.3 M NaCl at pH 6.6 as a eluent at 30 °C and a flow rate of 1.0 mL/min calibrated using pullulan standards. Branched glycopolymers were analyzed by GPC on a Waters system equipped with a refractive index detector and four Waters styragel columns (100-5K, 500-30K, 50-100K, 5K-600K) using tetrahydrofuran at a flow rate of 1.0 mL/min and calibrated using linear poly(methyl methacrylate) standards. Fmoc-protected glycopolymers were analyzed by GPC on a Jasco system equipped with a UV detector, a refractive index detector, and four Waters styragel columns (100-5K, 500-30K, 50-100K, 5K-600K) using tetrahydrofuran at 30 °C or dimethylformamide with 0.01 M lithium bromide at 40 °C with a flow rate of 1.0 mL/min and calibrated using linear polystyrene standards or a Shimazu system equipped with a UV detector, a Wyatt Optilab T-rEX, a Wyatt DAWN HELEOS-II (MALS), and four Waters styragel columns (100-5K, 500-30K, 50-100K, 5K-600K) using tetrahydrofuran at 30 °C with a flow rate of 1.0 mL/min. Amine quantification was conducted with the CBQCA Protein Quantification Kit (Molecular Probes) and read on a BioTek Synergy H1 multi-mode reader with an excitation of 465 nm and an emission of 550 nm.

Potentiometric titration was conducted using 0.1 M HCl and measured using a Thermo Scientific Orion Star A111 pH meter.

4.8.3. Bis(thiobenzyl) disulfide (BTBD)

Carbon disulfide (5.25 mL, 87 mmol) was added dropwise to a phenylmagnesium bromide solution in 2-methyl tetrahydrofuran (30 mL, 2.9M) diluted with tetrahydrofuran (THF) (15 mL) at 0°C and stirred under argon. The solution was stirred for 45 minutes and quenched by the addition of water dropwise. The THF was removed in vacuo and the solution was filtered. The product was extracted with DCM as hydrochloric acid was added until the aqueous layer was colorless. The organic layer was washed with brine (2×) and reduced to a red oil in vacuo. The oil was crystallized with ethanol (10 mL), DMSO (2 mL), and catalytic amounts of crystalline iodine at 0 °C. The magenta crystals were filtered and washed with water (4.18 g, 31%).

^{1}H NMR (300 MHz, $CDCl_3$): δ7.40-8.10 (m, 10H, ϕ).

4.8.4. 4-Cyano-4-(thiobenzoylthio)pentanoic acid

4,4'-Azobis(4-cyanovaleric acid) (584 mg, 2.1 mmol) and bis(thiobenzyl) disulfide (425 mg, 1.4 mmol) were dissolved in distilled ethyl acetate (8 mL) and heated to 80 °C for 18 hours. The product was isolated as a magenta solid by silica column chromatography using 1:1 ethyl acetate in hexanes as an eluent (470 mg, 60%).

^{1}H NMR (300 MHz, $CDC1_3$): δ7.40-8.00 (m, 5H, ϕ), 2.76 (m, CH_2CH_2COOH), 2.45-2.63 (m, CH_2CH_2COOH), 1.96 (s, CH_3).

4.8.5. RAFT polymerization of glycomonomer attached through a glycosidic bond

Glycomonomer (100 equivalents), 4-cyano-4-(thiobenzoylthio)pentanoic acid (1 equivalent), and 4,4'-azobis(4-cyanovaleric acid) (0.3 equivalents) were dissolved in a solution of water/ethanol (3:1). The solution was degassed via freeze/pump/thaw cycles (5×) and heated at

70 °C for 18 hours followed by quenching in liquid nitrogen and exposure to air. The reaction was diluted with water, and a sample was lyophilized to determine conversion via ^{1}H NMR. The remainder of the polymer solution was dialyzed in DI water over 16 hours, changing the water every two hours, and lyophilized. The resultant polymer were analyzed by ^{1}H NMR and GPC.

4.8.6. Representative RAFT polymerization of glycomonomer attached through a glycosidic bond

2-*O*-(α-D-Mannosyl)hydroxyethyl acrylate (517.5 mg, 1.86 mmol), 4-cyano-4-(thiobenzoylthio)pentanoic acid (5.2 mg, 0.019 mmol), and 4,4'-azobis(4-cyanovaleric acid) (1.6 mg, 0.006 mmol) were dissolved in a solution of water/ethanol (2 mL, 3:1). The solution was degassed via freeze/pump/thaw cycles (5×) and heated at 70 °C for 18 hours followed by quenching in liquid nitrogen and exposure to air. The reaction was diluted with water, and a sample was lyophilized to determine conversion via ^{1}H NMR. The remainder of the polymer solution was dialyzed in DI water over 16 hours, changing the water every two hours, and lyophilized. The resultant polymer were analyzed by ^{1}H NMR and GPC.

4.8.7. Poly(acryloyl-1,2:3,4-di-*O*-isopropylidene-α-D-galactose)

For each molecular weight, acryloyl-1,2:3,4-di-*O*-isopropylidene-α-D-galactose was added to ethyl 2-(phenylcarbonothioylthio) propionate in toluene (3 mL) and aliquoted into three equal portions. The corresponding amount of polymerizable CTA was added as calculated respectively for no branching, one branch per polymer, and five branches per polymer. Azobisisobutyronitrile (AIBN) (0.1 mol/mol of CTA) was added, and the total amount of toluene was increased to 2.54 mL. The solution was degassed via freeze-pump-thaw cycles (5×), backfilled with argon, and heated to 80°C for 72 hours. Each polymerization was quenched by cooling with liquid

nitrogen followed by exposure to air. When possible, the polymers were precipitated in cold methanol and analyzed by ^{1}H NMR and GPC.

4.8.8. Representative synthesis of poly(acryloyl-1,2:3,4-di-*O*-isopropylidene-α-D-galactose) (DP = 50, 0 branch)

Acryloyl-1,2:3,4-di-*O*-isopropylidene-α-D-galactose (2.9 g, 9 mmol) was added to ethyl 2-(phenylcarbonothioylthio) propionate (46.5 mg, 0.18 mmol) dissolved in toluene (3 mL). A third of this solution was aliquoted, AIBN (1 mg, 0.006 mmol) was added, and the solution was diluted with 1.54 mL of toluene. This solution was degassed via freeze-pump-thaw cycles (5×), backfilled with argon, and heated to 80°C for 72 hours. The polymerization was quenched by cooling with liquid nitrogen followed by exposure to air. The polymer was precipitated in cold methanol and analyzed by ^{1}H NMR and GPC.

4.8.9. Poly(methyl acrylate) macro-CTA (PMA CTA)

Ethyl 2-(phenylcarbonothioylthio) propionate (120 mg, 0.47 mmol), AIBN (12 mg, 0.07 mmol), and methyl acrylate (1.07 mL, 11.8 mmol) were dissolved in toluene (1.07 mL) and degassed via freeze-pump-thaw cycles (5×), backfilled with argon, and heated to 80°C for 18 hours. The polymerization was quenched by cooling with liquid nitrogen followed by exposure to air. Residual monomer was washed away with hexanes, and the polymer was analyzed by ^{1}H NMR and GPC (586.2 mg). By ^{1}H NMR, the polymer was determined to have a degree of polymerization of 24.8 corresponding to a molecular weight of 2388 Da by comparing the ethyl chain end to the methyl side chain integrations. The PMA CTA had a M_n = 4100 Da and a M_w = 5269 Da, resulting in a molecular weight distribution (*Đ*) of 1.3 via GPC.

4.8.10. Poly(methyl acrylate-co-acryloyl-1,2:3,4-di-*O*-isopropylidene-α-D-galactose)

The same batch of PMA CTA was used in all chain-extension polymerizations. For each molecular weight, acryloyl-1,2:3,4-di-*O*-isopropylidene-α-D-galactose was added to the PMA CTA in toluene (3 mL) and aliquoted into three equal portions. The corresponding amount of polymerizable CTA was added as calculated respectively for no branching, one branch per copolymer, and five branches per copolymer. AIBN (0.3 mol/mol of CTA) was added and the total amount of toluene was increased to 2 mL. The solution was degassed via freeze-pump-thaw cycles (5×), backfilled with argon, and heated to 80°C for 24 hours. The polymerization was quenched by cooling with liquid nitrogen followed by exposure to air. When possible, the copolymers were precipitated in cold methanol and analyzed by ^{1}H NMR and GPC.

4.8.11. Representative synthesis of poly(methyl acrylate-co-acryloyl-1,2:3,4-di-*O*-isopropylidene-α-D-galactose) (DP = 25 methyl acrylate, 50 acryloyl-1,2:3,4-di-*O*-isopropylidene-α-D-galactose, 0 branch)

Acryloyl-1,2:3,4-di-*O*-isopropylidene-α-D-galactose (964.5 mg, 3.07 mmol) was added to PMA CTA (146.6 mg, 0.06 mmol) dissolved in toluene (3 mL). A third of this solution was separated, AIBN (1.0 mg, 0.006 mmol) was added, and the solution was diluted with 1 mL of toluene. This solution was degassed via freeze-pump-thaw cycles (5×), backfilled with argon, and heated to 80°C for 24 hours. The polymerization was quenched by cooling with liquid nitrogen followed by exposure to air. The copolymer was precipitated in cold methanol and analyzed by ^{1}H NMR and GPC.

4.8.12. Deprotection of isopropylidene protecting groups

All glycopolymers and amphiphilic copolymers were deprotected in similar fashion. Polymers (70 mg) were stirred in formic acid (10 mL, 90%) for 2.5 hours after which water

(4 mL) was added, and the reaction mixture was allowed to stir for an additional 3 hours. The acid was removed by dialysis in water over at least 24 hours, changing the water every 2 hours as possible, no less than 5 times. The deprotected polymers were lyophilized and verified via ^{1}H NMR in DMSO-d_6 by the disappearance of the isopropylidene peaks at 1.35-1.5 ppm and the disappearance of the anomeric peak of the protected saccharide at 5.5 ppm.

4.8.13. Representative acidolysis of poly(methyl acrylate-co-acryloyl-1,2:3,4-di-*O*-isopropylidene-α-D-galactose) (DP = 25 methyl acrylate, 50 acryloyl-1,2:3,4-di-*O*-isopropylidene-α-D-galactose, 0 branch)

The copolymer (70 mg, 0.05 mmol) was stirred in formic acid (10 mL, 90%) for 2.5 hours after which water (4 mL) was added, and the reaction mixture was allowed to stir for an additional 3 hours. The acid was removed by dialysis in water over at least 24 hours, changing the water every 2 hours as possible, no less than 5 times. The deprotected copolymer was lyophilized (40.4mg, 77.4%).

4.8.14. Aminolysis of RAFT chain end

All glycopolymer and amphiphilic copolymer chain ends were removed in similar fashion. TCEP (50 µL) and ethanolamine (50 µL) were added to polymer (10 mg) dissolved in water (1 mL) when possible, otherwise dissolved in DMSO (1 mL). After 1 hour, the solution was filtered and dialyzed in water over at least 24 hours, changing the water every 2 hours as possible, no less than 5 times. The polymers were lyophilized and verified via ^{1}H NMR by the disappearance of the aromatic peaks at 7.4-8.0 ppm.

4.8.15. Polymerization of Fmoc-protected cationic glycomonomer

4.8.15.1. Thermo-initiator

Fmoc-protected glycomonomer (1000 equivalents) and ACVA (1 equivalent) were dissolved in THF, degassed via freeze-pump-thaw cycles (5×), backfilled with argon, and heated at 70 °C for 90 hours. The polymerization was quenched by cooling with liquid nitrogen followed by exposure to air. The polymer was precipitated in cold methanol and analyzed by ^{1}H NMR and GPC.

4.8.15.2. Photoinitiator

Fmoc-protected glycomonomer (1000 equivalents) and Irgacure 2959 (1 equivalent) were dissolved in THF, degassed via freeze-pump-thaw cycles (5×), backfilled with argon, and irradiated with 2.6 mW/cm^2 of 365 nm UV light (Figure 4.16) for 16 hours. The polymerization was quenched by exposure to air, and the polymer was precipitated in cold methanol and analyzed by ^{1}H NMR and GPC.

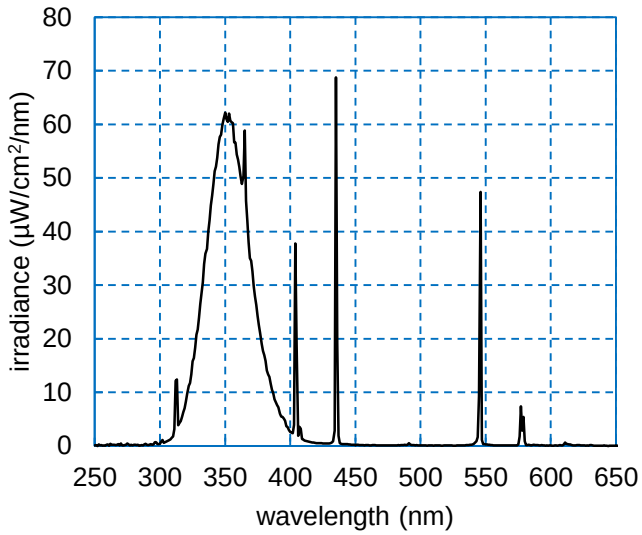

Figure 4.16. Irradiance spectrum of 365 nm UV light source.

4.8.16. Representative polymerization of Fmoc-protected cationic glycomonomer

4.8.16.1. Thermo-initiator

Methyl *N*-Fmoc-6-acryloyl-β-D-glucosaminoside (185 mg, 0.40 mmol) and ACVA (0.1 mg, 0.4 μmol) were dissolved in THF (0.5 mL), degassed via freeze-pump-thaw cycles (5×), backfilled with argon, and heated at 70 °C for 90 hours. The polymerization was quenched by cooling with liquid nitrogen followed by exposure to air. The polymer was precipitated in cold methanol and analyzed by ^{1}H NMR and GPC.

4.8.16.2. Photoinitiator

Methyl *N*-Fmoc-6-acryloyl-β-D-glucosaminoside (196 mg, 0.42 mmol) and Irgacure 2959 (0.09 mg, 0.4 μmol) were dissolved in THF (0.5 mL), degassed via freeze-pump-thaw cycles (5×), backfilled with argon, and irradiated with 2.6 mW/cm^2 of 365 nm UV light for 16 hours. The polymerization was quenched by exposure to air, and the polymer was precipitated in cold methanol and analyzed by ^{1}H NMR and GPC.

4.8.17. Fractional precipitation of glycopolymer

Fmoc-protected glycopolymer was dissolved in THF and methanol was gradually added until precipitate formed an opaque solution. The solution was stored at -20 °C for 16 hours, and the precipitate was isolate by centrifugation at 4000 rpm for 10 minutes. The process of addition of methanol and centrifugation was repeated until an opaque solution cannot be formed. The supernatant was then concentrated in vacuo. Each fraction was analyzed by GPC.

4.8.18. Deprotection of Fmoc protecting group

Polymer (~50 mg) was stirred in a solution of piperidine in DCM (1 mL, 20%) for 30 minutes. The reaction was diluted with DCM, and the polymer was precipitated and washed with

petroleum ether. The deprotected polymers were dried in vacuo and analyzed via ^{1}H NMR for the absence of the Fmoc group (δ7.00-8.00).

4.8.19. *N*-Fmoc-2-aminoethanol

Fmoc-Cl (500 mg, 1.9 mmol) was added to a suspension of sodium bicarbonate (974 mg, 11.6 mmol) and ethanolamine (0.13 mL, 2.1 mmol) in DCM (6 mL) at 0 °C and stirred for 16 hours. The product was extracted with DCM (100 mL, 3×), washed with cold DI water (30 mL), washed with brine (30 mL), and dried with sodium sulfate. The solvent was removed in vacuo (519 mg, 95%).

^{1}H NMR (300 MHz, $CDCl_3$): δ7.20-7.80 (m, 8H, Fmoc), 5.18 (br, NH), 3.71 (d, 2H, Fmoc), 4.22 (t, 1H, Fmoc), 3.71 (br, CH_2CH_2OH), 3.35 (q, CH_2CH_2OH), 2.14 (br, OH).

4.8.20. *N*-Fmoc-2-aminoethyl acrylate

Acryloyl chloride (299 mg, 3.30 mmol) in DCM (5 mL) was added dropwise to a solution of triethylamine (510 µL, 3.66 mmol) and *N*-Fmoc-2-aminoethanol (519 mg, 1.83 mmol) dissolved in DCM (21 mL) at 0 °C and stirred for 16 hours. The reaction was washed with DI water, saturated sodium bicarbonate solution (4×), and dried with sodium sulfate. The DCM was removed in vacuo. The product was dissolved in acetone, precipitated into water, dissolved in DCM, and passed through a silica plug with DCM (300 mg, 49%).

^{1}H NMR (300 MHz, $CDCl_3$): δ7.20-7.80 (m, 8H, Fmoc), 6.45 (d, 1H, CH_2═CH), 6.17 (m, CH_2═C*H*), 5.86 (d, 1H, CH_2═CH), 5.06 (br, -NH), 4.42 (d, 2H, Fmoc), 4.25 (m, 3H, $NHCH_2CH_2O$, Fmoc), 3.52 (q, $NHCH_2CH_2O$).

4.8.21. 2-(*N*-Fmoc-2-aminoethoxy)ethanol

Fmoc-Cl (1.2 g, 4.5 mmol) dissolved in *p*-dioxanes (4.5 mL) was added to a solution of 2-(2-aminoethoxy)ethanol (300 µL, 3 mmol) and sodium bicarbonate (1 g, 12 mmol) in water (9

mL) and *p*-dioxanes (4.5 mL) at 0 °C and stirred for 16 hours. The product was extracted with ethyl acetate, washed with 1 M HCl and brine, dried with sodium sulfate, and purified with silica column chromatography using ethyl acetate as an eluent. The fractions were concentrated and the product was crystallized at -20 °C (609 mg, 62%).

^{1}H NMR (300 MHz, $CDCl_3$): δ7.16-7.80 (m, 8H, Fmoc), 5.64 (br, NH), 4.40 (d, 2H, Fmoc), 4.16 (t, 1H, Fmoc), 3.64 (t, $NHCH_2C\mathit{H}_2OCH_2CH_2OH$), 3.46 (m, $NHCH_2CH_2OC\mathit{H}_2C\mathit{H}_2OH$), 3.32 (q, $NHC\mathit{H}_2CH_2OCH_2CH_2OH$), 2.99 (br, OH).

4.8.22. 2-(*N*-Fmoc-2-aminoethoxy)ethyl acrylate

Acryloyl chloride (270 µL, 3.4 mmol) in DCM (5 mL) was added dropwise to a solution of 2-(*N*-Fmoc-2-aminoethoxy)ethanol (609 mg, 1.86 mmol) with triethylamine (520 µL, 3.7 mmol) in DCM (20 mL) at 0 °C. After 4 hours, the reaction was washed with water (3×), saturated sodium bicarbonate (3×), brine (2x), and dried with sodium sulfate. The product was passed through silica and basic alumina plugs with DCM (441 mg, 62%).

^{1}H NMR (300 MHz, $CDCl_3$): δ7.22-7.84 (m, 8H, Fmoc), 6.43 (d, 1H, $C\mathit{H}_2$═CH), 6.14 (m, CH_2═C*H*), 5.82 (d, 1H, $C\mathit{H}_2$═CH), 5.18 (br, NH), 4.38 (d, 2H, Fmoc), 4.32 (t, $NHCH_2CH_2OCH_2C\mathit{H}_2OC$═O), 4.23 (t, 1H, Fmoc), 3.70 (t, $NHCH_2C\mathit{H}_2OCH_2CH_2OC$═O), 3.57 (t, $NHCH_2CH_2OC\mathit{H}_2CH_2OC$═O), 3.40 (q, $NHC\mathit{H}_2CH_2OCH_2CH_2OC$═O).

4.8.23. Fmoc-glycine-HEA

Fmoc-glycine-OH (1.00 g, 3.36 mmol), EDC•HCl (1.29 g, 6.74 mmol), and DMAP (82 mg, 0.68 mmol) were dissolved in THF (20 mL) and stirred for 15 minutes before adding hydroxyethyl acrylate (1.540 mL, 13.46 mmol) and stirred for 16 hours. The product was precipitated into DI water and collected. The product was recrystallized in methanol (857 mg, 65%).

^{1}H NMR (300 MHz, $CDCl_3$): δ7.19-7.90 (m, 8H, Fmoc), 6.44 (d, 1H, C*H*$_2$═CH), 6.11 (m, CH$_2$═C*H*), 5.84 (d, 1H, C*H*$_2$═CH), 5.29 (br, -NH), 4.38 (m, 6H, OC*H*$_2$C*H*$_2$O, Fmoc), 4.23 (t, 1H, Fmoc), 4.03 (d, NHC*H*$_2$CO$_2$).

4.8.24. Boc-glycine

Di-*tert*-butyl dicarbonate (4.8 mL, 20.8 mmol) in *p*-dioxanes (10 mL) was added dropwise to NaOH (834 mg, 20.8 mmol) and glycine (1.05 g, 14.0 mmol) in water (20 mL) and *p*-dioxanes (10 mL) at 0 °C and stirred for 16 hours at room temperature. The reaction was washed with diethyl ether (3×), and the product was extracted from the diethyl ether with a saturated sodium bicarbonate solution (3×). The aqueous layers were combined and acidified using Na_2HPO_4. The product was extracted with ethyl acetate (3×), washed with water, and dried with sodium sulfate. The ethyl acetate was removed in vacuo to yield a white solid (2.4 g, 97%).

^{1}H NMR (300 MHz, $CDCl_3$): δ6.58, 5.38 (br, NH), 3.90 (m, NHC*H*$_2$COOH), 1.45 (s, OC(C*H*$_3$)$_3$).

4.8.25. Boc-glycine-HEA

Boc-glycine (500 mg, 2.8 mmol) was dissolved in DCM (10 mL) and DMAP (70 mg, 0.6 mmol) and EDC•HCl (1.094 g, 5.7 mmol) were added and stirred for 15 min. Hydroxyethyl acrylate (1.31 mL, 11.4 mmol) was added, and the reaction was stirred for 16 hours. The reaction was washed with water (3×) and brine and dried with sodium sulfate. The product was purified by silica column chromatography using 3:2 ethyl acetate in hexanes as an eluent. The product was passed through a basic alumina with DCM. The solvent was removed in vacuo (585 mg, 75%).

^{1}H NMR (300 MHz, $CDCl_3$): δ6.45 (d, 1H, C*H*$_2$═CH), 6.14 (m, CH$_2$═C*H*), 5.89 (d, 1H, C*H*$_2$═CH), 3.49 (m, NHC*H*$_2$CO$_2$), 4.36 (m, OC*H*$_2$C*H*$_2$O), 1.46 (s, OC(C*H*$_3$)$_3$).

4.8.26. RAFT polymerization of model amine-protected cationic monomers

Model amine-protected cationic monomer (25 equivalents), ethyl 2-(phenylcarbonothioylthio) propionate (1 equivalent), and AIBN (0.3 equivalents) were dissolved in toluene. The solution was degassed via freeze/pump/thaw cycles (5×), backfilled with argon, and heat at 80 °C for 70 hours. After quenching with liquid nitrogen and exposure to atmosphere, monomer conversion was evaluated by ^{1}H NMR.

4.8.27. Representative RAFT polymerization of model amine-protected cationic monomers

2-(*N*-Fmoc-2-aminoethoxy)ethyl acrylate (233 mg, 0.61 mmol), ethyl 2-(phenylcarbonothioylthio) propionate (6.2 mg, 0.024 mmol), and AIBN (1.2 mg, 0.007 mmol) were dissolved in toluene (1 mL). The solution was degassed via freeze/pump/thaw cycles (5×), backfilled with argon, and heat at 80 °C for 70 hours. After quenching with liquid nitrogen and exposure to atmosphere, monomer conversion was evaluated by ^{1}H NMR.

CHAPTER 5

Bacterial attachment to surfaces modified with various glycopolymers

5.1. Introduction

In order for bacteria to establish a colony and initiate an infection, the bacteria must first land and attach to a surface, such as the epithelial layer of the digestive tract. These surfaces, however, are often subjected to continuous shear forces that can sweep bacteria away. To facilitate adhesion, bacteria have a number of cell-surface proteins on the tips of cell appendages, such as fimbriae or pili, which recognize and bind to eukaryotic glycans. *Escherichia coli*, for example, has been extensively studied for its ability to adhere to surfaces containing mannose,[226] galabiose,[227] and *N*-acetyl glucosamine.[228] More recently, *Vibrio cholerae*, often found in contaminated drinking water, and *Shewanella oneidensis*, capable of reducing heavy metal ions and producing electrically conductive appendages,[229] have garnered increased attention. *Vibrio cholerae* is known to display mannose and *N*-acetyl glucosamine-recognition domains for attachment,[230–233] and *Shewanella oneidensis* primarily utilizes mannose-recognition domains for attachment.[234] Utilizing the specificity of bacterial adhesion lectins for particular sugars, devices can be constructed to direct, isolate, or concentrate mobile bacteria onto surfaces.

Self-assembled monolayers (SAMs) are a common approach to functionalize a surface in a well-defined manner, typically using small molecules. SAMs can be created on gold substrates through the attachment of thiol-terminated molecules. The Whitesides group has created carboxylic acid-terminated SAMs on a gold surface and attached monosaccharide moieties.[235]

Although bacterial lectins have low affinity for monosaccharides, the presentation of saccharides on a SAM increases the density of the saccharides to induce a higher avidity.[91]

In contrast to small molecules, macromolecules are more difficult to self-assemble, and are typically grafted onto a surface instead. There are four main strategies for grafting polymers onto a surface: 1) grafting to, where a surface is functionalized and polymer is conjugated to the surface 2) grafting from, where an initiator is attached to the surface and a polymer is grown from the initiator 3) grafting through, where a monomer is attached to the surface and incorporated into a growing polymer chain and 4) direct immobilization, where a preformed polymer is attached directly with the surface.[236] While grafting from and grafting through techniques ensures high conjugation density to the surface, the surface-bound polymers are difficult to characterize. Grafting to and direct immobilizations affords the ability to fully characterize the polymers prior to attachment to the surface. The choice between grafting to or direct immobilization techniques is often determined by the reactivity of the surface. Glass, for example, is extremely inert making direct immobilization difficult. Coated surfaces on glass substrates are typically created through the functionalization of the glass surface with an organofunctional alkoxysilane. Gold substrates, on the other hand, are often utilized with direct immobilization due to its selectivity for interaction with free thiols.

Reversible addition-fragmentation chain transfer (RAFT) polymerization is an ideal method for creating polymers for attachment to gold surfaces. Not only does RAFT polymerization afford the ability to create polymers with control over chain length, but it also provides a convenient protected-thiol chain end that can be deprotected under mild conditions. The McCormick group has synthesized a variety of water soluble polymers via RAFT polymerization using 4,4‘-azobis(4-cyanopentanoic acid) and 4-cyanopentanoic acid dithiobenzoate as an

initiator and chain transfer agent, respectively, and created polymer-modified surfaces following reduction of the dithioester chain end with sodium borohydride.[237] More recently, the Narain group in collaboration with the Liu group created a surface by immobilizing glycopolymers created by RAFT polymerization onto a sensor surface for studies of bacterial adhesion by quartz crystal microbalance with dissipation.[155]

In this collaborative investigation with the research groups of Professor Paul S. Weiss and Professor Gerard C. L. Wong, a set of glycopolymers of various saccharide identities was used to create glycopolymer surfaces, and the surfaces were studied for their ability to promote bacterial attachment.

5.2. Formation of glycopolymer surfaces

Using the set of glycopolymers that have various saccharides attached to the polymer backbone through a glycosidic bond from Section 4.2, various glycopolymer surfaces can be created to control bacterial adhesion. Four glycopolymers were previously created containing glucose, galactose, mannose, and *N*-acetyl glucosamine with a degree of polymerization (DP) of approximately 100. In addition, one mannose-containing glycopolymer was created with a DP of 215. In collaboration with the Weiss lab, glycopolymer surfaces were created by applying solutions of glycopolymer pre-reacted with ethanolamine to form a thiol chain end to substrates coated with gold via vapor deposition. The surfaces were rinsed and analyzed by X-ray photoelectron spectroscopy (XPS) for characterization of glycopolymer conjugation (Figure 5.2).

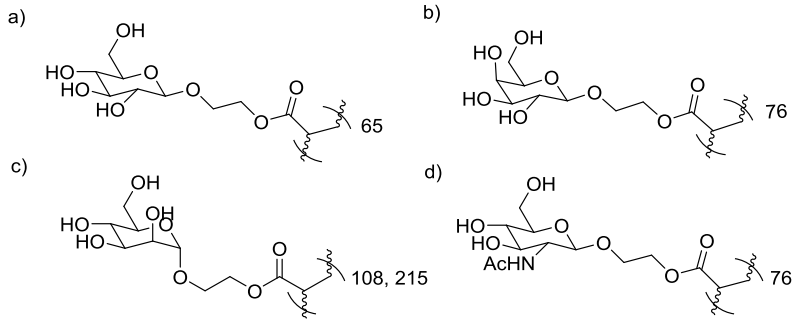

Figure 5.1. Set of glycopolymers synthesized in Section 4.2 containing a) glucose DP 65, b) galactose DP 76, c) mannose DP 108 and 215, and d) *N*-acetyl glucosamine DP 76

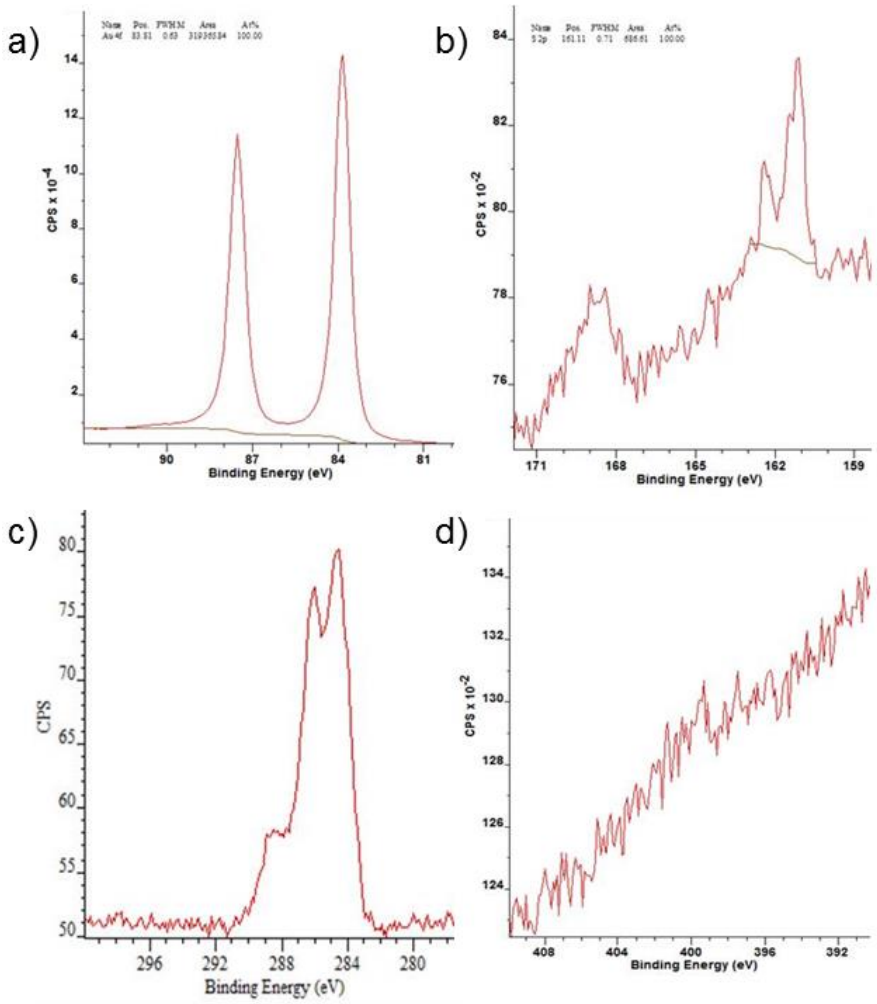

Figure 5.2. X-ray photoelectron spectroscopy analysis of a) gold 4f, b) sulfur 2p, c) carbon 1s, and d) nitrogen 1s electrons on a polymeric mannose-bearing surface.

From the XPS analysis, we can clearly see the gold from the surface (Figure 5.2a), the sulfur from the glycopolymer chain end (Figure 5.2b), and the carbon from the polymer backbone and saccharides (Figure 5.2c). Figure 5.2d shows no obvious peak for nitrogen, which indicates that the ethanolamine did not bind to the surface nor conjugate to the glycopolymer. By comparing the percent composition of carbon (34.66%) to gold (42.86%), there were approximately 175 surface gold atoms per polymer chain. Infrared spectroscopy of the surfaces exhibited peaks characteristic of alcohol and ether C-O stretching at 1100 cm^{-1} from the saccharide moieties and

ester stretching at 1250 cm^{-1} and carbonyl stretching at 1740 cm^{-1} from the linkage of the saccharides to the polymer backbone (Figure 5.3).

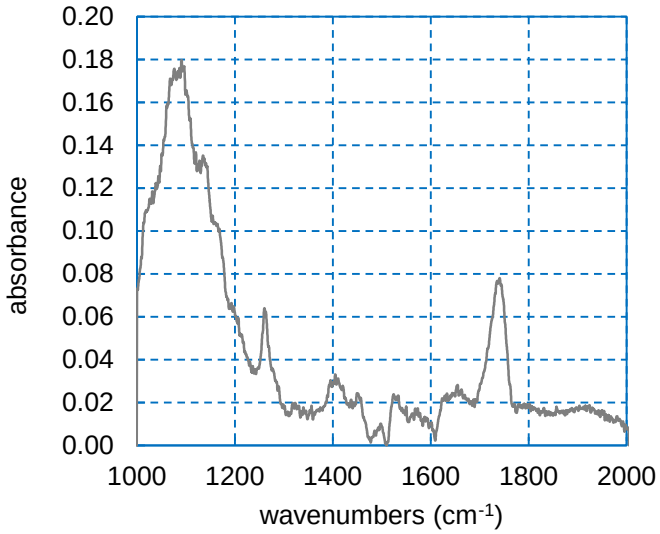

Figure 5.3. Infrared spectrum of a polymeric mannose-bearing surface.

5.3. Biological interaction with bacteria

5.3.1. Attachment of *Shewanella oneidensis*

In collaboration with the Weiss lab, glycopolymer surfaces were created in quadruplicate in the wells of a 96-well plate by coating the plate with gold via vapor deposition and incubating each well with a solution of glycopolymer pre-reacted with ethanolamine. After rinsing the plate to remove excess polymer, each well was incubated overnight with a solution of *Shewanella oneidens*is MR-1 strains wild type with GFP-containing plasmid p519nGFP in phosphate buffer saline (PBS) followed by rinses with PBS. The green fluorescent protein (GFP) emission, representative of the amount of bacteria attached to the surface in each well, was quantified with an excitation of 470 nm and an emission of 507 nm light. The galactose DP 76 and *N*-acetyl glucosamine DP 76 polymers exhibited significantly less bacterial adhesion, 78% and 89% respectively, compared to the mannose DP 108 polymer ($p < 0.01$) (Figure 5.4).

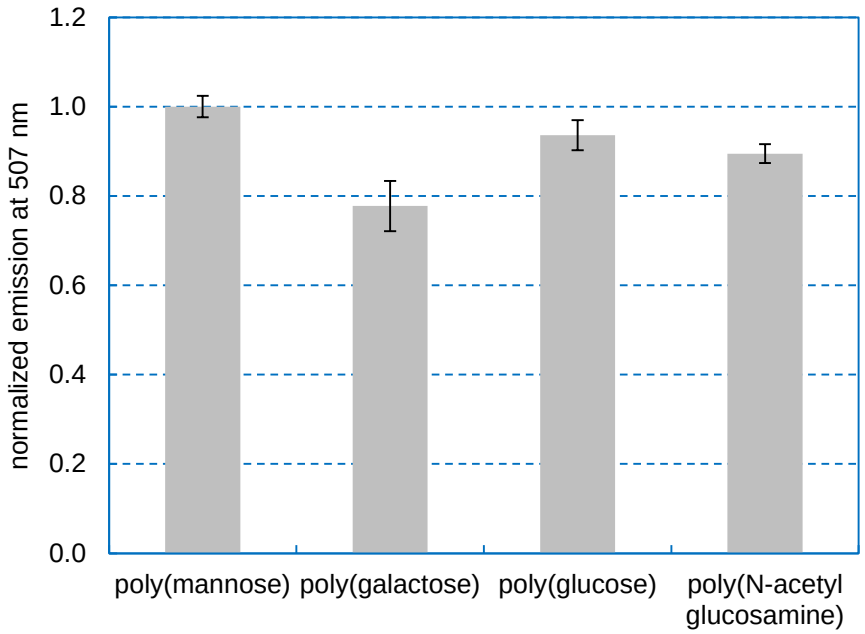

Figure 5.4. Normalized GFP emission at 507 nm from 470 nm excitation of *Shewanella oneidens*is MR-1 strains wild type with GFP-containing plasmid p519nGFP attached to various glycopolymer surfaces in quadruplicate.

In evaluating the effect of molecular weight, surfaces were created with polymeric mannose DP 108 and 215, and *Shewanella oneidens*is attachment was quantified relative to a chain-terminated mannose surface (Figure 5.5). Surfaces with polymeric mannose DP 108 and DP 215 exhibited a 3.2× and 2.2× amount of cell adhesion, respectively, compared to monomeric mannose. Higher molecular weight glycopolymers should have more bacterial attachment due to the cluster glycoside effect.[91] As expected, both polymeric surfaces bound more bacteria than the monomeric surface, but surprisingly, less bacteria bound to the high molecular weight polymeric mannose surface compared to the low molecular weight polymeric mannose surface. To further investigate this effect, a 250 mM solution of methyl α-D-mannopyranoside was applied to competitively inhibit the attachment of the bacteria to the surface, and while all surfaces saw a decrease in bacteria, the low molecular weight polymeric mannose surface retained a statistically significant higher amount of bacteria compared to the other surfaces ($p < 0.01$) (Figure 5.5) and maintained the most bacteria (37%) compared to the high molecular weight polymeric mannose

surface (19%) and the monomeric mannose surface (27%) (Table 5.1). Thus, the difference in bacterial adhesion in not just a difference in bacteria density, but it is a difference in avidity for the surface. While the high molecular weight glycopolymer is expected to have higher avidity compared to the low molecular weight glycopolymer, this observation was made with glycopolymers in solution. When the glycopolymers are attached to a substrate, only the saccharide residues exposed on the surface are accessible for bacterial adhesion. With higher molecular weight glycopolymer, the bulk of the sugar content may be hidden and inaccessible to the bacteria resulting in a decreased amount of avidity. In addition, the higher molecular weight polymer may create a surface with a saccharide density that surpasses an optimal density for bacterial interaction. A similar effect was observed by Serizawa *et al*. with saccharides attached to a nanoparticle surface.[198] When saccharide density reached a critical density (0.43 < critical density < 0.71 μg/cm^2) lectin binding becomes suppressed, presumably due to steric hindrance.

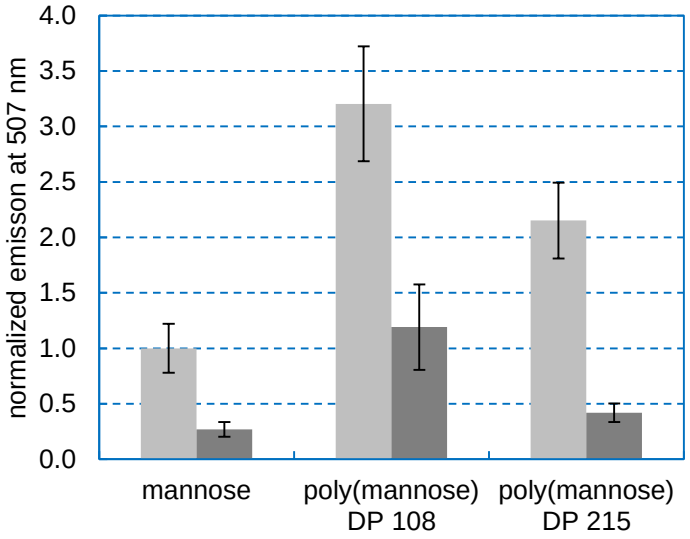

Figure 5.5. Normalized GFP emission at 507 nm from 470 nm excitation of *Shewanella oneidens*is MR-1 strains wild type with GFP-containing plasmid p519nGFP attached to a monomeric mannose and various molecular weight polymeric mannose surfaces in quadruplicate (light gray) and after incubation with a 250 mM solution of methyl α-D-mannopyranoside for 13 hours (dark gray).

Table 5.1. Percentage of GFP emission remaining after incubation with a 250 mM solution of methyl α-D-mannopyranoside for 13 hours.

mannose	poly(mannose) DP 108	poly(mannose) DP 215
27%	37%	19%

5.3.2. Attachment of *Vibrio cholerae*

Using the mannose polymer that exhibited the most bacterial attachment, (poly(mannose) DP 108), the movement of *Vibrio cholerae* was tracked on a surface in a flow cell in collaboration with the Wong lab (Figure 5.6). Looking at the trajectories of the bacteria, we observe that *Vibrio cholerae* interacts with glass and move in an orbital path with a diameter of approximately 10 μm (Figure 5.6a). When the bacteria interact with the polymeric mannose surface, the orbital paths decrease in size and number, indicating a stronger interaction with the surface (Figure 5.6b). When bacteria without MSH pili are introduced to the polymeric mannose surface, the orbital paths are lost entirely, indicating that there is no interaction between the bacteria and the surface (Figure 5.6c). Therefore, the interaction of the bacteria with the polymeric mannose surface is dependent on the expression of MSH. Analyzing the movement speed of the bacteria on the different surfaces, we observed that about 24% of the bacteria are stationary (moving < 5 μm/sec) on the polymeric mannose surface, whereas only about 5% of the cells are stationary on the glass surface and none of the cells are stationary without MSH pili (Figure 5.7).

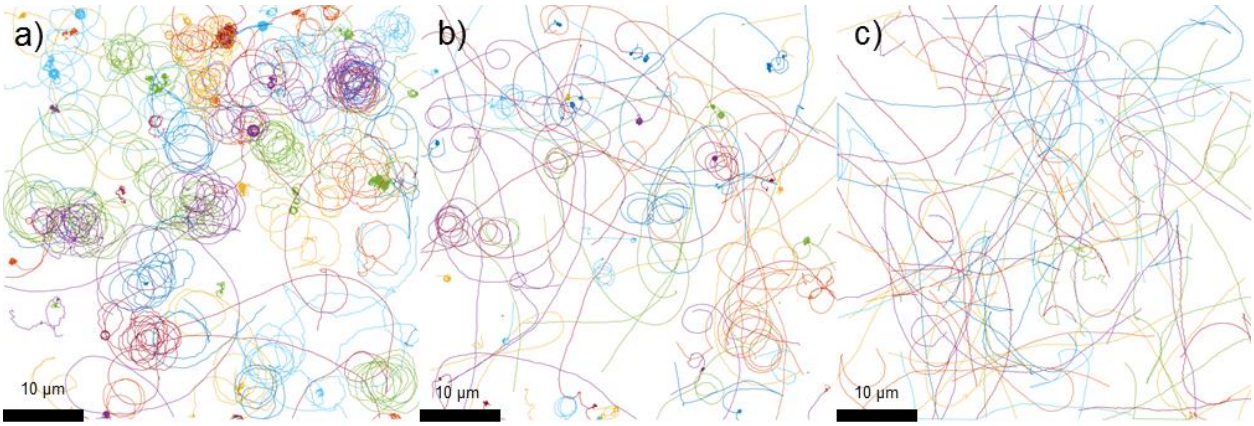

Figure 5.6. Trajectory of a) *Vibrio cholerae* on glass, b) *Vibrio cholerae* on a poly(mannose) surface, and c) *Vibrio cholerae ΔmshA* on a poly(mannose) surface.

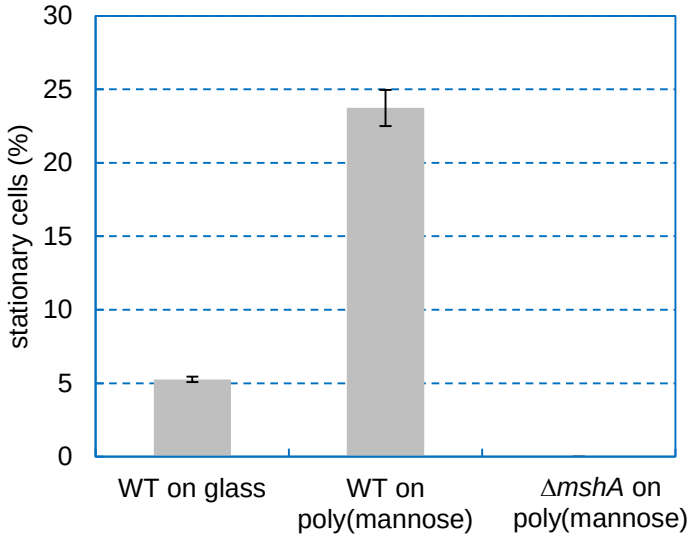

Figure 5.7. Percentage of stationary *Vibrio cholerae* cells (moving < 5 µm/sec).

5.4. Conclusions

Various glycopolymers composed of different saccharide identities were used to construct glycopolymer-modified surfaces on gold-coated substrates and characterized via X-ray photoelectron spectroscopy and infrared spectroscopy, which verified the presence of the glycopolymers on the gold substrates. Using these substrates, the ability to attach and direct the movement of *Shewanella oneidens*is and *Vibrio cholerae* was investigated since both bacteria facilitate adhesion using mannose-sensitive hemagglutinin (MSH). Using *Shewanella oneidens*is MR-1 strains wild type with GFP-containing plasmid p519nGFP on surfaces created on a gold-coated 96-well plate, the total amount of bacterial adhesion was quantified and demonstrated preferential attachment to mannose surfaces over galactose and *N*-acetyl glucosamine surfaces. In addition, we observed that surfaces constructed from higher molecular weight glycopolymer resulted in a decrease in bacterial adhesion in number and in avidity. When movement of *Vibrio cholerae* was tracked on a polymeric mannose surface in a flow cell, increased adhesion was observed when MSH was expressed. Using a combination of saccharide identity and molecular weight, patterned surfaces can be created that direct bacteria using the differences in cellular interaction with the various glycopolymer surfaces.

5.5. Experimentals

5.5.1. Materials

2-(2-[2-(11-Mercaptoundecyloxy)-ethoxy]-ethoxy)-ethoxy-acetic acid (Toronto Research Chemicals), 2-(2-[2-(11-mercaptoundecyloxy)-ethoxy]-ethoxy)-ethanol (Toronto Research Chemicals), 4-aminophenyl-α-D-mannopyranoside (LC scientific, 98%), trifluoroacetic acid (Sigma-Aldrich, 99%), ethanolamine (Sigma, 98%), triethylamine (Alfa Aesar, 99%), 1-ethyl-3-(3-dimethylaminopropyl) carbodiimide hydrochloride (Advanced Chem Tech, 98%), *N*-hydroxysuccinimide (Aldrich, 98%), ethanol (Decon Labs, 200 proof), and phosphate-buffered saline (PBS) (Cellgro) were used as received. *Shewanella oneidensis* MR-1 strains wild type with GFP-containing plasmid p519nGFP were used in cell attachment experiments. The WT O1 Serotype, El tor Biotype, A1552 strain of *Vibrio cholerae* and the isogenic mutant strains Δ*mshA* (lacking MSHA pilin) were used in the cell tracking experiments. Luria-Bertani (LB) media was made from LB broth powder (Fisher, 25 g/L). LB plates were poured using agar powder (Fisher, 15 g/L) in LB media.

5.5.2. Analytical techniques

X-ray photoelectron spectra were acquired using a Kratos Axis Ultra spectrometer (Chestnut Ridge, NY) with a monochromatic Al KR source (20 mA, 1.4 keV). Samples were fixed to a holder by a metal bar to complete a conductive path. The spectra were acquired at a pressure of 10^{-8} torr, anode voltage of 15 kV, emission of 20 mA, and a spot size of 300 μm × 700 μm. Survey spectra were acquired at a pass energy of 160 eV, while high-resolution spectra of the O 1s, N 1s, C 1s, S 2p, and Au 4f regions were collected at a pass energy of 20 eV. High-resolution spectra were averaged over 10 sweeps and had a 250 ms dwell time. Infrared absorption spectra were collected using a Nicolet 6700 FTIR spectrometer (Thermo Electron

Corp., Madison, WI) equipped with a liquid-nitrogen-cooled mercury-cadmium-telluride detector. The spectrometer was purged with dry and CO_2-free nitrogen. The substrate is placed at a grazing angle to the IR beam, 82 degrees relative to the surface normal. The polarization of the IR beam was modulated elliptically. Spectra were transformed using Norton-Beer (N-B) medium apodization, averaged over 2056 scans with a resolution of 2 cm^{-1}. Quantification of *Shewanella oneidensis* attachment to surfaces was conducted on a BioTek Synergy H1 multi-mode reader with excitation at 470 nm and emission at 507 nm. High-speed movies of *V. cholerae* motion in the flow-cells were captured with a Phantom V12.1 high-speed camera (Vision Research), collecting ~20,000 bright-field images at 5 ms resolution with a 100× oil objective on an IX81 Olympus microscope.

5.5.3. Vapor deposition of gold surfaces

5.5.3.1. Glass cover slips

Glass coverslips were cleaned by sonicating in ethanol, rinsing with 1% Alconox detergent in water, and rinsing with water for 30 minutes each. The substrates were then submerged in piranha solution (3:1 sulfuric acid with 30% hydrogen peroxide) for 1 hour and rinsed thoroughly with Millipore filtered water and dried with a nitrogen stream. Metal layers (2 nm of titanium followed by 2 nm of gold) were deposited by electron beam metal evaporation (Kurt J. Lesker Company, Jefferson Hills, PA) at a pressure beneath 1 x 10^{-7} torr to ensure even metal coverage at a rate of 0.3 Å/sec. Substrates, were flame annealed by passing a 4 cm hydrogen flame over the substrate once a second for 60 seconds.

5.5.3.2. 96-Well plate

96-Well plates were used as received and coated with 10 nm of titanium followed by 80 nm of gold by electron beam metal evaporation (Kurt J. Lesker Company, Jefferson Hills, PA) at a

pressure around 10^{-6} torr to soften shadows in the deposition at a rate of 1 Å/sec. Well plates were visually inspected and wells that were not fully covered by gold were not used in glycopolymer surface formation.

5.5.4. Creation of saccharide surfaces

5.5.4.1. Monomeric mannose surface

A solution of 0.5 mM 2-(2-[2-(11-mercaptoundecyloxy)-ethoxy]-ethoxy)-ethoxy-acetic acid, 0.5 mM 2-(2-[2-(11-mercaptoundecyloxy)-ethoxy]-ethoxy)-ethanol, and 130 mM trifluoroacetic acid was mixed in ethanol and added to the gold substrate for three days. The solution was removed and the substrates were rinsed with triethylamine in ethanol (10 v/v%) followed by ethanol. A solution of *N*-hydroxysuccinimide (0.05 M) and 1-ethyl-3-(3-dimethylaminopropyl) carbodiimide (0.2 M) in water was added for 30 minutes to form an NHS ester. The surface was rinsed with water and dried with a nitrogen stream. A solution of 4-aminophenyl-α-D-mannopyranoside (2 mg/mL) in sodium phosphate buffer (25 mM, pH 8.0) was applied to the surface for two days.

5.5.4.2. Polymeric saccharide surface

A glycopolymer solution (0.5 mM) was reacted with ethanolamine (80 mM) in water for 30 minutes before addition to the gold surface for three days followed by rinsing with water, ethanol, and PBS (pH 7.2).

5.5.5. Quantification of attachment through green-fluorescent protein (GFP) emission

Shewanella oneidensis MR-1 WT p519nGFP from frozen stock incubated for 24 hours at 32 °C was streaked on LB agar plates containing kanamycin. The bacteria were precultured by inoculating LB media (20 mL) in a 125mL flask and incubating at 32 °C for 24 hours. The preculture (1 mL) was diluted into LB media with 50 mg/L kanamycin (20 mL). The culture was

incubated until the optical density at 600 nm reached 0.9 (approximately two hours). The cell were washed by centrifugation (2300 RCF, 5 minutes) and resuspended in PBS (3×). The bacteria solution was diluted 10× in PBS and aliquoted into each sample well (250 μL) and incubated at 32 °C for 18 hours to allow for cell attachment. The wells were rinsed with PBS (4×) and covered with PBS (100 μL). The green fluorescent protein emission was quantified by a plate reader at an excitation of 470 nm and emission of 507 nm. Gold-coated surfaces covered with PBS without bacteria (100 μL) were used as a negative control and subtracted from the fluorescence of each well prior to normalization.

5.5.6. Cell tracking

The bacteria were cultured in LB media overnight under shaking at 30 °C. Prior to inoculation, a subculture was made by diluting the overnight culture into 2% LB (containing 171 mM NaCl) to an optical density at 600 nm in the range of 0.01–0.03. *V. cholerae* were then injected into a sterile flow-cell heated at 30 °C containing the same media and high-speed movies of *V. cholerae* motion in the flow-cells were captured.

5.5.7. Cell-tracking algorithm and analysis

We preprocess every frame of a movie in Matlab (Mathworks) by subtracting the background, scaling, smoothing, and thresholding to generate a binary image using Otsu thresholding[238]. Bacteria appear as bright regions. Tracking is done by locating all bright objects that overlap objects in the next frame by combining the two frames into a three-dimensional (3D) matrix and then by locating 3D connected components.

We store the results in a tree-like structure with multiple roots[239]; every newly detected bacterium that appears is recorded as a ‘root’ of the tree. When bacteria interact, they are recorded as a ‘node’ of the tree; when they depart, they are recorded as a ‘leaf’. Each root or

node stores the sequence of pixel lists that comprise the bacterium in all frames until the next interaction or detachment event. We measure the instantaneous shape properties of the bacteria using the Matlab regionprops function. From these properties we can calculate the MSD, $\Delta x^2(t) = \langle(\vec{x}(t+t_2) - \vec{x}(t_i))^2\rangle$, where $\vec{x}(t_j) = \vec{R}_j$ and is the position vector of the j^{th} point on the trajectory and the angled brackets indicate an average over all times t_i. The MSD gives information about the average displacement between points in the trajectory separated by a fixed time lag[240]. The instantaneous speed is calculated as, $v_i = |\vec{x}(t+t_{i+1}) - \vec{x}(t_i)|/\Delta t$, where $\Delta t = t_{i+1} - t_i$. The angle difference is defined as the angle between a bacterium's instantaneous velocity and its body axis, limited to the range $\left[0, \frac{\pi}{2}\right]$[241,242].

CHAPTER 6

Biological interaction of hyperbranched glycopolymers presented in 3D

The contents of this chapter were adapted from with permission from *Biomacromolecules* 16, 284–94 (2015).

6.1. Introduction

Lectins are saccharide-binding proteins that are important in biological recognition and immune response. Lectins typically exhibit weak interactions with monosaccharides, but the clustering of saccharide ligands and increased density of their presentation (e.g. through branching) enhances these interactions. Lectins contain multiple carbohydrate recognition domains (CRDs). Although lectins from diverse sources lack primary sequence homology, they share similarities in tertiary structure. This implies that the primary sequence may be important for recognizing specific monosaccharide residues, but that the 3D presentation of the saccharides to the lectin is a key determinant in the avidity of this interaction.[243]

Since the natural binding partners of lectin may be polysaccharides and/or glycoproteins, our group has investigated the interactions of synthetic binding analogues of these partners, both glycopolymers and protein-glycopolymer conjugates, with lectin.[19,119] In particular, we demonstrated that branched polymers incorporating a saccharide unit (mannose) into the branching repeat unit show a higher affinity for the corresponding lectin (mannose binding lectin, MBL) than linear polymers of the same molecular weight or branched polymers with the same number of mannose residues but without mannose incorporation in the branching repeat unit. Furthermore, we demonstrated that the lectin affinity increases with increasing polymer

branching density, which has also been recently verified by another group.[244] In addition to linear and branched glycomimetics, synthetic glycoproteins[245] and protein glycoconjugates[246–250] have also been reported in literature and synthesized by our group[251]. We polymerized glycomonomers from protein-based initiators to obtain protein-glycomimetic conjugates. Interestingly, the 3D presentation of the glycoresidues (mannose) from the protein surface appears to significantly enhance their interaction with lectin (MBL). This indicates that the 3D presentation of the sugar groups may more strongly influence their interaction with lectins than the chain length, consistent with observations about the distribution of CRDs on lectins.

While using protein-glycoconjugates to study the role of 3D presentation is promising, there are several synthetic limitations. First, the distribution of glycopolymer chains and the 3D shape of the protein are inherently limited by the sequence and 3D structure of the protein and are not easy to systematically vary. The distribution of glycopolymer chains on the surface of the protein is limited to available reactive amino acids, such as lysine, which can be converted into initiating groups. Second, polymerization would ideally be conducted in water to maintain the 3D protein structure, but this polymerization is difficult to control and requires the use of a sacrificial initiator.[140] Finally, the characterization of this protein-glycopolymer conjugates is difficult, especially the determination of the glycopolymer chain length.[251]

As an alternative, the relationship between glycopolymer structure, glycoresidue density, and 3D presentation to lectins can be systematically studied using amphiphilic copolymers that self-assemble into nanoparticles. Nanoparticles offer several advantages, including facile synthesis and tunable size and surface chemistry. Glyconanoparticles can be created by surface modification of nanoparticles, by conjugation of hydrophobic polymers to glycopolymers or natural polysaccharides, by post-polymerization modifications of reactive block copolymers, or

by direct polymerization of glycomonomers from macroinitiators. In the first approach, nanoparticles are fabricated prior to conjugation of saccharide moieties onto their surface.[252–254] While this ensures the formation of nanoparticles, the conjugation of saccharide moieties is limited due to the nanoparticles' insolubility and the steric hindrance of grafting to the surface. Direct conjugation of hydrophobic polymers to natural polysaccharides or growth of hydrophobic polymers from polysaccharide macroinitiators allows direct incorporation of natural residues.[255–262] However, natural polysaccharides may offer little control over architecture or molecular weight, can be difficult to purify, and can suffer from batch-to-batch variability. Amphiphilic block copolymers incorporating a glycopolymer block can be synthesized via post-polymerization modification of a reactive block (such as an azide-alkyne Huisgen cycloaddition)[24,120,263–266] or by direct polymerization of glycomonomers from a living macroinitiator. For example, the Sanderson group created an amphiphilic glycopolymer via direct polymerization of methacryloyl-1,2:5,6-di-*O*-isopropylidene-D-glucofuranose and then extending the chain with styrene or methyl acrylate, followed by deprotection of the isopropylidene protecting groups.[267] Controlled radical polymerizations are particularly useful for making such block copolymers as they tolerate a wide variety of polymerization conditions and monomers. Controlled radical polymerization has been used to create amphiphilic glycopolymers via nitroxide-mediated polymerization (NMP),[258,268] atom transfer radical polymerization (ATRP),[269–275] and radical addition-fragmentation chain transfer (RAFT) polymerization.[151,267] RAFT polymerization is of particular interest as it avoids the use of biotoxic metal catalysts and is susceptible to facile chain-end modification.[276–278] Once the amphiphilic polymers are synthesized, they can be assembled into nanoparticles via techniques such as solvent evaporation, nanoprecipitation, emulsification/solvent diffusion, salting out, or

dialysis.[279] For example, Pati *et al.* used nanoprecipitation to self-assemble glycopolypeptide-dendrons,[280] and Bonduelle *et al.* used nanoprecipitation to self-assemble tree-like glycopolypeptides.[281]

After self-assembly, the 3D glyconanoparticles can interact with lectins that also have a 3D conformation. A common method to determine the bioactivity of glycopolymers is to investigate their ability to bind native lectins through *in vitro* experiments. Increased molecular weights and branching in glycopolymers have been seen to enhance lectin interactions.[19,91–93] The enhancement in interaction is attributed to the lectin having multiple carbohydrate recognition domains as with *Ricinus communis* (castor bean) agglutinin 120 (RCA_{120}).[95,96] Multiple carbohydrate recognition domains allow the lectin to bind multiple saccharides on the same polymer when properly spaced. Spain *et al.* has reported increased binding of RCA_{120} with increasing molecular weight of linear glycopolymer.[282] Lee *et al.* has reported that an oligosaccharide with three branches presented a 1000-fold increase in binding to hepatic lectin even though it contained only three times as much galactose compared to a similar linear oligosaccharide.[98] The increased interaction due to clusters of saccharides has been termed "the cluster glycoside effect."[91] These examples, however, only present the glycopolymer in solution.

Since nanoparticles are composed of densely packed amphiphilic molecules, lectins may not be able to penetrate into the nanoparticle such that only the ligands presented on the surface may be available for binding. Increased lectin binding has been observed with nanoparticles that present monomeric saccharides on their surface compared to monomeric saccharides in solution.[254,275] Functionalization of the surface of polymer vesicles and nanoparticles with dendritic saccharides further amplifies this effect.[254] The Akashi group has reported that saccharide surface density is directly proportional to the size of the nanoparticle when size is

adjusted by increasing the length of the hydrophobic block.[283] In addition, there is an optimal surface density for lectin binding, above which lectin interaction decreases.[198,283]

To better understand structure-activity relationships between glycopolymers and lectins, it is important to study the combined effects of branching and 3D presentation. Using the set of amphiphilic glycopolymer with systematic variation of molecular weight and branching created in Section 4.4 (Table 6.1), nanoparticles were self-assembled via nanoprecipitation, and the bioactivity of the nanoparticles was examined using two representative biological assays, an inhibitory enzyme-linked lectin assay and the hemagglutination assay. By adjusting the molecular weight and degree of branching of the glycoblock of the copolymer, the size of the self-assembled nanoparticle and the saccharide density on its surface can be tuned, impacting its interaction with lectin.

Table 6.1. Summary of amphiphilic copolymers synthesized in Section 4.4.

	^{1}H NMR			GPC†		
copolymer	conversion of chain-extension	DP of sugar	M_n	M_w	M_n	$Đ$
25:50 0 branch	88%	44	16190	10270	6480	1.58
25:50 1 branch	86%	43	16170	7790	5610	1.39
25:50 5 branch	92%	46	18290	7700	5830	1.32
25:25 0 branch	90%	23	9480	7580	5870	1.29
25:25 1 branch	71%	18	8220	6790	4980	1.36
25:25 5 branch	78%	20	9800	5420	3920	1.38
25:12 0 branch	42%	5	4060	6310	4800	1.31
25:12 1 branch	30%	4	3680	4820	4130	1.17
25:12 5 branch	80%	10	6850	4230	3350	1.26

†Gel permeation chromatography (GPC) was performed in THF and calibrated using linear poly(methyl methacrylate) standards.

6.2. Self-assembly into 3D micelles

Each copolymer from Section 4.4 was named according to the ratio of the degree of polymerization of methyl acrylate, the expected degree of polymerization of acryloyl-1,2:3,4-di-*O*-isopropylidene-α-D-galactose, and the expected number of branches per chain. For example, a copolymer with poly(methyl acrylate) with a degree of polymerization of 25, poly(acryloyl-1,2:3,4-di-*O*-isopropylidene-α-D-galactose) with a target degree of polymerization of 50, and a target of five branches per chain would be named 25:50 5 branch. First, the isopropylidene-deprotected copolymer samples were self-assembled via direct hydration, but only the 25:50 copolymers were observed to form well-defined structures (Table 6.2). Nanoprecipitation was conducted by quickly injecting a solution of copolymer dissolved in DMSO into water (Method 1) or by adding water dropwise to the DMSO solution (Method 2). Transmission electron microscopy (TEM) images of the samples created via direct hydration revealed a continuous gradient of sizes ranging from 10 to 200 nm in diameter, whereas the samples created via nanoprecipitation revealed more homogeneous nanoparticles (Figure 6.1). Nanoprecipitation Method 1 tended to produce more polydisperse nanoparticles than Method 2 (Table 6.2). Therefore, nanoprecipitation Method 2 was employed, and the resulting nanoparticles were analyzed via dynamic light scattering (DLS) and recorded via TEM (Figure 6.2).

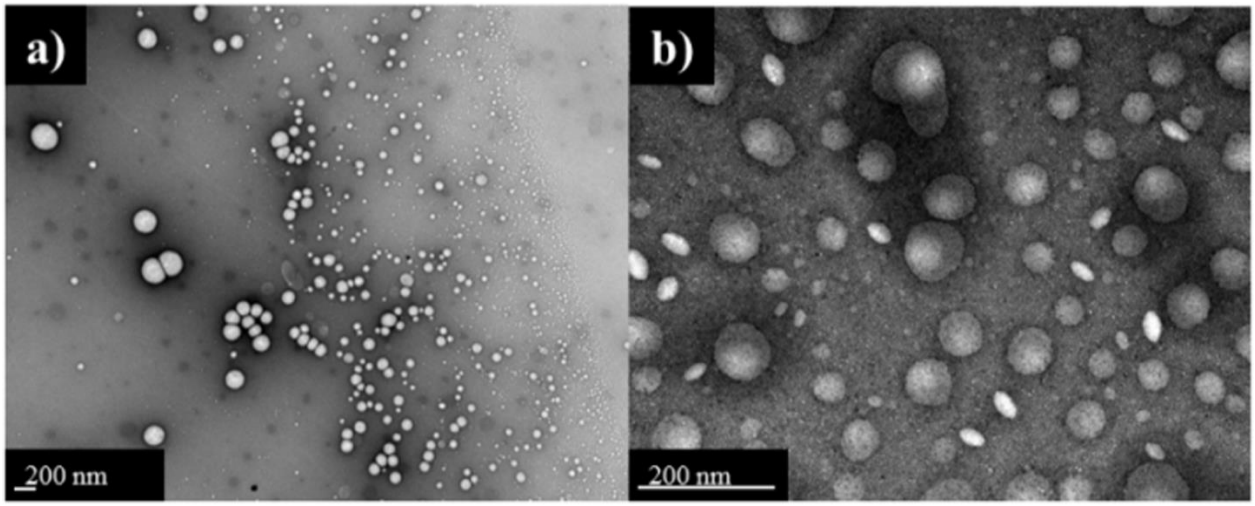

Figure 6.1. TEM images of nanoparticles formed from 25:50 0 branch copolymers by a) direct hydration (DH) and b) nanoprecipitation Method 2.

Table 6.2. Average diameter and polydispersity index (PDI) of 25:50 copolymers using the following methods of self-assembly: direct hydration (DH) measured after 2 hours and 2 days; nanoprecipitation by addition of the DMSO solution into water (Method 1) or addition of water dropwise into the DMSO solution (Method 2).

	0 branch		1 branch		5 branch	
	diameter (nm)	PDI	diameter (nm)	PDI	diameter (nm)	PDI
DH (2 hours)	280	0.32	219	0.48	319	0.54
DH (2 days)	244	0.19	198	0.48	261	0.45
Nanoprecipitation Method 1	81	0.41	46	0.39	70	0.50
Nanoprecipitation Method 2	107	0.20	57	0.44	85	0.36

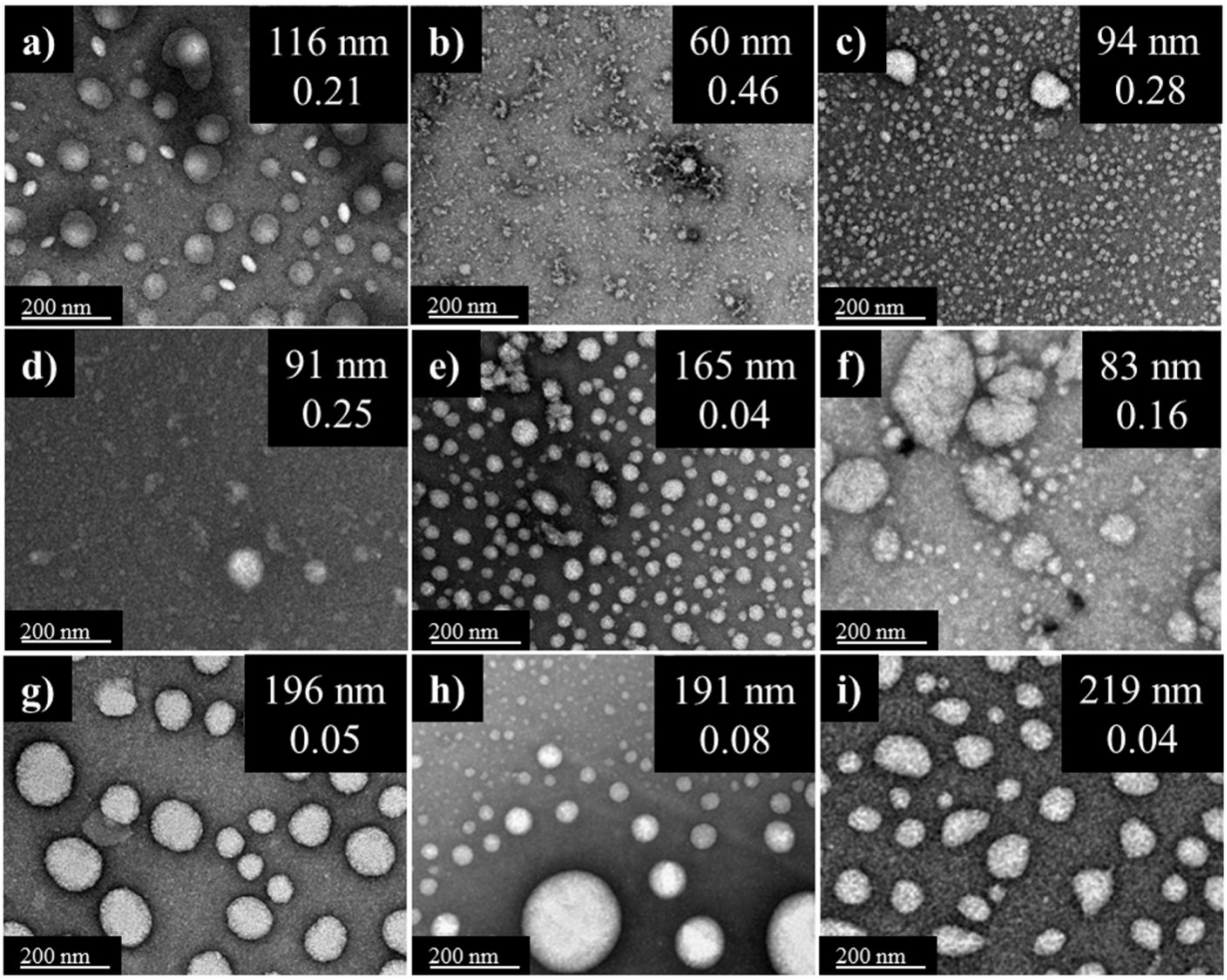

Figure 6.2. TEM images of copolymer nanoparticles with corresponding diameter and PDI from DLS of a) 25:50 0 branch, b) 25:50 1 branch, c) 25:50 5 branch, d) 25:25 0 branch, e) 25:25 1 branch, f) 25:25 5 branch, g) 25:12 0 branch, h) 25:12 1 branch, and i) 25:12 5 branch.

In general, decreasing the length of the hydrophilic segment of the copolymer produced larger nanoparticles with lower polydispersity. Some of the samples produced abnormally high polydispersities (Figure 6.2b) compared to other samples of similar molecular weight (Figure 6.2a). We suspect that a more gradual and continuous solvent displacement method might be necessary. The non-circular shape observed in some TEM samples may indicate a non-spherical morphology that may be explained by the glassy character of the hydrophobic domain, which can lead to out of equilibrium structures. In addition, the increase in size with decreasing molecular weight indicates that we do not have simple micelles.

The samples that appeared to be monodisperse by TEM were further analyzed by multi-angle light scattering (MALS). The calculated hydrodynamic radius (R_H) from MALS (Table 6.3) was in close agreement with the measurement obtained from DLS. Static light scattering was also conducted on the 25:12 0 branch nanoparticles to obtain the radius of gyration (R_g). By taking the ratio for R_g/R_H, a shape factor of 0.84 was calculated (Figure 6.3). A solid sphere has a shape factor of 0.78, while a hollow sphere has a shape factor that approaches 1.[265,284–286] Based on the shape factor and the TEM analysis, we conclude that the nanoparticles were solid spheres, possibly stabilized by the hydrophobic CTA chain ends.

Table 6.3. Hydrodynamic radius (R_H) as determined from multi-angle light scattering.

nanoparticle sample	R_H (nm)
25:50 0 branch	52
25:50 5 branch	44
25:25 1 branch	81
25:12 0 branch	96
25:12 5 branch	105

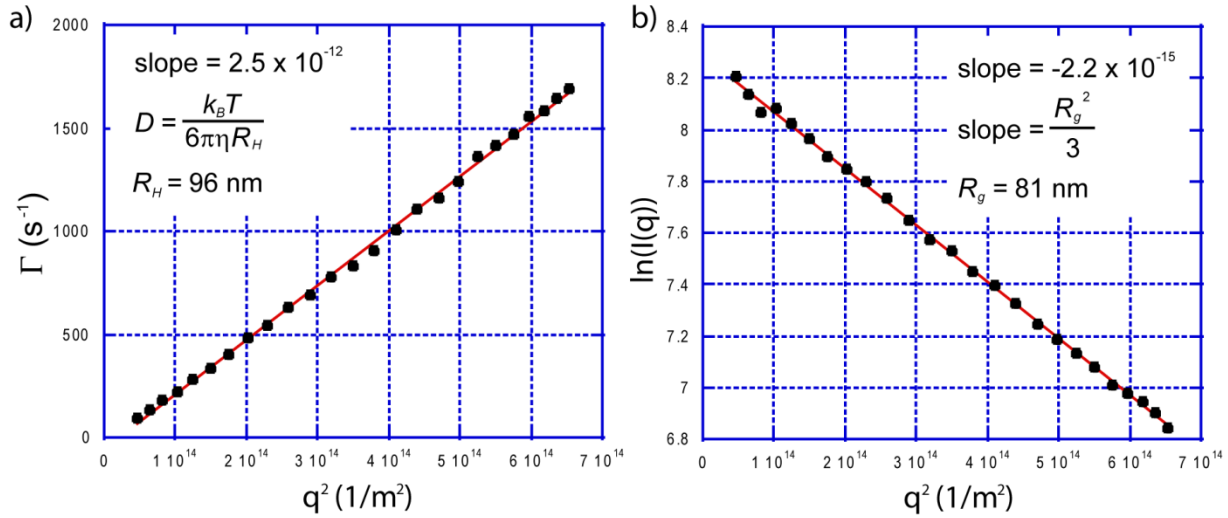

Figure 6.3. Multi-angle light scattering analysis of 25:12 0 branch copolymer nanoparticles for determining shape factor: a) decay constant (Γ) versus squared magnitude of the scattering vector (q^2) for determining hydrodynamic radius (R_H) using the Stokes-Einstein equation and b) Guinier plot for determining radius of gyration (R_g).

To further investigate the possibility of an aggregated construct facilitated by the CTA chain end, the copolymer chain ends were modified by aminolysis into a free thiol and self-assembled via nanoprecipitation and investigated by DLS (Figure 6.4). The resulting nanoparticles constructed from the lowest molecular weight copolymers were significantly smaller in size (Table 6.4). When the copolymers with higher proportion of hydrophilic block were subject to the same end group modification, monodisperse nanoparticles could not be formed, suggesting that the hydrophobic CTA chain end assists in the formation of stable nanoparticles. Aminolysis, therefore, may be a viable method of dissolution of these nanoparticles.

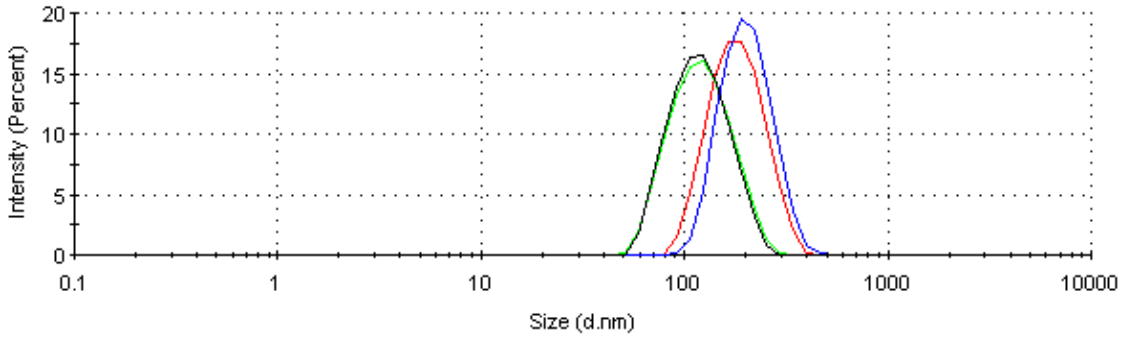

Figure 6.4. Histogram of DLS of 25:12 0 branch (red) and 25:12 5 branch (blue) copolymer nanoparticles prior to aminolysis and 25:12 0 branch (black) and 25:12 5 branch (green) copolymer nanoparticles after aminolysis.

Table 6.4. Diameter and PDI of nanoparticles before and after aminolysis as measured by DLS.

	before aminolysis		after aminolysis	
	dia. (nm)	PDI	dia. (nm)	PDI
25:12 0 branch	196	0.05	112	0.09
25:12 5 branch	219	0.04	113	0.10

6.3. Biomolecular interaction with linear and branched glycopolymers presented in 3D

In addition to observing the morphology of these self-assembled nanoparticles, the biological relevance of the nanoparticles was assessed via lectin binding assays.[9] First, we qualitatively investigated the direct interaction of the nanoparticles with *Ricinus communis* (castor bean)

agglutinin 120 ($RCA_{120,}$ an R-type galactose binding lectin) via a lectin precipitation assay. While it is generally accepted that RCA_{120} is specific for non-reducing β-linked D-galactose, Fais *et al*. demonstrated that both terminal galactose and 6-substituted galactose can interact with the carbohydrate binding site of RCA_{120}.[88] At the same concentration of galactose, the high molecular weight copolymer nanoparticles induced more crosslinking/precipitation of RCA_{120} than the low molecular weight copolymer nanoparticles as observed the absorbance at 450 nm (Figure 6.5). The high molecular weight copolymer nanoparticles have more saccharides per copolymer. Since the nanoparticles are smaller, the high molecular weight copolymer nanoparticles also have a higher surface area to volume ratio. Thus, they have more saccharide residues available for lectin interaction.

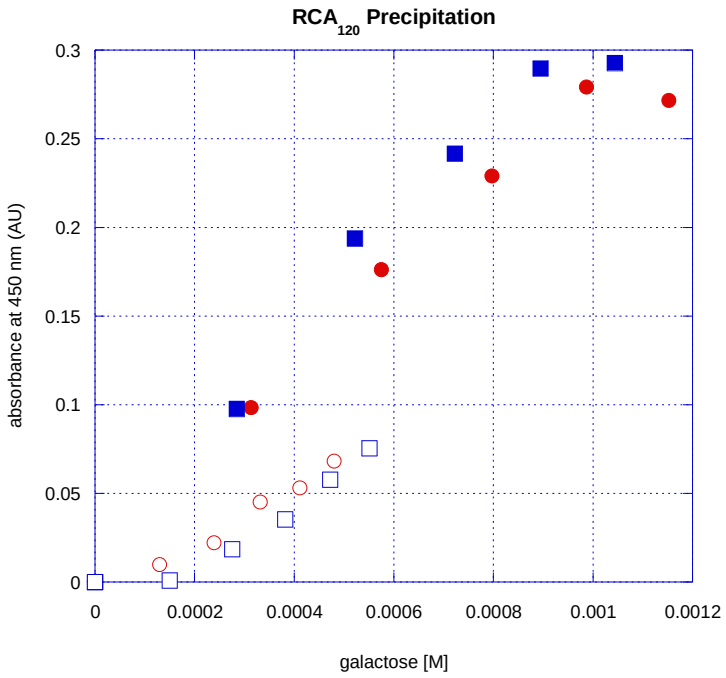

Figure 6.5. Absorbance at 450 nm versus total galactose in solution of 25:50 0 branch (●), 25:50 5 branch (■), 25:12 0 branch (○), and 25:12 5 branch (□) nanoparticles added to a RCA_{120} solution (2 mg/mL).

To obtain a more quantitative measure of lectin activity, the hemagglutination assay and an inhibitory enzyme-linked lectin assay (ELLA) were used. The hemagglutination assay is an

inhibition assay which indirectly quantifies nanoparticle-lectin interactions. In the absence of nanoparticles, the lectin will cause red blood cell precipitation, but if nanoparticles are present and bind the lectin, the red blood cells will not precipitate. Varying concentrations of nanoparticles in solution are prepared, and lectin is added and allowed to interact with the nanoparticles. Red blood cells are subsequently added to the lectin-nanoparticle solution, and the minimum concentration of nanoparticles needed to prevent red blood cell precipitation is recorded. In the inhibitory ELLA, well plates are coated with a high molecular weight polysaccharide or glycopolymer that competitively binds to the lectin. Solutions of lectin and varying concentrations of nanoparticles are added to the well plate, and the amount of lectin that binds to the wells is quantified as the concentration of nanoparticles decreases. The percent inhibition versus saccharide concentration is plotted and curve fitted. The concentration at which 50% inhibition of interaction is observed can be reported and used to calculate relative potency.

The galactose concentrations listed for the hemagglutination assay (Figure 6.6) and ELLA (Figure 6.7) describe the total galactose concentration in the system. This concentration represents the maximum amount of galactose residues available for interaction, although the number of residues actually available may be significantly less. That is, unless the lectin is able to intercalate the glycopolymer layer, only the residues displayed on the surface of the nanoparticle may interact. The 25:50 nanoparticles exhibit no significant inhibition in either assay, in contrast to samples with shorter glycoblocks. In the literature, the interaction between galactose-functionalized nanoparticles and RCA_{120} has been shown to depend on the density of saccharide residues on the surface. Increasing potency is observed with increasing galactose density on the surface until a critical density of saccharide residues is reached ($0.43 <$ critical density < 0.71 $\mu g/cm^2$), at which point binding becomes suppressed, presumably due to steric

hindrance.[198] With the increased galactose content per copolymer, the 25:50 nanoparticles may exceed the critical galactose surface density, thus sterically limiting their interaction with RCA_{120}. Relative potencies for the remainder of the nanoparticles were reported relative to poly(galactose acrylate) with a DP of 12 and 5 branches per chain (Table 6.5).

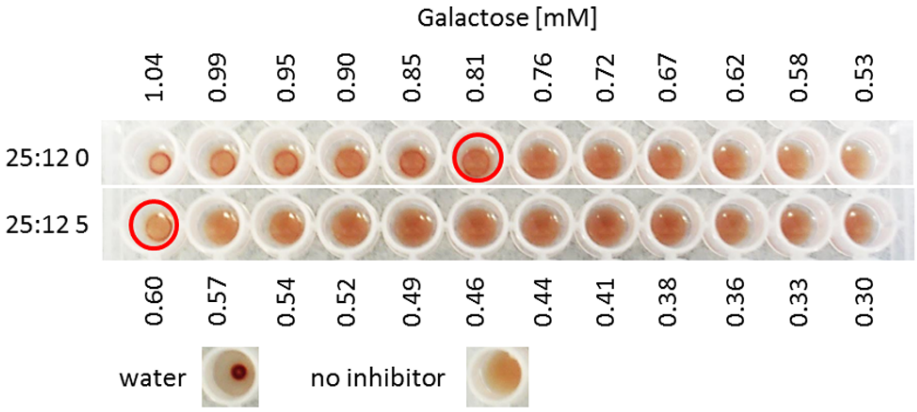

Figure 6.6. Example of the hemagglutination assay plate with the lowest nanoparticle concentration where red blood cell precipitation is inhibited circled.

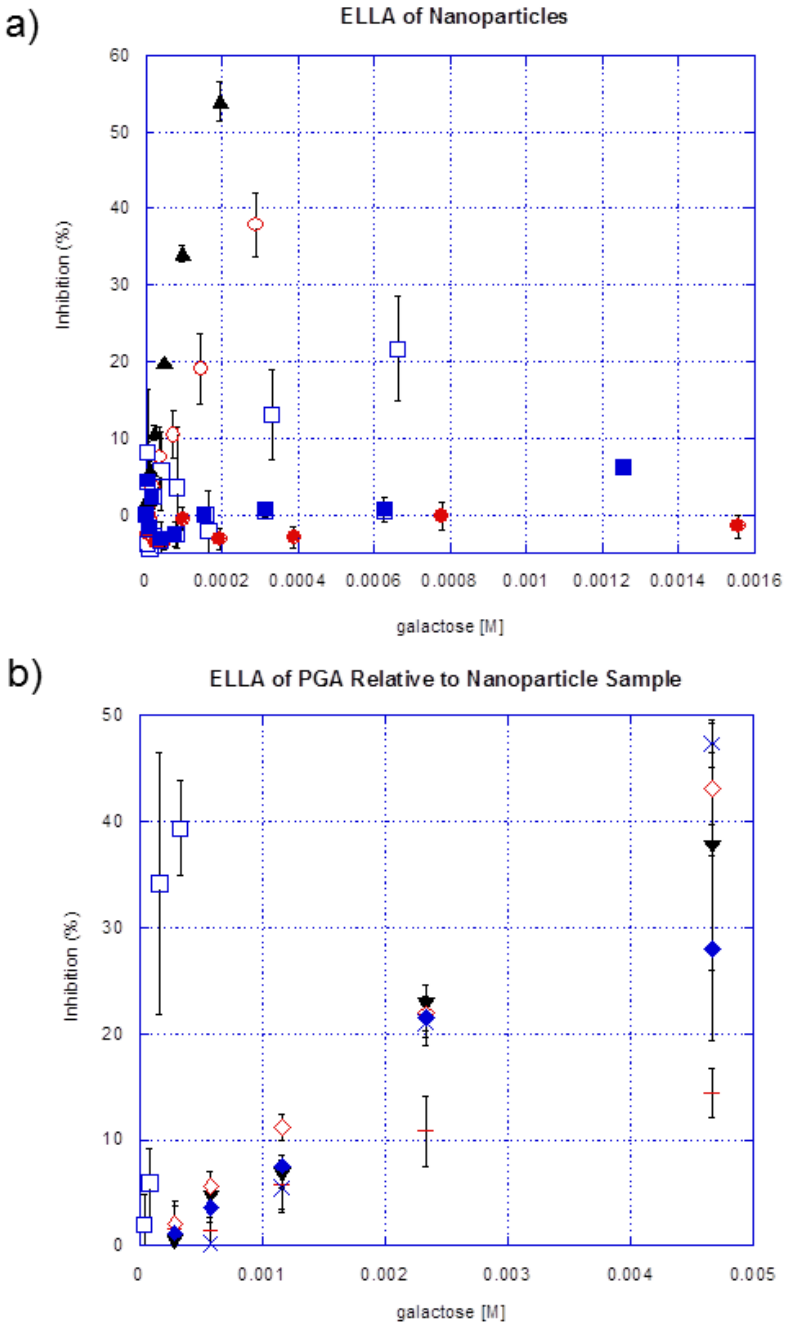

Figure 6.7. a) Percent RCA_{120} inhibition as a function of galactose content in 25:50 0 branch (●), 25:50 5 branch (■), 25:25 1 branch (▲), 25:12 0 branch (○), and 25:12 5 branch (□) nanoparticles and b) 25:12 5 branch (□) nanoparticle with a 3D structure exhibit increased lectin binding compared to 12 0 branch (-), 12 5 branch (×), 25 1 branch (▼), 50 0 branch (◊), and 50 5 branch (♦) glycopolymers in solution. The ratios in the samples represent the degree of polymerization of the copolymer PMA:poly(galactose acrylate) followed by the number of branches per chain. When no ratio is present, the number represents the degree of polymerization of poly(galactose acrylate) (PGA) followed by the number of branches per chain.

Table 6.5. Relative potencies of glycopolymer and nanoparticle interactions with RCA_{120}.

compound	hemagglutination relative potency†	ELLA relative potency‡
poly(galactose acrylate)		
12 0 branch	-	0.3
12 5 branch	1	1
25 1 branch	-	0.8
50 0 branch	-	0.9
50 5 branch	-	0.6
nanoparticle		
25:12 0 branch	4.8	26
25:12 5 branch	6.5	13
25:25 1 branch	16	58

† Relative potency is calculated as the ratio of the concentration at which inhibition of precipitation is last observed for the 12 5 branch glycopolymer divided by the concentration at which inhibition of precipitation is last observed for the compound.
‡ Relative potency is calculated as the ratio of the concentration at which 50% inhibition is observed for the 12 5 branch glycopolymer divided by the concentration at which 50% inhibition is observed for the compound.

In both assays, the nanoparticle of intermediate size and galactose content (25:25 1 branch) exhibits the highest potency. Nanoparticles of larger size and lower galactose content exhibit lower potency than the 25:25 1 branch nanoparticles, but higher potency than free glycopolymers in solution. These particles may have a lower density of galactose on the surface than the 25:25 1 branch particles, which is consistent with both the particle size and the (relatively) shorter glycoblocks.

The apparent discrepancies between the hemagglutination assay and the inhibitory ELLA may be attributed to inherent differences between the two assays. RCA_{120} is a 120 kDa divalent β-galactose binding lectin with the two binding sites separated by 12 nm.[96,287] In the hemagglutination assay, each RCA_{120} can bind either a) monovalently to a red blood cell (RBC) with one binding site free; b) monovalently to a nanoparticle with one binding site free; c) divalently to a single nanoparticle or single RBC; or d) divalently to bridge two separate species (two nanoparticles, two RBCs, one RBC and one nanoparticle). The hemagglutination

assay measures the amount of crosslinking species in solution (free RCA_{120} that binds to two different red blood cells and nanoparticles with multiple RCA_{120} attached through only one binding site each that can then bind two or more red blood cells). It does not account for nanoparticles with only one RCA_{120} attached through one binding site nor RCA_{120} divalently attached to a single nanoparticle or RBC. The inhibitory ELLA quantifies the amount of RCA_{120} bound to the well plate (RCA_{120} unbound to nanoparticles and RCA_{120} monovalently bound to a nanoparticle, along with all the RCA_{120} bound to that nanoparticle). Due to these differences, the ELLA tends to amplify measured potencies compared to the hemagglutination assay. The inversion in relative potency between the two 25:12 nanoparticles suggests that when the nanoparticles are mixed with RCA_{120}, the samples without branches produce more crosslinking species whereas the samples incorporating branches allow more RCA_{120} to be bound to the plate.

If we consider a nanoparticle with multiple lectins bound to it, the difference can be explained by an increase in monovalent lectin bound to the nanoparticles, which allow for denser packing on the nanoparticle (Figure 6.8). With a higher galactose density on the surface of the branched nanoparticle, lectin can bind in greater density, which can hinder divalent binding to the nanoparticle. The higher lectin density on the nanoparticle does not necessarily translate into more crosslinking species since both types of nanoparticles may still bind multiple RCA_{120} molecules monovalently; furthermore, increased density of RCA_{120} on the surface of the nanoparticle incorporating branched glycoblocks may result in steric hindrance when interacting with the RCA_{120} receptors on the surface of RBCs. However, increased lectin density on the nanoparticles incorporating branched glycoblocks will translate into more lectin absorbing to the well plate in the inhibitory ELLA.

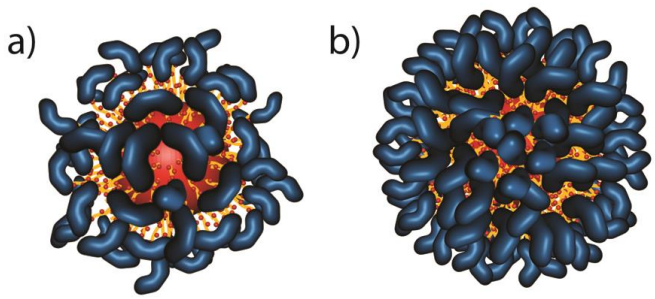

Figure 6.8. Representation of RCA_{120} (blue) saturated a) linear copolymer nanoparticle b) branched copolymer nanoparticle.

To verify that nanoparticles incorporating branched glycoblocks bind more RCA_{120} than their linear analogues, we analyzed the total amount of RCA_{120} bound to nanoparticles made from 25:12 0 branch and 25:12 5 branch copolymers via a dot blot assay (using an equal mass of nanoparticles for each compound), which revealed that the branched copolymer nanoparticles bind 1.64 times as much RCA_{120} compared to the unbranched copolymer nanoparticles (Figure 6.9). The mass ratio of total galactose content for the nanoparticles with the branched block to the nanoparticles with the linear block is 1.14. While this could, in theory, explain some of the enhancement of binding to the branched particles over the linear particles, not all of the galactose is accessible, as some is likely sequestered in the interior of the nanoparticle.

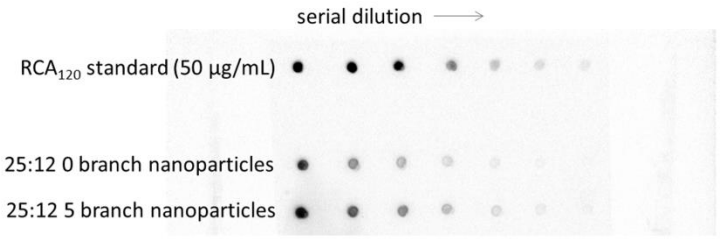

Figure 6.9. Dot blot quantification of RCA_{120} bound to nanoparticle samples.

If we consider only the galactose exposed on the surface of the nanoparticles, we can calculate the total surface area of all the nanoparticles of each sample beginning from the total mass of polymer used in each sample. The total mass of all the nanoparticles in a sample is the

product of the volume of each nanoparticle, the density of each nanoparticle, and the number of nanoparticles. Since the same total mass of polymer was used in each nanoparticle solution (Equation 6.1) and assuming equal nanoparticle density, the ratio of the number of nanoparticles in the linear sample to the branched sample is the ratio of the cube of the radius of the branched nanoparticle to the cube of the radius of the linear nanoparticle (Equation 6.2).

$$\frac{4}{3}\pi r_{lin}^3(N_{lin}\rho) = \frac{4}{3}\pi r_{br}^3(N_{br}\rho) \quad \text{Equation 6.1}$$

$$\frac{N_{lin}}{N_{br}} = \frac{r_{br}^3}{r_{lin}^3} \quad \text{Equation 6.2}$$

The total surface area in a sample is the surface area of one nanoparticle multiplied by the total number of nanoparticles in that sample. The ratio of the total surface area of the linear sample to the total surface area of the branched sample is thus equal to the ratio of the radius of the branched sample to the radius of the linear sample (Equation 6.3). From DLS, the radius of the branched particles is approximately 10% larger than the linear particles, resulting in approximately 10% lower surface area per unit mass. Therefore, the increase in amount of lectin bound to the branched nanoparticles cannot be explained by differences in galactose content or particle diameter, and must be due to an enhanced interaction.

$$\frac{N_{lin}}{N_{br}}\frac{4\pi r_{lin}^2}{4\pi r_{br}^2} = \frac{r_{br}^3}{r_{lin}^3}\frac{4\pi r_{lin}^2}{4\pi r_{br}^2} = \frac{r_{br}}{r_{lin}} \quad \text{Equation 6.3}$$

In summary, previously in glycomimetics, studies have been conducted with polymers in solution, but the natural binding partners of lectins are presented in 3D. To better mimic the natural binding partners of lectins, we have used protein-glycomimetic conjugates but were faced with inherent synthetic limitations. Glyconanoparticles offer a method of presenting glycomimetics in a 3D fashion with more synthetic control. The approach we report introduces a way to create well-defined glyconanoparticles that allow for independent control of size and

surface saccharide density through the chain-extension of a hydrophobic polymer with a glycomonomer and a heterobifunctional branching unit. The separate control of these two variables enables the creation of nanoparticles with a broader range of attributes.

6.4. Conclusions

Using RAFT polymerization, tunable amphiphilic copolymers with variable monomer identity, molecular weight, and degree of branching were previously synthesized. In this chapter, these copolymers were self-assembled using the nanoprecipitation method to create solid spherical nanoparticles with saccharide moieties on the nanoparticle surface available for lectin binding. Nanoparticle size was observed to be inversely proportional to copolymer molecular weight. The nanoparticles are stabilized by the CTA chain ends, which may lead to an aggregated construct. Saccharide density on the surface of the nanoparticles can be increased via branching without affecting the size and morphology of the nanoparticle, allowing for intricate studies of multivalent lectin binding to a 3D substrate. These results add another aspect of control to the design of synthetic glyconanoparticles for improved biological activity.

6.5. Experimentals

6.5.1. Materials

Dimethyl sulfoxide (Scharlau, HPLC grade) were used as received. Water was purified using an ELGA PURELAB Classic. Dialysis was conducted using a Spectra/Por® dialysis membrane (1000 Da). *Ricinus communis* (castor bean) agglutinin 120 (Sigma-Aldrich, 10 mg/mL in 0.005 M sodium phosphate, 0.2 M sodium chloride, pH 7.2, 0.1% NaN_3 buffered aqueous solution), rabbit red blood cells in saline with 0.1% NaN_3 (Fitzgerald), goat anti-*Ricinus communis* RCA_{60},RCA_{120} (MyBioSource, MBS6011813), rabbit anti-goat HRP (Life Technologies, A16136), slow (3,3',5,5'-tetramethylbenzidine) (TMB) substrate (Pierce), Nunc Maxisorp 96 well plates, SuperSignal West Pico Chemiluminescent substrate (Pierce), and Protran BA 85 nitrocellulose membrane (Whatman, 0.45 μm) were used as received.

6.5.2. Analytical techniques

Dynamic light scattering (DLS) used to obtain average nanoparticle size was performed on a Malvern Zetasizer Nano ZS90 with a 90° backscattering at room temperature. Multi-angle light scattering (MALS) measurements were performed using an ALV laser goniometer, with a 22 mW linearly polarized laser (632.8 nm HeNe) and an ALV- 5000/EPP multiple tau digital correlator at 25°C. The scattering angle was varied between 30° and 150° in 5° increments. Hydrodynamic radius (R_H) was determined from the apparent diffusion coefficient and the Stokes-Einstein equation. The radius of gyration (R_g) was determined from a Guinier plot resulting from the measurement of the average scattered intensity at the same angles. Transmission electron microscopy (TEM) images were recorded using a Hitachi H7650 microscope working at 80 kV equipped with a GATAN Orius 11 Megapixel camera. TEM samples were prepared by aerosolizing a 1 mg/mL solution of nanoparticles by a flow of

nitrogen as it was dispensed from a pipet onto an Agar Scientific formvar/carbon 200 mesh copper grid positively charged via glow discharge. The samples were air dried for 3.5 minutes, followed by staining with a 1.3% uranyl acetate solution for 1.5 minutes. Lectin precipitation assays were quantified using a Molecular Devices SpectraMax M2 microplate reader. Inhibitory enzyme-linked lectin assays (ELLA) were quantified using a Beckman Coulter DTX880 Multimode plate reader. Dot blots were read using a Bio-Rad ChemiDoc XRS+ System with Image Lab Software.

6.5.3. Self-assembly

6.5.3.1. Direct hydration

Water (1 mL) was filtered through a 0.8μm Supor membrane syringe filter and added to the copolymer (1 mg) and agitated on an IKA Vibrex VSR shaker plate.

6.5.3.2. Nanoprecipitation

Copolymers (2 mg) were dissolved in DMSO (200 μL) and agitated on an IKA Vibrex VSR shaker plate overnight. The DMSO solutions were filtered through a 0.2 μm PTFE syringe filter. Water (1.8 mL) was filtered through a 0.8 μm Supor membrane syringe filter. Nanoprecipitation was conducted by quickly injecting the DMSO solutions into water (Method 1) or by gradually adding water dropwise to the DMSO solutions (Method 2). The DMSO was removed by dialysis in water over at least 24 hours, changing the water every 2 hours as possible, no less than 5 times. The self-assembled nanoparticle solutions were analyzed via DLS, and those created via Method 2 were recorded by TEM. Samples that appeared monodisperse by TEM were further investigated by MALS.

6.5.4. Biological assays

6.5.4.1. Lectin precipitation

Lectin precipitation assays were conducted with *Ricinus communis* (castor bean) agglutinin 120 (RCA_{120}). Nanoparticle solutions (10 µL, 1 mg/mL) were added 5 times, once every 5.5 minutes, to a lectin solution (100 µL, 2 mg/mL). Absorbance was measured at 450 nm by a Molecular Devices SpectraMax M2 microplate reader 5 minutes after each addition of nanoparticle solution.

6.5.4.2. Hemagglutination

A solution (95 µL) including RCA_{120} (5 µL, 33.3 µg/mL) and galactose containing sample (glycopolymer/nanoparticle of interest) diluted to a prescribed concentration was added to each well of a 96 U-bottom well plate. After 10 minutes, rabbit red blood cells (RBC) (5 µL) were added and mixed via pipet and allowed to sit without agitation for 1 hour. MIC values were recorded as the minimum concentration at which inhibition of RBC precipitation was observed.

6.5.4.3. Inhibitory enzyme-linked lectin assay (ELLA)

Poly(galactose acrylate) polymerized using 0.5% Irgacure dissolved in coating buffer (15 mM Na_2CO_3, 35 mM $NaHCO_3$, pH 9.6) (100 µL, 10 µg/mL) was incubated at room temperature overnight in immunosorp wells. The solution was removed and replaced with blocking buffer (200 µL, 5 mg/mL BSA, 10 mM TrisCl, 145 mM NaCl, pH 7.4) and incubated at 37°C for two hours. While blocking the wells, lectin solution (0.08 µg/mL RCA_{120}, 1 mg/mL BSA, 20 mM TrisCl, 1 M NaCl, 0.05% Triton X-100, pH 7.4) was combined in equal volume with a serial dilution of the inhibitor (glycopolymer/nanoparticle of interest) and incubated at room temperature for 30 minutes. The wells were washed three times with washing buffer (100 mM TrisCl, 0.9% NaCl, 0.05% Tween 20, pH 7.5) before adding the inhibitor/lectin

solution (100 µL) and incubated at 4°C overnight. The wells were washed three times with washing buffer, and goat anti-RCA in washing buffer (100 µL, 1 µg/mL) was incubated at room temperature for two hours. The wells were washed three times with washing buffer, and rabbit anti-goat HRP in washing buffer (100 µL, 0.05 µg/mL) was incubated at room temperature for two hours. The wells were washed three times with washing buffer, and slow TMB substrate (100 µL) was used to develop the wells at room temperature for 25 minutes. The development was stopped with sulfuric acid (100 µL, 2 M), and the absorbance of the wells was recorded at 450 nm. 0% inhibition was measured as the absorbance of wells that had a lectin solution added without any inhibitory nanoparticles/glycopolymer, and 100% inhibition was measured as the absorbance of wells that were not coated with poly(galactose acrylate) (non-specific adsorption of lectin to the well). Percent inhibition was calculated as $100\text{-}100(Abs_{inhibitior}/Abs_{noninhibitor})$. Error was calculated as the standard deviation of the mean between the four replicates within the same plate. Plots were curve fitted and IC_{50} values were recorded as the concentration at which 50% inhibition occurs.

6.5.4.4. Dot blot assay

A solution of nanoparticles (100 µL, 0.8 mg/mL) was combined with a solution of RCA_{120} (100 µL, 100 µg/mL) and incubated at room temperature for 30 minutes. The nanoparticle solutions were centrifuged at 5000 rpm for 10 minutes, and the supernatant was removed. The nanoparticles were washed twice with DI water (200 µL) and resuspended in DI water (200 µL). The solutions were serially diluted and blotted (1 µL) on a nitrocellulose membrane. The membrane was allowed to dry before immersing in blocking buffer (5% BSA, 0.05% Tween 20, 20 mM Tris-Cl, 150 mM NaCl, pH 7.5) and incubated at room temperature for two hours. Following removal of the blocking solution, the membrane was incubated at room temperature

for 30 minutes with goat anti-RCA in blocking buffer. The membrane was washed with TBS-T (0.05% Tween 20, 20 mM Tris-Cl, 150 mM NaCl, pH 7.5) (3 × 5 minutes) and incubated at room temperature for 30 minutes with rabbit anti-goat HRP in blocking buffer. The membrane was washed with TBS-T (2 × 5 minutes) and TBS (20 mM Tris-Cl, 150 mM NaCl, pH 7.5) (2 × 5 minutes), before developing with SuperSignal West Pico Chemiluminescent Substrate. The chemiluminescence was recorded by a Bio-Rad ChemiDoc XRS+ System with Image Lab Software and analyzed with ImageJ. Serial dilutions were conducted to ensure the chemiluminescence recorded were within an acceptable range for analysis by ImageJ.

CHAPTER 7

Antibacterial activity of cationic glycopolymers

7.1. Introduction

Cationic polymers have been investigated extensively for antibacterial activity.[288] In particular, chitosan has been shown to inhibit the growth of a wide range of bacteria and fungi.[289] While the antimicrobial characteristic of chitosan is well known, the mechanism of this characteristic is still not fully understood. The antimicrobial property of chitosan is dependent on a number of parameters, such as pH, degree of deacetylation, concentration, and molecular weight.[289]

In general, the antimicrobial activity of chitosan increases with decreasing pH and exhibits no activity at neutral or basic pH due to a lack of solubility.[290–293] The concentration of acid used to decrease the pH, however, can also inhibit bacterial growth and should be considered.[294] Likewise, antimicrobial activity increases with decreasing degree of acetylation.[295] With regards to the concentration and molecular weight of chitosan, there is a more complex interdependence. Liu *et al.* has observed that chitosan promotes bacterial growth at low concentrations (20 ppm) for all molecular weights tested (55-155 kDa).[294] As the concentration is increased, lower molecular weight chitosan (< 70 kDa) exhibits antimicrobial activity against *E. coli* before higher molecular weight chitosan (> 88k Da). It has also been determined that chitosan should have a molecular weight of at least 10 kDa (DP_n = 62) to exhibit antimicrobial activity.[296] All these parameters ultimately affect the solubility of chitosan, which has been suggested to be a key factor in its antimicrobial activity.[297,298]

Currently, three prominent theories exist regarding the antibacterial mode of action for chitosan: 1) the cationic charge on chitosan interacts with the anion cell surface altering the permeability,[299–305] 2) chitosan penetrates the cell and interacts with the microbial DNA to prevent mRNA and protein synthesis,[306] or 3) the amino group in chitosan chelates essential nutrients and metals[307,308]. Most investigations into the antimicrobial mechanism of chitosan have been conducted through observations of cell morphology and released components of modified chitin. Rather than using naturally-derived polysaccharides, glycomimetics can be used to construct polymer with more precise control over saccharide identity, molecular weight, and functionalization. In this chapter, we investigated the antibacterial characteristic of a chitosan-mimic, poly(methyl 6-acryloyl-β-D-glucosaminoside) synthesized in Section 4.6. Poly(methyl 6-acryloyl-β-D-glucosaminoside) maintaining the same number of exposed functional groups and preserves the glycosidic bond, which also maintains a similar pKa compared to chitosan (Figure 7.1).

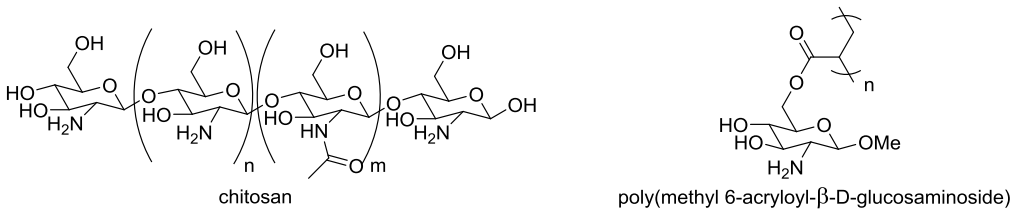

Figure 7.1. Structure of chitosan (pKa 6.5) and poly(methyl 6-acryloyl-β-D-glucosaminoside) (pKa 6.61).

7.2. Fractional precipitation of chitosan

In an initial investigation, a stock solution of chitosan was fractionally precipitated to obtain a series of molecular weights with low dispersity. As a naturally-derived polysaccharide, chitosan is highly disperse. In addition, chitosan is only soluble in acidic aqueous solutions and forms a highly viscous fluid even at low concentration. For fractional precipitation, chitosan was initially dissolved in an acetic acid solution, and the pH was adjusted with a sodium hydroxide solution until precipitate formed but dissolved upon agitation. Gradually, methanol was added until precipitate formed and was isolated by centrifugation. The process of addition of methanol and isolation of precipitate was repeated for each fraction. The precipitate was dissolved in acetate buffer (0.2 M acetic acid/0.1 M sodium acetate) and diluted to a series of concentrations to determine viscosity by rheology. By plotting the reduced viscosity (η_{red}) (Equation 7.1) and inherent viscosity (η_{inh}) (Equation 7.2) versus concentration, intrinsic viscosity ($[\eta]$) (Equation 7.3) was determined by extrapolation, where η is the viscosity of the solution, η_s is the viscosity of the solvent, and *c* is the concentration of the solution (Figure 7.2).

$$\eta_{red} = \frac{\eta - \eta_s}{c\eta_s} \qquad \text{Equation 7.1}$$

$$\eta_{inh} = \frac{\ln\left(\eta/\eta_s\right)}{c} \qquad \text{Equation 7.2}$$

$$[\eta] = \lim_{n\to 0}(\eta_{red}) = \lim_{n\to 0}(\eta_{inh}) \qquad \text{Equation 7.3}$$

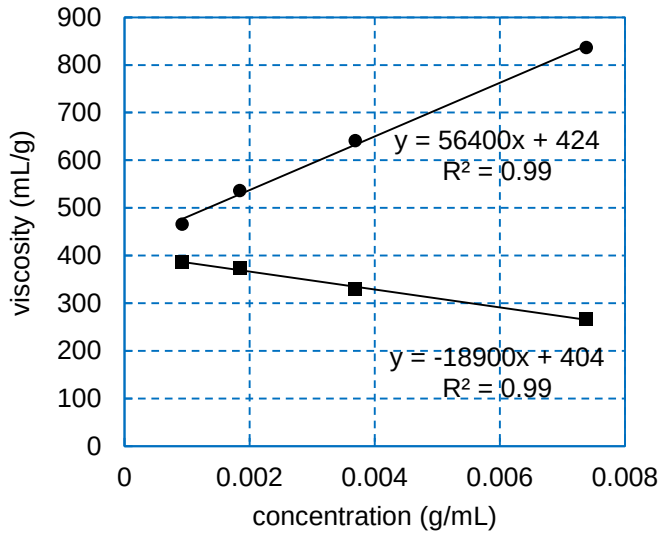

Figure 7.2. Sample linear curve fits of reduced viscosity (•) and inherent viscosity (■) versus chitosan concentration extrapolated to determine intrinsic viscosity.

The intrinsic viscosity and molecular weight can be related by the Mark-Houwink equation developed for chitosan solutions in 0.2 M acetic acid/0.1 M sodium acetate buffer (Equation 7.4) by Wang *et al*., where DD equals the percent degree of deacetylation.[309] Using the degree of deacetylation determined by ^{1}H NMR in deuterium oxide with trifluoroacetic acid and the intrinsic viscosity determined by rheology, molecular weights were determined for each chitosan fraction (Table 7.1). Due to the lack of uniformity and the complex effect of degree of deacetylation and molecular weight on solvent interactions, the precipitated fractions lack a trend in either degree of deacetylation or molecular weight. These results further exemplify the limitations of working with chitosan as a naturally-derived polysaccharide.

$[\eta] = KM_v{}^{a}$, with $K = 1.64\times10^{-30} \times \mathrm{DD}^{14}$ and $a = -1.02\times10^{-2} \times \mathrm{DD} + 1.82$ Equation 7.4

Table 7.1. Degree of deacetylation (DD), intrinsic viscosity ([η]), and viscosity molecular weight (M_v) of fractionated chitosan.

sample	DD (%)[a]	[η] (mL/g)[b]	M_v (kDa)[c]
unfractionated chitosan	86.7	413	428
fraction 1	79.8	415	550
fraction 2	77.0	415	620
fraction 3	72.5	426	786
fraction 4	78.9	460	632
fraction 5	80.6	378	486
fraction 6	80.2	405	529

[a] Determined by ^{1}H NMR in deuterium oxide with trifluoroacetic acid
[b] Determined using plots of viscosity versus concentration
[c] Determined using the Mark-Houwink equation

7.3. Antibacterial properties

Chitosan is only soluble in acidic solutions, most commonly acetic acid solutions. Before evaluating the antibacterial capacity of saccharide-containing polymers, the effect of acetic acid on bacterial growth was investigated. Acetic acid concentrations was serially diluted and incubated overnight with a typical gram-negative bacteria, *E. coli*. At acetic acid concentrations greater than 0.125%, acetic acid inhibits the growth of bacteria (Figure 7.3).

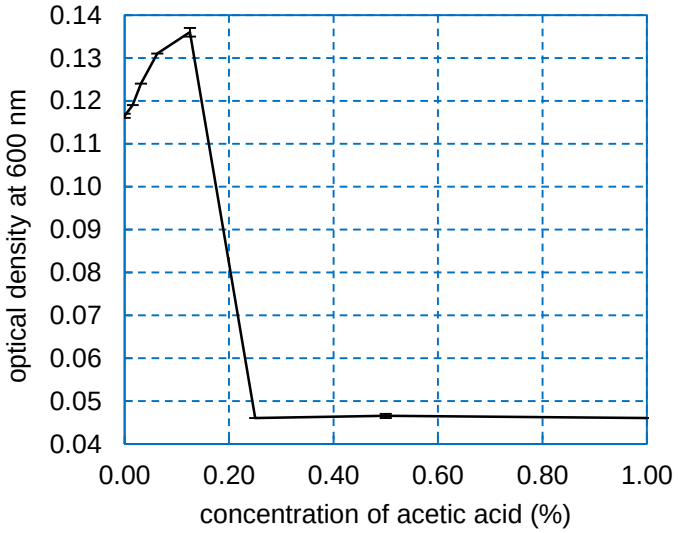

Figure 7.3. Optical density of *E. coli* incubated overnight at various concentrations of acetic acid in M9 salt buffer.

In order to minimize the inhibitory effect of acetic acid, a minimal amount of acetic acid should be used. With chitosan, however, the concentration of acetic acid drastically affects its solubility. In order to create solutions of chitosan with low concentrations of acetic acid, a stock solution of chitosan was dissolved overnight in M9 salts buffer with 1% acetic acid. Immediately prior to use, the stock solution was diluted to the appropriate concentration of acetic acid. In order to create a "0% acetic acid" solution, the stock solution was dialyzed and a sample aliquot was lyophilized to determine the chitosan concentration. While dialysis may not completely remove all the acetic acid due to electrostatic interactions between the acetic acid and the protonated amine, it reduces the acetic acid to the minimum amount required to maintain chitosan in solution.

Using this series of chitosan solutions in various concentrations of acetic acid, the synergistic antibacterial effects of chitosan and acetic acid were investigated using the minimum inhibitory concentration (MIC) assay (Figure 7.4). The solution that contained only a minimal amount of acetic acid exhibited no antibacterial activity whatsoever. At acetic acid concentrations higher than 0.20%, bacterial growth was completely inhibited even without chitosan. Between 0.10% and 0.20% acetic acid, the solutions were only antibacterial with the inclusion of chitosan. A solution of 0.20% acetic acid buffer had a partial inhibitory effect on the bacteria, indicating an upper concentration limit of acetic acid tolerance by the bacteria. At a concentration of 0.10% acetic acid, a chitosan concentration-dependent inhibitory effect was observed, indicating a lower acetic acid concentration limit.

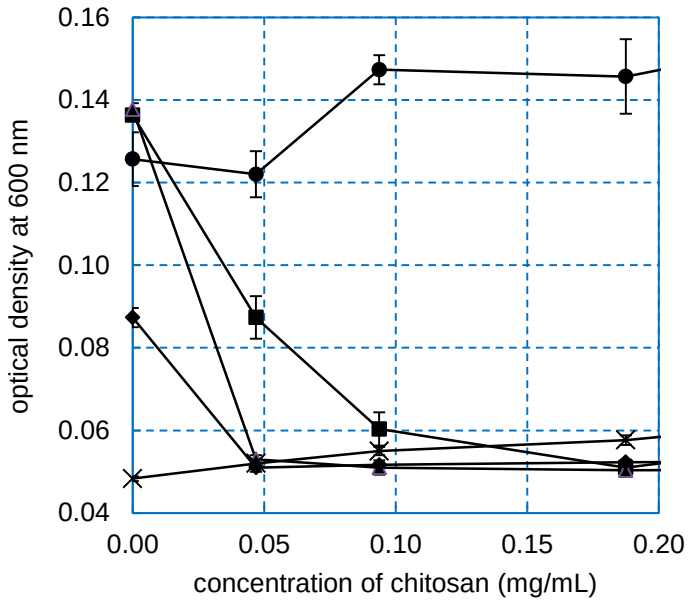

Figure 7.4. Optical density of *E. coli* incubated overnight with various concentrations of chitosan in 0% (•), 0.10% (■), 0.15% (▲), 0.20% (♦), and 0.25% (×) acetic acid concentrations in M9 salt buffer.

Using a concentration of 0.10% acetic acid, the poly(methyl 6-acryloyl-β-D-glucosaminoside) series was investigated for its antibacterial properties. The MIC assay showed a clear relationship between the molecular weight of the glycopolymer and its efficacy in inhibiting bacterial growth (Figure 7.5). Sometimes at the concentration just below the MIC, higher optical density was observed with higher variability due to visible aggregation of bacteria forming a heterogeneous suspension. Fraction 3 of the poly(methyl 6-acryloyl-β-D-glucosaminoside) series has a degree of polymerzation of 81 repeat units and showed a partial inhibitory effect at concentrations of 62.5 μg/mL and above, suggesting it is near the lower molecular weight limit for inihibiting bacterial growth. The minimum molecular weight limit observed with poly(methyl 6-acryloyl-β-D-glucosaminoside) is similar to chitosan, which exhibits antimicrobial activity with molecular weights above 10 kDa (DP_n = 62).[296] Fractions with molecular weights lower than fraction 3 exhibited no inhibitory effect on bacteria up to a concentration of 1 mg/mL, whereas fractions 1 and 2, which have higher molecular weights than

fraction 3, exhibited an inhibitory effect at 62.5 μg/mL and 125 μg/mL, respectively, approaching the MIC of chitosan at 31.3 μg/mL (Table 7.2). Adjusting the MICs to reflect the concentration of glucosamine, the MIC of chitosan, poly(methyl 6-acryloyl-β-D-glucosaminoside) fraction 1, and poly(methyl 6-acryloyl-β-D-glucosaminoside) fraction 2 are 0.194 mM, 0.253 mM, and 0.506 mM, respectively.

In expanding the scope of bacteria investigated, a similar inhibitory effect was observed for chitosan and poly(methyl 6-acryloyl-β-D-glucosaminoside) fraction 1 on *P. aeruginosa* with an MIC of 62.5 μg/mL (0.388 mM of glucosamine) and 125 μg/mL (0.506 mM of glucosamine), respectively (Figure 7.6). *P. aeruginosa* infections are known to be particularly difficult to treat, which is observed in the slightly higher MICs of chitosan and poly(methyl 6-acryloyl-β-D-glucosaminoside) compared to *E. coli*.

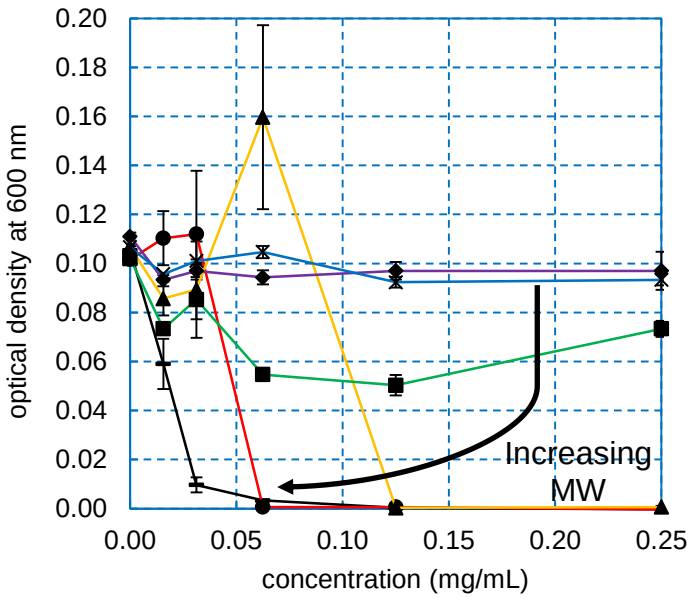

Figure 7.5. Minimum inhibitory concentration assay of chitosan (black) and poly(methyl 6-acryloyl-β-D-glucosaminoside) fraction 1 (red), fraction 2 (orange), fraction 3 (green), fraction 4 (purple), and filtrate (blue) on *E. coli* in 0.10% acetic acid in M9 salts.

Table 7.2. Minimum inhibitory concentration of chitosan and fractionated poly(methyl 6-acryloyl-β-D-glucosaminoside) on *E. coli* in 0.1% acetic acid in M9 salts.

sample	DP_n [†]	MIC (μg/mL)	MIC [‡] (mM glucosamine)
chitosan	2660	31.3	0.194
fraction 1	179	62.5	0.253
fraction 2	149	125	0.506
fraction 3	81	–	–
fraction 4	41	–	–
filtrate	14	–	–

[†] Determined for chitosan from M_v divided by the molecular weight of the repeat unit and determined previously in Section 4.6 for poly(methyl 6-acryloyl-β-D-glucosaminoside).
[‡] Determined by dividing the MIC (μg/mL) by the molecular weight of the respective repeat unit.

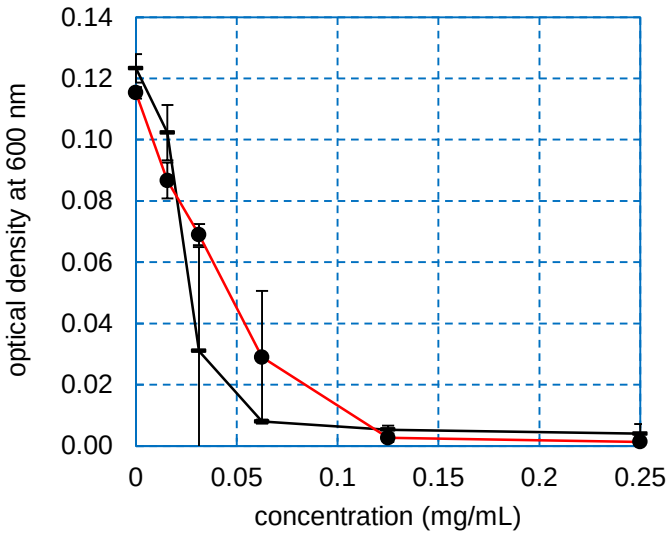

Figure 7.6. Minimum inhibitory concentration assay of chitosan (black) and poly(methyl 6-acryloyl-β-D-glucosaminoside) fraction 1 (red) on *P. aeruginosa* in 0.1% acetic acid in M9 salts. The minimum inhibitory concentration for chitosan and poly(methyl 6-acryloyl-β-D-glucosaminoside) fraction 1 were 62.5 μg/mL (0.388 mM of glucosamine) and 125 μg/mL (0.506 mM of glucosamine), respectively.

Although chitosan is only soluble in acidic aqueous solutions, poly(methyl 6-acryloyl-β-D-glucosaminoside) was soluble at neutral and basic pH. Extreme pHs were still avoided due to the inherent antibacterial nature under those conditions and the possibility of hydrolysis of poly(methyl 6-acryloyl-β-D-glucosaminoside). When the MIC of poly(methyl 6-acryloyl-β-D-glucosaminoside) was tested using M9 salts without acetic acid (pH 7.0) and a basic

solution of ammonium hydroxide in M9 salts (pH 7.8), similar antibacterial potency was observed relative to acetic acid in M9 salts (pH 6.7) (Figure 7.7). This result has profound implications concerning the scope of usefulness and the interaction of poly(methyl 6-acryloyl-β-D-glucosaminoside) with bacteria. Unlike chitosan, poly(methyl 6-acryloyl-β-D-glucosaminoside) has the potential to be used as a potent antibacterial agent regardless of pH. This greatly expands the scope of applications in areas such as food additives and cosmetics. In addition, since no apparent effect on the antibacterial activity of poly(methyl 6-acryloyl-β-D-glucosaminoside) was observed with the increase of pH, even far beyond its pKa of 6.61, it suggests that the inhibitory activity in bacteria is more complex than simply an electrostatic interaction with the bacterial membrane.

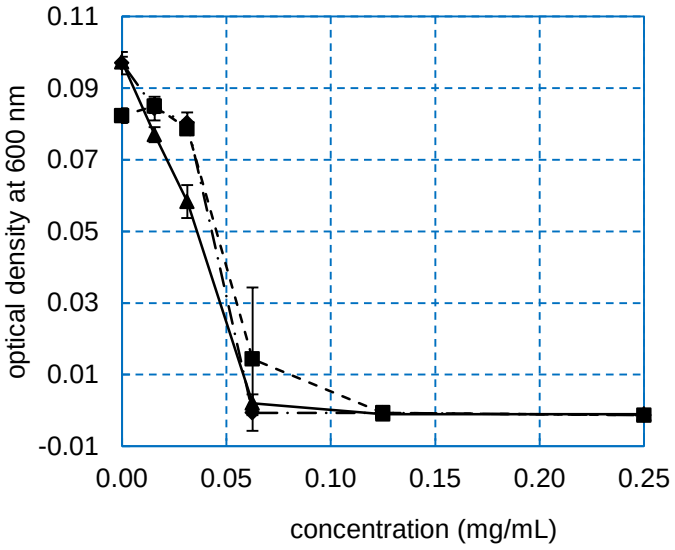

Figure 7.7. Minimum inhibitory concentration assay of poly(methyl 6-acryloyl-β-D-glucosaminoside) fraction 1 on *E. coli* in 0.1% acetic acid in M9 salts (pH 6.7) (– · ♦ – ·), M9 salts (pH 7.0) (- -■ - -), and 0.017 M ammonium hydroxide in M9 salts (pH 7.8) (— ▲ —).

7.4. Cell viability of cationic polymers in solution

For most cationic polymers, an increase in cytotoxicity is observed with increasing molecular weight.[167,168,187,188,310] In order to investigate the selectivity of poly(methyl 6-acryloyl-β-D-glucosaminoside) for inhibiting bacterial growth without cytotoxicity towards mammalian

cells, the cytotoxicity of poly(methyl 6-acryloyl-β-D-glucosaminoside) was evaluated using HEK293 cells. Cells were seeded on a 96-well plate at a density of 10,000 cells per well and incubated overnight. Polymers were dissolved in an acetate buffer (0.3 acetic acid/0.2 sodium acetate, pH 4.4) at 2 mg/mL and diluted to prescribed concentrations. Each sample was diluted 10× with serum-free media, and the media in each well was replaced with the polymer solutions and incubated for 48 hours. The cell viability was assessed using an MTT assay (Figure 7.8). From the MTT assay, a clear trend was seen with increasing molecular weight resulting in increased cytotoxicity. When compared to common compounds used with HEK293 cells (Figure 7.9), the glycopolymer fractions exhibited similar cytotoxicity to Glycofect with the higher molecular fractions approaching the cytotoxicity of PEI (Table 7.3).

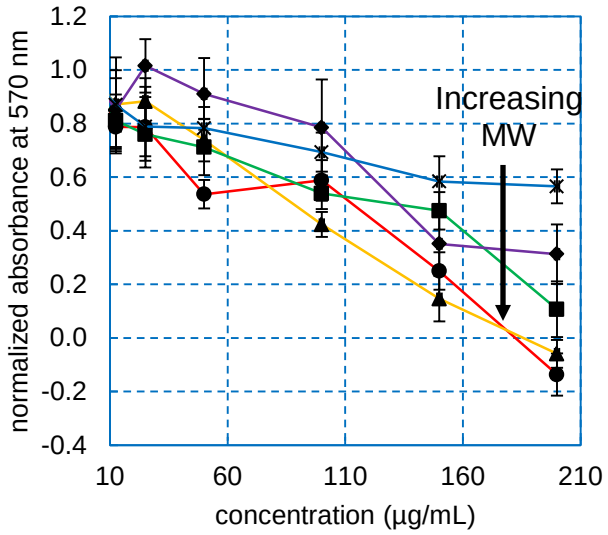

Figure 7.8. HEK293 cell viability via MTT assay in the presence of poly(methyl 6-acryloyl-β-D-glucosaminoside) fraction 1 (red), fraction 2 (orange), fraction 3 (green), fraction 4 (purple), and filtrate (blue) in pH 4.4 acetate buffer diluted with serum-free media.

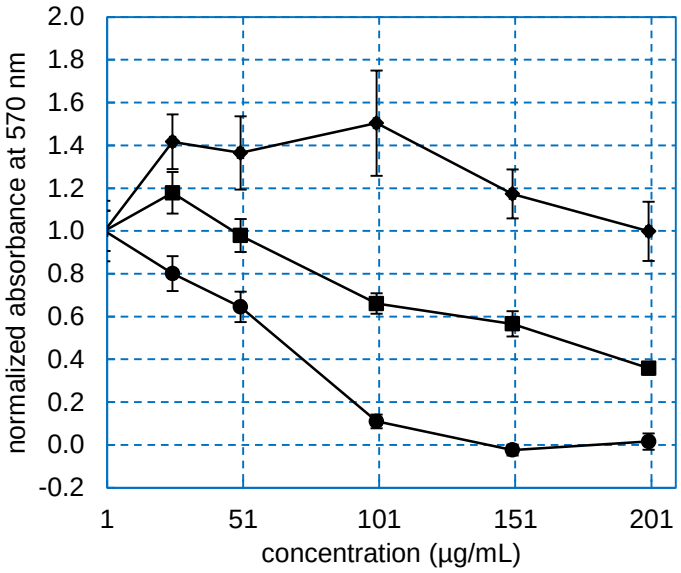

Figure 7.9. HEK293 cell viability via MTT assay in the presence of chitosan (♦), Glycofect (■), and poly(ethyleneimine) (PEI) (•) in pH 4.4 acetate buffer diluted with serum-free media.

Table 7.3. Cytotoxicity of Glycofect and various molecular weights of poly(methyl 6-acryloyl-β-D-glucosaminoside) relative to PEI in pH 4.4 acetate buffer diluted with serum-free media.

sample	relative cytotoxicity[†]
PEI	1
Glycofect	0.36
fraction 1	0.69
fraction 2	0.66
fraction 3	0.53
fraction 4	0.42
filtrate	0.28

[†] Relative cytotoxicity is calculated as the ratio of the concentration at which 50% viability is observed for PEI divided by the concentration at which 50% inhibition is observed for the compound.

Since poly(methyl 6-acryloyl-β-D-glucosaminoside) was soluble and inhibited bacteria at neutral pH, its cytotoxicity was also examined at pH 7.2 by dissolving the polymer in distilled water and diluting with serum-free media. Under these conditions, no significant cytotoxicity was observed up to a concentration of 200 µg/mL (Figure 7.10). This suggests that the cationic charge plays a direct role in the cytotoxicity of these glycopolymers towards mammalian cells.

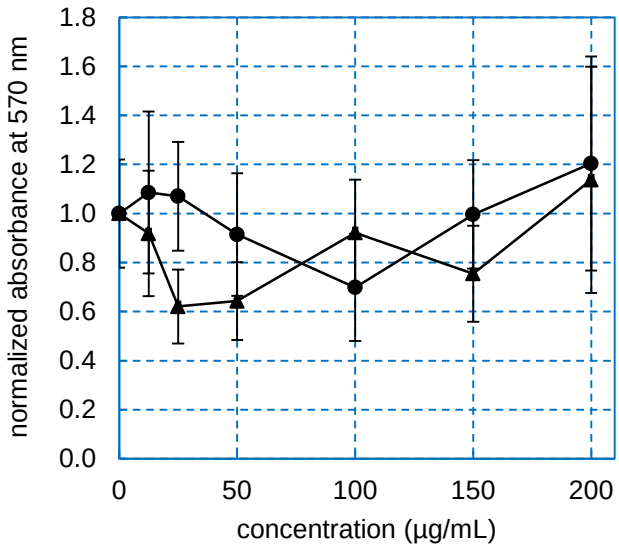

Figure 7.10. HEK293 cell viability via MTT assay in the presence of poly(methyl 6-acryloyl-β-D-glucosaminoside) fraction 1 (•) and fraction 2 (▲) in distilled water diluted with serum-free media (pH 7.2).

7.5. Conclusions

Using poly(methyl 6-acryloyl-β-D-glucosaminoside) due to its structural similarity to chitosan, we investigated the antibacterial properties associated with chitosan. The reported potency of chitosan, however, varies greatly due to inconsistent experimental conditions, such as various concentrations of acetic acid and various molecular weights and degrees of deacetylation of chitosan due to its derivation from natural sources. Although acetic acid is necessary to dissolve chitosan, the investigations in this chapter determined that less than 0.2% acetic acid should be used to prevent an inhibitory effect from acetic acid on bacteria. When poly(methyl 6-acryloyl-β-D-glucosaminoside) was investigated to mimic the antibacterial activity of chitosan on *E. coli*, a similar molecular weight dependence was observed as previously reported for chitosan. Unlike chitosan, poly(methyl 6-acryloyl-β-D-glucosaminoside) was soluble at neutral and basic pH and maintained its ability to inhibit bacterial growth. In evaluating the cytotoxicity of poly(methyl 6-acryloyl-β-D-glucosaminoside) on a model eukaryotic cell (HEK293), cytotoxicity was seen to increase with molecular weight. When poly(methyl 6-acryloyl-β-D-glucosaminoside) was dissolved at neutral pH, no cytotoxic effect was observed.

7.6. Experimentals

7.6.1. Materials

Chitosan (Aldrich, high purity, M_v 60-120 kDa), linear PEI (Alfa Aesar, 25 kDa), acetic acid (Macron, ACS grade), and ammonium hydroxide (Fisher, ACS grade plus) were used as received. Glycofect was synthesized according to the protocol found in Liu *et al.*[182] Luria-Bertani (LB) media was made from LB broth powder (Fisher, 25 g/L). LB plates were poured using agar powder (Fisher, 15 g/L) in LB media. M9 salts buffer was made from Difco M9 minimal salts (BD, 11.28 g/L). HEK293 were cultured in 10% fetal bovine serum in Dulbecco's Modification of Eagle's Medium (Cellgro) with 4.5 g/L glucose and L-glutamine at 37 °C and 5% CO_2.

7.6.2. Analytical techniques

Rheology of chitosan solutions was conducted on an Anton Paar Physica MCR 301 rheometer with a CP50-1 measuring cone (50 mm diameter, 1° cone angle). Minimum inhibitory concentration plates were read on a BioTek ELx800 plate reader. Cell viability was determined by MTT assay (ATCC) read on a BioTek Synergy H1 multi-mode reader.

7.6.3. Fractional precipitation of chitosan

Chitosan (100 mg) was dissolved in 2% acetic acid (1 mL) and diluted with distilled water (9 mL) and the pH was adjusted to approximately 5.5 with 0.1 M sodium hydroxide. Methanol was added gradually with swirling until a cloudy solution was obtained and the solution was stored overnight at 4 °C. The precipitate was collected by centrifugation and washed with 0.1 M sodium hydroxide and distilled water and dried in vacuo. Molecular weights were determined by rheology in acetate buffer (0.2 M acetic acid/0.1 M sodium acetate) and application of the Mark-

Houwink equation ($[\eta]=KM_v^a$, with $K=1.64\times10^{-30} \times DD^{14}$ and $a= - 1.02\times10^{-2} \times DD + 1.82$, where DD is the percent degree of deacetylation).[309]

7.6.4. Minimum inhibitory concentration (MIC)

Escherichia coli (MG1655 WT) and *Pseudomonas aeruginosa* (PAO1 WT) from a frozen stock were streaked onto a fresh LB agar plate and grown overnight at 37 °C. A single colony from the streaked plate was grown in LB media overnight in a 37 °C shaker. Bacteria from the overnight culture was added to fresh LB media and shaken at 37 °C for two hours to achieve log-phase bacteria. The bacteria culture was diluted to a working density of ~8×10^6 CFU/mL. In a 96-well plate, each sample (90 μL) in triplicate was serially diluted using the appropriate buffer with the last well containing only buffer as a positive control. The diluted bacteria culture (10 μL) was added to each well. The plate was sealed with Parafilm and shaken overnight at 37 °C, and the optical density at 600 nm was read for each well.

7.6.5. Cell viability assay of polymers in solution

HEK293 cells (100 μL, 100 cells/μL) were seeded in each well of a 96-well plate and incubated overnight at 37 °C and 5% CO_2. Stock solutions of each sample were prepared at a concentration of 2 mg/mL in buffer and passed through a 0.22 μm syringe filter into a sterile centrifuge tube. Each sample in triplicate was diluted to the prescribed concentration (10 μL) and diluted with serum-free media (90 μL). The media in the plate was replaced with each polymer sample and incubated at 37 °C and 5% CO_2 for 48 hours. Control wells were filled with serum-free media. The polymer solutions were replaced with serum-free media (100 μL) and MTT reagent (10 μL) and incubated for 2 hours at 37 °C and 5% CO_2 followed by the addition of detergent (100 μL) and incubation at room temperature overnight. The absorbance at 570 nm was read for each well. Error was calculated as the standard deviation between the three

replicates within the same plate. Plots were curve fitted and LC_{50} values were recorded as the concentration at which 50% cell viability was observed.

CHAPTER 8

Transfection potential of cationic glycopolymers

8.1. Introduction

Cationic polymers are often utilized in gene delivery due to the ability of the cationic charge to complex with anionic nucleic acids. With the introduction of gene therapy in the 1970s and the completion of the Human Genome Project, there has been an impending need to develop effective gene delivery methods. Current methods include viral vectors, non-viral vectors, and physical methods.[311] Although viral vectors are a highly effective method for delivering genetic material, issues with carcinogenesis[312] and immunogenicity[313–316] were observed in clinical trials. Alternatively, non-viral vectors, while lacking high gene delivery efficacy, allow for more design control, particularly with synthetic polymers.

One of the most extensively studied synthetic polymers for gene delivery is poly(ethyleneimine) (PEI). PEI has been observed to avoid lysosomal degradation and complex/release DNA efficiently.[163–165] Cytotoxicity, non-specific interactions, and elicitation of an immune response limit the usefulness of PEI.[166–168] In an effort to mitigate the cytotoxicity of PEI, Reineke *et al.* developed ring-opened poly(glycoamidoamine) copolymers[317] that exhibit high transfection efficiency due to transport via the endoplasmic reticulum and the Golgi complex with limited cell toxicity due to reduced membrane disruption.[318] Their poly(galactaramidoamine) copolymer has since been commercialized as Glycofect^{TM} (Figure 8.1a).[319] More recently, both the Narain group (Figure 8.1b) and the Reineke group (Figure 8.1c) have developed block-copolymers that employ a cationic block

(e.g. 2-aminoethylmethacrylamide) to complex nucleic acids and a saccharide block for reducing cytotoxicity and enable cell targeting.[187,320]

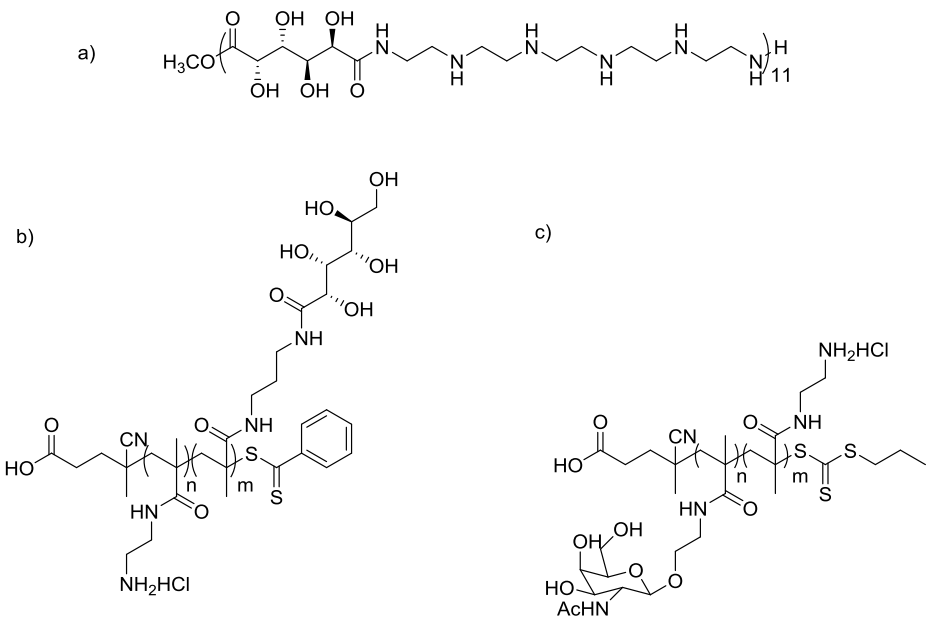

Figure 8.1. a) Glycofect,[317] b) poly(2-amino ethyl methacrylamide-*block*-3-gluconamidopropyl methacrylamide),[187] c) poly(methacrylamido *N*-acetyl-D-galactosamine-*block*-2-amino ethyl methacrylamide).[320]

In order to create gene delivery vehicles that are more biocompatible than PEI, chitosan has also been investigated as a gene delivery vehicle.[321–324] Effective transfection of genetic material has been seen to be dependent on a number of factors,[325] many of which change the charge density of the polysaccharide, including deacetylation[326,327] and pH.[328] Zhao *et al.* observed that polyplexes constructed from mixing PEI and chitosan maintained high transfection efficacy with no sign of cytotoxicity.[329] Pezzoli *et al.* demonstrated that grafting PEI off a chitosan backbone also decreased cytotoxicity relative to PEI alone.[330]

To bridge the gap between copolymerizing glycomonomers with synthetic cationic monomers and modification of a natural cationic polysaccharide, we utilized poly(methyl 6-acryloyl-β-D-glucosaminoside), synthesized in Section 4.6 (Table 8.1), to investigate its potential as a transfection agent. Due to its structural similarity to chitosan, we hypothesized that

we would observe decreased cytotoxicity compared to PEI. In addition, the lower pKa of poly(methyl 6-acryloyl-β-D-glucosaminoside) (6.61) compared to PEI (~8.0) and the degradability of the ester linkages connecting the saccharides to the polymer backbone may facilitate release of the complexed genetic material increasing its transfection efficiency compared to chitosan.

Table 8.1. Molecular weights of poly(methyl 6-acryloyl-β-D-glucosaminoside) from Section 4.6.

fraction	M_w (kDa)	M_n (kDa)	DP_n
1	79.7	44.2	179
2	56.7	37.0	149
3	22.9	20.1	81
4	11.6	10.1	41
filtrate	4.51	3.42	14

8.2. Polyplex formation

In evaluating the potential usage of poly(methyl 6-acryloyl-β-D-glucosaminoside) as a transfection agent, its ability to complex nucleic acids was first investigated. Select molecular weights (fraction 1, fraction 4, and filtrate) of poly(methyl 6-acryloyl-β-D-glucosaminoside) were dissolved in acetate buffer (0.3 M acetic acid/0.2 M sodium acetate, pH 4.4) at various concentrations corresponding to a particular nitrogen to phosphate (N/P) ratio, added to a solution of pEGFP-C1, and allowed to complex at room temperature for 30 minutes. The resultant solutions were analyzed via agarose gel electrophoresis (Figure 8.2). When the glycopolymer has effectively complex the nucleic acid, the resultant polyplexes will be unable to travel down the gel. At high molecular weight (fraction 1), poly(methyl 6-acryloyl-β-D-glucosaminoside) was observed to begin complexing nucleic acid at an N/P of 30, similar to what was used by the Narain group with their sugar containing copolymer.[187] At lower molecular weights (fraction 4), partial complexation was observed at an N/P of 30 with a faint free nucleic acid band remaining and complete complexation was observed at an N/P of 60. At the lowest molecular weight (filtrate), only a loose interaction was observed between the polymer and the nucleic acid resulting in a smeared band that still travelled down the agarose gel, albeit slower than free nucleic acid.

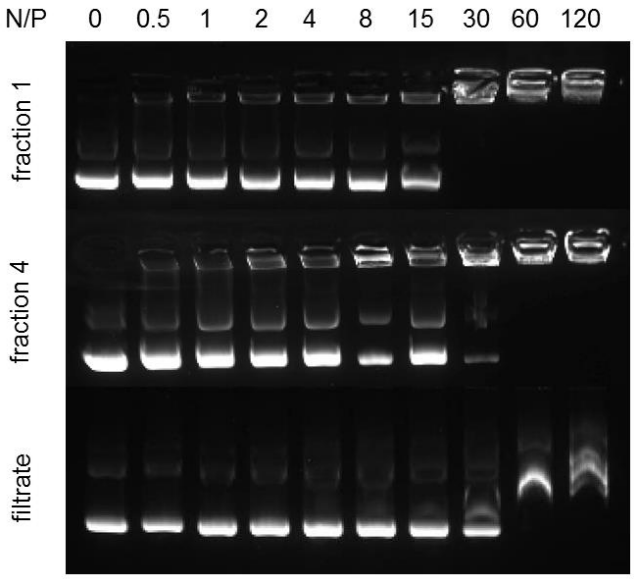

Figure 8.2. Agarose gel of select molecular weights of poly(methyl 6-acryloyl-β-D-glucosaminoside) complexed with pEGFP-C1 at increasing nitrogen to phosphate ratios.

Using the N/P ratios at which complexation was observed, samples were created using 2 μg of pEGFP-C1 and diluted to 1 mL with water for analysis by dynamic light scattering (Table 8.2). The glycopolymer from the filtrate fraction was observed to only form aggregates with the nucleic acid. Using the glycopolymer from fraction 4, large, polydisperse polyplexes were formed at an N/P of 30 with the size decreasing with increasing N/P ratio. With the highest molecular weight glycopolymer from fraction 1, polyplexes with approximately 150 nm diameters were formed with relatively low polydispersity at all N/P ratios tested. In general, increased molecular weight glycopolymers and increased N/P ratios both contribute to forming polyplexes for transfection.

Table 8.2. Diameter and zeta-potential of polyplexes formed from select molecular weights of poly(methyl 6-acryloyl-β-D-glucosaminoside).

	filtrate			fraction 4			fraction 1		
N/P	diameter (nm)	PDI	zeta-potential	diameter (nm)	PDI	zeta-potential	diameter (nm)	PDI	zeta-potential
30	9280	0.76	12.7	663	0.51	29.0	152	0.24	9.60
60	14900	0.88	14.7	265	0.28	18.9	145	0.25	10.3
120	10600	0.97	9.67	218	0.37	14.6	179	0.26	11.9

8.3. Cytotoxicity of polyplexes

While polyplex formation is important in successful transfection, the cytotoxicity of the polyplexes must also be considered. Polyplex solutions were formed by dissolving each fraction of poly(methyl 6-acryloyl-β-D-glucosaminoside) in acetate buffer (0.3 M acetic acid/0.2 M sodium acetate, pH 4.4) at various concentrations corresponding to an N/P of 30 and 60, adding a solution of pEGFP-C1, and allowing the polyplexes to complex at room temperature for 30 minutes. The solutions were diluted with serum-free Dulbecco's Modification of Eagle's Medium (DMEM) and incubated with HEK293 cells for 48 hours at 37 °C and 5% CO_2. Afterwards, the polyplex solutions were aspirated and replaced with serum-free DMEM for quantification of cell viability via MTT assay (Figure 8.3). Initially, the MTT assay was conducted without replacing the polyplex solutions, but significant interaction was observed between the polyplex solutions and the MTT assay. In general, polyplexes constructed of higher molecular weight polymer and higher N/P ratios exhibited higher levels of cytotoxicity. This is consistent with what has been reported for other cationic polymers used in transfection.[170,331] The source of the cytotoxicity is reportedly due to the presence of unbound cationic polymers, which increases in toxicity with molecular weight and are more abundant with increased N/P ratios. In comparison to other common cationic transfection vectors, the polyplexes formed using poly(methyl 6-acryloyl-β-D-glucosaminoside) mirror the cytotoxicity of the free polymer, less cytotoxic than PEI, more cytotoxic than chitosan, and in the same range of cytotoxicity as Glycofect (Figure 8.4).

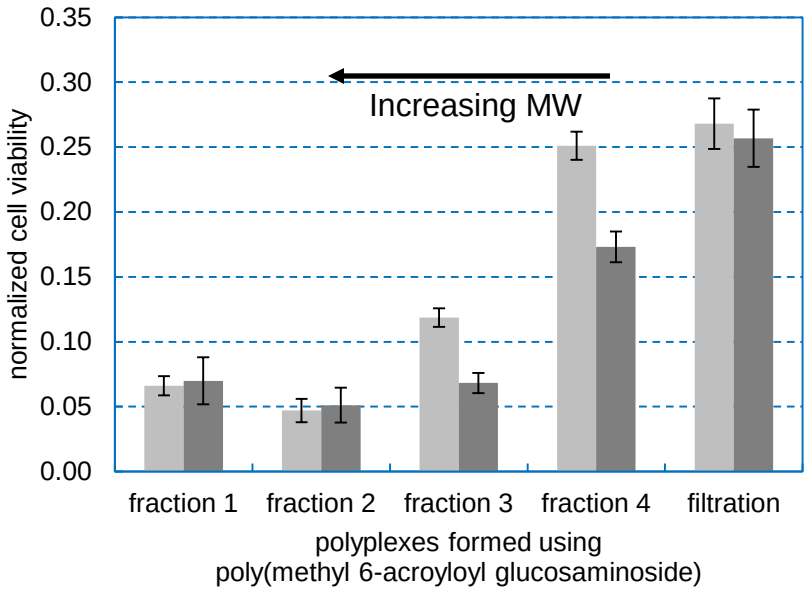

Figure 8.3. HEK293 cell viability (normalized to HEK293 cells grown in serum-free media) in the presence of polyplexes formed from poly(methyl 6-acryloyl-β-D-glucosaminoside) of various molecular weights and pEGFP-C1 at an N/P ratio of 30 (light gray) and 60 (dark gray).

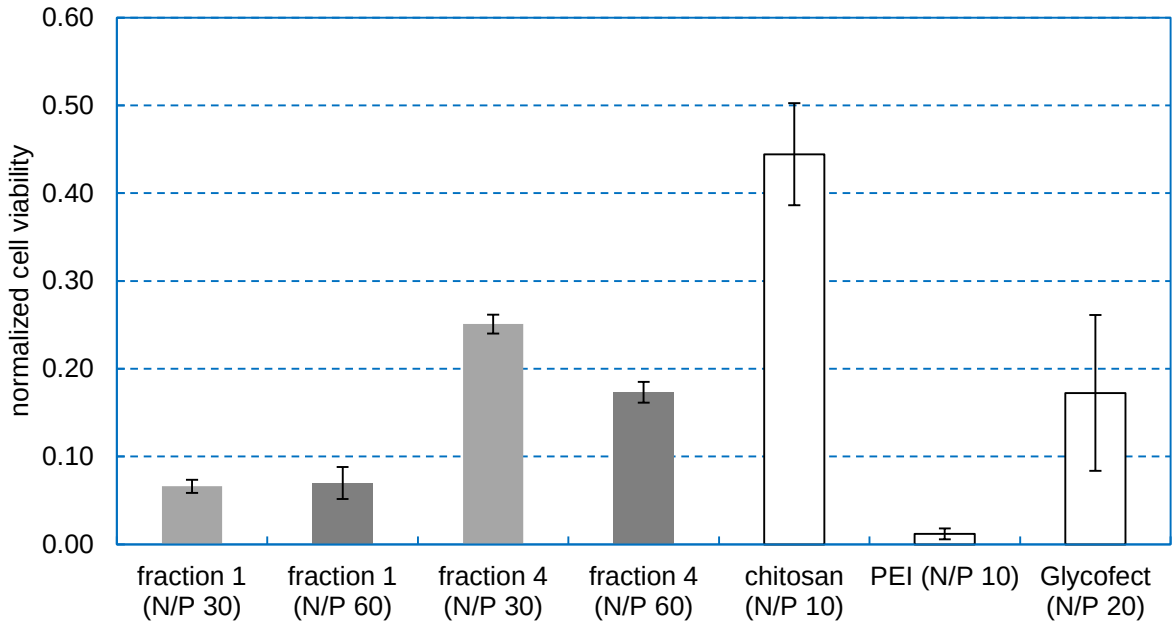

Figure 8.4. HEK293 cell viability (normalized to HEK293 cells grown in serum-free media) in the presence of polyplexes formed from poly(methyl 6-acryloyl-β-D-glucosaminoside) compared to reported transfection conditions for chitosan, PEI, and Glycofect.

8.4. Transfection of HEK293 cells

HEK293 cells were transfected with polyplex solutions created with PEI (N/P 10), chitosan (N/P 10), Glycofect (N/P 20), poly(methyl 6-acryloyl-β-D-glucosaminoside) fraction 1 (N/P 30 and 60), and poly(methyl 6-acryloyl-β-D-glucosaminoside) fraction 4 (N/P 30 and 60). Cationic polymer solutions were allowed to complex with pEGFP-C1 (0.4 μg) at room temperature for 30 minutes, diluted with serum-free DMEM, and incubated with HEK293 cells for 48 hours at 37 °C and 5% CO_2. The cells were imaged every 24 hours, and the media was changed every two days with 10% fetal bovine serum in DMEM. After 48 hours, significant expression of green fluorescent protein (GFP) was observed in wells transfected with PEI (Figure 8.5b2), Glycofect (Figure 8.5d2), and poly(methyl 6-acryloyl-β-D-glucosaminoside) fraction 1 (Figure 8.6a2 and Figure 8.6b2). Sparse expression of GFP was observed in wells transfected with chitosan (Figure 8.5c2) and poly(methyl 6-acryloyl-β-D-glucosaminoside) fraction 4 (Figure 8.6c2 and Figure 8.6d2). No noticeable amount of cell death was observed except with PEI (Figure 8.5b1).

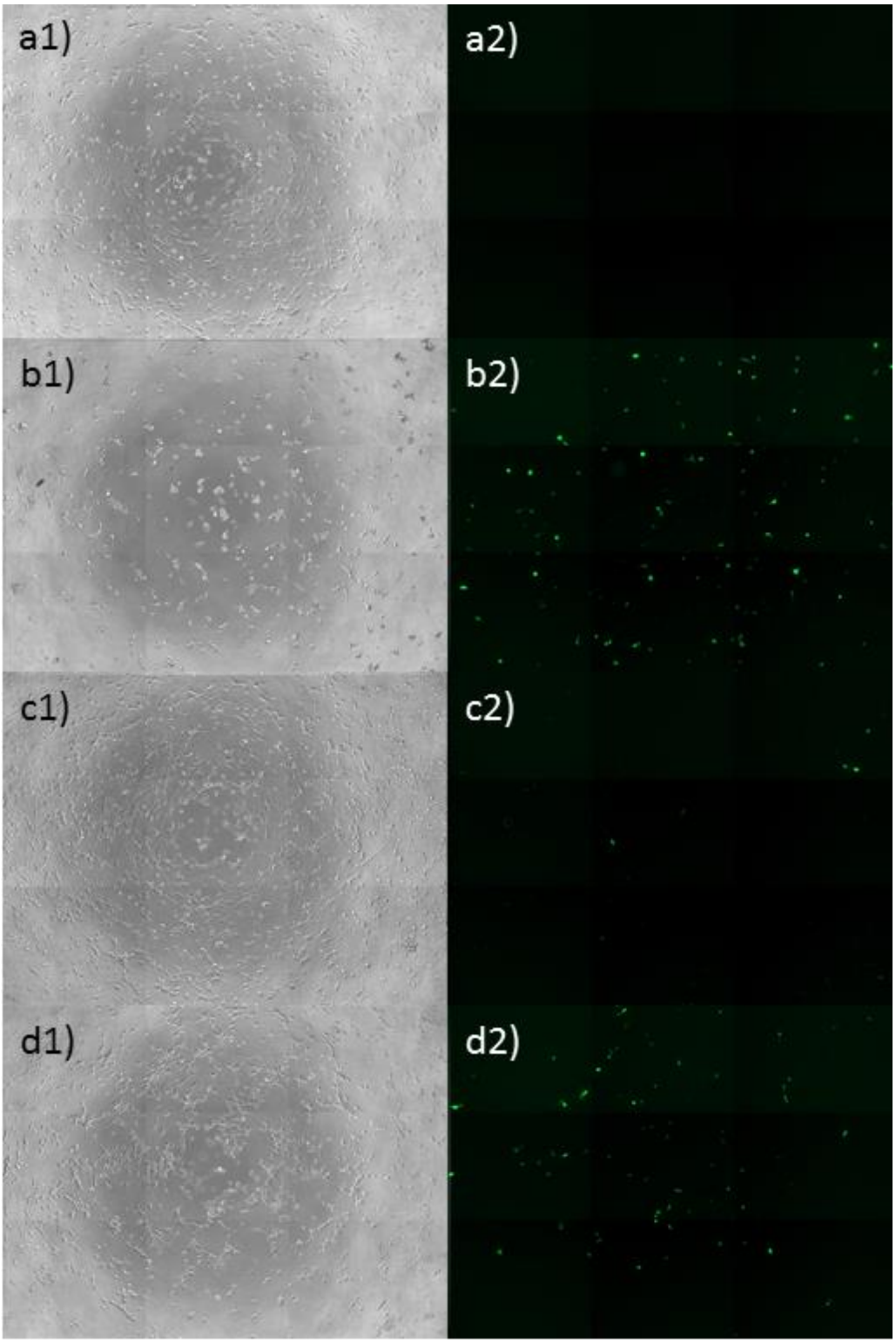

Figure 8.5. 1) Phase-contrast and 2) fluorescence images of HEK293 cells transfected with a) DNA, b) PEI (N/P 10), c) chitosan (N/P 10), and d) Glycofect (N/P 20) after 48 hours.

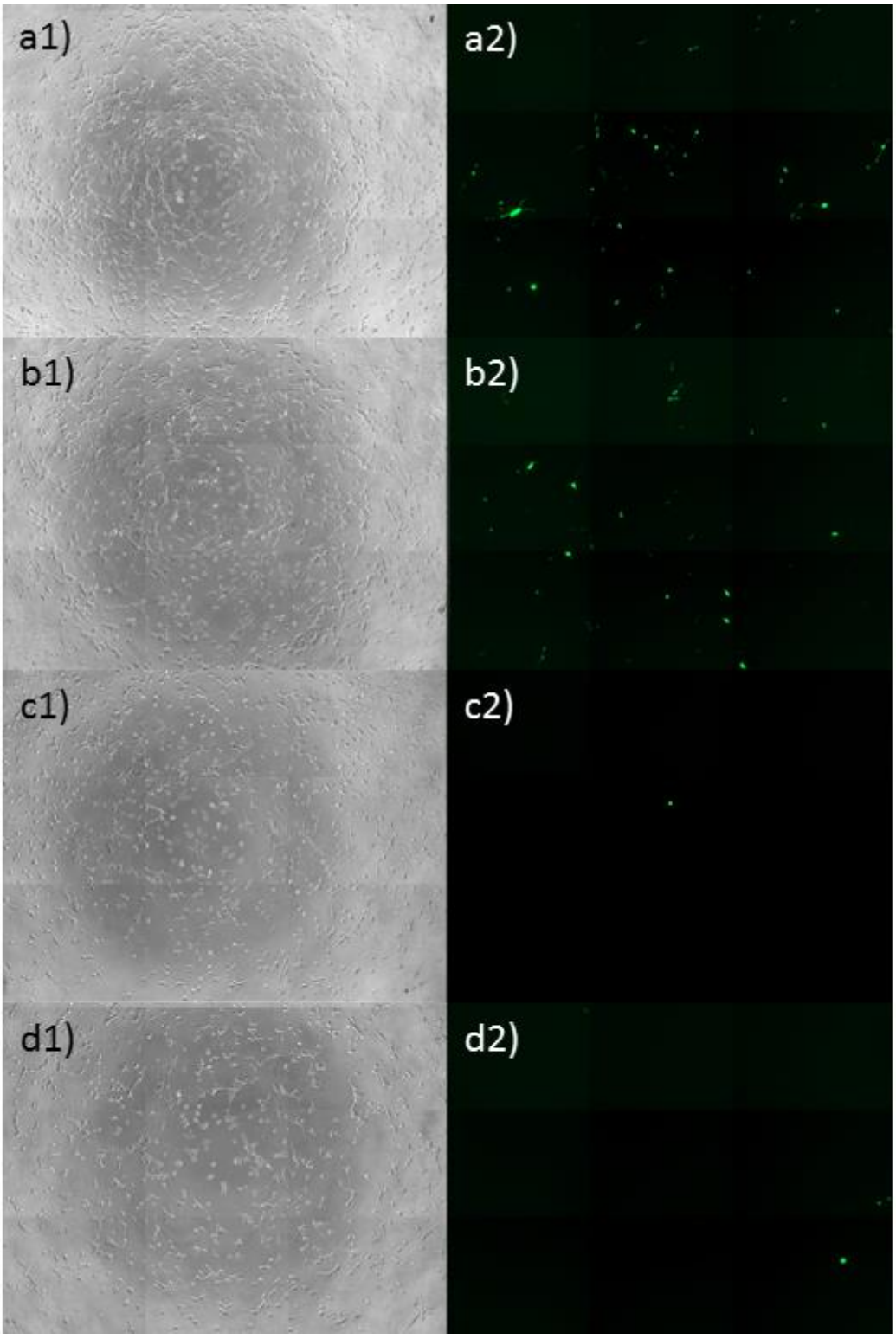

Figure 8.6. 1) Phase-contrast and 2) fluorescence images of HEK293 cells transfected with poly(methyl 6-acryloyl-β-D-glucosaminoside) a) fraction 1 (N/P 30), b) fraction 1 (N/P 60), c) fraction 4 (N/P 30), and d) fraction 4 (N/P 60) after 48 hours.

After five days, significant GFP expression was observed in wells transfected with chitosan, while no significant increase in GFP expression was seen with wells transfected with poly(methyl 6-acryloyl-β-D-glucosaminoside) fraction 4 (Figure 8.7). The delay in gene expression when using chitosan as a transfection agent has been previously observed to reach a maximum after five days, with the fraction of cells expressing GFP increasing 202% between the two-day time point and the five-day time point after transfection.[332] Replenishing the cells with 10% fetal bovine serum media was also seen to facilitate gene expression after transfection with chitosan.[333] Unfortunately, no increase in GFP expression was observed in using poly(methyl 6-acryloyl-β-D-glucosaminoside) fraction 4 even after five days with a replenishment of 10% fetal bovine serum media on day 2. When the concentration of polyplexes was increased fivefold, however, transfection was observed using poly(methyl 6-acryloyl-β-D-glucosaminoside) fraction 4 although considerable cell debris was also observed (Figure 8.8).

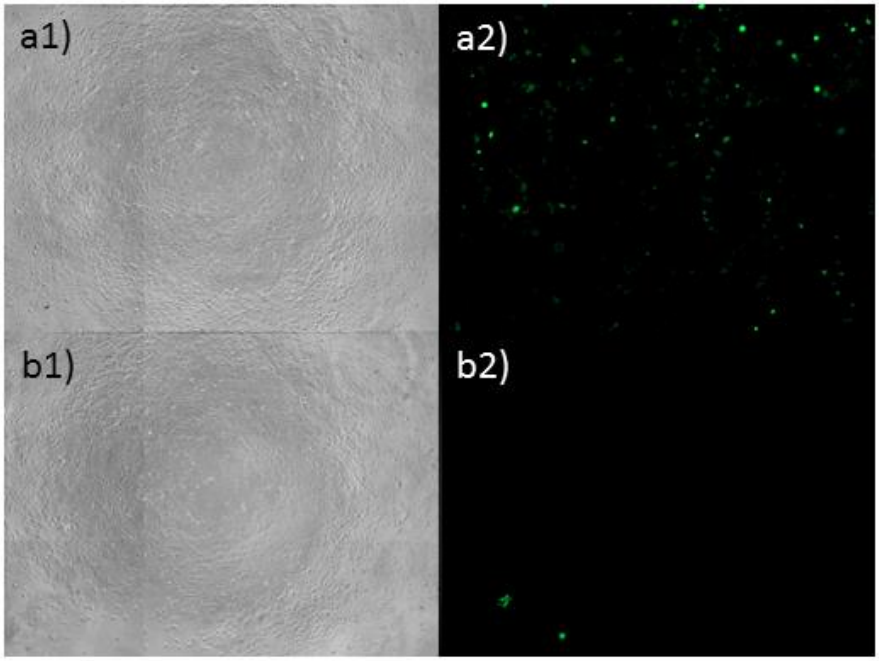

Figure 8.7. 1) Phase-contrast and 2) fluorescence images of HEK293 cells transfected with a) chitosan (N/P 10) and b) poly(methyl 6-acryloyl-β-D-glucosaminoside) fraction 4 (N/P 60) after 5 days.

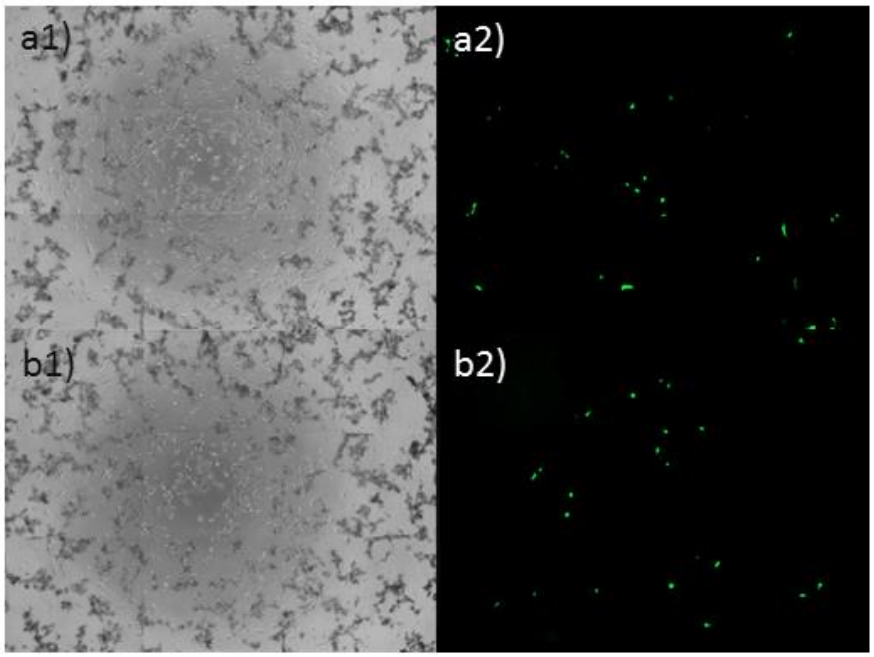

Figure 8.8. 1) Phase-contrast and 2) fluorescence images of HEK293 cells transfected with 5× poly(methyl 6-acryloyl-β-D-glucosaminoside) fraction 4 a) N/P 30 and b) N/P 60 after 2 days.

8.5. Conclusions

Due to its cationic nature and biocompatibility with eukaryotic cells, chitosan has been investigated as a transfection agent, but is limited by the drawbacks of naturally-derived polysaccharides including a lack of control of molecular weight and difficulty in purification. As an alternative, poly(methyl 6-acryloyl-β-D-glucosaminoside) was evaluated for its potential as a transfection agent. Complexation of nucleic acids was observed at approximately an N/P ratio of 30, with higher molecular weight glycopolymer and higher N/P ratios creating smaller and more homogeneous polyplexes. Higher molecular glycopolymer and higher N/P ratios, however, also exhibited higher cytotoxicity towards HEK293 cells, a common cell line for transfection. A dilute solution of polyplexes created with high molecular weight poly(methyl 6-acryloyl-β-D-glucosaminoside) demonstrated significant gene expression while exhibiting no visual signs of cell death. A more concentrated solution of low molecular weight poly(methyl 6-acryloyl-β-D-glucosaminoside) also demonstrated significant gene expression but exhibited significant signs of cell death. In order to maximize gene expression while limiting cytotoxicity, the transfection conditions should be optimized with consideration given to the molecular weight of glycopolymer, N/P ratio, and concentration of the polyplex solution.

8.6. Experimentals

8.6.1. Materials

Chitosan (Aldrich, high purity, M_v 60-120 kDa), linear PEI (Alfa Aesar, 25 kDa), acetic acid (Macron, ACS grade), sodium acetate trihydrate (Fisher, ACS grade), agarose (Apex BioResearch Products, general purpose), DNA loading dye (New England BioLabs Nucleic Acid Gel Loading Dye Purple (6×)), Biotium GelRed Nucleic Acid Gel Stain (10,000× in water), and phosphate-buffered saline (Cellgro) were used as received. Glycofect was synthesized according to the protocol found in Liu *et al.*[182] Water was distilled. HEK293 were cultured in 10% fetal bovine serum in Dulbecco's Modification of Eagle's Medium (Cellgro) with 4.5 g/L glucose and L-glutamine at 37 °C and 5% CO_2.

8.6.2. Analytical techniques

Agarose gels were visualized using a ChemiDoc Touch imaging system. Polyplex size and zeta-potential were determined by on a Malvern Zetasizer Nano ZS. Cell viability was determined by MTT assay (ATCC) read on a BioTek Synergy H1 multi-mode reader. Transfection images were captured on a Zeiss Axiovert Observer Z1 inverted fluorescent microscope.

8.6.3. Agarose gel

Cationic polymers were dissolved in acetate buffer (0.3 M acetic acid/0.2 M sodium acetate) and diluted to the appropriate concentration using acetate buffer. An equal volume of plasmid DNA solution (0.5 µg, pEGFP-C1) was added to each polymer solution and allowed to complex at room temperature for 30 minutes. Loading dye (2 µL) was added, the sample was loaded into a 1% agarose gel with Biotium GelRed Nucleic Acid Gel Stain in TAE buffer, and 100 volts was applied for 45 minutes.

8.6.4. Polyplex size and zeta-potential

Cationic polymers were dissolved in acetate buffer (0.3 M acetic acid/0.2 M sodium acetate) and diluted to the appropriate concentration using acetate buffer. An equal volume of plasmid DNA solution (2 μg, pEGFP-C1) was added to each polymer solution and allowed to complex at room temperature for 30 minutes followed by dilution with distilled water to 1 mL.

8.6.5. Cell viability assay of polyplexes

HEK293 cells (100 μL, 100 cells/μL) were seeded in each well of a 96-well plate and incubated overnight at 37 °C and 5% CO_2. Polyplexes were formed by adding the cationic polymer in acetate buffer (0.3 acetic acid/0.2 sodium acetate, pH 4.4) at the appropriate concentration (10 μL) to pEGFP-C1 dissolved in distilled water (10 μL, 200 ng/μL) and incubated at room temperature for 30 minutes. Each sample in triplicate was diluted with serum-free media (80 μL). The media in the plate was replaced with each polyplex solution and incubated at 37 °C and 5% CO_2 for 48 hours. Control wells were filled with serum-free media. The media was replaced with serum-free media (100 μL) and the MTT reagent (10 μL) and incubated for 2 hours at 37 °C and 5% CO_2 followed by the addition of detergent (100 μL) and incubation at room temperature overnight. The absorbance at 570 nm was read for each well.

8.6.6. Transfection

HEK293 cells (100 μL, 100 cells/μL) were seeded in each well of a 96-well plate and incubated overnight at 37 °C and 5% CO_2. Polyplexes were formed by adding the solution of cationic polymer in acetate buffer (0.3 acetic acid/0.2 sodium acetate, pH 4.4) (2 μL) to pEGFP-C1 dissolved in distilled water (2 μL, 200 ng/μL) and incubated at room temperature for 30 minutes. Each sample in quadruplicate was diluted with serum-free media (96 μL). The media in the plate was replaced with each polyplex solution and incubated at 37 °C and 5% CO_2. The

cells were imaged every 24 hours for seven days, changing the media every two days with 10% fetal bovine serum in DMEM.

CHAPTER 9

Conclusions and future directions

9.1. Conclusions

This dissertation creates new tools for the synthesis of glycopolymers and utilizes these glycopolymers to explore three aspects of glycomimetic research: 1) utilization of glycopolymers to create a 2D substrate for bacterial attachment, 2) utilization of a polymerizable RAFT CTA to create branched glycopolymers with control of saccharide density on 3D substrates, and 3) utilization of a cationic glycomimetic to investigate its potential biomedical applications.

9.1.1. Utilization of glycopolymers to create a 2D substrate for bacterial attachment

We synthesized a set of glycopolymers with various saccharide identities via RAFT polymerization taking advantage of the ability to control molecular weight, limit dispersity, and modify the chain end into a free thiol. The various glycopolymers were used to modify the surfaces of gold-coated substrates, and the surfaces were characterized via X-ray photoelectron spectroscopy and infrared spectroscopy. Using these substrates, we investigated the attachment and movement of mannose-sensitive hemagglutinin expressing *Shewanella oneidens*is and *Vibrio cholerae*. We observed preferential attachment to mannose surfaces over galactose and *N*-acetyl glucosamine surfaces and decreased cell adhesion to surfaces constructed from higher molecular weight glycopolymer. Using a combination of saccharide identity and molecular weight, patterned surfaces can be created to direct bacteria using the differences in cellular interaction with the various glycopolymer surfaces.

9.1.2. Utilization of a polymerizable RAFT CTA to create branched glycopolymers with control of saccharide density on 3D substrates

Using RAFT chain transfer agent (CTA) synthesis techniques, we developed two alcohol-bearing RAFT CTAs. Using one of these alcohol-bearing RAFT CTAs, a polymerizable group or a glycomonomer was attached, allowing for the polymerization of hyperbranched structures without crosslinking. Using one of these polymerizable CTAs, a series of glycopolymers was synthesized with varying molecular weight and degree of branching. Expanding upon this work, tunable amphiphilic copolymers with variable monomer identity, molecular weight, and degree of branching were synthesized. Using methyl acrylate as a hydrophobic monomer and galactose acrylate as a hydrophilic monomer, we created amphiphilic block copolymers of various molecular weights and degrees of branching in the hydrophilic domain. The saccharide moieties were observed to retain their natural ability to isomerize even though connected to the polymer backbone. These copolymers were self-assembled using the nanoprecipitation method to create solid, spherical nanoparticles with saccharide moieties on the nanoparticle surface available for lectin binding. Nanoparticle size was observed to be inversely proportional to copolymer molecular weight, and the nanoparticles were stabilized by the CTA chain ends, which may lead to an aggregated construct. Saccharide density on the surface of the nanoparticles was increased via branching without affecting the size and morphology of the nanoparticle, allowing for intricate studies of multivalent lectin binding to a 3D substrate.

9.1.3. Utilization of a cationic glycomimetic to investigate its potential biomedical applications

We synthesized a series of glycomonomers incorporating an Fmoc protecting group and a polymerizable acrylate moiety. Each glycomonomer was designed with a slight structural

variation of glucosamine and variation in the saccharide attachment site to the polymer backbone. Design focused on methyl *N*-Fmoc-6-acryloyl-β-D-glucosaminoside, which most closely mimics the structure of glucosamine in chitosan, containing a β-glycosidic bond and maintaining only two free alcohols. Methyl *N*-Fmoc-6-acryloyl-β-D-glucosaminoside was polymerized via a UV-photoinitiator, and a series of molecular weights was obtained through fractional precipitation. After deprotection of the Fmoc protecting group, the glycopolymers were characterized by an amine quantification assay for amine content and potentiometric titration for pKa.

Using poly(methyl 6-acryloyl-β-D-glucosaminoside), we investigated two biomedical applications that are commonly studied for chitosan, as an antimicrobial and as a gene transfection vector. Although acetic acid is necessary to dissolve chitosan, less than 0.2% acetic acid should be used to prevent an inhibitory effect from acetic acid. When poly(methyl 6-acryloyl-β-D-glucosaminoside) was investigated for its inhibitory effect on *E. coli*, it demonstrated a similar molecular weight dependence as previously reported for chitosan. Unlike chitosan, poly(methyl 6-acryloyl-β-D-glucosaminoside) is soluble without acetic acid and was found to maintain its inhibitory effect in neutral and basic pH buffers. In evaluating the cytotoxicity of poly(methyl 6-acryloyl-β-D-glucosaminoside) on eukaryotic cells, cytotoxicity was observed to increase with the molecular weight of the polymer. When poly(methyl 6-acryloyl-β-D-glucosaminoside) was dissolved at neutral pH, however, no cytotoxic effect was observed.

Furthermore, we evaluated the potential of poly(methyl 6-acryloyl-β-D-glucosaminoside) as a transfection agent. Complexation of nucleic acids was observed at approximately an N/P ratio of 30, with higher molecular weight glycopolymer and higher N/P ratios creating smaller and

more homogeneous polyplexes. Higher molecular glycopolymer and higher N/P ratios, however, also exhibited higher cytotoxicity towards HEK293 cells, a common cell line for transfection. A dilute solution of polyplexes created with high molecular weight poly(methyl 6-acryloyl-β-D-glucosaminoside) demonstrated significant gene expression while exhibiting no visual signs of cell death. A more concentrated solution of low molecular weight poly(methyl 6-acryloyl-β-D-glucosaminoside) also demonstrated significant gene expression but exhibited significant signs of cell death. In order to maximize gene expression while limiting cytotoxicity, the transfection conditions should be optimized with consideration given to the molecular weight of glycopolymer, N/P ratio, and concentration of the polyplex solution.

Overall, this dissertation has presented a number of synthetic tools for expanding the scope of glycomimetic research. While much of glycomimetic research had previously focused on linear glycopolymers in solution, the work in this dissertation extends the scope of glycopolymer investigations to include the design of more complex 2D substrates, the control of saccharide density on the surface of 3D structures, and the inclusion of cationic charge on the saccharide moiety. These advances can be utilized in numerous biomedical applications for studying biological interactions with glycomimetics, controlling biological responses due to glycomimetics, and developing novel therapeutics using glycomimetics.

9.2. Future directions

The results of this dissertation provide the initial basis for further glycomimetic investigations. While the direction of future investigations may progress in many ways, we present a few immediate possibilities.

From the work in Chapter 5, glycopolymer surfaces have been constructed on gold-coated substrates. While gold is a convenient medium for attaching chain end modified RAFT glycopolymers, it is difficult to construct a gold substrate that is also optically transparent to allow for the imaging of bacterial activity on the substrate. As an alternative, glass substrates can be modified with thiol-reactive acrylate moieties as presented by Biggs *et al*.[334] for the attachment of RAFT glycopolymers. The surface modification of glass also opens the possibility of functionalizing the surface with different moieties for attachment of different glycopolymer populations. For example, a glass substrate can be patterned with an atom-transfer radical polymerization (ATRP) initiator and a maleimide moiety. Glycopolymers can be created by polymerization from the ATRP initiator, and a thiol-terminated glycopolymer can be attached to the maleimide. In this fashion, patterned substrates can be created with control over saccharide identity, molecular weight, and architecture.

From the work in Chapter 6, a non-crosslinking branching unit was created for RAFT polymerizations from which branched amphiphilic glycopolymers were created. Linear and branched amphiphilic glycopolymers were self-assembled into nanoparticles with control over saccharide density at their surface. Using these nanoparticles, we studied the interaction of lectins with saccharide-bearing 3D constructs. Building on this work, additional saccharide identities can be studied including polymers containing multiple saccharide identities to mimic a

natural glycocalyx. In addition, the nanoparticle platform can be used to investigate cellular interactions and potentially used as a carrier for hydrophobic therapeutics.

From the work in Chapters 7 and 8, a cationic glycopolymer was synthesized and used to investigate potential applications as an antimicrobial and as a transfection vector. The cationic glycopolymer with its series of molecular weights can be used to investigate bacterial membrane behavior in model systems to further elucidate the antibacterial mechanism of chitosan. Furthermore, the effect of pH on the release of genetic material complexed to the cationic glycopolymer should be studied. The lower pKa of the cationic glycopolymer relative to poly(ethyleneimine) is potentially advantageous for disassociation of anionic material in near neutral conditions, such as the delivery of siRNA in the cytoplasm. In addition, the polymerization and deprotection conditions can be tuned to facilitate creation of glycopolymers from the remaining cationic glycomonomers that vary the structure of the saccharide unit to probe structural dependencies in biomedical applications. Furthermore, copolymerization of these cationic glycomonomers with other glycomonomers can be used to create glycopolymers with varied charge densities that might also have profound effects on bioactivity. In addition, visible light-initiated RAFT polymerization can be explored as a technique for producing Fmoc-protected glycopolymers. Additional glycomonomers can, also, be designed to include different amine protecting groups, such as *tert*-butyl carbamate, which would allow for amine deprotection prior to polymerization using acidic conditions that would protonate the amine and prevent a Michael addition reaction with the polymerizable acrylate. Finally, the synthetic techniques for creating cationic glycomonomers can be applied to other amino-saccharides, such as galactosamine and mannosamine for studies of the importance of saccharide identity in cationic glycopolymers.

REFERENCES

(1) Rinaudo, M. *Prog. Polym. Sci.* **2006**, *31*, 603–632.

(2) Crout, D. H.; Vic, G. *Curr. Opin. Chem. Biol.* **1998**, *2*, 98–111.

(3) Flitsch, S. L. *Curr. Opin. Chem. Biol.* **2000**, *4*, 619–625.

(4) Manzoni, L.; Castelli, R. *Org. Lett.* **2004**, *6*, 4195–4198.

(5) Park, G.; Ko, K. S.; Zakharova, A.; Pohl, N. L. *J. Fluor. Chem.* **2008**, *129*, 978–982.

(6) Plante, O. J.; Palmacci, E. R.; Seeberger, P. H. *Science* **2001**, *291*, 1523–1527.

(7) Ladmiral, V.; Melia, E.; Haddleton, D. M. *Eur. Polym. J.* **2004**, *40*, 431–449.

(8) Okada, M. *Prog. Polym. Sci.* **2001**, *26*, 67–104.

(9) Ting, S. R. S.; Chen, G.; Stenzel, M. H. *Polym. Chem.* **2010**, *1*, 1392–1412.

(10) Ahmed, M.; Wattanaarsakit, P.; Narain, R. *Eur. Polym. J.* **2013**, *49*, 3010–3033.

(11) Ghadban, A.; Albertin, L. *Polymers.* **2013**, *5*, 431–526.

(12) Miura, Y. *J. Polym. Sci. Part A Polym. Chem.* **2007**, *45*, 5031–5036.

(13) *Engineered Carbohydrate-Based Materials for Biomedical Applications*; Narain, R., Ed.; John Wiley & Sons, Inc.: Hoboken, NJ, USA, 2011.

(14) Varma, A. .; Kennedy, J. .; Galgali, P. *Carbohydr. Polym.* **2004**, *56*, 429–445.

(15) Muthukrishnan, S.; Mori, H.; Müller, A. H. E. *Macromolecules* **2005**, *38*, 3108–3119.

(16) Muthukrishnan, S.; Jutz, G.; André, X.; Mori, H.; Müller, A. H. E. *Macromolecules* **2005**, *38*, 9–18.

(17) Muthukrishnan, S.; Erhard, D. P.; Mori, H.; Müller, A. H. E. *Macromolecules* **2006**, *39*, 2743–2750.

(18) Gao, C.; Muthukrishnan, S.; Li, W.; Yuan, J.; Xu, Y.; Müller, A. H. E. *Macromolecules* **2007**, *40*, 1803–1815.

(19) Lin, K.; Kasko, A. M. *Biomacromolecules* **2013**, *14*, 350–357.

(20) Matyjaszewski, K. *Macromolecules* **2012**, *45*, 4015–4039.

(21) Chiefari, J.; Chong, Y. K. B.; Ercole, F.; Krstina, J.; Jeffery, J.; Le, T. P. T.; Mayadunne, R. T. A.; Meijs, G. F.; Moad, C. L.; Moad, G.; Rizzardo, E.; Thang, S. H. *Macromolecules* **1998**, *31*, 5559–5562.

(22) Barner-Kowollik, C.; Perrier, S. *J. Polym. Sci. Part A Polym. Chem.* **2008**, *46*, 5715–5723.

(23) Vo, C. D.; Rosselgong, J.; Armes, S. P.; Billingham, N. C. *Macromolecules* **2007**, *40*, 7119–7125.

(24) Semsarilar, M.; Ladmiral, V.; Perrier, S. S. *Macromolecules* **2010**, *43*, 1438–1443.

(25) Wang, R.; Luo, Y.; Li, B. G.; Zhu, S. *Macromolecules* **2009**, *42*, 85–94.

(26) Liu, B.; Kazlauciunas, A.; Guthrie, J. T.; Perrier, S. *Macromolecules* **2005**, *38*, 2131–2136.

(27) Liu, J.; Willför, S.; Xu, C. *Bioact. Carbohydrates Diet. Fibre* **2014**, *5*, 31–61.

(28) Varki, A. *Glycobiology* **1993**, *3*, 97–130.

(29) Dube, D. H.; Bertozzi, C. R. *Nat. Rev. Drug Discov.* **2005**, *4*, 477–488.

(30) Mueller, R. L.; Scheidt, S. *Circulation* **1994**, *89*, 432–449.

(31) McLean, J. *Am J Physiol* **1916**, *41*, 250–257.

(32) Linhardt, R.; Gunay, N. *Semin. Thromb. Hemost.* **1999**, *25*, 5–16.

(33) Hedlund, K. D.; Coyne, D. P.; Sanford, D. M.; Huddelson, J. *Perfusion* **2013**, *28*, 61–65.

(34) Blixt, O.; Razi, N. In *Glycoscience*; Fraser-Reid, B. O.; Tatsuta, K.; Thiem, J., Eds.; Springer Berlin Heidelberg: Berlin, Heidelberg, 2008; pp. 1361–1385.

(35) Bülter, T.; Elling, L. *Glycoconj. J. 16*, 147–159.

(36) Seibel, J.; Jördening, H. J.; Buchholz, K. *Biocatal. Biotransformation* **2009**.

(37) Bojarová, P.; Rosencrantz, R. R.; Elling, L.; Křen, V. *Chem. Soc. Rev.* **2013**, *42*, 4774–4797.

(38) van der Vlist, J.; Schönen, I.; Loos, K. *Biomacromolecules* **2011**, *12*, 3728–3732.

(39) van der Vlist, J.; Faber, M.; Loen, L.; Dijkman, T. J.; Asri, L. A. T. W.; Loos, K. *Polymers.* **2012**, *4*, 674–690.

(40) Thimm, J.; Thiem, J. In *Glycoscience*; Springer Berlin Heidelberg: Berlin, Heidelberg, 2008; pp. 1387–1409.

(41) Perugino, G.; Trincone, A.; Rossi, M.; Moracci, M. *Trends Biotechnol.* **2004**, *22*, 31–37.

(42) Mackenzie, L. F.; Wang, Q.; Warren, R. A. J.; Withers, S. G. *J. Am. Chem. Soc.* **1998**, *120*, 5583–5584.

(43) Faijes, M.; Planas, A. *Carbohydr. Res.* **2007**, *342*, 1581–1594.

(44) Davis, B. G. *J. Chem. Soc. Perkin Trans. 1* **2000**, 2137–2160.

(45) Toshima, K. In *Glycoscience*; Fraser-Reid, B. O.; Tatsuta, K.; Thiem, J., Eds.; Springer Berlin Heidelberg: Berlin, Heidelberg, 2008; pp. 429–449.

(46) Koenigs, W.; Knorr, E. *Berichte der Dtsch. Chem. Gesellschaft* **1901**, *34*, 957–981.

(47) Fischer, E.; Delbrück, K. *Berichte der Dtsch. Chem. Gesellschaft* **1909**, *42*, 1476–1482.

(48) Schmidt, R. R.; Michel, J. *Angew. Chemie Int. Ed. English* **1980**, *19*, 731–732.

(49) Mootoo, D. R.; Konradsson, P.; Udodong, U.; Fraser-Reid, B. *J. Am. Chem. Soc.* **1988**, *110*, 5583–5584.

(50) Lemieux, R. U.; Cipera, J. D. T. *Can. J. Chem.* **1956**, *34*, 906–910.

(51) Juaristi, E.; Cuevas, G. *Tetrahedron* **1992**, *48*, 5019–5087.

(52) Reynolds, D. D.; Evans, W. L. In *Organic Syntheses*; John Wiley & Sons, Inc.: Hoboken, NJ, USA, 2003; pp. 56–56.

(53) Daranas, A. H.; Shimizu, H.; Homans, S. W. *J. Am. Chem. Soc.* **2004**, *126*, 11870–11876.

(54) Jalsa, N. K. *Tetrahedron Lett.* **2011**, *52*, 6587–6590.

(55) Bennett, C. S. *Org. Biomol. Chem.* **2014**, *12*, 1686.

(56) Kröck, L.; Esposito, D.; Castagner, B.; Wang, C. C.; Bindschädler, P.; Seeberger, P. H. *Chem. Sci.* **2012**, *3*, 1617.

(57) Calin, O.; Eller, S.; Seeberger, P. H. *Angew. Chem. Int. Ed. Engl.* **2013**, *52*, 5862–5865.

(58) Boltje, T. J.; Li, C.; Boons, G. J. *Org. Lett.* **2010**, *12*, 4636–4639.

(59) Kandasamy, J.; Hurevich, M.; Seeberger, P. H. *Chem. Commun.* **2013**, *49*, 4453.

(60) Ganesh, N. V.; Fujikawa, K.; Tan, Y. H.; Stine, K. J.; Demchenko, A. V. *Org. Lett.* **2012**, *14*, 3036–3039.

(61) Curran, D. P.; Ferritto, R.; Hua, Y. *Tetrahedron Lett.* **1998**, *39*, 4937–4940.

(62) Miura, T.; Hirose, Y.; Ohmae, M.; Inazu, T. *Org. Lett.* **2001**, *3*, 3947–3950.

(63) Jaipuri, F. A.; Pohl, N. L. *Org. Biomol. Chem.* **2008**, *6*, 2686–2691.

(64) Yang, B.; Jing, Y.; Huang, X. *European J. Org. Chem.* **2010**, *2010*, 1290–1298.

(65) Zong, C.; Venot, A.; Dhamale, O.; Boons, G. J. *Org. Lett.* **2013**, *15*, 342–345.

(66) Manabe, S.; Ishii, K.; Ito, Y. *European J. Org. Chem.* **2011**, *2011*, 497–516.

(67) Ando, H.; Manabe, S.; Nakahara, Y.; Ito, Y. *Angew. Chemie Int. Ed.* **2001**, *40*, 4725–4728.

(68) Douglas, S. P.; Whitfield, D. M.; Krepinsky, J. J. *J. Am. Chem. Soc.* **1995**, *117*, 2116–2117.

(69) Ito, Y.; Kanie, O.; Ogawa, T. *Angew. Chemie Int. Ed. English* **1996**, *35*, 2510–2512.

(70) Jiang, L.; Hartley, R. C.; Chan, T. H. *Chem. Commun.* **1996**, 2193.

(71) Zhu, T.; Boons, G. J. *J. Am. Chem. Soc.* **2000**, *122*, 10222–10223.

(72) Manabe, S.; Nakahara, Y.; Ito, Y. *Synlett* **2000**, *2000*, 1241–1244.

(73) Yan, F.; Gilbert, M.; Wakarchuk, W. W.; Brisson, J. R.; Whitfield, D. M. *Org. Lett.* **2001**, *3*, 3265–3268.

(74) de Paz, J. L.; Mar Kayser, M.; Macchione, G.; Nieto, P. M. *Carbohydr. Res.* **2010**, *345*, 565–571.

(75) Galan, M. C.; Jones, R. A.; Tran, A. T. *Carbohydr. Res.* **2013**, *375*, 35–46.

(76) Ma, Q.; Sun, S.; Meng, X. B.; Li, Q.; Li, S. C.; Li, Z. J. *J. Org. Chem.* **2011**, *76*, 5652–5660.

(77) Yerneni, C. K.; Pathak, V.; Pathak, A. K. *J. Org. Chem.* **2009**, *74*, 6307–6310.

(78) Tran, A. T.; Burden, R.; Racys, D. T.; Galan, M. C. *Chem. Commun.* **2011**, *47*, 4526–4528.

(79) He, X.; Chan, T. *Synthesis.* **2006**, *2006*, 1645–1651.

(80) Huang, J. Y.; Lei, M.; Wang, Y. G. *Tetrahedron Lett.* **2006**, *47*, 3047–3050.

(81) Sharon, N.; Lis, H. *Science.* **1972**, *177*, 949–959.

(82) Lis, H.; Sharon, N. *Chem. Rev.* **1998**, *98*, 637–674.

(83) Sharon, N.; Lis, H. *Essays Biochem.* **1995**, *30*, 59–75.

(84) Goldstein, I. J.; Poretz, R. D. In *The Lectins: Properties, Functions, and Applications in Biology and Medicine*; Liener, I. E.; Sharon, N.; Goldstein, I. J., Eds.; Elsevier, 2012; pp. 33–247.

(85) Sumner, J. B. *J. Biol. Chem.* **1919**, *37*, 137–142.

(86) Sumner, J. B.; Howell, S. F. *J. Bacteriol.* **1936**, *32*, 227–237.

(87) Goldstein, I. J.; Hollerman, C. E.; Smith, E. E. *Biochemistry* **1965**, *4*, 876–883.

(88) Fais, M.; Karamanska, R.; Allman, S.; Fairhurst, S. A.; Innocenti, P.; Fairbanks, A. J.; Donohoe, T. J.; Davis, B. G.; Russell, D. A.; Field, R. A. *Chem. Sci.* **2011**, *2*, 1952–1959.

(89) Wang, Y.; Yu, G.; Han, Z.; Yang, B.; Hu, Y.; Zhao, X.; Wu, J.; Lv, Y.; Chai, W. *FEBS Lett.* **2011**, *585*, 3927–3934.

(90) Ohtsuka, I.; Sadakane, Y.; Higuchi, M.; Hada, N.; Hada, J.; Kakiuchi, N.; Sakushima, A. *Bioorg. Med. Chem.* **2011**, *19*, 894–899.

(91) Lundquist, J. J.; Toone, E. J. *Chem. Rev.* **2002**, *102*, 555–578.

(92) Becer, C. R. *Macromol. Rapid Commun.* **2012**, *33*, 742–752.

(93) Jayaraman, N. *Chem. Soc. Rev.* **2009**, *38*, 3463–3483.

(94) Wang, J. L.; Cunningham, B. A.; Waxdal, M. J.; Edelman, G. M. *J. Biol. Chem.* **1975**,

250, 1490–1502.

(95) Sweeney, E. C.; Tonevitsky, A. G.; Temiakov, D. E.; Agapov, I. I.; Saward, S.; Palmer, R. A. *Proteins* **1997**, *28*, 586–589.

(96) Mahajan, S. S. Glycans for ricin and Shiga toxins : Synthesis and biophysical characterization, University of Cincinnati, 2011.

(97) Lee, Y. C.; Townsend, R. R.; Hardy, M. R.; Lönngren, J.; Bock, K. In *Biochemical and Biophysical Studies of Proteins and Nucleic Acids*; Lo, T. B.; Liu, T. Y.; Li, C. H., Eds.; Elsevier, 1984; pp. 349–360.

(98) Lee, Y. C.; Townsend, R. R.; Hardy, M. R.; Lönngren, J.; Arnarp, J.; Haraldsson, M.; Lonn, H. *J. Biol. Chem.* **1983**, *258*, 199–202.

(99) Lee, Y. C.; Lee, R. T. *Acc. Chem. Res.* **1995**, *28*, 321–327.

(100) Woller, E. K.; Cloninger, M. J. *Org. Lett.* **2002**, *4*, 7–10.

(101) Cloninger, M. J. *Curr. Opin. Chem. Biol.* **2002**, *6*, 742–748.

(102) Lahmann, M. *Top. Curr. Chem.* **2009**, *288*, 183–65.

(103) Burke, S. D.; Zhao, Q.; Schuster, M. C.; Kiessling, L. L. *J. Am. Chem. Soc.* **2000**, *122*, 4518–4519.

(104) André, S.; Lahmann, M.; Gabius, H. J.; Oscarson, S. *Mol. Pharm.* **2010**, *7*, 2270–2279.

(105) Patel, A.; Lindhorst, T. K. *Carbohydr. Res.* **2006**, *341*, 1657–1668.

(106) Zistler, A.; Koch, S.; Schlüter, A. D. *J. Chem. Soc. Perkin Trans. 1* **1999**, 501–508.

(107) Gauthier, M. A.; Gibson, M. I.; Klok, H. A. *Angew. Chem. Int. Ed. Engl.* **2009**, *48*, 48–58.

(108) Bahulekar, R.; Tokiwa, T.; Kano, J.; Matsumura, T.; Kojima, I.; Kodama, M. *Carbohydr.*

Polym. **1998**, *37*, 71–78.

(109) Pasparakis, G.; Cockayne, A.; Alexander, C. *J. Am. Chem. Soc.* **2007**, *129*, 11014–11015.

(110) García-Oteiza, M. C.; Sánchez-Chaves, M.; Arranz, F. *Macromol. Chem. Phys.* **1997**, *198*, 2237–2247.

(111) Schofield, C. L.; Mukhopadhyay, B.; Hardy, S. M.; McDonnell, M. B.; Field, R. A.; Russell, D. A. *Analyst* **2008**, *133*, 626–634.

(112) Dintinger, T.; Dutheil-Bouëdec, D.; Bouchonneau, M.; Tellier, C. *Biotechnol. Lett.* **1994**, *16*, 689–692.

(113) Cohen, S. B.; Halcomb, R. L. *Org. Lett.* **2001**, *3*, 405–407.

(114) Gamblin, D. P.; Garnier, P.; van Kasteren, S.; Oldham, N. J.; Fairbanks, A. J.; Davis, B. G. *Angew. Chemie* **2004**, *116*, 846–851.

(115) Murakami, T.; Hirono, R.; Sato, Y.; Furusawa, K. *Carbohydr. Res.* **2007**, *342*, 1009–1020.

(116) Kefurt, K.; Kefurtová, Z.; Jarý, J. *Collect. Czechoslov. Chem. Commun.* **1988**, *53*, 1795–1805.

(117) Susaki, H.; Sszuki, K.; Ikeda, M.; Yamada, H.; Watanabe, H. K. *Chem. Pharm. Bull. (Tokyo).* **1994**, *42*, 2090–2096.

(118) Wong, L.; Boyer, C.; Jia, Z.; Zareie, H. M.; Davis, T. P.; Bulmus, V. *Biomacromolecules* **2008**, *9*, 1934–1944.

(119) Lin, K. Synthesis of glycopolyers for biomedical applications, University of California, Los Angeles, 2013.

(120) Slavin, S.; Burns, J.; Haddleton, D. M.; Becer, C. R. *Eur. Polym. J.* **2011**, *47*, 435–446.

(121) Hu, Z.; Fan, X.; Zhang, G. *Carbohydr. Polym.* **2010**, *79*, 119–124.

(122) Ladmiral, V.; Mantovani, G.; Clarkson, G. J.; Cauet, S.; Irwin, J. L.; Haddleton, D. M. *J. Am. Chem. Soc.* **2006**, *128*, 4823–4830.

(123) Kobayashi, K.; Sumitomo, H.; Ina, Y. *Polym. J.* **1985**, *17*, 567–575.

(124) Spain, S. G.; Gibson, M. I.; Cameron, N. R. *J. Polym. Sci. Part A Polym. Chem.* **2007**, *45*, 2059–2072.

(125) Kloosterman, W. M. J.; Roest, S.; Priatna, S. R.; Stavila, E.; Loos, K. *Green Chem.* **2014**, *16*, 1837–1846.

(126) Hennen, W. J.; Sweers, H. M.; Wang, Y. F.; Wong, C. H. *J. Org. Chem.* **1988**, *53*, 4939–4945.

(127) Filice, M.; Bavaro, T.; Fernandez-Lafuente, R.; Pregnolato, M.; Guisan, J. M.; Palomo, J. M.; Terreni, M. *Catal. Today* **2009**, *140*, 11–18.

(128) Barz, M.; Götze, S.; Loges, N.; Schüler, T.; Theato, P.; Tremel, W.; Zentel, R. *Eur. Polym. J.* **2015**, *69*, 628–635.

(129) Song, E. H.; Manganiello, M. J.; Chow, Y. H.; Ghosn, B.; Convertine, A. J.; Stayton, P. S.; Schnapp, L. M.; Ratner, D. M. *Biomaterials* **2012**, *33*, 6889–6897.

(130) Helferich, B. *Adv. Carbohydr. Chem.* **1948**, *3*, 79–111.

(131) Mahkam, M.; Mohammadi, R.; Ranaei Siadat, S. O.; Ranaei-siadat, S. E. *e-Polymers* **2006**, *6*, 58–68.

(132) Shi, H.; Liu, L.; Wang, X.; Li, J. *Polym. Chem.* **2012**, *3*, 1182.

(133) Dan, K.; Ghosh, S. *Macromol. Rapid Commun.* **2012**, *33*, 127–132.

(134) Guo, T. Y.; Liu, P.; Zhu, J. W.; Song, M. D.; Zhang, B. H. *Biomacromolecules* **2006**, *7*, 1196–1202.

(135) Zhou, D.; Li, C.; Hu, Y.; Zhou, H.; Chen, J.; Zhang, Z.; Guo, T. *Int. J. Biol. Macromol.* **2012**, *50*, 965–973.

(136) Moira Ambrosi; S. Batsanov, A.; R. Cameron, N.; G. Davis, B.; K. Howard, J. A.; Rob Hunter. *J. Chem. Soc. Perkin Trans. 1* **2002**, 45–52.

(137) Ambrosi, M.; Cameron, N. R.; Davis, B. G.; Stolnik, S. *Org. Biomol. Chem.* **2005**, *3*, 1476.

(138) Odian, G. G. *Principles of polymerization*; 4th ed.; John Wiley & Sons, 2004.

(139) Solomon, D. H.; Rizzardo, E.; Paul, C. Polymerization process and polymers produced thereby. 4,581,429, 1986.

(140) Jakubowski, W.; Matyjaszewski, K. *Macromolecules* **2005**, *38*, 4139–4146.

(141) Moad, G. In *Controlled Radical Polymerization: Mechanisms*; Matyjaszewski, K.; Sumerlin, B. S.; Tsarevsky, N. V.; Chiefari, J., Eds.; ACS Symposium Series; American Chemical Society: Washington, DC, 2015; Vol. 1187, pp. 211–246.

(142) John Chiefari; Roshan T. A. Mayadunne; Catherine L. Moad; Graeme Moad, *; Ezio Rizzardo, *; Almar Postma; Melissa A. Skidmore, and; Thang*, S. H. **2003**.

(143) Barner-Kowollik, C. *Handbook of RAFT Polymerization*; John Wiley & Sons, 2008.

(144) Keddie, D. J.; Moad, G.; Rizzardo, E.; Thang, S. H. *Macromolecules* **2012**, *45*, 5321–5342.

(145) Thang, S. H.; Chong, (Bill) Y.K.; Mayadunne, R. T. A.; Moad, G.; Rizzardo, E.

Tetrahedron Lett. **1999**, *40*, 2435–2438.

(146) Wager, C. M.; Haddleton, D. M.; Bon, S. A. . *Eur. Polym. J.* **2004**, *40*, 641–645.

(147) Pissuwan, D.; Boyer, C.; Gunasekaran, K.; Davis, T. P.; Bulmus, V. *Biomacromolecules* **2010**, *11*, 412–420.

(148) Lowe, A. B.; Sumerlin, B. S.; McCormick, C. L. *Polymer*. **2003**, *44*, 6761–6765.

(149) Albertin, L.; Stenzel, M. H.; Barner-Kowollik, C.; Davis, T. P. *Polymer*. **2006**, *47*, 1011–1019.

(150) Boyer, C.; Bulmus, V.; Davis, T. P.; Ladmiral, V.; Liu, J.; Perrier, S. *Chem. Rev.* **2009**, *109*, 5402–5436.

(151) Stenzel, M. H. *Chem. Commun.* **2008**, 3486–3503.

(152) Esko, J. D.; Sharon, N. *Microbial Lectins: Hemagglutinins, Adhesins, and Toxins*; Cold Spring Harbor Laboratory Press, 2009.

(153) Disney, M. D.; Zheng, J.; Swager, T. M.; Seeberger, P. H. *J. Am. Chem. Soc.* **2004**, *126*, 13343–13346.

(154) Yang, Q.; Strathmann, M.; Rumpf, A.; Schaule, G.; Ulbricht, M. *ACS Appl. Mater. Interfaces* **2010**, *2*, 3555–3562.

(155) Wang, Y.; Narain, R.; Liu, Y. *Langmuir* **2014**, *30*, 7377–7387.

(156) Goodarzi, N.; Varshochian, R.; Kamalinia, G.; Atyabi, F.; Dinarvand, R. *Carbohydr. Polym.* **2013**, *92*, 1280–1293.

(157) Pearson, S.; Scarano, W.; Stenzel, M. H. *Chem. Commun.* **2012**, *48*, 4695–4697.

(158) Zhang, L.; Bernard, J.; Davis, T. P.; Barner-Kowollik, C.; Stenzel, M. H. *Macromol.*

Rapid Commun. **2008**, *29*, 123–129.

(159) Suriano, F.; Pratt, R.; Tan, J. P. K.; Wiradharma, N.; Nelson, A.; Yang, Y. Y.; Dubois, P.; Hedrick, J. L. *Biomaterials* **2010**, *31*, 2637–2645.

(160) Xiao, N. Y.; Liang, H.; Lu, J.; Rapoport, N.; Nostrum, C. F. van; Lo, C. L.; Huang, G. K.; Lin, K. M.; Hsiue, G. H.; Prabaharan, M.; Grailer, J. J.; Pilla, S.; Steeber, D. A.; Gong, S. Q.; Ganta, S.; Devalapally, H.; Shahiwala, A.; Amiji, M.; Li, M. H.; Keller, P.; Zha, L.; Banikb, B.; Alexis, F.; Ulbrich, K.; Etrych, T.; Chytil, P.; Pechar, M.; Jelinkova, M.; Rihova, B.; Hruby, M.; Konak, C.; Ulbrich, K.; Chytil, P.; Etrych, T.; Konak, C.; Sirova, M.; Mrkvan, T.; Rihova, B.; Ulbrich, K.; Etrych, T.; Chytil, P.; Jelinkova, M.; Rihova, B.; Ulbrich, K.; Ulbrich, K.; Subr, V.; Strohalm, J.; Plocova, D.; Jelinkova, M.; Rihova, B.; Liu, G. Y.; Lv, L. P.; Chen, C. J.; Liu, X. S.; Hu, X. F.; Ji, J.; Huynh, C. T.; Nguyen, M. K.; Kim, J. H.; Kang, S. W.; Kim, B. S.; Lee, D. S.; Chen, W.; Meng, F. H.; Li, F.; Ji, S. J.; Zhong, Z. Y.; Toncheva, V.; Schacht, E.; Ng, S. Y.; Barr, J.; Heller, J.; Bae, Y. H.; Fukushima, S.; Harada, A.; Kataoka, K.; Yasugi, K.; Nakamura, T.; Nagasaki, Y.; Kato, M.; Kataoka, K.; Wang, Q.; Dordick, J. S.; Linhardt, R. J.; Kopecek, J.; Duncan, R.; Bó, A. G. D.; Soldi, V.; Giacomelli, F. C.; Jean, B.; Pignot-Paintrand, I.; Borsali, R.; Fort, S.; Albertin, L.; Stenzel, M. H.; Barner-Kowollik, C.; Foster, L. J. R.; Davis, T. P.; Ladmiral, V.; Melia, E.; Haddleton, D. M.; Xiao, N. Y.; Li, A. L.; Liang, H.; Lu, J.; Bailey, W. J.; Ni, Z.; Wu, S. R.; Ren, L.; Agarwal, S.; Lutz, J. F.; Andrieu, J.; Üzgün, S.; Rudolph, C.; Agarwal, S.; Wlckel, H.; Agarwal, S.; Wlckel, H.; Agarwal, S.; Greiner, A.; Godwin, A.; Hartenstein, M.; Muller, A. H. E.; Brocchini, S.; Shi, M.; Li, A. L.; Liang, H.; Lu, J.; Sun, G.; Cheng, C.; Wooley, K. L.; Xiao, Z. P.; Yang, K. M.; Liang, H.; Lu, J.; Shuai, X. T.; Ai, H.; Nasongkla, N.; Kim, S.; Gao, J.; Quinn, J. F.; Rizzardo, E.; Davis, T. P.; Ting, S.

R. S.; Gregory, A. M.; Stenzel, M. H.; Na, K.; Lee, K. H.; Bae, Y. H.; Jiang, G. B.; Quan, D. P.; Liao, K.; Wang, H.; Schmalenberg, K. E.; Frauchiger, L.; Nikkhouy-Albers, L.; Uhrich, K. E. *Soft Matter* **2011**, *7*, 10834.

(161) Ahmed, M.; Lai, B. F. L.; Kizhakkedathu, J. N.; Narain, R. *Bioconjug. Chem.* **2012**, *23*, 1050–1058.

(162) Ibraheem, D.; Elaissari, A.; Fessi, H. *Int. J. Pharm.* **2014**, *459*, 70–83.

(163) Boussif, O.; Lezoualc'h, F.; Zanta, M. A.; Mergny, M. D.; Scherman, D.; Demeneix, B.; Behr, J. P. *Proc. Natl. Acad. Sci. U. S. A.* **1995**, *92*, 7297–7301.

(164) Lungwitz, U.; Breunig, M.; Blunk, T.; Göpferich, A. *Eur. J. Pharm. Biopharm.* **2005**, *60*, 247–266.

(165) Godbey, W. T.; Wu, K. K.; Mikos, A. G. *J. Control. Release* **1999**, *60*, 149–160.

(166) Jäger, M.; Schubert, S.; Ochrimenko, S.; Fischer, D.; Schubert, U. S. *Chem. Soc. Rev.* **2012**, *41*, 4755–4767.

(167) Lv, H.; Zhang, S.; Wang, B.; Cui, S.; Yan, J. *J. Control. Release* **2006**, *114*, 100–109.

(168) Parhamifar, L.; Larsen, A. K.; Hunter, a. C.; Andresen, T. L.; Moghimi, S. M. *Soft Matter* **2010**, *6*, 4001–4009.

(169) Fischer, D.; Bieber, T.; Li, Y.; Elsässer, H. P.; Kissel, T. *Pharm. Res.* **1999**, *16*, 1273–1279.

(170) Kunath, K.; von Harpe, A.; Fischer, D.; Petersen, H.; Bickel, U.; Voigt, K.; Kissel, T. *J. Control. Release* **2003**, *89*, 113–125.

(171) Wiseman, J. W.; Goddard, C. A.; McLelland, D.; Colledge, W. H. *Gene Ther.* **2003**, *10*,

1654–1662.

(172) Mady, M. M.; Mohammed, W. A.; El-Guendy, N. M.; Elsayed, A. A. *Rom. J. Biophys.* **2011**, *21*, 151–165.

(173) Dai, Z.; Gjetting, T.; Mattebjerg, M. a; Wu, C.; Andresen, T. L. *Biomaterials* **2011**, *32*, 8626–8634.

(174) Godbey, W.; Wu, K.; Mikos, A. *J. Biomed. Mater. Res.* **1999**, *45*, 268–275.

(175) Godbey, W.; Wu, K.; Mikos, A. *Biomaterials* **2001**, *22*, 471–480.

(176) Godbey, W.; Wu, K.; Hirasaki, G.; Mikos, A. *Gene Ther.* **1999**, *6*.

(177) Burke, R. S.; Pun, S. H. *Bioconjug. Chem.* **2008**, *19*, 693–704.

(178) Kichler, A.; Chillon, M.; Leborgne, C.; Danos, O.; Frisch, B. *J. Control. Release* **2002**, *81*, 379–388.

(179) Malek, A.; Czubayko, F.; Aigner, A. *J. Drug Target.* **2008**, *16*, 124–139.

(180) Shuai, X.; Merdan, T.; Unger, F.; Wittmar, M.; Kissel, T. *Macromolecules* **2003**, *36*, 5751–5759.

(181) Liu, Y.; Wenning, L.; Lynch, M.; Reineke, T. M. *J. Am. Chem. Soc.* **2004**, *126*, 7422–7423.

(182) Liu, Y.; Reineke, T. M. *J. Am. Chem. Soc.* **2005**, *127*, 3004–3015.

(183) Wongrakpanich, A.; Joshi, V. B.; Salem, A. K. *Pharm. Dev. Technol.* **2013**, *18*, 1255–1258.

(184) Prevette, L. E.; Kodger, T. E.; Reineke, T. M.; Lynch, M. L. *Langmuir* **2007**, *23*, 9773–9784.

(185) Smith, A. E.; Sizovs, A.; Grandinetti, G.; Xue, L.; Reineke, T. M. *Biomacromolecules* **2011**, *12*, 3015–3022.

(186) Zhang, X. Q.; Wang, X. L.; Zhang, P. C.; Liu, Z. L.; Zhuo, R. X.; Mao, H. Q.; Leong, K. W. *J. Control. Release* **2005**, *102*, 749–763.

(187) Ahmed, M.; Narain, R. *Biomaterials* **2011**, *32*, 5279–5290.

(188) Ahmed, M.; Narain, R. *Biomaterials* **2012**, *33*, 3990–4001.

(189) Kurtulus, I.; Yilmaz, G.; Ucuncu, M.; Emrullahoglu, M.; Becer, C. R.; Bulmus, V. *Polym. Chem.* **2014**, *5*, 1593–1604.

(190) Pries, A. R.; Secomb, T. W.; Gaehtgens, P. *Pflügers Arch. - Eur. J. Physiol.* **2000**, *440*, 653–666.

(191) Lipowsky, H. H. *Ann. Biomed. Eng.* **2012**, *40*, 840–848.

(192) Yang, Q.; Kaul, C.; Ulbricht, M. *Langmuir* **2010**, *26*, 5746–5752.

(193) Linden, S. K.; Sutton, P.; Karlsson, N. G.; Korolik, V.; McGuckin, M. A. *Mucosal Immunol.* **2008**, *1*, 183–197.

(194) Chen, X.; Lee, G. S.; Zettl, A.; Bertozzi, C. R. *Angew. Chemie Int. Ed.* **2004**, *43*, 6111–6116.

(195) Rabuka, D.; Parthasarathy, R.; Lee, G. S.; Chen, X.; Groves, J. T.; Bertozzi, C. R. *J. Am. Chem. Soc.* **2007**, *129*, 5462–5471.

(196) Rabuka, D.; Forstner, M. B.; Groves, J. T.; Bertozzi, C. R. *J. Am. Chem. Soc.* **2008**, *130*, 5947–5953.

(197) Mia L. Huang, R. A. A. S. G. W. T. K. G. *J. Am. Chem. Soc.* **2014**, *136*, 10565.

(198) Serizawa, T.; Uchida, T.; Akashi, M. *J. Biomater. Sci. Polym. Ed.* **1999**, *10*, 391–401.

(199) Toyoshima, M.; Oura, T.; Fukuda, T.; Matsumoto, E.; Miura, Y. *Polym. J.* **2010**, *42*, 172–178.

(200) Su, L.; Zhao, Y.; Chen, G.; Jiang, M. *Polym. Chem.* **2012**, *3*, 1560.

(201) Hoppe-Seyler, F. *Berichte der Dtsch. Chem. Gesellschaft* **1894**, *27*, 3329–3331.

(202) Song, Y.; Sun, Y.; Zhang, X.; Zhou, J.; Zhang, L. *Biomacromolecules* **2008**, *9*, 2259–2264.

(203) Kamiński, K.; Płonka, M.; Ciejka, J.; Szczubiałka, K.; Nowakowska, M.; Lorkowska, B.; Korbut, R.; Lach, R. *J. Med. Chem.* **2011**, *54*, 6586–6596.

(204) Luten, J. Biodegradable cationic polymers as gene delivery carriers: From synthesis to in vivo application, Utrecht University, 2007.

(205) Zhang, C.; Zhou, Y.; Liu, Q.; Li, S.; Perrier, S.; Zhao, Y. *Macromolecules* **2011**, *44*, 2034–2049.

(206) Wei, Z.; Hao, X.; Gan, Z.; Hughes, T. C. *J. Polym. Sci. Part A Polym. Chem.* **2012**, *50*, 2378–2388.

(207) Yamada, B.; Konosu, O.; Tanaka, K.; Oku, F. *Polymer.* **2000**, *41*, 5625–5631.

(208) Bergmeier, S. C.; Arason, K. M. *Tetrahedron Lett.* **2000**, *41*, 5799–5802.

(209) Pugh, C.; Raveendra, B.; Singh, A.; Samuel, R.; Garcia, G. *Synlett* **2010**, 1947–1950.

(210) Billing, J. F.; Nilsson, U. J. *Tetrahedron* **2005**, *61*, 863–874.

(211) Burchard, W. In *Branched Polymers II*; Springer Berlin Heidelberg, 1999; pp. 113–194.

(212) Müller, A. H. E.; Yan, D.; Wulkow, M. *Macromolecules* **1997**, *30*, 7015–7023.

(213) Mackie, W.; Perlin, A. S. *Can. J. Chem.* **1966**, *44*, 2039–2049.

(214) Sun, H.; Gao, C. *Biomacromolecules* **2010**, *11*, 3609–3616.

(215) Höck, S.; Marti, R.; Riedl, R.; Simeunovic, M. *Chim. Int. J. Chem.* **2010**, *64*, 200–202.

(216) Flory, P. J. *Principles of polymer chemistry*; Cornell University Press, 1953.

(217) Lu, L.; Zhang, H.; Yang, N.; Cai, Y. *Macromolecules* **2006**, *39*, 3770–3776.

(218) Lu, L.; Yang, N.; Cai, Y. *Chem. Commun.* **2005**, *0*, 5287.

(219) Quinn, J. F.; Barner, L.; Barner-Kowollik, C.; Rizzardo, E.; Davis, T. P. *Macromolecules* **2002**, *35*, 7620–7627.

(220) Yin, H.; Zheng, H.; Lu, L.; Liu, P.; Cai, Y. *J. Polym. Sci. Part A Polym. Chem.* **2007**, *45*, 5091–5102.

(221) Yeow, J.; Sugita, O. R.; Boyer, C. *ACS Macro Lett.* **2016**, *5*, 558–564.

(222) Brandrup, J.; Immergut, E.; Grulke, E. *Polymer handbook*; 4th ed.; John Wiley & Sons, Inc.: New York, 1999.

(223) Hrynets, Y.; Ndagijimana, M.; Betti, M. *J. Agric. Food Chem.* **2015**, *63*, 6249–6261.

(224) Domard, A. *Int. J. Biol. Macromol.* **1987**, *9*, 98–104.

(225) Bichsel, Y.; von Gunten, U. *Environ. Sci. Technol.* **2000**, *34*, 2784–2791.

(226) Krogfelt, K. A.; Bergmans, H.; Klemm, P. *Infect. Immun.* **1990**, *58*, 1995–1998.

(227) Roberts, J.; Marklund, B.; Ilver, D. *Proc.* **1994**.

(228) Lintermans, P. F.; Bertels, A.; Schlicker, C.; Deboeck, F.; Charlier, G.; Pohl, P.; Norgren, M.; Normark, S.; van Montagu, M.; De Greve, H. *J. Bacteriol.* **1991**, *173*, 3366–3373.

(229) Gorby, Y. A.; Yanina, S.; McLean, J. S.; Rosso, K. M.; Moyles, D.; Dohnalkova, A.;

Beveridge, T. J.; Chang, I. S.; Kim, B. H.; Kim, K. S.; Culley, D. E.; Reed, S. B.; Romine, M. F.; Saffarini, D. A.; Hill, E. A.; Shi, L.; Elias, D. A.; Kennedy, D. W.; Pinchuk, G.; Watanabe, K.; Ishii, S.; Logan, B.; Nealson, K. H.; Fredrickson, J. K. *Proc. Natl. Acad. Sci. U. S. A.* **2006**, *103*, 11358–11363.

(230) Tarsi, R.; Pruzzo, C. *Appl. Environ. Microbiol.* **1999**, *65*, 1348–1351.

(231) Watnick, P.; Fullner, K.; Kolter, R. *J. Bacteriol.* **1999**.

(232) Chiavelli, D. A.; Marsh, J. W.; Taylor, R. K. *Appl. Environ. Microbiol.* **2001**, *67*, 3220–3225.

(233) Utada, A. S.; Bennett, R. R.; Fong, J. C. N.; Gibiansky, M. L.; Yildiz, F. H.; Golestanian, R.; Wong, G. C. L.; Colwell, R. R.; Huq, A.; Faruque, S. M.; Albert, M. J.; Mekalanos, J. J.; Faruque, S. M.; Lipp, E. K.; Huq, A.; Colwell, R. R.; Yildiz, F. H.; Schoolnik, G. K.; Meibom, K. L.; Chiavelli, D. A.; Marsh, J. W.; Taylor, R. K.; Huq, A.; O'Toole, G.; Kaplan, H. B.; Kolter, R.; Berk, V.; Beyhan, S.; Yildiz, F. H.; Costerton, J. W.; Gibiansky, M. L.; Zhao, K.; Watnick, P. I.; Lauriano, C. M.; Klose, K. E.; Croal, L.; Kolter, R.; Watnick, P. I.; Kolter, R.; Berke, A.; Turner, L.; Berg, H. C.; Lauga, E.; Goto, T.; Nakata, K.; Baba, K.; Nishimura, M.; Magariyama, Y.; Riedel, I. H.; Kruse, K.; Howard, J.; Lauga, E.; DiLuzio, W. R.; Whitesides, G. M.; Stone, H. A.; Shum, H.; Gaffney, E. A.; Smith, D. J.; Leonardo, R. Di; Dell'Arciprete, D.; Angelani, L.; Iebba, V.; Spagnolie, S. E.; Lauga, E.; Berg, H. C.; Turner, L.; Kudo, S.; Imai, N.; Nishitoba, M.; Sugiyama, S.; Magariyama, Y.; DiLuzio, W. R.; Kojima, S.; Yamamoto, K.; Kawagishi, I.; Homma, M.; Crocker, J. C.; Grier, D. G.; Frymier, P. D.; Ford, R. M.; Berg, H. C.; Cummings, P. T.; Ebbens, S.; Jones, R. A. L.; Ryan, A. J.; Golestanian, R.; Howse, J. R.; Watnick, P. I.; Fullner, K. J.; Kolter, R.; Pratt, L. A.; Kolter, R.; Otsu, N.; Qian, H.; Sheetz, M. P.; Elson,

E. L.; Conrad, J. C.; Gray, J.; Hancock, G. J.; Katz, D. F.; Blake, J. R.; Paveri-Fontana, S. L. *Nat. Commun.* **2014**, *5*, 4913.

(234) Thormann, K. M.; Saville, R. M.; Shukla, S.; Pelletier, D. A.; Spormann, A. M. *J. Bacteriol.* **2004**, *186*, 8096–8104.

(235) Qian, X.; Metallo, S. J.; Choi, I. S.; Wu, H.; Liang, M. N.; Whitesides, G. M. *Anal. Chem.* **2002**, *74*, 1805–1810.

(236) Murugan, P.; Krishnamurthy, M.; Jaisankar, S. N.; Samanta, D.; Mandal, A. B. *Chem. Soc. Rev.* **2015**, *44*, 3212–3243.

(237) Sumerlin, B. S.; Lowe, A. B.; Stroud, P. A.; Zhang, P.; Urban, M. W.; McCormick, C. L. *Langmuir* **2003**, *19*, 5559–5562.

(238) Otsu, N. *Automatica* **1975**.

(239) Knuth, D. E. *The art of computer programming*; Addison-Wesley, 1997.

(240) Qian, H.; Sheetz, M.; Elson, E. *Biophys. J.* **1991**.

(241) Gibiansky, M. L.; Conrad, J. C.; Jin, F.; Gordon, V. D.; Motto, D. A.; Mathewson, M. A.; Stopka, W. G.; Zelasko, D. C.; Shrout, J. D.; Wong, G. C. L. *Science.* **2010**, *330*.

(242) Conrad, J.; Gibiansky, M.; Jin, F.; Gordon, V.; Motto, D. *Biophys. J.* **2011**.

(243) Varki, A. *Proc. Natl. Acad. Sci.* **1994**, *91*, 7390–7397.

(244) Byrne, M.; Mildner, R.; Menzel, H.; Heise, A. *Macromol. Biosci.* **2014**.

(245) Bonduelle, C.; Lecommandoux, S. *Biomacromolecules* **2013**, *14*, 2973–2983.

(246) Gestwicki, J. E.; Cairo, C. W.; Strong, L. E.; Oetjen, K. A.; Kiessling, L. L. *J. Am. Chem. Soc.* **2002**, *124*, 14922–14933.

(247) Geng, J.; Mantovani, G.; Tao, L.; Nicolas, J.; Chen, G.; Wallis, R.; Mitchell, D. A.; Johnson, B. R. G.; Evans, S. D.; Haddleton, D. M. *J. Am. Chem. Soc.* **2007**, *129*, 15156–15163.

(248) Lipinski, T.; Kitov, P. I.; Szpacenko, A.; Paszkiewicz, E.; Bundle, D. R. *Bioconjug. Chem.* **2011**, *22*, 274–281.

(249) Mancini, R. J.; Lee, J.; Maynard, H. D. *J. Am. Chem. Soc.* **2012**, *134*, 8474–8479.

(250) Narain, R. *React. Funct. Polym.* **2006**, *66*, 1589–1595.

(251) Lin, K.; Kasko, A. M. *Bioconjug. Chem.* **2015**, *26*, 1504–1512.

(252) Wang, Y. C.; Liu, X. Q.; Sun, T. M.; Xiong, M. H.; Wang, J. *J. Control. Release* **2008**, *128*, 32–40.

(253) Hu, Y. C.; Pan, C. Y. *Macromol. Rapid Commun.* **2005**, *26*, 968–972.

(254) Martin, A. L.; Li, B.; Gillies, E. R. *J. Am. Chem. Soc.* **2009**, *131*, 734–741.

(255) Bathfield, M.; D'Agosto, F.; Spitz, R.; Charreyre, M. T.; Delair, T. *J. Am. Chem. Soc.* **2006**, *128*, 2546–2547.

(256) Haddleton, D. M.; Ohno, K. *Biomacromolecules* **2000**, *1*, 152–156.

(257) Felici, M.; Marzá-Pérez, M.; Hatzakis, N. S.; Nolte, R. J. M.; Feiters, M. C. *Chemistry* **2008**, *14*, 9914–9920.

(258) Kakuchi, T.; Narumi, A.; Miura, Y.; Matsuya, S.; Sugimoto, N.; Satoh, T.; Kaga, H. *Macromolecules* **2003**, *36*, 3909–3913.

(259) Houga, C.; Le Meins, J. F.; Borsali, R.; Taton, D.; Gnanou, Y. *Chem. Commun.* **2007**, 3063–3065.

(260) Houga, C.; Giermanska, J.; Lecommandoux, S.; Borsali, R.; Taton, D.; Gnanou, Y.; Le Meins, J. F. *Biomacromolecules* **2009**, *10*, 32–40.

(261) Schatz, C.; Louguet, S.; Le Meins, J. F.; Lecommandoux, S. *Angew. Chem. Int. Ed. Engl.* **2009**, *48*, 2572–2575.

(262) Bonduelle, C.; Huang, J.; Ibarboure, E.; Heise, A.; Lecommandoux, S. *Chem. Commun. (Camb).* **2012**, *48*, 8353–8355.

(263) Nurmi, L.; Lindqvist, J.; Randev, R.; Syrett, J.; Haddleton, D. M. *Chem. Commun. (Camb).* **2009**, 2727–2729.

(264) Otman, O.; Boullanger, P.; Drockenmuller, E.; Hamaide, T. *Beilstein J. Org. Chem.* **2010**, *6*.

(265) Huang, J.; Bonduelle, C.; Thévenot, J.; Lecommandoux, S.; Heise, A. *J. Am. Chem. Soc.* **2012**, *134*, 119–122.

(266) Bonduelle, C.; Huang, J.; Mena-Barragán, T.; Ortiz Mellet, C.; Decroocq, C.; Etamé, E.; Heise, A.; Compain, P.; Lecommandoux, S. *Chem. Commun.* **2014**, *50*, 3350–3352.

(267) Ramiah, V.; Matahwa, H.; Weber, W.; McLeary, J. B.; Sanderson, R. D. *Macromol. Symp.* **2007**, *255*, 70–80.

(268) Ting, S. R. S.; Min, E. H.; Escalé, P.; Save, M.; Billon, L.; Stenzel, M. H. *Macromolecules* **2009**, *42*, 9422–9434.

(269) Narain, R.; Armes, S. P. *Macromolecules* **2003**, *36*, 4675–4678.

(270) Lu, F. Z.; Meng, J. Q.; Du, F. S.; Li, Z. C.; Zhang, B. Y. *Macromol. Chem. Phys.* **2005**, *206*, 513–520.

(271) Suriano, F.; Coulembier, O.; Degee, P.; Dubois, P. *J. Polym. Sci. Part A Polym. Chem.* **2008**, *46*, 3662–3672.

(272) Dai, X. H.; Dong, C. M. *J. Polym. Sci. Part A Polym. Chem.* **2008**, *46*, 817–829.

(273) Dai, X. H.; Dong, C. M.; Yan, D. *J. Phys. Chem. B* **2008**, *112*, 3644–3652.

(274) Bes, L.; Angot, S.; Limer, A.; Haddleton, D. M. *Macromolecules* **2003**, *36*, 2493–2499.

(275) Joralemon, M. J.; Murthy, K. S.; Remsen, E. E.; Becker, M. L.; Wooley, K. L. *Biomacromolecules* **2004**, *5*, 903–913.

(276) Deletre, M.; Levesque, G. *Macromolecules* **1990**, *23*, 4733–4741.

(277) Li, M.; De, P.; Gondi, S. R.; Sumerlin, B. S. *J. Polym. Sci. Part A Polym. Chem.* **2008**, *46*, 5093–5100.

(278) Vogt, A. P.; Sumerlin, B. S. *Soft Matter* **2009**, *5*, 2347–2351.

(279) Nagavarma, B.; Yadav, H.; Ayaz, A.; Vasudha, L.; Shivakumar, H. *Asian J. Pharm. Clin. Res.* **2012**, *5*, 16–23.

(280) Pati, D.; Kalva, N.; Das, S.; Kumaraswamy, G.; Sen Gupta, S.; Ambade, A. V. *J. Am. Chem. Soc.* **2012**, *134*, 7796–7802.

(281) Bonduelle, C.; Mazzaferro, S.; Huang, J.; Lambert, O.; Heise, A.; Lecommandoux, S. *Faraday Discuss.* **2013**, *166*, 137–150.

(282) Spain, S. G.; Cameron, N. R. *Polym. Chem.* **2011**, *2*, 1552–1560.

(283) Serizawa, T.; Yasunaga, S.; Akashi, M. *Biomacromolecules* **2001**, *2*, 469–475.

(284) Schurtenberger, P.; Newman, M. E. In *Enviromental particles*; Buffle, J.; van Leeuwen, H. P., Eds.; Lewis Publishers: Boca Raton, FL, 1993; Vol. 2, pp. 37–115.

(285) Burchard, W. In *Light Scattering from Polymers*; Springer-Verlag, 1983; Vol. 48, pp. 1–124.

(286) Moughton, A. O.; O'Reilly, R. K. *Chem. Commun.* **2010**, *46*, 1091–1093.

(287) Scheibe, C.; Wedepohl, S.; Riese, S. B.; Dernedde, J.; Seitz, O. *Chembiochem* **2013**, *14*, 236–250.

(288) Siedenbiedel, F.; Tiller, J. C. *Polymers.* **2012**, *4*, 46–71.

(289) Goy, R. C.; Britto, D. de; Assis, O. B. G. *Polímeros* **2009**, *19*, 241–247.

(290) Tsai, G. J.; Su, W. H. *J. Food Prot.* **1999**, *62*, 239–243.

(291) Yang, T. C.; Chou, C. C.; Li, C. F. *Int. J. Food Microbiol.* **2005**, *97*, 237–245.

(292) Fei Liu, X.; Lin Guan, Y.; Zhi Yang, D.; Li, Z.; De Yao, K. *J. Appl. Polym. Sci.* **2001**, *79*, 1324–1335.

(293) No, H. K.; Young Park, N.; Ho Lee, S.; Meyers, S. P. *Int. J. Food Microbiol.* **2002**, *74*, 65–72.

(294) Liu, N.; Chen, X. G.; Park, H. J.; Liu, C. G.; Liu, C. S.; Meng, X. H.; Yu, L. J. *Carbohydr. Polym.* **2006**, *64*, 60–65.

(295) Younes, I.; Sellimi, S.; Rinaudo, M.; Jellouli, K.; Nasri, M. *Int. J. Food Microbiol.* **2014**, *185*, 57–63.

(296) Jeon, Y. J.; Park, P. J.; Kim, S. K. *Carbohydr. Polym.* **2001**, *44*, 71–76.

(297) Chung, Y. C.; Wang, H. L.; Chen, Y. M.; Li, S. L. *Bioresour. Technol.* **2003**, *88*, 179–184.

(298) Qin, C.; Li, H.; Xiao, Q.; Liu, Y.; Zhu, J.; Du, Y. *Carbohydr. Polym.* **2006**, *63*, 367–374.

(299) Li, Z.; Yang, F.; Yang, R. *Int. J. Biol. Macromol.* **2015**, *75*, 378–387.

(300) Xing, K.; Chen, X. G.; Kong, M.; Liu, C. S.; Cha, D. S.; Park, H. J. *Carbohydr. Polym.* **2009**, *76*, 17–22.

(301) Xing, K.; Chen, X. G.; Liu, C. S.; Cha, D. S.; Park, H. J. *Int. J. Food Microbiol.* **2009**, *132*, 127–133.

(302) Helander, I. .; Nurmiaho-Lassila, E. L.; Ahvenainen, R.; Rhoades, J.; Roller, S. *Int. J. Food Microbiol.* **2001**, *71*, 235–244.

(303) Sudarshan, N. R.; Hoover, D. G.; Knorr, D. *Food Biotechnol.* **1992**, *6*, 257–272.

(304) Young, D. H.; Kohle, H.; Kauss, H. *PLANT Physiol.* **1982**, *70*, 1449–1454.

(305) Liu, H.; Du, Y.; Wang, X.; Sun, L. *Int. J. Food Microbiol.* **2004**, *95*, 147–155.

(306) Hadwiger, L. A.; Kendra, D. F.; Fristensky, B. W.; Wagoner, W. In *Chitin in Nature and Technology*; Springer US: Boston, MA, 1986; pp. 209–214.

(307) Cuero, R. G.; Osuji, G.; Washington, A. *Biotechnol. Lett.* **1991**, *13*, 441–444.

(308) Jia, Z.; Shen, D.; Xu, W. *Carbohydr. Res.* **2001**, *333*, 1–6.

(309) Wang, W.; Bo, S.; Li, S.; Qin, W. *Int. J. Biol. Macromol.* **1991**, *13*, 281–285.

(310) Cai, J.; Yue, Y.; Rui, D.; Zhang, Y.; Liu, S.; Wu, C. *Macromolecules* **2011**, *44*, 2050–2057.

(311) Kamimura, K.; Suda, T.; Zhang, G.; Liu, D. *Pharmaceut. Med.* **2011**, *25*, 293–306.

(312) Gore, M. *Gene Ther.* **2003**, *10*.

(313) Lehrman, S. *Nature* **1999**, *401*, 517–518.

(314) Marshall, E. *Gene therapy death prompts review of adenovirus vector.*; 1999; Vol. 286,

pp. 2244–2245.

(315) Liu, Q.; Muruve, D. A. *Gene Ther.* **2003**, *10*, 935–940.

(316) Sun, J. Y.; Anand-Jawa, V.; Chatterjee, S.; Wong, K. K. *Gene Ther.* **2003**, *10*, 964–976.

(317) Reineke, T. M. *J. Polym. Sci. Part A Polym. Chem.* **2006**, *44*, 6895–6908.

(318) Fichter, K. M.; Ingle, N. P.; McLendon, P. M.; Reineke, T. M. *ACS Nano* **2013**, *7*, 347–364.

(319) Akers, F. Press Release: Patent Claims Awarded for Techulon's Gene Delivery Polymers. *Business Wire*, 2011.

(320) Dhande, Y. K.; Wagh, B. S.; Hall, B. C.; Sprouse, D.; Hackett, P. B.; Reineke, T. M. *Biomacromolecules* **2016**, *17*, 830–840.

(321) Buschmann, M. D.; Merzouki, A.; Lavertu, M.; Thibault, M.; Jean, M.; Darras, V. *Adv. Drug Deliv. Rev.* **2013**, *65*, 1234–1270.

(322) Mao, S.; Sun, W.; Kissel, T. *Adv. Drug Deliv. Rev.* **2010**, *62*, 12–27.

(323) Sizovs, A.; McLendon, P. M.; Srinivasachari, S.; Reineke, T. M. *Top. Curr. Chem.* **2010**, *296*, 131–190.

(324) Almalik, A.; Day, P. J.; Tirelli, N. *Macromol. Biosci.* **2013**, *13*, 1671–1680.

(325) Ishii, T.; Okahata, Y.; Sato, T. *Biochim. Biophys. Acta* **2001**, *1514*, 51–64.

(326) Kiang, T.; Wen, J.; Lim, H. W.; Leong, K. W. *Biomaterials* **2004**, *25*, 5293–5301.

(327) Huang, M.; Fong, C. W.; Khor, E.; Lim, L. Y. *J. Control. Release* **2005**, *106*, 391–406.

(328) Sato, T.; Ishii, T.; Okahata, Y. *Biomaterials* **2001**, *22*, 2075–2080.

(329) Zhao, Q. Q.; Chen, J. L.; Lv, T. F.; He, C. X.; Tang, G. P.; Liang, W. Q.; Tabata, Y.; Gao,

J. Q. *Biol. Pharm. Bull.* **2009**, *32*, 706–710.

(330) Pezzoli, D.; Olimpieri, F.; Malloggi, C.; Bertini, S.; Volonterio, A.; Candiani, G. *PLoS One* **2012**, *7*, 1–9.

(331) Gary, D. J.; Min, J.; Kim, Y.; Park, K.; Won, Y. Y. *Macromol. Biosci.* **2013**, *13*, 1059–1071.

(332) Cifani, N.; Chronopoulou, L.; Pompili, B.; Di Martino, A.; Bordi, F.; Sennato, S.; Di Domenico, E. G.; Palocci, C.; Ascenzioni, F. *Biotechnol. Lett.* **2015**, *37*, 557–565.

(333) Nimesh, S.; Thibault, M. M.; Lavertu, M.; Buschmann, M. D. *Mol. Biotechnol.* **2010**, *46*, 182–196.

(334) Biggs, C. I.; Walker, M.; Gibson, M. I. *Biomacromolecules* **2016**, *17*, 2626–2633.